frontiers | Research Topics

Metabolic barriers in cancer and cancer therapy

Edited by
Martin Böttcher, Sascha Kahlfuss and Jérôme Paggetti

Published in
Frontiers in Oncology

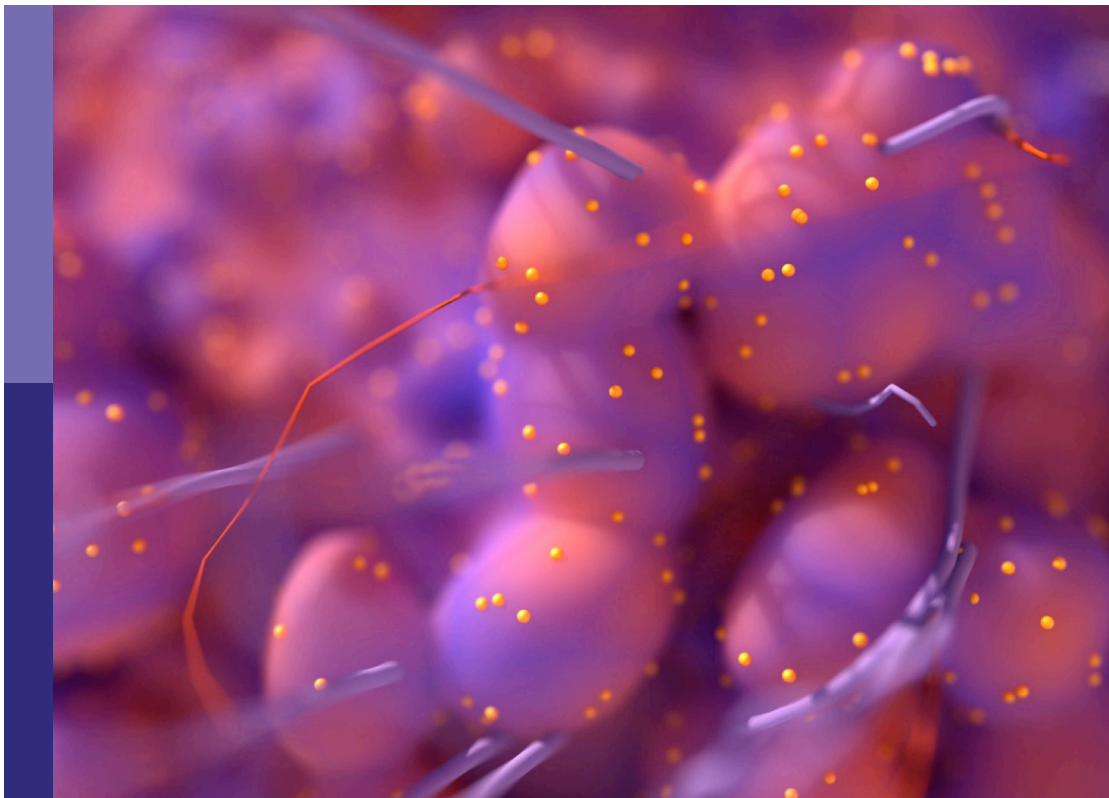

ISSN 1664-8714
ISBN 978-2-8325-4838-7
DOI 10.3389/978-2-8325-4838-7

About Frontiers

Frontiers is more than just an open access publisher of scholarly articles: it is a pioneering approach to the world of academia, radically improving the way scholarly research is managed. The grand vision of Frontiers is a world where all people have an equal opportunity to seek, share and generate knowledge. Frontiers provides immediate and permanent online open access to all its publications, but this alone is not enough to realize our grand goals.

Frontiers journal series

The Frontiers journal series is a multi-tier and interdisciplinary set of open-access, online journals, promising a paradigm shift from the current review, selection and dissemination processes in academic publishing. All Frontiers journals are driven by researchers for researchers; therefore, they constitute a service to the scholarly community. At the same time, the *Frontiers journal series* operates on a revolutionary invention, the tiered publishing system, initially addressing specific communities of scholars, and gradually climbing up to broader public understanding, thus serving the interests of the lay society, too.

Dedication to quality

Each Frontiers article is a landmark of the highest quality, thanks to genuinely collaborative interactions between authors and review editors, who include some of the world's best academicians. Research must be certified by peers before entering a stream of knowledge that may eventually reach the public - and shape society; therefore, Frontiers only applies the most rigorous and unbiased reviews. Frontiers revolutionizes research publishing by freely delivering the most outstanding research, evaluated with no bias from both the academic and social point of view. By applying the most advanced information technologies, Frontiers is catapulting scholarly publishing into a new generation.

What are Frontiers Research Topics?

Frontiers Research Topics are very popular trademarks of the *Frontiers journals series*: they are collections of at least ten articles, all centered on a particular subject. With their unique mix of varied contributions from Original Research to Review Articles, Frontiers Research Topics unify the most influential researchers, the latest key findings and historical advances in a hot research area.

Find out more on how to host your own Frontiers Research Topic or contribute to one as an author by contacting the Frontiers editorial office: frontiersin.org/about/contact

Metabolic barriers in cancer and cancer therapy

Topic editors

Martin Böttcher — University Hospital Magdeburg; Otto-von-Guericke University Magdeburg, Germany

Sascha Kahlfuss — Universitätsklinikum Magdeburg, Germany

Jérôme Paggetti — Luxembourg Institute of Health, Luxembourg

Citation

Böttcher, M., Kahlfuss, S., Paggetti, J., eds. (2024). *Metabolic barriers in cancer and cancer therapy*. Lausanne: Frontiers Media SA. doi: 10.3389/978-2-8325-4838-7

Table of contents

04 Editorial: Metabolic barriers in cancer and cancer therapy
Sascha Kahlfuss, Jérôme Paggetti and Martin Böttcher

07 Decreased Efficacy of Doxorubicin Corresponds With Modifications in Lipid Metabolism Markers and Fatty Acid Profiles in Breast Tumors From Obese vs. Lean Mice
Ilze Mentoor, Theo Nell, Zaakiyah Emjedi, Paul J. van Jaarsveld, Louis de Jager and Anna-Mart Engelbrecht

28 Cytosolic NUAK1 Enhances ATP Production by Maintaining Proper Glycolysis and Mitochondrial Function in Cancer Cells
Emilia Escalona, Marcelo Muñoz, Roxana Pincheira, Álvaro A. Elorza and Ariel F. Castro

40 Inhibition of Fatty Acid Synthase Upregulates Expression of CD36 to Sustain Proliferation of Colorectal Cancer Cells
James Drury, Piotr G. Rychahou, Daheng He, Naser Jafari, Chi Wang, Eun Y. Lee, Heidi L. Weiss, Bernard Mark Evers and Yekaterina Y. Zaytseva

53 TIGIT signaling and its influence on T cell metabolism and immune cell function in the tumor microenvironment
Nouria Jantz-Naeem, Romy Böttcher-Loschinski, Katrin Borucki, Marisa Mitchell-Flack, Martin Böttcher, Burkhart Schraven, Dimitrios Mougiakakos and Sascha Kahlfuss

64 Lactate mediated metabolic crosstalk between cancer and immune cells and its therapeutic implications
Seyedeh Sahar Mortazavi Farsani and Vivek Verma

75 Crosstalk between arginine, glutamine, and the branched chain amino acid metabolism in the tumor microenvironment
Tanner J. Wetzel, Sheila C. Erfan, Lucas D. Figueroa, Leighton M. Wheeler and Elitsa A. Ananieva

84 LC–MS-based serum metabolomics analysis for the screening and monitoring of colorectal cancer
Yanan Yi, Jianjian Wang, Chengtong Liang, Chuanli Ren, Xu Lian, Chongxu Han and Wei Sun

95 The cross-talk between macrophages and tumor cells as a target for cancer treatment
Muhammad Aizaz, Aakif Khan, Faisal Khan, Maria Khan, Ebraheem Abdu Musad Saleh, Maryum Nisar and Natalia Baran

119 Moving from conventional to adaptive risk stratification for oropharyngeal cancer
Vlad C. Sandulache, R. Parker Kirby and Stephen Y. Lai

frontiers | Frontiers in Oncology

TYPE Editorial
PUBLISHED 08 May 2024
DOI 10.3389/fonc.2024.1411579

OPEN ACCESS

EDITED AND REVIEWED BY
Michael P. Lisanti,
University of Salford, United Kingdom

*CORRESPONDENCE
Martin Böttcher
martin.boettcher@med.ovgu.de

RECEIVED 03 April 2024
ACCEPTED 15 April 2024
PUBLISHED 08 May 2024

CITATION
Kahlfuss S, Paggetti J and Böttcher M (2024) Editorial: Metabolic barriers in cancer and cancer therapy.
Front. Oncol. 14:1411579.
doi: 10.3389/fonc.2024.1411579

Editorial: Metabolic barriers in cancer and cancer therapy

Sascha Kahlfuss[1,2,3,4], Jérôme Paggetti[5] and Martin Böttcher[3,6]*

[1]Institute of Molecular and Clinical Immunology, Medical Faculty, Otto-von-Guericke University Magdeburg, Magdeburg, Germany, [2]Institute of Medical Microbiology and Hospital Hygiene, Medical Faculty, Otto-von-Guericke University Magdeburg, Magdeburg, Germany, [3]Health Campus Immunology, Infectiology and Inflammation (GCI), Medical Faculty, Otto-von-Guericke University Magdeburg, Magdeburg, Germany, [4]Center for Health and Medical Prevention (CHaMP), Otto-von-Guericke-University, Magdeburg, Germany, [5]Tumor Stroma Interactions, Department of Cancer Research, Luxembourg Institute of Health, Luxembourg, Luxembourg, [6]Department of Hematology, Oncology and Cell Therapy, University Hospital Magdeburg, Otto-von-Guericke University Magdeburg, Magdeburg, Germany

KEYWORDS

cancer metabolism, immunometabolism, cancer therapy, therapy resistance, personalized medicine

Editorial on the Research Topic
Metabolic barriers in cancer and cancer therapy

Cancer is a complex and heterogeneous disease with various entities originating from multiple tissues/sites with different genetic backgrounds. However, all types of tumors are characterized by a dysregulated cellular metabolism. This not only fuels tumorigenesis but also confers growth advantages and resistance to immune cells and (immune-based) therapy. Outstanding research efforts over the past 20–30 years have led to the emergence of three major concepts in the field of cancer immunometabolism: 1) metabolic competition, 2) secretion of regulatory (onco-)metabolites, and 3) induction and recruitment of tolerogenic innate and adaptive immune cells by providing a metabolically favorable microenvironment for these cell types. In terms of metabolic competition, tumor cells have often undergone metabolic rewiring that allows them to consume available metabolites, such as glucose, fatty acids, and amino acids, more efficiently and abundantly than their attacking immune cells. This gives them an advantage in growth and proliferation while disarming the immune cells and hindering their ability to mount an effective anti-tumor immune response (1, 2). At the same time, this metabolic rewiring leads to the secretion of large amounts of metabolic by-products, such as lactate, kynurenine, or reactive oxygen species. While malignant cells have evolved mechanisms to cope with this overabundance of metabolites, many immune effector cells, including T and NK cells and tumorigenic macrophages, are detrimentally inhibited in their function (3–5). The altered metabolic microenvironment leads to the accumulation of tolerogenic immune cells, such as Tregs and myeloid-derived suppressor cells (6, 7). The latter cell types are more resistant to the 'toxic' metabolites secreted and do not rely on metabolic pathways/substrates that are primarily used and depleted by tumor cells. The metabolic status of malignant cells can create metabolic barriers for immune cells and immune-based therapies at multiple levels. Therefore, understanding the underlying mechanisms is a crucial goal of current research. This will provide more precise targets for therapeutic intervention.

The current Research Topic frames recent developments in this context and summarizes current knowledge.

The articles by Aizaz et al. and Jantz-Naeem et al. focus on the interplay between the tumor microenvironment (TME) and immune checkpoints as metabolic regulatory circuits. Macrophages, particularly tumor-associated macrophages (TAMs), undergo metabolic reprogramming in response to the tumor milieu, promoting tumor growth and immune evasion. These alterations in macrophage metabolism contribute to the immunosuppressive TME. These pathways represent promising targets for cancer therapy. The CD47 protein, recognized as a "don't eat me" signal on cancer cells, is involved in metabolic crosstalk between tumor cells and macrophages, influencing immune evasion and tumor progression. Targeting CD47 and other metabolism-directed strategies offers new avenues for cancer treatment by disrupting metabolic interactions within the TME and enhancing anti-tumor immune responses. In addition, immune checkpoint molecules such as TIGIT, PD-1, and CTLA-4 exert regulatory effects on immune cell metabolism within the TME. TIGIT, for example, not only modulates T cell exhaustion but also affects cellular metabolism, potentially altering the balance between pro- and anti-tumor immune responses. Understanding the metabolic regulation of immune checkpoints provides insights into novel therapeutic strategies for cancer treatment, particularly those targeting metabolic vulnerabilities in the TME.

In addition, the manuscripts by Mentoor et al. and Drury et al. highlight the special role of fatty acid metabolism as a critical determinant of cancer progression and response to therapy. Breast cancer cells exhibit a pronounced ability to modulate lipid metabolism, a process that is intricately linked to tumor growth and inflammation within the TME, particularly under conditions of diet-induced obesity (DIO). In addition, dysregulated fatty acid synthase (FASN), a key enzyme in *de novo* lipogenesis, represents a promising therapeutic target. Inhibition of FASN triggers metabolic rewiring in cancer cells, leading to compensatory upregulation of the fatty acid transporter CD36. This upregulation promotes tumor growth and survival, underscoring the importance of fatty acid metabolism in breast cancer progression, particularly in obese individuals. Obesity-induced alterations in lipid metabolism also affect the efficacy of chemotherapy, highlighting the importance of understanding the interplay between fatty acid metabolism and treatment outcomes. Modulation of fatty acid metabolism provides an avenue for the development of targeted therapeutic strategies aimed at disrupting the metabolic dependencies of breast cancer cells and enhancing treatment efficacy. By elucidating the intricate mechanisms governing fatty acid metabolism in breast cancer, novel interventions can be developed to overcome therapeutic resistance and improve patient outcomes.

The manuscripts by Escalona et al., Farsani and Verma, and Wetzel et al. focus on the role of specific pathways and their metabolites in the regulation of cancer progression and persistence. On the one hand, the Warburg effect, characterized by enhanced glycolysis even in the presence of oxygen, underscores the metabolic adaptations of cancer cells. Glucose-derived lactate, a hallmark of the Warburg effect, not only fuels tumor growth but also influences immune cell function within the TME. This glucose-lactate-mediated crosstalk between tumor and immune cells poses a challenge to the efficacy of immunotherapy, highlighting the importance of metabolic intervention in improving treatment outcomes. On the other hand, amino acid metabolism, particularly arginine, glutamine, and branched-chain amino acids (BCAAs), plays a pivotal role in supporting cancer cell growth and immune evasion within the TME. Cancer cells exploit metabolic flexibility to outcompete infiltrating immune cells for essential nutrients, thereby promoting tumor progression and immune suppression. Targeting amino acid metabolism represents a promising therapeutic approach to disrupt the metabolic symbiosis between cancer and immune cells, thereby enhancing immune-mediated tumor control.

Finally, the manuscript by Yi et al. provides insight into the utility of metabolomics as a diagnostic tool, specifically in colorectal cancer (CRC). The metabolomic analysis distinguishes CRC patients from healthy individuals and identifies potential biomarkers associated with disease progression. Monitoring changes in serum metabolites after surgery provides valuable insights into treatment response and disease recurrence. Serum metabolomics offers a comprehensive approach to CRC screening and monitoring, improving early detection and personalized treatment strategies.

In summary, understanding the complex interplay between tumor cells, immune cells, and the TME, as well as metabolic alterations in cancer cells is critical for developing effective cancer therapies and improving patient outcomes.

Author contributions

SK: Writing – review & editing. JP: Writing – review & editing. MB: Conceptualization, Writing – original draft, Writing – review & editing.

Acknowledgments

In this editorial, we used ChatGPT, an AI language model developed by OpenAI, based on the GPT-3.5 architecture, to improve language quality, readability, and conciseness. We declare that all text generated by ChatGPT has undergone thorough verification and review.

Conflict of interest

The authors declare that the research was conducted in the absence of any commercial or financial relationships that could be construed as a potential conflict of interest.

The author(s) declared that they were an editorial board member of Frontiers, at the time of submission. This had no impact on the peer review process and the final decision.

Publisher's note

References

1. Lu J, Böttcher M, Walther T, Mougiakakos D, Zenz T, Huber W. Energy metabolism is co-determined by genetic variants in chronic lymphocytic leukemia and influences drug sensitivity. *Haematologica*. (2019) 104:1830–40. doi: 10.3324/haematol.2018.203067

2. Qorraj M, Bruns H, Böttcher M, Weigand L, Saul D, Mackensen A, et al. The pd-1/pd-L1 axis contributes to immune metabolic dysfunctions of monocytes in chronic lymphocytic leukemia. *Leukemia*. (2017) 31:470–8. doi: 10.1038/leu.2016.214

3. Böttcher M, Renner K, Berger R, Mentz K, Thomas S, Cardenas-Conejo ZE, et al. D-2-hydroxyglutarate interferes with hif-1α Stability skewing T-cell metabolism towards oxidative phosphorylation and impairing th17 polarization. *Oncoimmunology*. (2018) 7:e1445454. doi: 10.1080/2162402x.2018.1445454

4. Böttcher M, Böttcher-Loschinski R, Kahlfuss S, Aigner M, Gießl A, Mackensen A, et al. Cll-derived extracellular vesicles impair T-cell activation and foster T-cell exhaustion via multiple immunological checkpoints. *Cells*. (2022) 11(14):2176. doi: 10.3390/cells11142176

5. Gargiulo E, Viry E, Morande PE, Largeot A, Gonder S, Xian F, et al. Extracellular vesicle secretion by leukemia cells in vivo promotes cll progression by hampering antitumor T-cell responses. *Blood Cancer Discov*. (2023) 4:54–77. doi: 10.1158/2643–3230.Bcd-22–0029

6. Tohumeken S, Baur R, Böttcher M, Stoll A, Loschinski R, Panagiotidis K, et al. Palmitoylated proteins on aml-derived extracellular vesicles promote myeloid-derived suppressor cell differentiation via tlr2/akt/mtor signaling. *Cancer Res*. (2020) 80:3663–76. doi: 10.1158/0008–5472.Can-20–0024

7. Mougiakakos D, Johansson CC, Jitschin R, Böttcher M, Kiessling R. Increased thioredoxin-1 production in human naturally occurring regulatory T cells confers enhanced tolerance to oxidative stress. *Blood*. (2011) 117:857–61. doi: 10.1182/blood-2010–09-307041

frontiers in Oncology

ORIGINAL RESEARCH
published: 17 March 2020
doi: 10.3389/fonc.2020.00306

Decreased Efficacy of Doxorubicin Corresponds With Modifications in Lipid Metabolism Markers and Fatty Acid Profiles in Breast Tumors From Obese vs. Lean Mice

Ilze Mentoor[1], Theo Nell[1], Zaakiyah Emjedi[1], Paul J. van Jaarsveld[2,3], Louis de Jager[4] and Anna-Mart Engelbrecht[1]**

[1] Department of Physiological Sciences, Faculty of Natural Sciences, University of Stellenbosch, Stellenbosch, South Africa, [2] Non-Communicable Diseases Research Unit, South African Medical Research Council, Cape Town, South Africa, [3] Division of Medical Physiology, Faculty of Medicine and Health Sciences, Stellenbosch University, Tygerberg, South Africa, [4] Division of Anatomical Pathology, Faculty of Medicine and Health Sciences, Stellenbosch University, Tygerberg, South Africa

OPEN ACCESS

Edited by:
Federica Sotgia,
University of Salford, United Kingdom

Reviewed by:
Cesare Indiveri,
University of Calabria, Italy
Olivier Peulen,
University of Liège, Belgium

***Correspondence:**
Anna-Mart Engelbrecht
ame@sun.ac.za
Ilze Mentoor
mentoor@sun.ac.za

Specialty section:
This article was submitted to Cancer Metabolism, a section of the journal Frontiers in Oncology

Received: 14 November 2019
Accepted: 20 February 2020
Published: 17 March 2020

Citation:
Mentoor I, Nell T, Emjedi Z, van Jaarsveld PJ, de Jager L and Engelbrecht A-M (2020) Decreased Efficacy of Doxorubicin Corresponds With Modifications in Lipid Metabolism Markers and Fatty Acid Profiles in Breast Tumors From Obese vs. Lean Mice. Front. Oncol. 10:306. doi: 10.3389/fonc.2020.00306

Breast cancer cells modulate lipid and fatty acid metabolism to sustain proliferation. The role of adipocytes in cancer treatment efficacy remains, however, to be fully elucidated. We investigated whether diet-induced obesity (DIO) affects the efficacy of doxorubicin treatment in a breast tumor-bearing mouse model. Female C57BL6 mice were fed a high fat or low fat diet for the full duration of the study (12 weeks). After 8 weeks, mice were inoculated with E0771 triple-negative breast cancer cells in the fourth mammary gland to develop breast tumor allographs. Tumor-bearing mice received either vehicle (Hank's balanced salt solution) or doxorubicin (chemotherapy). Plasma inflammatory markers, tumor, and mammary adipose tissue fatty acid composition, as well as protein expression of lipid metabolism markers were determined. The high fat diet (HFD) attenuated the treatment efficacy of doxorubicin. Both leptin and resistin concentrations were significantly increased in the HFD group treated with doxorubicin. Suppressed lipogenesis (decreased stearoyl CoA-desaturase-1) and lipolysis (decreased hormone-sensitive lipase) were observed in mammary adipose tissue of the DIO animals, whereas increased expression was observed in the tumor tissue of doxorubicin treated HFD mice. Obesogenic conditions induced altered tissue fatty acid (FA) compositions, which reduced doxorubicin's treatment efficacy. In mammary adipose tissue breast cancer cells suppressed the storage of FAs, thereby increasing the availability of free FAs and favored inflammation under obesogenic conditions.

Keywords: obesity, breast cancer, adipose tissue, fatty acids, treatment efficacy

INTRODUCTION

The incidence of lifestyle associated conditions including obesity is a rising epidemic (1), this is especially alarming since breast cancer remains a major health risk for women globally (2). Obesity is identified as a casual factor in both the development as well as the progression of breast carcinogenesis (3, 4), and is characterized by rapid adipose tissue remodeling (hypertrophy and

hyperplasia) (5), increased synthesis of several adipokines such as leptin, resistin, tumor necrosis factor-alpha (TNF-α), interleukin (IL)-1β, IL-6, macrophage chemoattractant protein-1 (MCP-1), and immune cell infiltration, all of which lead to a state of sustained low-grade inflammation. Mammary adipose tissue serves as a exogenous source of energy metabolites which favors the proliferation demand of breast cells in the tumor microenvironment (6, 7). On the other hand, breast cancer cells can also modulate lipid metabolism by altering both *de novo* fatty acid (FA) synthesis as well as the catabolic break down of triacylglycerol's (TAGs) a process known as lipolysis. This subsequently results in the release of free fatty acids (FFAs) which become available metabolic substrates for the benefit of breast cancer cell survival, either by storage in the form of lipid droplets, membrane lipids or energy production *via* β-oxidation supplying energy to these proliferating breast cancer cells (6, 8).

The role of FAs in cancer progression and treatment resistance implicates various physiological functions of FAs in relation to both dietary intake and *de novo* synthesized FAs. It is proposed to be achieved by *(i) alterations in cell membrane composition, (ii) the biosynthesis of lipid-signaling molecules, and (iii) its role in metabolic reprogramming as an energy source* [reviewed in (9, 10)]. Both SFAs and MUFAs are implicated in alterations within cancer cell membrane composition known as *membrane lipid saturation*. These FA classes are more resistant to lipid peroxidation, which in turn protects cancerous cells against oxidative stress induced by therapies (11, 12). The role of omega-6 (n-6) PUFAs in breast cancer development, progression as well as treatment resistance, includes n-6 PUFAs exhibiting pro-inflammatory effects mediated by lipid-derived bioactive mediators i.e., eicosanoids, prostaglandins and leukotrienes (13, 14). These lipid-derived bioactive mediators upregulate signaling pathways that are involved in inflammation, which exacerbate angiogenesis, cell-proliferation and inflammation (15), to contribute to an ideal microenvironment favoring mammary carcinogenesis.

Recently, findings from cell culture and animal models identified obesity as a main contributing factor in the underlying pathophysiology implicated in the development of breast cancer chemotherapeutic drug resistance (16, 17). Patients suffering from obesity and breast cancer presented with poor clinical outcomes when treated with first line adjuvant regimens such as doxorubicin (18, 19). Despite doxorubicin's high efficacy in killing cancer cells, its' clinical efficacy is hindered by the development of various cellular toxicities which contributes to the development of chemotherapeutic drug resistance (20). Doxorubicin treatment is also associated with cellular toxicities in adipose tissue (primary storage site for FAs) which in turn leads to dysfunctional lipid/FA storage (21, 22). Therefore, FA tissue composition may also be significantly altered by chemotherapeutic agents.

A lack of evidence highlighting the role of FAs in breast cancer treatment efficacy, as well as an incomplete understanding of cellular mechanisms whereby obesity affects chemotherapy outcomes, necessitates further investigation. We therefore aimed to determine whether diet-induced obesity (DIO) affects the efficacy of doxorubicin treatment in a breast tumor-bearing mouse model and to explore possible mechanisms of action.

METHODS

Female C57BL6 mice were fed a low fat diet (LFD) or a high fat diet (HFD) for 12 weeks. After developing the DIO phenotype, syngeneic breast tumors were induced, followed by respective treatments.

Animals and Handling

Animal handling and interventions were carried out under the supervision of a registered small animal handling expert at the Stellenbosch University. Ethical clearance was obtained from Stellenbosch University animal research committee (SU-ACUM13-00015). All protocols strictly adhered to the standard care guidelines of laboratory animals implemented at Stellenbosch University and according to the South African National Standards 10386:2008 for the use of animals in research and teaching.

Three-week-old female C57BL6 mice ($n = 40$) were maintained in the animal research facility at the University of Stellenbosch in static micro-isolation sterilized cages ($n = 5$ per cage) with filtered air. The mice were provided with chow and water *ad libitum* in a regular 12:12 h light-dark cycle. All animals were acclimated for 1 week followed by the assignment to either HFD or LFD groups. The general welfare of all animals were monitored daily.

Diet Regimens

A HFD was used to induce obesity since reported evidence showed that genetic models of obesity (i.e., *ob/ob*, *db/db*, and *leptin/ leptin* receptor-deficient mice) demonstrated resistance in developing mammary cancer (23). C57BL6 mice are particularly

Abbreviations: Σ MUFAs, Total Monounsaturated fatty acids; Σ n-3 PUFA, Total omega-3 polyunsaturated fatty acids; Σ n-6 PUFAs, Total omega-6 polyunsaturated fatty acids; Σ PUFAs, Total polyunsaturated fatty acids; Σ SFAs, Total saturated fatty acids; AA (C20:4n-6), Arachidonic Acid; ACC, Acetyl-CoA carboxylase; ADA (C22:4n-6), Adrenic Acid; ALA (C18:3n-3), α-Linolenic Acid; ARA (C20:0), Arachidic Acid; ATGL, Adipose triglyceride lipase; CMS, Chloroform:Methanol:Saline; DGLA (C20:3n-6), Dihomo-γ-Linolenic Acid; DHA (C22:6n-3), Docosahexaenoic Acid; DIO, Diet-induced obesity; Dox-H, Tumor doxorubicin-HFD; Dox-L, Tumor doxorubicin-LFD; DPA (C22:5n-6), Docosapentaenoic Acid; EA (C22:1 n-9), Erucic Acid; ECL, Enhanced chemiluminescence; EDA (C20:2n-6), Eicosadienoic Acid; EPA (C20:5n-3), Eicosapentaenoic Acid; FABP4, Fatty acid binding protein 4; FAMEs, Fatty acid methyl esters; GA (C20:1n-9), Gondoic Acid; GLC, Gas-liquid chromatography; HBSS, Hanks Balanced Salt Solution; HFD, High-fat diet; HSL, Hormone-sensitive lipase; IL, Interleukin; LA (C18:2n-6), Linoleic Acid; γ-LA (C18:3n-6), γ-Linolenic Acid; LFD, Low-fat diet; MA (C14:0), Myristic Acid; MCP-1, Macrophage chemoattractant protein-1; MGA (C17:0), Margaric Acid; n-3, Omega-3; n-6, Omega-6; NA (C24:1n-9), Nervonic Acid; NFκB, Nuclear factor kappa B; OA (C18:1n-9), Oleic Acid; PA (C16:0), Palmitic Acid; PAI-1, Plasminogen activator inhibitor-1; PenStrep, Penicillin Streptomycin; PI3K, Phosphoinositide-3-kinase; PTA (C16:1n-7), Palmitoleic Acid; PVDF, Polyvinylidene fluoride; RIPA, Radio-immunoprecipitation assay buffer; SA (C18:0), Stearic Acid; SCD-1, Stearoyl CoA-desaturase-1; SFAs, Saturated fatty acids; SEM, Standard error of the mean; TAG, triacylglycerols; TBS-T, Tris Buffered Saline-Tween 20; TNF-α, Tumor necrosis factor-alpha; TPL, Total phospholipid; VA (C18:1n-7), cis-Vaccenic Acid; VEGF, Vascular endothelial growth factor; Vehicle-H, Tumor vehicle-HFD; Vehicle-L, Tumor vehicle-LFD.

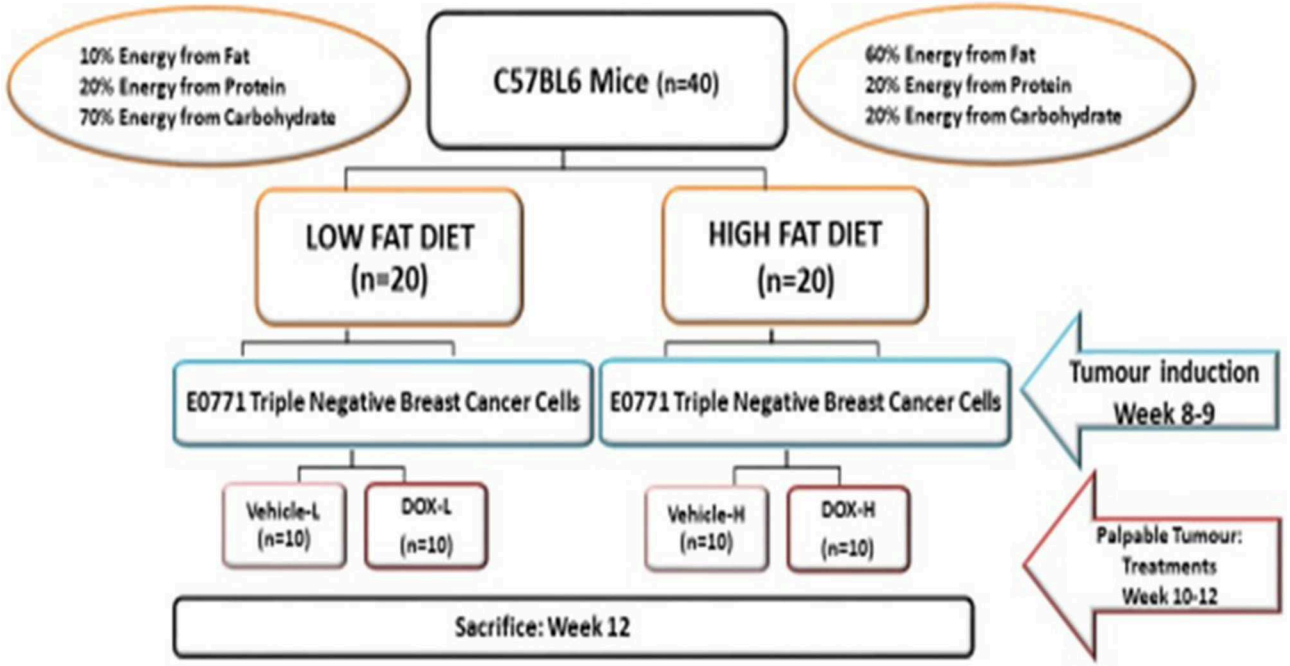

FIGURE 1 | Representative summary of the *in vivo* model and respective experimental groups.

sensitive to DIO (24). Forty mice ($n = 40$) were randomly assigned into two equal groups ($n = 20$) and allocated one of two respective diets for 12 weeks (**Figure 1**). The energy content of the HFD (D12492, Research diet Inc., New Jersey, USA) consisted of 60% energy from fat, 20% energy from protein, and 20% energy from carbohydrates, compared to the LFD (D12450J, Research diet Inc., New Jersey, USA), containing 10% energy from fat, 20% energy from protein, and 70% energy from carbohydrates (**Table 1**). The dietary FA composition of the respective diets is summarized in **Supplementary Table 1**. Body weight was monitored weekly over the study period and the DIO phenotype was confirmed after 8 weeks followed by tumor induction.

Tumor Induction

Cell Culture

An aggressive triple-negative breast cancer cell line with metastatic capabilities (E0771) that originated from a tumor after a spontaneous mutation in a C57BL6 mouse, was used in this *in vivo* model. The cells were cultured in T75 flasks (75 cm^2, SPL Life Sciences, Pocheon-si, South Korea) with Dulbecco's Modified Eagle's medium (DMEM, Gibco®, ThermoFisher Scientific, Massachusetts, United States) under standard incubation conditions (37°C and 5% CO_2 humidity), supplemented with 10% fetal bovine serum (FBS, Capricorn Scientific, Germany) and 1% Penicillin Streptomycin (PenStrep Gibco, ThermoFisher Scientific, Massachusetts, United States). Growth media was replaced every 2 day. Regular sub-culturing was performed once cultures reached 70–80% confluency.

Inoculation of Tumors

E0771 cells were prepared for each mouse. The mice were anesthetized under 3% (v/v) isoflurane (Isofor, Safeline Pharmaceuticals, Johannesburg, South Africa) in an anesthetic chamber. Mice were inoculated subcutaneously (using a 23-gauge needle syringe) in the fourth left mammary fat pad with 1.2×10^5 E0771 triple-negative breast cancer cells suspended in Hanks Balanced Salt Solution (HBSS) (Sigma Chemical Co., St Louis, MO, USA) as illustrated in **Figure 1**.

Drug Administration

Once tumors became palpable (200–300 mm^2), LFD and HFD mice were randomly assigned to the respective treatment groups (**Figure 1**). The treatment groups included: (1) vehicle control (isovolumetric intra-peritoneal injection of HBSS), and (2) doxorubicin treatment (D5794, LKT® laboratories, Minnesota, USA). Mice were restrained and treated with three dosages of 4 mg/kg doxorubicin (cumulative dosage of 12 mg/kg) *via* intraperitoneal injection. The dosage of 12 mg/kg doxorubicin is equivalent to 36 mg/m^2 in humans which is within the clinically relevant dosage range of doxorubicin treatment (15–90 mg/m^2) (25).

The experimental groups were assigned as follows: (i) tumor vehicle-LFD (vehicle-L), (ii) tumor vehicle-HFD (vehicle-H), (iii) tumor doxorubicin-LFD (Dox-L), and (iv) tumor doxorubicin-HFD (Dox-H). Humane endpoints were implemented when tumor growth influenced the general welfare or restricted mobility of the mice, or when the mice began to bite their tumors and exhibit changes in posture and facial expression, as determined by the grimace scale. The final sample size per

TABLE 1 | Dietary composition of low fat diet and high fat diet.

	Low Fat Diet (LFD)		High Fat Diet (HFD)	
	Research diet D12450J		Research diet D12492	
	gram%	kcal%	gram%	kcal%
Protein	19.2	20	26.2	20
Carbohydrates	67.3	70	26.3	20
Fat	4.3	10	34.9	60
Total		100		100
Kcal/gm	3.85		5.24	
INGREDIENTS	**gram**	**kcal**	**gram**	**kcal**
Casein, 30 Mesh 200	200	800	200	800
L-Cystine	3	12	3	12
Corn starch	506.2	2024.8	0	0
Maltodextrin 10	125	500	125	500
Sucrose	68.8	275.2	68.8	275.2
Cellulose BW200	50	0	50	0
Soybean oil	25	225	25	225
Lard	20	180	245	2,205
Mineral mix S10026	10	0	10	0
Dicalcium phosphate	13	0	13	0
Calcium carbonate	5.5	0	5.5	0
Potassium citrate, 1 H_2O	6.5	0	6.5	0
Vitamin mix V10001	10	40	10	40
Choline bitartrate	2	0	2	0
FD&C yellow dye #5	0.04	0		
FD&C blue dye #1	0.01	0	0.05	0
TOTAL	1055.1	4,057	773.9	4057.0
Cholesterol (mg)/4057 kcal	–	54.4	–	216.4
Cholesterol (mg)/kg	–	51.6	–	279.6

As per manufacturer product data sheet (Research diet Inc., New Jersey, USA).

experimental group were as follows: vehicle-L ($n = 8$), vehicle-H ($n = 9$), Dox-L ($n = 10$), and Dox-H ($n = 9$).

Measurements, Blood Collection, and Tumor- and Fat Tissue Excision

Every second day, animals were weighed and tumor location and volume were recorded. The absolute body weight was calculated after subtracting tumor weight. Tumor growth was measured using a Harpenden caliper (in mm) to determine tumor volume using the following equation:

$$\textbf{Tumour Volume } \left(\textbf{mm}^3\right) = \frac{1}{2\left(\textbf{length} \times \textbf{width}^2\right)} \quad (26)$$

Animals were euthanised 72 h after the last scheduled doxorubicin administration. Mice were anesthetized under 3% isoflurane and sacrificed by cervical dislocation after a deep sleep was confirmed by the absence of pedal reflex. Whole blood was immediately collected into pediatric EDTA tubes (Lasec, Cape Town, South Africa) from the thoracic cavity. Collected blood samples were placed on ice and centrifuged (1,000 RCF (g), 10 min), to collect and aliquot plasma which was stored at −80°C for subsequent analysis. Mammary adipose tissue was collected from the third and fourth quadrant of the mice and tumor tissue were dissected, weighed, snap-frozen with liquid nitrogen and stored at −80°C or stored in formalin at room temperature for immunohistochemistry analysis.

Blood Analysis

Plasma samples were used to quantify TNF-α, IL-6, IL-10, leptin (PPX-04-MXCE327, Thermo Fisher Scientific, United States), IL-1β and vascular endothelial growth factor (VEGF-A) (PPX-02-MXFVKXT, Thermo Fisher Scientific, United States) using a custom ProcartaPlex panel and matched mouse Luminex kits. A Milliplex mouse adipokine magnetic bead panel MAP kit was used to quantify MCP-1, insulin, total plasminogen activator inhibitor-1 (PAI-1) and resistin (MADKMAG-71K, Burlington, Massachusetts, United States). All analyses were performed according to the manufacturers' protocols and specifications. Analytes were measured simultaneously using a MAGPIX system plate reader (APX1042, Bio-Rad, California, United States) and data (expressed in pg/ml) was processed on Bioplex Software 6.1 (Bio-Rad, California, United States).

Determination of Tissue Fatty Acid Profiles

For tumor tissue, FA composition of the total phospholipid (TPL) and the FFA fractions were determined, whereas for the mammary adipose tissue, the total lipid FA composition was determined. Frozen tumor tissue and mammary adipose tissue were allowed to thaw at room temperature. Approximately 100 mg of tumor tissue and 30 mg of adipose tissue were weighed for lipid extraction using chloroform:methanol (C:M; 2:1; v:v; Sigma-Aldrich, St. Louis, Missouri, United States) according to a method adapted from Folch et al. (27) as previously described by Hon et al. (28). The extraction solvent contained 0.01% butylated hydroxytoluene (Sigma-Aldrich, St. Louis, Missouri, United States), acting as an antioxidant.

Briefly, lipids of tumor tissue were extracted with 9 mL of C:M (2:1; v:v) by homogenisation for 1 min using a Polytron® PT-MR 3100D homogeniser (Kinematica, Luzern, Switzerland). The homogenate was filtered through a sintered glass funnel with the filter pad lined with a glass microfiber filter disk (GF/A, Whatman, England) into a round bottom flask. The Polytron® shaft was rinsed with another 7 mL of the extracting solvent and filtered, collecting the rinse into a round bottom flask. The microfiber filter disk containing the homogenized tissue was removed and placed into an extraction tube and extracted again with 10 mL C:M (2:1; v:v) by 20-min shaking and a filtering step (repeated twice). The combined extraction phases containing the lipids were concentrated to dryness through rotary evaporation in a 37°C water bath (BÜCHI Labortechnik, Postfach, Switzerland). Lipids were transferred from the round bottom flask to a 12 mL glass tube with screw cap using 5 × 2 mL chloroform:methanol:saline (CMS; 86:14:1; v:v:v; Sigma-Aldrich) transfer volumes. Saline saturated with CMS (1 mL) was added, mixed and centrifuged, and the top saline layer was completely removed in order to concentrate the bottom phase to dryness under nitrogen gas flow in a 37°C water bath.

Neutral lipids were separated from the TPL fraction using thin-layer chromatography (TLC) silica gel 60 plates (10 × 10 cm;

No. 1.05626.0001; Merck, Darmstadt, Germany) and eluted with the solvent system petroleum ether (B&M Scientific, Cape Town, South Africa):diethyl ether (Merck):acetic acid (Merck) (90:30:1; v:v:v). The lipid bands containing the TPL and FFA fractions were demarcated by visualization under long-wave UV light after plates were sprayed with C:M (1:1; v:v) containing 2,5-bis-(5′-tert-butylbenzoxazolyl-[2′]) thiophene (10 mg/100 mL; Sigma-Aldrich). These lipid bands were scraped off the plates into glass tubes with screw caps. The lipids were trans-esterified through trans-methylation with 2 mL methanol:sulphuric acid (H2SO4; BDH Chemicals, Poole, England) (95:5; v:v) at 70°C for 2 h to yield FA methyl esters (FAMEs). After cooling, the FAMEs were extracted with distilled water (1 mL) and n-hexane (3 mL) (Sigma-Aldrich). The upper hexane layer containing the FAMEs was collected and evaporated to dryness for subsequent gas-liquid chromatography (GLC) analysis.

Total lipids were extracted from mammary adipose tissue with 9 mL C:M (2:1; v:v) by shaking for 20 min with a mechanical shaker. Subsequently, 1.8 mL saline saturated with CMS was added, mixed and centrifuged at 60 RCF (g) for 10 min at 4°C. The bottom phase was collected and transferred to a 12 mL glass tube with a screw cap and the lipid extract evaporated to dryness under nitrogen gas flow using a 37°C water bath. The dried lipids were re-dissolved in 3 mL C:M (2:1; v:v) of which a 50 μL aliquot was transferred to a clean 12 mL glass tube and the lipid aliquot was evaporated to dryness as described before. These lipids were trans-methylated with 2 mL methanol:sulphuric acid (70°C for 2 h) with subsequent sample FAME isolation for GLC analysis as described above.

All FAMEs were re-dissolved in n-hexane and analyzed (sample injection volume 1 μl) by GLC on a Finnigan Focus Gas Chromatograph (Thermo Electron Corporation, Austin, TX, USA) equipped with a flame-ionization detector and a 30 m capillary column of 0.32 mm internal diameter (BPX70 0.25 μm; SGE International, Ringwood, Victoria, Australia). Gas flow rates were: N2 (make up gas), 25 mL/min; synthetic air, 250 mL/min; and H2 (carrier gas), 25 mL/min, with a 20:1 split ratio. Oven temperature programming was linear at 4.5°C/min, initial temperature 140°C (hold-time 1 min), final temperature 220°C (hold-time 5 min), injector temperature 220°C, and detector temperature 250°C [as previously described (29)].

All sample FAMEs were subsequently identified by analyzing and comparing sample retention times with those a known standard FAME mixture (27 FAMEs, NuChek Prep, Elysian, MN, USA). Relative percentages of each individual FAME was calculated by determining the area count of a specific FAME as a percentage of the total area count of all FAMEs identified in the sample. Estimated desaturase indexes were estimated by product to precursor FA ratios which included stearoyl CoA-desaturase-1 (SCD1)-16 calculated as the ratio of palmitoleic acid (PTA) to palmitic acid (PA) and SCD1-18 calculated as the ratio of oleic acid (OA) to stearic acid (SA) (30, 31).

Protein Analysis and Western Blot Analysis

Mammary adipose tissue and tumor tissue samples were placed on ice and allowed to thaw at 4°C. Total protein extraction was performed where samples were suspended in 300 μl of cold modified radio-immunoprecipitation (RIPA) assay buffer containing protease and phosphatase inhibitors (2.5 mM Tris-HCL, 0.1 mM phenylmethylsulfonyl fluoride, 10 mg/ml leupeptin, 1 mM EDTA, 1 mM benzamidine, 50 mM sodium fluoride, 1 mM dithiothreitol, 4 mg/ml soybean trypsin inhibitor, 0.1% sodium dodecyl sulfate (SDS), 0.5% sodium deoxycholate, and 1% NP-40, pH 7.4). Samples were homogenized on ice under sterile conditions to prevent protein cross-contamination. Next, all samples were centrifuged (35,000 RCF (g), 60 min, 4°C), to yield distinct layers. The supernatant layer was removed using a sterile 23-gauge needle and syringe and transferred into sterile Eppendorf tubes, followed by another centrifugation step (35,000 RCF (g), 30 min, 4°C). The process of removing the supernatant was repeated and samples were run through Amicon® Ultra 0.5 mL filters (Merck, Darmstadt, Germany) for protein purification and concentration and stored at −80°C, until protein quantification using a Direct Detect® infrared spectrometer (DDHW00010-WW, Merck). This was followed by preparation of protein aliquots containing 20–50 μg protein diluted with Laemmli sample buffer and boiled for 5 min (to denature proteins) before being loaded into 4–15% polyacrylamide fast cast gels (mini-PROTEAN® TGX™ Gels, Bio-Rad) for separation by sodium dodecyl sulfate polyacrylamide gel electrophoresis (SDS-PAGE). Gels were run at 100 V (constant) and 400 mA for approximately 60 min (Power Pac 300, BioRad). The electro-transfer of proteins from the gel to prepared polyvinylidene fluoride (PVDF) membranes was achieved using a semi-dry electro-transfer system (TransBlot® Turbo™ v1.02, BioRad) for 30 min at 25 V and 1.0 A. Transfer efficiency was evaluated using the stain-free blot protocol provided on a Chemi-Doc™ MP (BioRad) system. Subsequently, all membranes were washed with 0.1% Tris Buffered Saline-Tween 20 (TBS-T) and blocked for 60 min in 5% (w/v) non-fat milk and TBS-T at room temperature to prevent non-specific binding. The PVDF membranes were then incubated overnight in primary antibody solutions (1:1,000, diluted in 5% w/v BSA, 1X TBS-T, refer to **Supplementary Table 2**) at 4°C. The following day, membranes were washed three times for 5 min each with TBS-T, prior to incubation with an anti-rabbit IgG horseradish peroxidase conjugated secondary antibody (1:10,000) (Cell Signaling Technologies, Massachusetts, United States), for 60 min at room temperature. A wash step followed, using TBS-T (five times for 5 min each), before specific bands were visualized and detected using the enhanced chemiluminescence (ECL) western blotting substrate detection kit (Pierce®, Thermo Scientific) and ImageLab 4.0 software on a Chemi-Doc™ MP (BioRad) imaging system. Protein quantification of samples were normalized to total protein signal in each lane present on the same membrane after blotting (ImageLab 4.0 software, Biorad USA), as determined by the Stain-Free™ (ImageLab 4.0 software, Biorad USA) properties of the blot and is expressed as a percentage of the control.

Haematoxylin and Eosin Stained Tumor Tissue

Sectioning, deparaffinization and rehydration of tumor tissue samples was performed as previously described (32). Tumor tissue samples were stained for histological

changes using haemotoxylin and eosin (H&E) staining. Staining was achieved by using an automated tissue stainer (Leica Biosystems, ST4020), during which section slides where dipped into haemotoxylin. This was followed by various subsequent 2-min dipping steps in distilled water, scott's tap water, distilled water, eosin and distilled water followed by coverslips being mounted using DPX mounting media.

Statistical Analysis

Statistical analyses were performed using Statistica version 13.3 (TIBCO Software, California, United States). Normality was assessed using the Shapiro-Wilk test and results were reported as mean ± standard error of the mean (SEM). To describe differences between two groups, *t*-tests were used, and to describe differences between the three/more groups two- or three-way ANOVA were used, followed by the Fisher's LSD *post-hoc* test. Pearson's correlations were used on selected parameters in each group and 2D scatter plots were drawn up in GraphPad Prism version 7 (GraphPad Software, San Diego, United States). Statistical significance was accepted at $p < 0.05$.

RESULTS

A High Fat Diet Increased Body Weight and Mammary Adipose Tissue Weight

Body Weight and Food Consumption

During the DIO period, mice that were fed the HFD showed significantly higher body weights at week 6 ($p < 0.01$), week 7 ($p < 0.001$) and week 8 ($p < 0.0001$), compared to the LFD group (**Figure 2A**), therefore DIO was established after 8 weeks. It was also observed that mice fed a HFD showed significantly lower food consumption per cage at week 2 ($p < 0.001$), 3 ($p < 0.01$) and 4 ($p < 0.05$) compared to the LFD group (**Figure 2B**).

Following tumor induction, mice in the vehicle-H group showed significantly higher body weight compared to vehicle-L mice during week 8–12 (all $p < 0.001$) (**Figure 3A**). A similar and statistically significant observation was made for body weight of mice in the Dox-H group, when compared to Dox-L mice at week 8–12 (all $p < 0.01$) (**Figure 3A**). The Dox-H mice also showed significantly lower food consumption compared to the vehicle-H mice at week 8 ($p < 0.0001$), 9 ($p < 0.0001$), 10 ($p < 0.001$), 11 ($p < 0.001$), and 12 ($p < 0.0001$) (**Figure 3B**). Lastly, the Dox-H mice revealed significantly lower food consumption than the

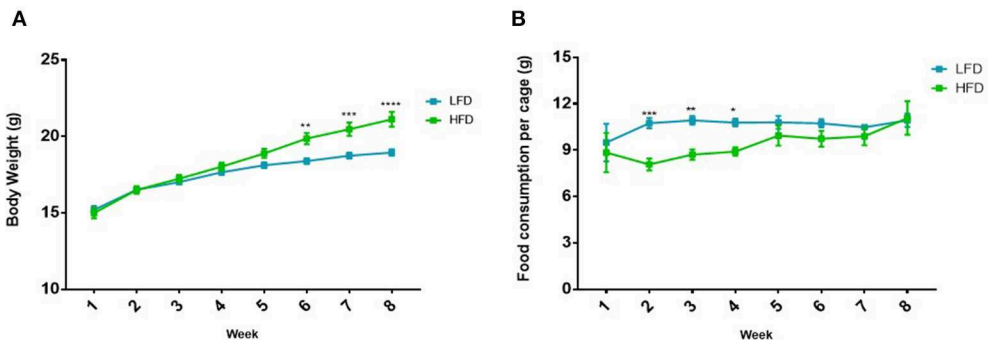

FIGURE 2 | Difference in **(A)** body weight and **(B)** food consumption in mice ($n = 5$ per cage) on the LFD and HFD for 8 weeks. Results are presented as mean ± SEM ($n = 20$ per group). *T*-tests were used for comparison between the LFD and the HFD mice for all weeks and $p < 0.05$ was considered as statistically significant. $^{*}p < 0.05$, $^{**}p < 0.01$, $^{***}p < 0.001$ and $^{****}p < 0.0001$.

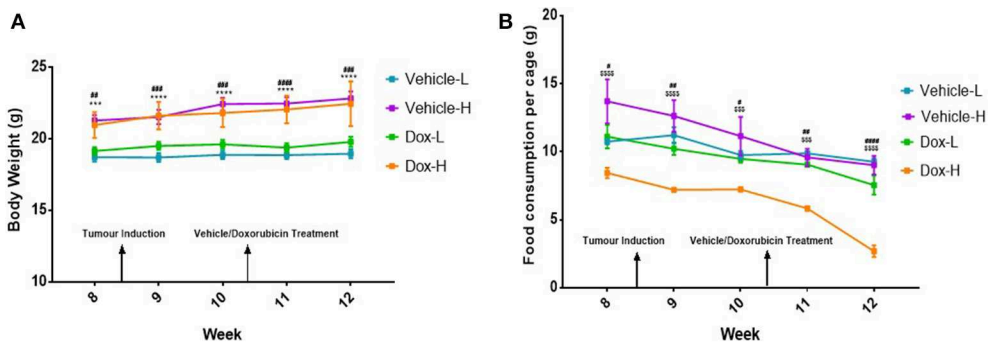

FIGURE 3 | (A) Mean body weight, and **(B)** food consumption of mice ($n = 5$ per cage) receiving vehicle-or doxorubicin treatment while on the LFD control compared to the HFD. Results are presented as mean ± SEM ($n = 10$ per group). Three-way ANOVA with Fisher's LSD *post hoc* correction was applied and $p < 0.05$ was considered as statistically significant. $^{***}p < 0.001$ and $^{****}p < 0.0001$. $^{\#}p < 0.05$, $^{\#\#}p < 0.01$, $^{\#\#\#\#}p < 0.0001$, $^{\$\$\$}p < 0.001$ and $^{\$\$\$\$}p < 0.0001$. *Vehicle-L vs. Vehicle-H, $^{\#}$Dox-L vs. Dox-H, and $^{\$}$Vehicle-H vs. Dox-H.

Dox-L mice at week 8 ($p < 0.05$), 9 ($p < 0.01$), 10 ($p < 0.05$), 11 ($p < 0.01$), and 12 ($p < 0.0001$) (**Figure 3B**).

Mammary Adipose- and Tumor Tissue Weight

The vehicle-H mice showed significantly higher mammary adipose tissue weight ($p < 0.01$) and tumor weight ($p < 0.05$) in comparison to the vehicle-L mice (**Figures 4A,B**). Mice in the Dox-H group presented with significantly higher mammary adipose tissue weight ($p < 0.05$) as well as tumor weight ($p < 0.01$) compared to Dox-L mice (**Figures 4A,B**).

Diet-Induced Obesity Decreased Doxorubicin Treatment Efficacy in Breast Tumors

Mice in the vehicle-H group showed significantly higher tumor volume compared to corresponding vehicle-L mice at day 18 ($p < 0.05$), 19 ($p < 0.05$), 20 ($p < 0.01$), 21 ($p < 0.001$), 22 ($p < 0.01$), 23 ($p < 0.01$), 24 ($p < 0.05$), 25 ($p < 0.01$), 26 ($p < 0.0001$), and 27 ($p < 0.0001$), as illustrated in **Figure 5**.

Similarly, mice in the Dox-H group showed significantly higher tumor volume compared to corresponding mice from the Dox-L group, at day 21 ($p < 0.05$), 23 ($p < 0.05$), 24 ($p < 0.001$), 25 ($p < 0.01$), 26 ($p < 0.0001$), and 27 ($p < 0.0001$) (**Figure 5**). Dox-L mice also had significantly lower tumor volumes at day 27 compared to vehicle-L mice ($p < 0.01$), and Dox-H mice yielded significantly lower tumor volume at day 26 ($p < 0.05$) and 27 ($p < 0.01$) compared to the vehicle-H mice (**Figure 5**).

Diet-Induced Obesity Induced Systemic Inflammation and Local Inflammatory Signaling in Mammary Adipose Tissue of Obese Mice Treated With Doxorubicin

A trend toward significance was observed for IL-6 in Dox-H mice compared to vehicle-H mice ($p = 0.067$, **Figure 6A**). Leptin

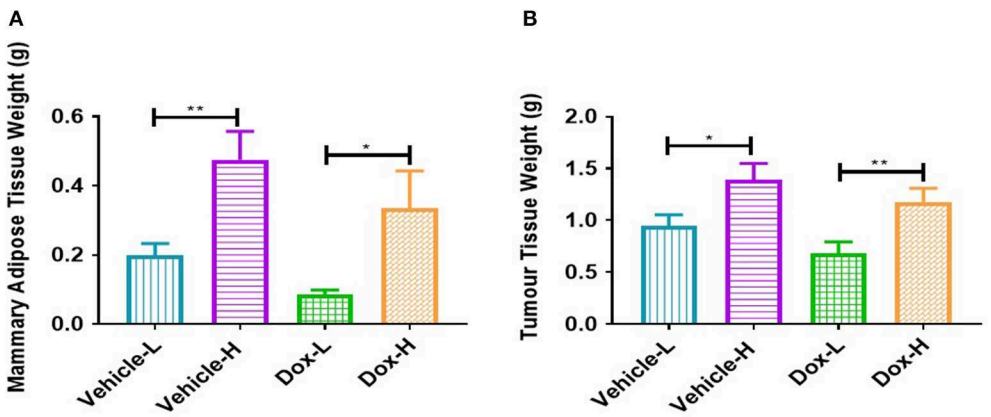

FIGURE 4 | Differences in **(A)** mammary adipose tissue weight, and **(B)** tumor weight of vehicle- and doxorubicin-treated groups on LFD control compared to HFD. Results are presented as mean ± SEM ($n = 9$–10 per group). Two-way ANOVA with Fisher's LSD *post hoc* correction were applied. $^{*}p < 0.05$, $^{**}p < 0.01$.

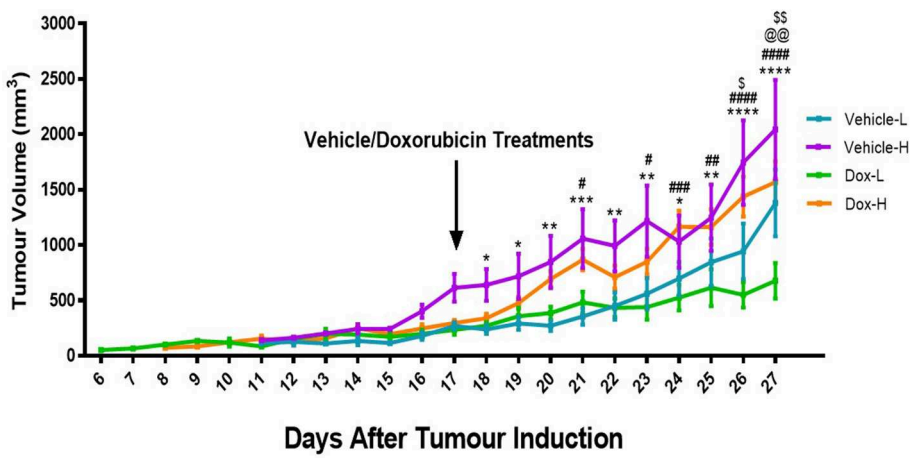

FIGURE 5 | Differences in tumor volume for the vehicle control and doxorubicin treatment groups on LFD and HFD. Results are presented as mean ± SEM ($n = 10$ per group). Three-way ANOVA with Fisher's LSD *post hoc* correction was applied and $p < 0.05$ was considered as statistically significant. $^{*}p < 0.05$, $^{**}p < 0.01$, $^{***}p < 0.001$, and $^{****}p < 0.0001$. $^{\#}p < 0.05$, $^{\#\#}p < 0.01$, $^{\#\#\#}p < 0.001$, and $^{\#\#\#\#}p < 0.0001$, $^{\$}p < 0.05$. $^{\wedge}$Vehicle-L vs. Vehicle-H, $^{\#}$Dox-L vs. Dox-H, $^{@}$Vehicle-L vs. Dox-L, $^{\$}$Vehicle-H vs. Dox-H. $^{@@}p < 0.01$, $^{\$\$}p < 0.01$.

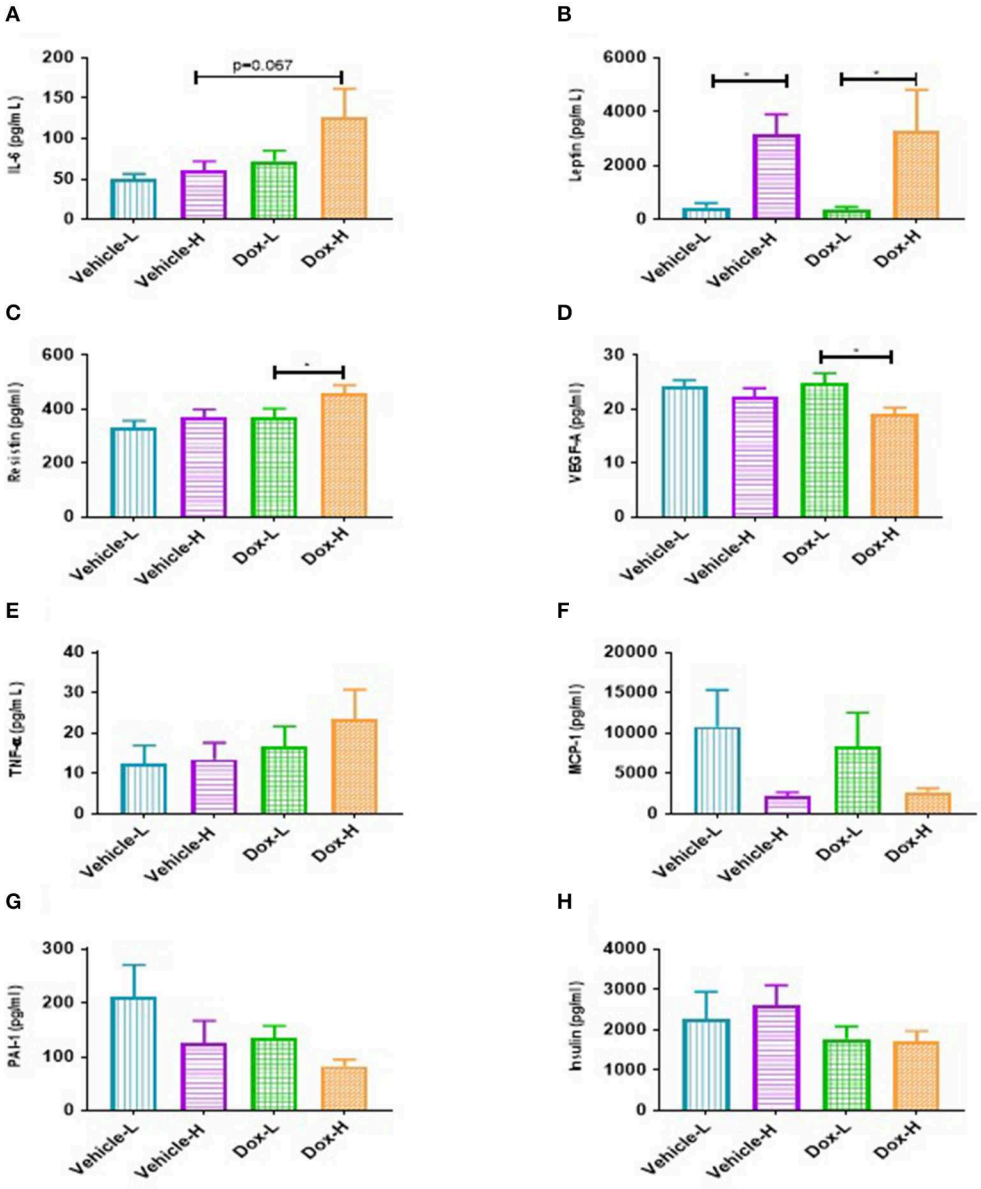

FIGURE 6 | Mean inflammatory marker concentrations for vehicle control and doxorubicin treatment groups on LFD and HFD. **(A)**, IL-6 **(B)** Leptin, **(C)** Resistin, **(D)** VEGF-A, **(E)** TNF-α, **(F)** MCP-1, **(G)** PAI-1, and **(H)** Insulin. Results are presented as mean ± SEM ($n = 6$–9). Two-way ANOVA with Fisher's LSD *post hoc* correction was employed and $p < 0.05$ was considered as statistically significant. *$p < 0.05$.

levels were significantly higher in vehicle-H compared to vehicle-L mice ($p < 0.05$, **Figure 6B**) and Dox-H compared to Dox-L mice ($p < 0.05$, **Figure 6B**), respectively. Mice in the Dox-H group showed significantly higher resistin ($p < 0.05$, **Figure 6C**) and decreased VEGF-A levels ($p < 0.05$, **Figure 6D**) compared to Dox-L mice. No significant differences were reported for TNF-α (**Figure 6E**), MCP-1 (**Figure 6F**), PAI-1 (**Figure 6G**), and insulin (**Figure 6H**) between any of the respective experimental groups. Interleukin-10 and IL-1β were undetectable within all samples of all the experimental groups.

Pearson's correlation analysis revealed some positive correlations between leptin and mammary adipose tissue weight (**Supplementary Figure 1**). Significant strong positive correlations were only observed for the doxorubicin treatment groups (Dox-L, $r = 0.78$, $p < 0.01$, and Dox-H, $r = 0.92$, $p = 0.001$; **Supplementary Figures 1C,D**).

Lastly, Dox-H mice showed significantly higher protein expression of nuclear factor kappa B (NFκB-p65) compared to both Vehicle-H ($p < 0.01$) and Dox-L ($p < 0.05$) mice, respectively (**Figure 7A**).

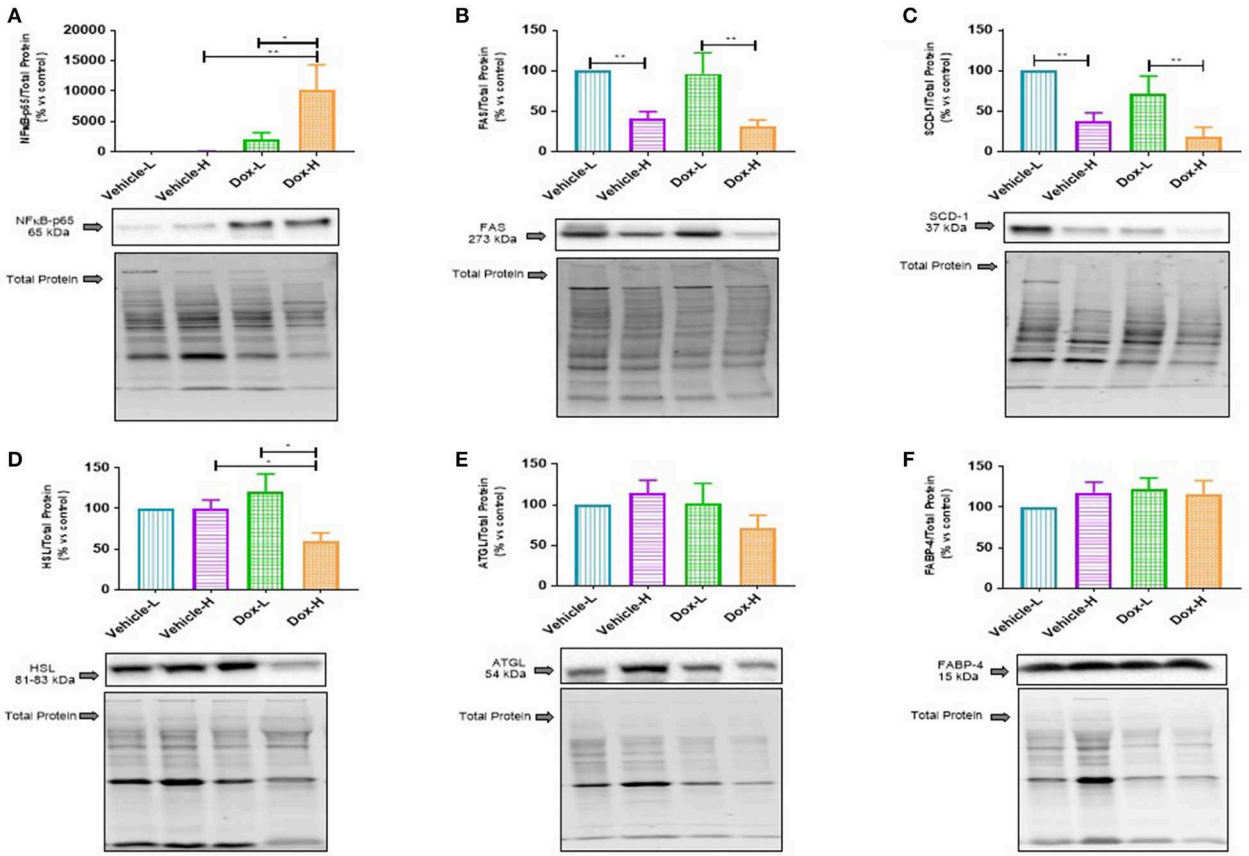

FIGURE 7 | Western blot analysis of lipid metabolism marker protein expression in mammary adipose tissue of vehicle control and doxorubicin treatment groups on LFD and HFD; **(A)** NFκB-p65, **(B)** FAS, **(C)** SCD-1, **(D)** HSL, **(E)** ATGL, and **(F)** FABP4. Results are presented as mean ± SEM ($n = 6$–8). Two-way ANOVA with Fisher's LSD *post hoc* correction was employed and $p < 0.05$ was considered as statistically significant. $^{*}p < 0.05$, $^{**}p < 0.01$.

Diet-Induced Obesity and Doxorubicin Treatment Suppressed *De novo* Lipogenesis and Lipolysis in Mammary Adipose Tissue

Fatty acid synthase (FAS) and sterol CoA-desaturase-1 (SCD-1) were found to be significantly decreased in the vehicle-H mice, compared to vehicle-L mice (FAS, $p < 0.01$ and SCD-1, $p < 0.01$ **Figures 7B,C**) and Dox-H mice compared to Dox-L mice (FAS, $p < 0.01$, and SCD-1, $p < 0.01$ **Figures 7B,C**), respectively. Moreover, hormone-sensitive lipase (HSL) was significantly decreased in Dox-H compared to both vehicle-H ($p < 0.05$, **Figure 7D**) and Dox-L mice ($p < 0.05$, **Figure 7D**). No significant differences were observed for adipose triglyceride lipase (ATGL) (**Figure 7E**) and fatty acid binding protein 4 (FABP4) (**Figure 7F**), between any of the respective experimental groups ($p > 0.05$).

Diet-Induced Obesity Increased *De novo* Lipogenesis and Lipolysis in Breast Tumors Treated With Doxorubicin

Dox-H mice showed a significant increase in the protein expression of SCD-1 and ATGL compared to vehicle-H (SCD-1, $p < 0.05$ and ATGL, $p < 0.01$) and Dox-L mice (SCD-1, $p < 0.05$ and ATGL, $p < 0.01$), in tumor tissue (**Figures 8A,B**). Pearson's correlation analysis showed a significantly strong negative correlation between mammary adipose tissue HSL protein expression and plasma resistin concentration in the Dox-H group ($r = -0.73$, $p < 0.05$; **Supplementary Figure 2D**).

Mammary Adipose- and Tumor Tissue Fatty Acid Composition

Fatty acids for both mammary adipose (total lipid) and tumor tissue (TPL) are summarized in **Supplementary Tables 3, 4**, and a select few FAs are presented in graphs. The predominant FA classes in mammary adipose tissue were monounsaturated FAs (MUFAs) ranging from 43 to 51%, followed by SFAs (27–30%) and polyunsaturated FAs (PUFAs; 21–27%) in the treatment groups (**Supplementary Figure 3**). In the tumor tissue TPL fraction the predominant FA classes were SFAs ranging from 40 to 43%, followed by PUFAs (32–38%) and MUFAs (19–28%) in all the experimental groups (**Supplementary Figure 4**).

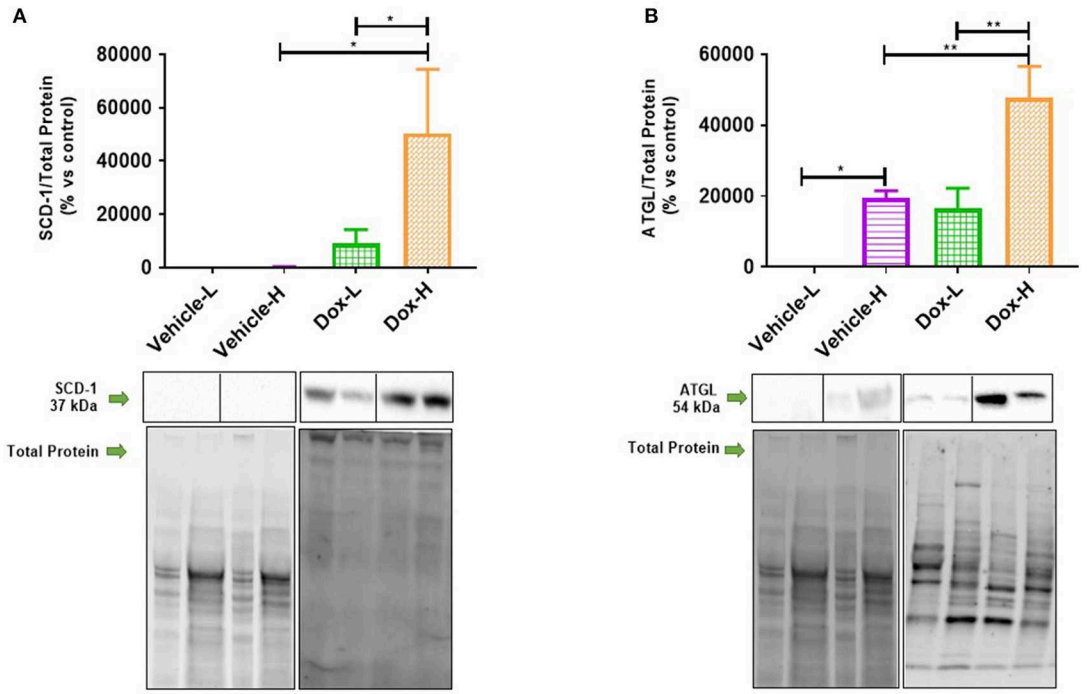

FIGURE 8 | Western blot analysis of lipid metabolism protein expression in tumor tissue of vehicle control and doxorubicin treatment groups on LFD and HFD; **(A)** SCD-1 ($n = 5$) and **(B)** ATGL ($n = 4$). Results are presented as mean ± SEM. Two-way ANOVA with Fisher's LSD *post hoc* correction was applied and $p < 0.05$ was considered as statistically significant. $^{*}p < 0.05$, $^{**}p < 0.01$.

Diet-Induced Obesity and Doxorubicin Differentially Altered Saturated Fatty Acids in the Tumor Microenvironment

Total SFAs (Σ SFAs) present in the tumor phospholipid fraction was significantly higher in vehicle-H compared to vehicle-L mice ($p < 0.0001$) and higher in Dox-H compared to Dox-L mice ($p < 0.0001$) (**Figure 9A**). In mammary adipose tissue, myristic acid (MA, C14:0) was significantly lower in the vehicle-H mice compared to vehicle-L ($p < 0.0001$) and lower in vehicle-L compared to Dox-L mice ($p < 0.001$), respectively (**Figure 9B**). Myristic acid was also significantly lower in the Dox-H mice compared to Dox-L mice in tumor tissue ($p < 0.05$; **Figure 9B**). Stearic acid (SA, C18:0) was significantly higher in vehicle-H mice compared to vehicle-L ($p < 0.0001$) in mammary adipose tissue. In addition, SA was also found to be significantly higher in the Dox-H mice compared to Dox-L mice ($p < 0.0001$; **Figure 9C**). The tumor tissue SA percentage was also higher in vehicle-H compared to vehicle-L mice ($p < 0.0001$) and higher in Dox-H compared to Dox-L mice ($p < 0.0001$), respectively (**Figure 9C**).

Diet-Induced Obesity and Doxorubicin Suppressed Monounsaturated Fatty Acids in the Tumor and in Surrounding Mammary Fat

A similar and significant trend was observed for various MUFAs in both mammary adipose tissue and tumor phospholipid FAs. The total MUFAs (Σ MUFAs) and palmitoleic acid (PTA, C16:1n-7) were significantly lower in vehicle-H compared to vehicle-L mice and significantly lower in Dox-H compared to Dox-L mice, respectively (all $p < 0.0001$, **Figures 10A,B**). In tumor tissue, oleic acid (OA, C18:1n-9) was significantly lower in vehicle-H vs. vehicle-L and Dox-H vs. Dox-L mice, respectively ($p < 0.0001$, **Figure 10C**).

Diet-Induced Obesity and Doxorubicin Selectively Increased Polyunsaturated Fatty Acids in the Tumor Microenvironment

The total n-6 PUFAs (Σ n-6 PUFAs), linoleic acid (LA, C18:2n-6) and eicosadienoic acid (EDA, C20:2n-6), were significantly higher in the mammary adipose tissue of vehicle-H compared to vehicle-L mice (Σ PUFAs, $p < 0.0001$, LA, $p < 0.0001$, EDA, $p < 0.0001$), and higher in Dox-H than Dox-L mice, respectively (Σ n-6 PUFAs, $p < 0.0001$, LA, $p < 0.0001$, EDA, $p < 0.0001$; **Figure 11**). Similar results were observed in the tumor tissue total phospholipid FA fraction i.e., higher Σ n-6 PUFAs, LA, EDA and adrenic acid (ADA, C22:4n-6) levels in vehicle-H compared to vehicle-L mice (Σ n-6 PUFAs, $p < 0.0001$, LA, $p < 0.0001$, EDA, $p < 0.0001$, and ADA, $p < 0.0001$) as well as higher percentages of these FAs in Dox-H compared to Dox-L mice (**Figure 11**).

Haematoxylin and Eosin Stained Tumors

Necrotic regions were detected in the tumor sections from the vehicle-L mice. Necrosis was identified by cells with pale

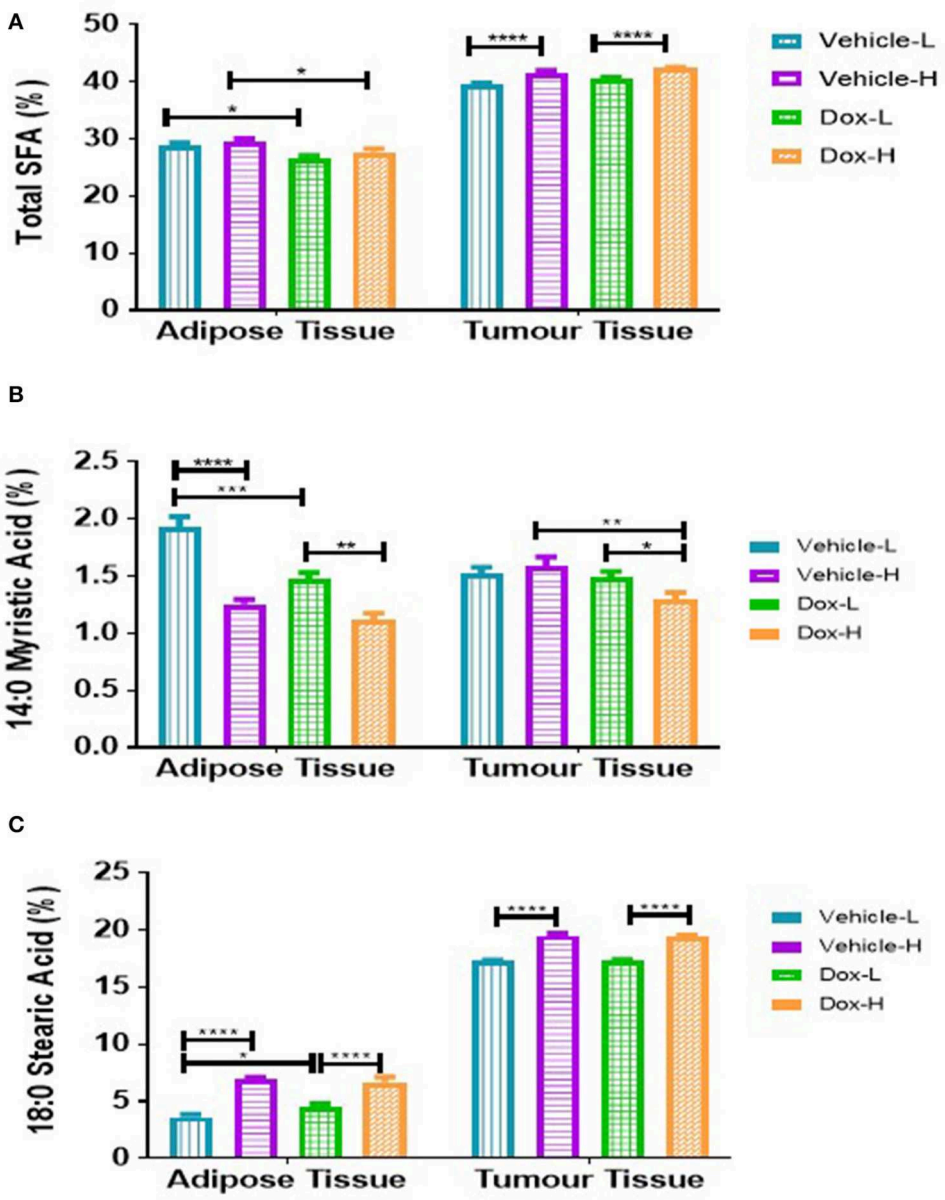

FIGURE 9 | Saturated fatty acid composition; **(A)** Total SFA, **(B)** Myristic Acid, and **(C)** Stearic Acid of mammary adipose- and tumor tissue of mice fed a LFD or HFD with either vehicle control or doxorubicin treatment. Results are presented as mean ± SEM ($n = 5$). Two-way ANOVA with Fisher's LSD *post hoc* correction was applied and $p < 0.05$ was considered as statistically significant. *$p < 0.05$, **$p < 0.01$, ***$p < 0.001$ and ****$p < 0.0001$.

pink cytoplasm and areas of karyorrhectic debris (**Figure 12A**). Necrosis was also detected in the tumors from the HFD vehicle treated mice. Viable tumor cells demonstrated hyperchromatic nuclei with coarse chromatin (**Figure 12B**). Tumors from both the LFD and HFD vehicle mice demonstrated hyper- and hypocellular regions and central areas of necrosis. Tumor sections from the Dox-L mice resembled those of the vehicle-L treated mice. In addition, multinucleated tumor cells were also noted (**Figure 12C**). Sections from Dox-H mice had a similar appearance (**Figure 12D**).

DISCUSSION

Diet-Induced Obesity Significantly Decreased Doxorubicin Treatment Efficacy in Breast Tumors

Similar to previous findings (33–35) we successfully establish weight gain in our animal model. Body weight of animals in the HFD group was significantly higher than those in the LFD group, before (**Figure 2A**) and after tumor induction irrespective of treatment (**Figure 3A**), which was corroborated

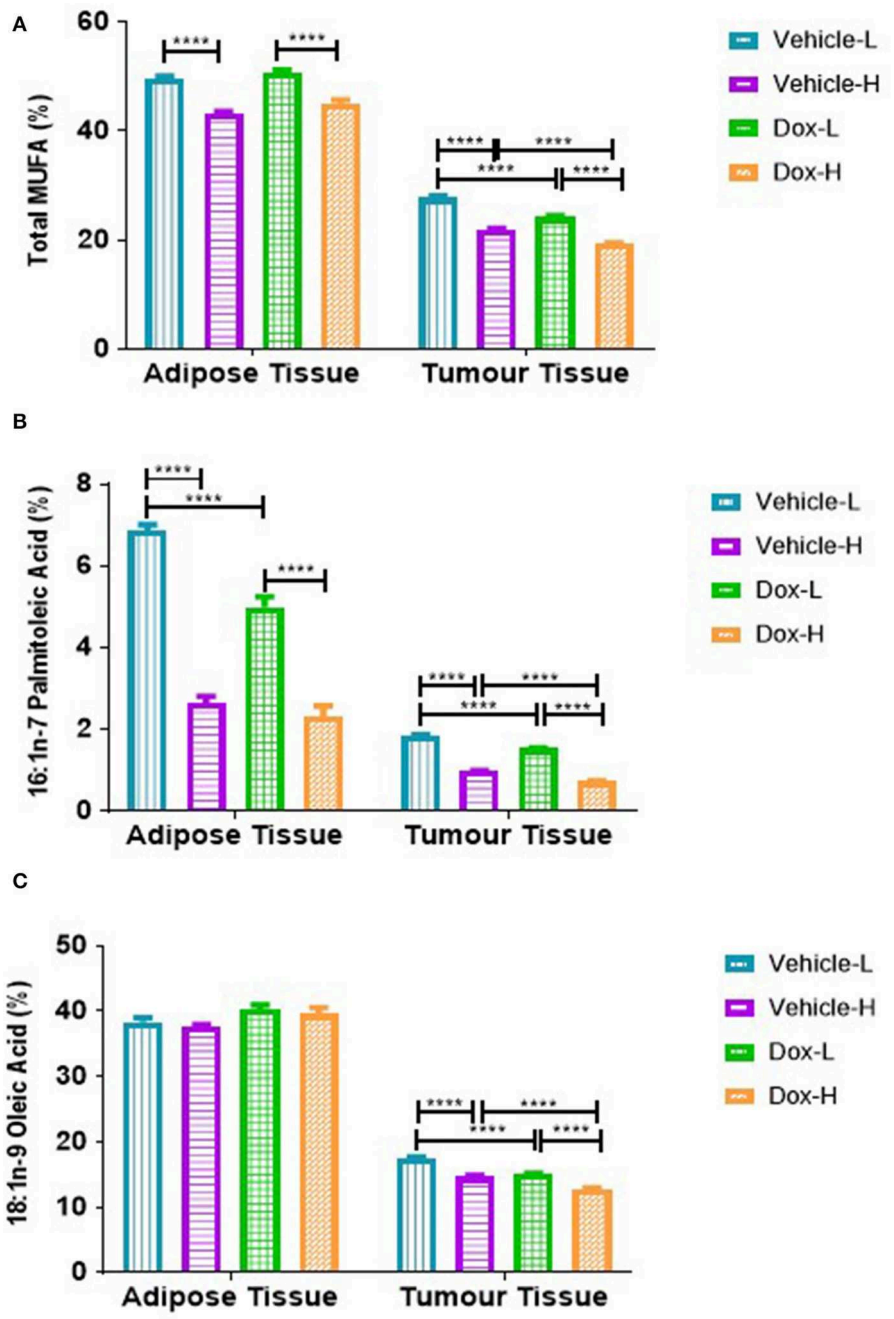

FIGURE 10 | Monounsaturated fatty acid composition; **(A)** Total MUFAs, **(B)** Palmitoleic Acid and **(C)** Oleic acid of mammary adipose- and tumor tissue of mice fed a LFD or HFD diet with either vehicle control or doxorubicin treatment. Results are presented as mean ± SEM ($n = 5$). Two-way ANOVA with Fisher's LSD *post hoc* correction was applied and $p < 0.05$ was considered as statistically significant. ****$p < 0.0001$.

by mammary adipose tissue weight. As expected, the Dox-H mice had significantly lower food consumption compared to vehicle-H mice (**Figure 3B**), which can be as a result of a well-known side-effect of doxorubicin treatment (36), however while the loss of appetite was visible, this had no effect on body weight. Furthermore, we reported a significantly higher volume (**Figure 5**) and weight (**Figure 4B**) of tumors in the vehicle-H mice and in the Dox-H mice. This is in agreement with previous studies reporting that DIO promoted tumor growth. For example, Lautenbach et al. (37), observed that female obese Sprague Dawley rats (HFD, 60% energy from fat for 8 weeks) were more susceptible to tumor induction by

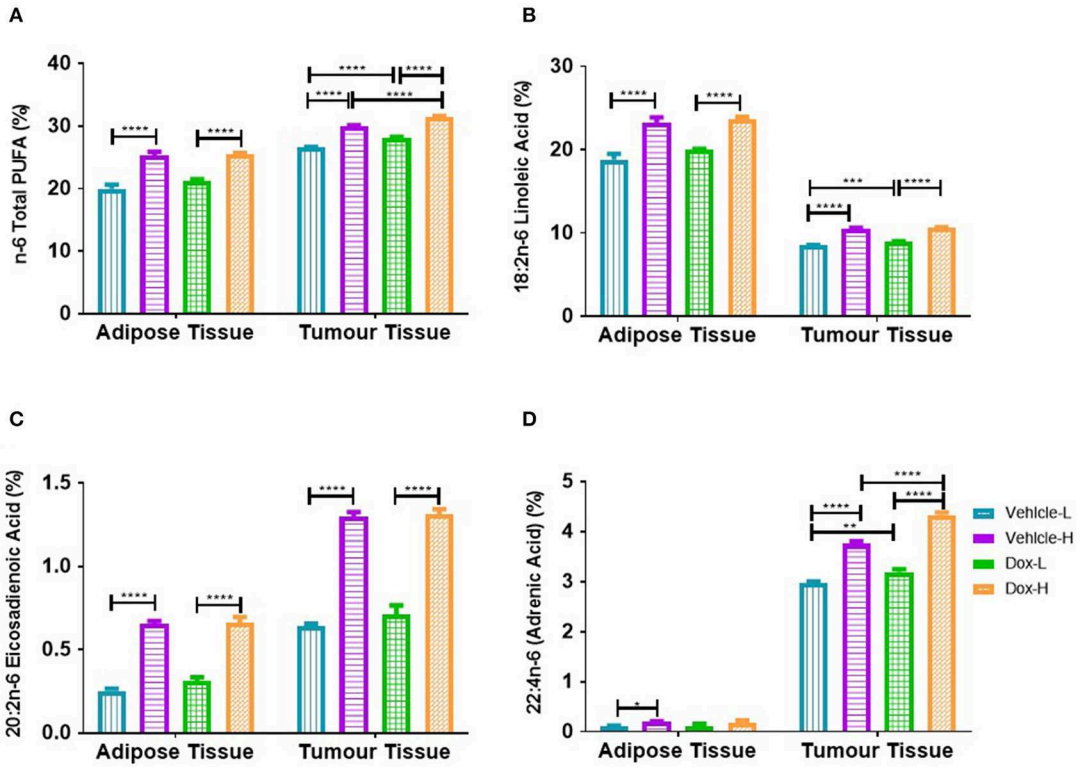

FIGURE 11 | Polyunsaturated fatty acid composition; **(A)** Total n-6 PUFAs, **(B)** Linoleic Acid, **(C)** Eicosadienoic Acid, and **(D)** Adrenic Acid of mammary adipose-and-tumor tissue of mice fed a LFD or HFD with either vehicle control or doxorubicin treatment. Results are presented as mean ± SEM ($n = 5$). Two-way ANOVA with Fisher's LSD *post hoc* correction was applied and $p < 0.05$ was considered as statistically significant. *$p < 0.05$, **$p < 0.01$, ***$p < 0.001$ and ****$p < 0.0001$.

dimethylbenzathracene and also showed increased tumor growth compared to controls. This was corroborated by Khalid et al. (38), who found that a HFD (45% energy from fat) significantly increased body weight and fat mass compared to mice on a LFD (10% energy from fat) in a MMTV-HER2/Neu transgenic breast cancer model, and that obesity promoted tumor growth, reflected by an increase in tumor size. Additionally, Cowen et al. (39) reported a higher body weight in female MMTV-PyMT mice on a HFD (35.7% energy from fat) compared to mice on a LFD (10% energy from fat), even after adjusting for tumor weight and tumor volume. Others reported that DIO promotes tumor growth, progression, and metastasis in animal models (40, 41), specifically in breast cancer (16, 17, 33). In addition, poor treatment outcomes are also reported in overweight and obese breast cancer patients evident by larger tumor sizes and poor clinical outcomes (7, 18, 42, 43) especially those treated with doxorubicin (42, 44). It was also reported that DIO decreased the efficacy of breast cancer treatment protocols in pre-clinical animal models (33, 45).

Inflammatory Markers: Diet-Induced Obesity Induces Systemic and Mammary Fat Inflammation

Leptin was significantly increased in both the vehicle-H and Dox-H groups compared to the respective control LFD groups (**Figure 6C**). Leptin concentrations also correlated positively with mammary adipose tissue weight (**Supplementary Figure 1**). These results indirectly implicate mammary adipose tissue, specifically adipocytes in the tumor microenvironment as a source of leptin secretion in obese mice, which also showed greater mammary adipose weight (**Figure 4A**). Since E0771 breast cancer cells have been shown not to produce leptin, even when co-cultured with adipocytes, it therefore does not significantly contribute to increased leptin levels (34). The increased mammary adipose tissue weight as a result of the HFD could possibly be one of the primary sources of leptin in our study. We also reported that the resistin concentrations were significantly increased in Dox-H compared to Dox-L mice (**Figure 6D**).

Obesity is well-known to increase various pro-inflammatory adipokine concentrations in serum and plasma as well as adipose tissue (34, 46), whereas mRNA expression levels showed that adipocytes co-cultivated with breast cancer cells also had significantly higher IL-6, IL-1β, and TNF-α levels (7). It has previously been shown that these elevated circulating cytokines (i.e., IL-6 and IL-8) exerted effects at distant sites (47, 48), this favors the progression of breast cancer by upregulating the secretion of pro-inflammatory adipokines as well as exacerbates immune cell infiltration, which in turn promoted cancer

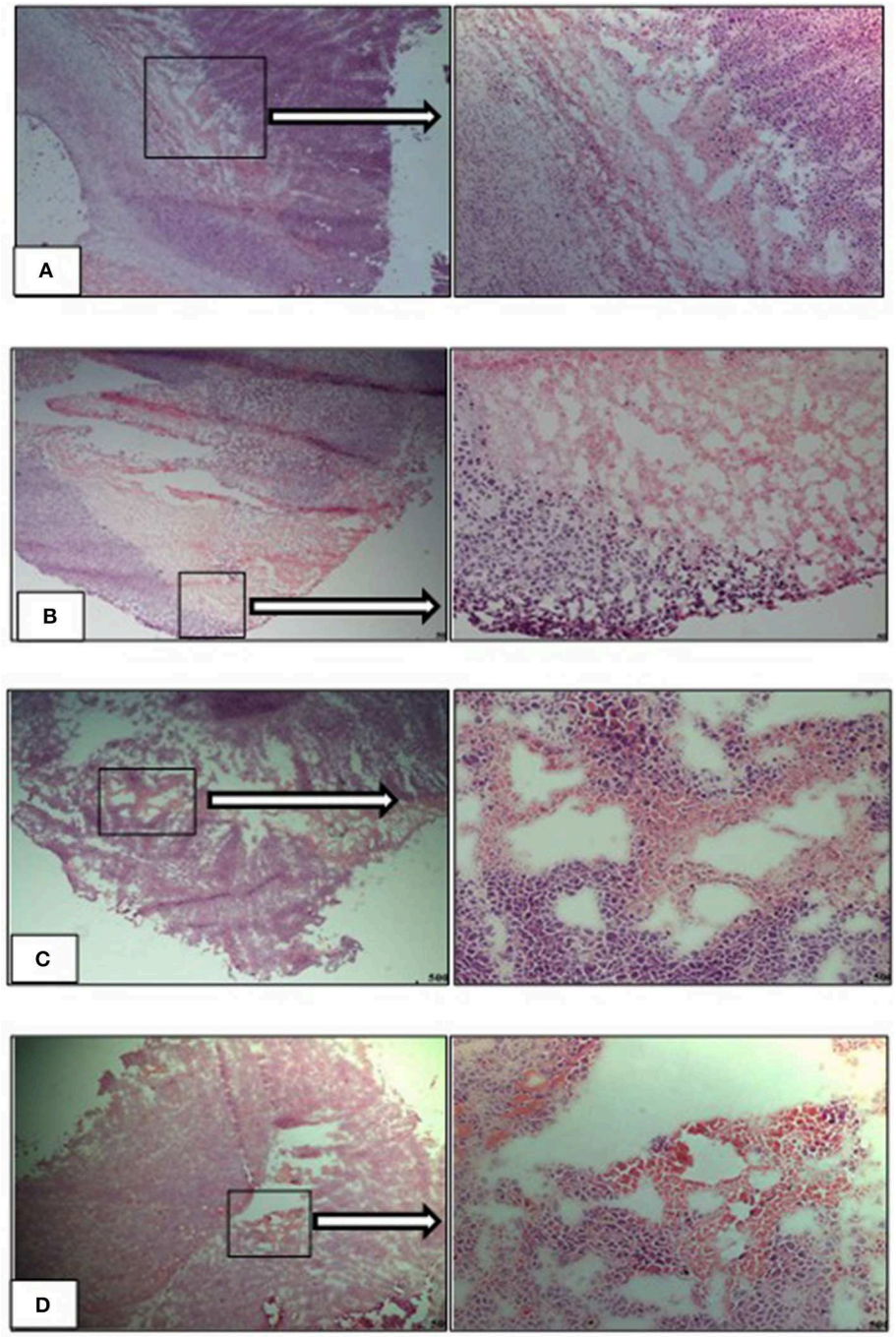

FIGURE 12 | Representative images of H&E stained tumor sections of the experimental treatment groups **(A)** vehicle-LFD, **(B)** vehicle-HFD, **(C)** Dox-L, **(D)** Dox-H, Magnification = 4 and 20 x. Scale = 500 μm.

progression through cellular proliferation, angiogenesis and the inhibition of apoptosis (38, 39, 49). Evidence also supports the role of obesity-induced inflammation (IL-6, TNF-α, and leptin) in Tamoxifen® and anti-VEGF acquired breast cancer drug resistance (33, 50).

Leptin and resistin are well-known adipokines linked to breast cancer (51). Both are secreted primarily by adipose tissue, increase with higher degrees of adiposity, and has been implicated for their role in obesity, inflammation, and breast tumorigenesis (51–53). Breast cancer patients are characterized by high serum leptin concentrations as well as increased leptin receptor expression especially in higher pathological grade tumor tissues and patients who develop resistance to anti-cancer treatments (54, 55). Both leptin and

resistin exacerbates an inflammatory microenvironment by favoring the secretion of other pro-inflammatory adipokines. Additionally, leptin favors breast cancer progression by inducing cellular proliferation by binding to its receptor followed by downstream signaling through NFκB, STAT3, ERK1/ERK2, and phosphoinositide-3-kinase (PI3K) pathways (56, 57). Both elevated leptin and resistin concentrations was associated with the promotion of cancer stem cell survival and the promotion of invasion and migration via epithelial to mesenchymal transition in breast cancer cells (55, 56, 58), which contributes to the development of treatment resistance.

High concentrations of leptin and resistin favor cancer cell proliferation and have recently been reported to be casual factors in acquired breast cancer treatment resistance (59). A well-known mechanism of developing breast cancer treatment resistance includes the evasion of apoptotic pathways (60, 61). Adipocytes attenuated Doxorubicin-induced apoptosis in cancer cells by increasing the protein expression of anti-apoptotic marker blc-2 as well as increasing the synthesis of resistin (59, 61). Resistin has also been identified as a causal factor for acquiring resistance to doxorubicin treatment in both MCF-7 and MDA-MB-231 breast cancer cells through the induction of autophagy (59).

Furthermore, we also determined the protein expression levels of NFκB, an important transcription factor regulating inflammation, in mammary adipose tissue to confirm local inflammation, and observed significantly higher levels of NFκB-p65 protein expression in Dox-H compared to both the Vehicle-H and Dox-L mice (**Figure 7A**). Mammary adipose tissue in the tumor microenvironment displays persistent inflammation and harbors crown like structures, which are well-known inflammatory foci (62). We therefore propose that mammary adipose tissue displays local inflammation (as a result of DIO) similar to what is observed in visceral adipose tissue of obese individuals (52, 63) and as a result may play a significant role in obesity-induced breast cancer treatment resistance. It is speculated that treatment resistance may be the result of inflammation found in the mammary adipose tissue as a result of the HFD and doxorubicin treatment. This is confirmed by the fact that doxorubicin treatment induces inflammation in metabolic tissues (64).

We, therefore conclude that inflammation as a result of adipokine dysfunction was observed in obese vehicle-treated mice and to a greater extent in doxorubicin treated mice. We propose that obesity drives both systemic and local inflammation in mammary adipose tissue and thereby induce downstream signaling pathways regulating cell growth, inhibition of apoptosis, and invasion, to ultimately contribute to the development of breast cancer treatment resistance. Therefore, it is plausible that DIO plays a key role as a causal factor in the underlying pathophysiology linked to the decreased efficacy of Doxorubicin treatment, involving systemic and local mammary fat inflammation as underlying molecular mechanisms.

Diet-Induced Obesity Distinctly Alters Lipid Metabolism in the Tumor Microenvironment Leading to Changes in Fatty Acid Composition in Mammary Adipose- and Tumor Tissue

We found that tumor tissue Σ SFA was increased in both vehicle-H and Dox-H (HFD) mice compared to LFD mice (**Figure 9A**). Stearic acid (SA) was also found to be increased in mammary adipose tissue and tumor tissue of Dox-H mice compared to Dox-L mice (**Figure 9C**). Furthermore, we observed decreased percentages of various MUFAs (PTA, OA, and VA) in both mammary adipose and tumor tissue of mice on the HFD, and even more profound decreases in doxorubicin-treated mice (**Figure 10**).

Clinical and experimental animal model evidence on tumor and adjacent adipose tissue induced FA composition alterations within the tumor microenvironment are lacking specifically under obesogenic conditions. Our results are in agreement with Maillard et al. (65), who showed that the most abundant FAs present in breast cancer tumors were OA, PA, SA, as well as LA, compared to controls. de Bree et al. (66), reported that breast cancer cases showed significantly higher Σ MUFA content in tumor tissue as well as lower Σ PUFAs and n-6 PUFAs content in breast adipose tissue, when compared to benign cases. Mohammadzadeh et al. (67), confirmed increased OA, arachidonic acid (AA) and MUFA:SFA ratio in breast tumors, compared to adjacent tissue.

Due to the abundance and close proximity of mammary adipose tissue (source of FAs) to breast cancer tumors, breast tumors rely on lipid metabolism to favor survival by increasing the expression of various proteins regulating lipid metabolism (68, 69). This is evident by an upregulation of various enzymes catalyzing *de novo* FA synthesis in breast cancer cells i.e., Acetyl-CoA carboxylase (ACC), FAS and SCD-1 (13, 70, 71). Supporting evidence includes increased exogenous lipid utilization, where breast cancer cells induce adipocytes to release FFA via activation of lipolysis (increased expression of ATGL and HSL) and inhibition of adipogenesis (through decreased expression of peroxisome proliferator-activated receptor-γ) (6, 8). Adipocyte-derived FFAs favor the proliferative nature of breast tumor cells in the tumor microenvironment (8), by serving as available metabolic substrates for energy production via β-oxidation or storage in the form of lipid droplets for later utilization. In contrast, microscopically, regions with varying cellularity were observed in tumor sections of both vehicle treated groups irrespective of diet (**Figures 12A,B**). Hyper-cellular regions also showed darker staining on low-power magnification, indicative of increased cell proliferation. Sections of the Dox-L mice showed mostly hyper-cellular regions (**Figure 12C**), whereas the tumor sections of the Dox-H mice were less cellular (**Figure 12D**). This may indicate a decrease in cellular proliferation in response to Doxorubicin treatment among the HFD fed mice. Therefore, it may also be plausible that adipocyte-derived FFAs can induce survival via other mechanisms of action other that proliferation. A recent report showed that lipid accumulation

(adipocyte derived FFA) leads to uncoupled FA oxidation, which favored invasion due to epithelial-mesenchymal-transition, but not proliferation (72).

Additionally, adipocyte-derived FFAs can also be incorporated into phospholipids and esterified with cholesterol to produce cholesteryl esters in cell membranes (73, 74) to induce lipid-saturated membranes. This is further supported by the increased amount and size of lipid droplets found in breast cancer tumors, specifically more aggressive phenotypes (6, 73). Therefore, it may also be plausible that the increased tumor volume in the HFD fed groups maybe be as a result of membrane lipid saturation and lipid droplet deposition within tumor tissue. In fact, tumors enriched with lipid droplets (TAGs and sterol esters) were found to be more resistant toward chemotherapeutic agents (75).

Fatty acids are essential components of cell membrane organization (phosphoglycerides) and fluidity (degree of carbon chain unsaturation), and it is known that the type of FA (i.e., increased saturated FAs characteristic of obesity) derived from the diet, affects phospholipid FA composition (densely-packed membranes) and physical-chemical properties (decreased transmembrane permeability) in cancer cells. This metabolic behavior protects breast cancer cells from oxidative damage induced by chemotherapeutic drugs by decreasing lipid peroxidation, ultimately leading to acquired treatment resistance (11, 76).

The decreased SFA and MUFA profiles observed in mammary adipose tissue could possibly be as a result of alterations in the expression of enzymes regulating lipogenesis, since PA can be elongated into SA, as well as desaturated (catalyzed by SCD-1) to produce PTA (77). We found a decrease in FAS (**Figure 7B**) and SCD-1 protein expression (**Figure 7C**) in HFD mice (both vehicle- and doxorubicin-treated) within mammary adipose tissue, which translate to a decrease in lipogenic activity in mammary adipose tissue of the HFD (obese) animals. This was further supported by decreased estimated activity of SCD1-16 and SCD1-18 (desaturation indexes) observed in HFD compared to LFD animals in mammary adipose tissue FA composition, specifically in the doxorubicin-treated mice (**Supplementary Table 3**). Our findings can be explained by the high dietary carbohydrate content of the LFD i.e., 70% energy from carbohydrates, which might partially explain why SCD-1 and FAS expression was higher in the LFD mice, irrespective of treatments, as dietary carbohydrates are substrates for *de novo* FA synthesis. Our results are in agreement with Liu et al. (78), who showed that rats fed a HFD (60% energy from fat) compared to a control diet (10% energy from fat), showed decreased SCD-1 estimated activity derived from FA composition in adipose tissue TAG and serum FFA fractions. Additionally, it may also be possible that a HFD suppresses SCD-1 expression to prevent adipose tissue storage of FAs in order to promote β-oxidation. This could have implications for tumor-cell survival since an increase in β-oxidation is linked to increased energy production which breast cancer cells utilize for survival, and/or to evade the toxic effects of cancer treatments. This provides a plausible explanation for the HFD-induced decreased lipogenic/lipolytic activity in mammary adipose tissue to increase the FFA "pool" by preventing fat storage (TAGs), which is also exacerbated by doxorubicin treatment—all of which may contribute to the attenuation of breast cancer treatment efficacy. We propose that the excess lipid "availability" in mammary adipose tissue of obese patients could explain the resistance to treatment protocols found in breast cancer patients, especially since dysfunctional adipose tissue (obesity) is implicated in breast cancer progression (79) and because "obese" adipocytes provide higher concentrations of FFAs to breast cancer cells to sustain survival and migration (8).

However, the increased SCD-1 expression observed in Dox-H compared to Dox-L mice in tumor tissue (**Figure 8A**) does not account for the decreased MUFAs found in the tumor tissue of Dox-H mice (**Figure 10**). Firstly, the decreased MUFA profile may be as a result of increased lipolysis of lipid droplets within the tumor itself, as evident by the increased expression of ATGL in the tumor tissue of the HFD mice (**Figure 8B**). Additionally, it could also be the result of breast tumor cells utilizing these MUFAs to decrease treatment efficacy, by increasing the release of MUFAs from the cell membrane. This is supported, by the decreased MUFAs observed within the tumor tissue FFA fraction, including PTA, VA, gondoic acid (GA), and nervonic acid (NA), in the Dox-H compared to Dox-L groups (**Supplementary Table 5**). Lastly, the decreased MUFAs found in tumor tissue TPL and FFA fractions can also be explained by the preferential release and low re-uptake of MUFAs in specific tissues, as well as the selective preference of SFAs compared to MUFAs, or the selective decrease of MUFAs-containing phosphatidylethanolamines and phosphatidylcholine lipids present in tumors under obesogenic conditions. Taken together, the HFD (obesity) induced both *de novo* FA synthesis and lipolysis in the tumor, which was exacerbated by the doxorubicin treatment itself and might therefore confer to the attenuation of breast cancer treatment efficacy under obesogenic conditions.

Furthermore, a dysregulation of cytokines (i.e., increased IL-6, TNF-α, and IL-1β) and adipokines, such as increased leptin and decreased adiponectin (80–83) has been shown to induces transcriptional changes. For example leptin has been shown to inhibit lipogenesis by altering the expression of transcription factors involved in lipid metabolism (7, 45). The outcome is altered adipocyte endocrine functionality which can favor tumor cells to produce more adipokines (83).

We observed increased leptin and resistin levels in Dox-H compared to Dox-L mice (**Figures 6C,D**). Previously, elevated TNF-α levels have been shown to inhibit adipocyte lipolysis (84) and high leptin levels have been shown to decrease adipose tissue SCD-1 expression (85). We believe that obesity-induced inflammation (increased resistin levels) may lead to lipolysis inhibition (decreased HSL in Dox-H vs. Dox-L mice) in mammary adipose tissue (**Figure 7D**). In agreement, we found a significant negative correlation between resistin concentration and HSL protein expression in mammary adipose tissue in the Dox-H mice (**Supplementary Figure 2**), which is supported by previous studies showing that high SFA levels induce the secretion of pro-inflammatory mediators via the NFκB signaling pathway, via the TLR-4 on macrophages (86, 87), which might in turn inhibit lipolysis (decreased HSL). This is also in agreement

with our results, since we found higher levels of NFκB protein expression in mammary adipose tissue of Dox-H compared Dox-L mice (**Figure 7**); all of which further promotes inflammation in the mammary adipose tissue environment, favoring breast cancer cell survival and thereby decreasing treatment efficacy in a paracrine manner.

Furthermore, both mammary adipose tissue and tumor tissue showed significant increases in various n-6 PUFAs (LA, EDA, and ADA) in vehicle-H and Dox-H mice compared to LFD mice (**Figure 11**). Linoleic acid and ALA are essential FAs derived from the diet (88). These FAs are desaturated (FA desaturases) and elongated (Elovl2 and Elovl5) to form their respective long-chain polyunsaturated products such as AA and eicosapentaenoic acid (EPA) (88). Both the low-fat and high-fat experimental diets in our study contained soybean oil, which is rich in both LA and ALA. Therefore, the increase in PUFAs found in both the mammary adipose tissue and the tumor tissue of the HFD mice may be reflective of the higher total fat content (and therefore PUFA content) of the HFD (60% energy from fat).

The proportions of FAs within the two respective diets differed significantly. Linoleic acid and AA accounted for the elevation of n-6 PUFAs in both mammary and tumor tissue of HFD-fed mice, suggesting an increased inflammatory profile, specifically in the obese doxorubicin-treated mice. The pro-inflammatory effects of n-6-PUFA is as a result of lipid-derived bioactive eicosanoid mediators, such as prostaglandins and leukotrienes (14, 89). These bioactive lipids are implicated in breast cancer progression by favoring angiogenesis, cellular proliferation and survival, cell migration, metastasis, as well as exacerbating inflammation (15, 90), in the breast tumor microenvironment possibly promoting acquired cancer resistance to anti-cancer treatment agents.

More importantly, doxorubicin treatment causes adipose tissue and/or adipocyte dysfunction, by altering lipogenesis (decreased FAS) and lipolysis (increased HSL) (20–22, 64, 91), which participate toward the disruption of adipose tissue homeostasis. The consequence here is an increase in FFA release that disrupts lipid storage (22). Doxorubicin-induced FFA release may further exacerbate the bioavailability of FFA, which cancer cells can utilize favorably for its survival and proliferation demands, and thereby indirectly promote breast cancer treatment resistance. Recently, Ebadi et al. (92), showed that chemotherapy treatment (5-fluorouracil and Irinotecan) in a colorectal cancer model diminished peri-uterine adipose tissues' function to store lipids by significantly downregulating the expression of ACC, FAS, and HSL, as well as markers of β-oxidation (i.e., CPT-2), compared to treatment-naïve rats. Additionally, they also showed that SFAs (PA) and MUFAs (PTA) were significantly decreased in chemotherapy-treated groups. However, the authors explained that it is still unknown whether the suppression of adipose tissue lipid storage capacity induced by chemotherapy is a result of decreased HSL expression, or due to mitochondrial dysfunction induced by the chemotherapy (92). Mehdizadeh et al. (93) showed that doxorubicin and 5-fluorouracil have

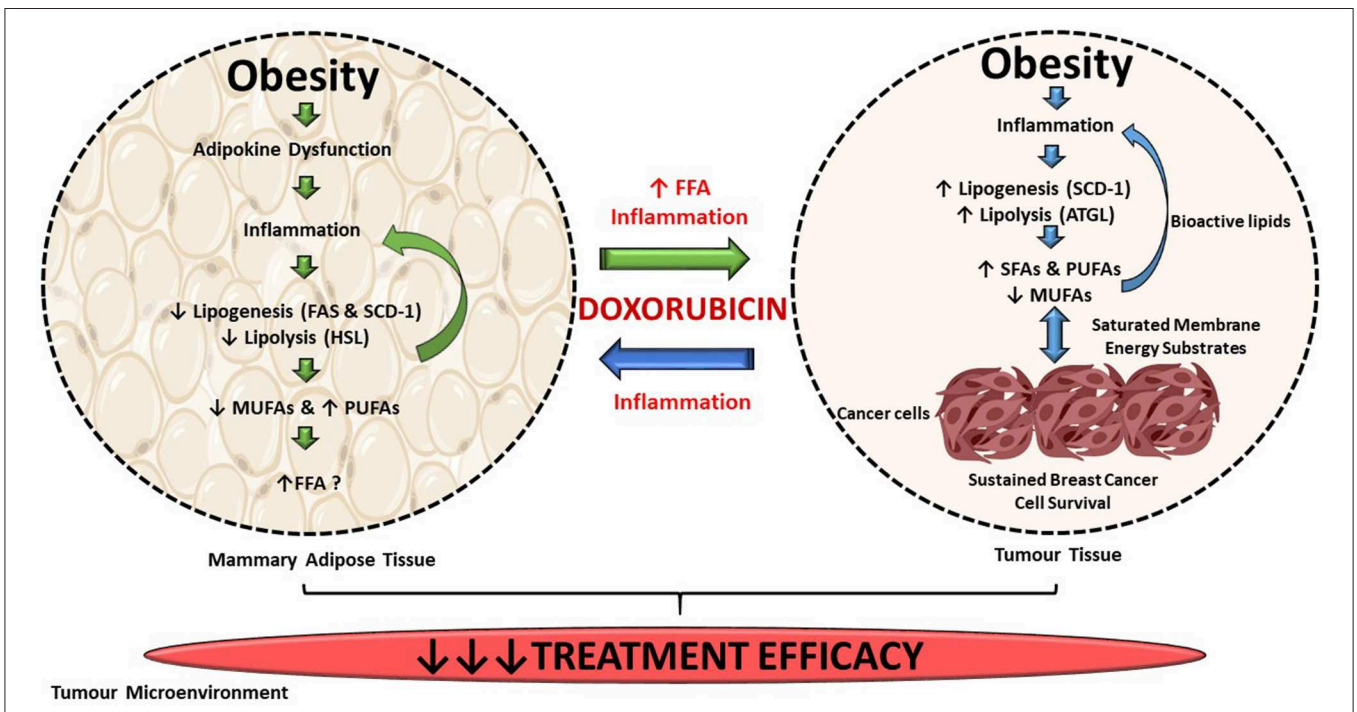

FIGURE 13 | Summary of findings. DIO selectively supresses *de novo* FA synthesis and lipolysis in mammary adipose tissue, but increased lipogenesis and lipolysis in tumor tissue. Exogenous dietary lipids can alter the energy metabolism of triple-negative breast cancer tumors in this current *in vivo* model. Alterations in FAs composition in both mammary adipose and tumor tissue could be a mechanism by which FAs composition can be altered in response to DIO within the tumor microenvironment and thereby contributing to the decreased efficacy of breast cancer treatment agent within our current model.

the ability to induce cancer cell invasion and metastasis by increasing lipid accumulation and membrane fluidity, by altering lipid metabolism. For example, doxorubicin and 5-fluorouracil treatment significantly increased the number of lipid droplets within HepG2 cancer cells. They also reported a significant increase in SFAs (PA) and PUFAs and a significant decrease in MUFAs (OA and PTA) following chemotherapy treatments in the phospholipid fractions of the membranes of cancer cells (93).

To summarize, evidence on FA profiles within the tumor microenvironment has not yet been explored in an obese breast cancer animal model to specifically illustrate its role in breast cancer treatment efficacy. We provide evidence that diet-induced obesity altered the FA profile of both the tumor tissue and its adjacent surrounding mammary adipose tissue. The expression of lipid metabolism enzymes in this study were also differentially altered by diet-induced obesity and it is very likely that the altered FA composition observed in both mammary adipose tissue and tumor tissue are as a result of alterations in lipogenesis and/or lipolysis, which may be a causal factor in decreasing the efficacy of doxorubicin a well-known breast cancer treatment agent. We acknowledge that the fat content used in the HFD (60% energy from fat) of the *in vivo* model is high in comparison to human consumption. However, Ervin et al. (94) suggested that although the total fat content is high, the proportion of specific FA classes (SFAs, MUFAs, and PUFAs) consumed in humans is similar to the HFD we used (94).

CONCLUSION

Diet-induced obesity significantly decreased the treatment efficacy of doxorubicin on triple-negative breast cancer tumors. Suppression of both *de novo* FA synthesis and lipolysis in mammary adipose tissue lead to the inhibition of FA storage (decreased MUFAs and increased PUFAs), exacerbating local inflammation in mammary adipose tissue which can enhance breast cancer cell survival in a paracrine manner, as illustrated in **Figure 13**. *De novo* FA synthesis and lipolysis were increased in breast tumor tissue. The incorporation of dietary FAs into phospholipid membranes of breast tumor cells suggests that exogenous dietary lipids can alter the energy metabolism of E0771 breast cancer cells. These selective alterations in lipid metabolism markers and FA composition in both mammary adipose and tumor tissue could be a novel mechanism by which FA composition can be altered in response to DIO within the tumor microenvironment and thereby contributing to the development of breast cancer treatment resistance. When doxorubicin is administered as a treatment in an obesogenic context, the treatment efficacy of this breast cancer treatment agent is decreased by conferring to a more lipid saturated cell membrane, known to protect cancer cells from the cytotoxic effects of chemotherapeutic agents.

DATA AVAILABILITY STATEMENT

All datasets generated for this study are included in the article/**Supplementary Material**.

ETHICS STATEMENT

The animal study was reviewed and approved by Animal research committee of Stellenbosch University (SU-ACUM13-00015).

AUTHOR CONTRIBUTIONS

IM performed and completed all analysis and wrote the first draft of this manuscript. ZE assisted with analysis. LJ completed and assisted with the histological analysis and interpretation of data. TN, PJ, and A-ME contributed to critical revision and intellectual input of the manuscript. All authors read and approved the final manuscript.

FUNDING

Work in this study was supported by research grants from the Cancer Association of South Africa (CANSA), the South African Medical Research Council (SAMRC) and the National Research Foundation (NRF) of South Africa. Funding bodies had no role in the preparation of this manuscript.

ACKNOWLEDGMENTS

We would also like to thank Johanna van Wyk of the Non-Communicable Diseases Research Unit of the South African Medical Research Council for her invaluable laboratory assistance with all the fatty acid analysis and ZE for her contribution to the animal study.

SUPPLEMENTARY MATERIAL

The Supplementary Material for this article can be found online at: https://www.frontiersin.org/articles/10.3389/fonc.2020.00306/full#supplementary-material

REFERENCES

1. Blüher M. Obesity: global epidemiology and pathogenesis. *Nat Rev Endocrinol.* (2019) 15:288–98. doi: 10.1038/s41574-019-0176-8
2. Bray F, Ferlay J, Soerjomataram I, Siegel RL, Torre LA, Jemal A. Global cancer statistics 2018: GLOBOCAN estimates of incidence and mortality worldwide for 36 cancers in 185 countries. *CA Cancer J Clin.* (2018) 68:394–424. doi: 10.3322/caac.21492
3. Nagrani R, Mhatre S, Rajaraman P, Soerjomataram I, Boffetta P, Gupta S, et al. Central obesity increases risk of breast cancer irrespective of menopausal and hormonal receptor status in women of South Asian ethnicity. *Eur J Cancer.* (2016) 66:153–61. doi: 10.1016/j.ejca.2016.07.022
4. Sparano JA, Wang M, Zhao F, Stearns V, Martino S, Ligibel JA, et al. Obesity at diagnosis is associated with inferior outcomes in hormone receptor-positive operable breast cancer. *Cancer.* (2012) 118:5937–46. doi: 10.1002/cncr.27527

5. Choe SS, Huh JY, Hwang IJ, Kim JI, Kim JB. Adipose tissue remodeling: its role in energy metabolism and metabolic disorders. *Front Endocrinol.* (2016) 7:1–16. doi: 10.3389/fendo.2016.00030
6. Balaban S, Lee LS, Varney B, Aishah A, Gao Q, Shearer RF, et al. Heterogeneity of fatty acid metabolism in breast cancer cells underlies differential sensitivity to palmitate-induced apoptosis. *Mol Oncol.* (2018) 12:1623–38. doi: 10.1002/1878-0261.12368
7. Dirat B, Bochet L, Dabek M, Daviaud D, Dauvillier S, Majed B, et al. Cancer-associated adipocytes exhibit an activated phenotype and contribute to breast cancer invasion. *Cancer Res.* (2011) 71:2455–65. doi: 10.1158/0008-5472.CAN-10-3323
8. Balaban S, Shearer RF, Lee LS, van Geldermalsen M, Schreuder M, Shtein HC, et al. Adipocyte lipolysis links obesity to breast cancer growth: adipocyte-derived fatty acids drive breast cancer cell proliferation and migration. *Cancer Metab.* (2017) 5:1. doi: 10.1186/s40170-016-0163-7
9. Mentoor I, Engelbrecht AM, van Jaarsveld PJ, Nell T. Chemoresistance: intricate interplay between breast tumor cells and adipocytes in the tumor microenvironment. *Front Endocrinol.* (2018) 9:758. doi: 10.3389/fendo.2018.00758
10. Mentoor I, Engelbrecht AM, Nell T. Fatty acids: adiposity and breast cancer chemotherapy, a bad synergy? *Prostaglandins Leukot Essent Fat Acids.* (2019) 140:18–33. doi: 10.1016/j.plefa.2018.11.009
11. Rysman E, Brusselmans K, Scheys K, Timmermans L, Derua R, Munck S, et al. *De novo* lipogenesis protects cancer cells from free radicals and chemotherapeutics by promoting membrane lipid saturation. *Cancer Res.* (2010) 70:8117–26. doi: 10.1158/0008-5472.CAN-09-3871
12. Zalba S, Hagen TLM. Cell membrane modulation as adjuvant in cancer therapy. *Cancer Treat Rev.* (2017) 52:48–57. doi: 10.1016/j.ctrv.2016.10.008
13. Greene ER, Huang S, Serhan CN, Panigrahy D. Regulation of inflammation in cancer by eicosanoids. *Prostaglandins Other Lipid Mediat.* (2011) 96:27–36. doi: 10.1016/j.prostaglandins.2011.08.004
14. Kremmyda LS, Tvrzicka E, Stankova B, Zak A. Fatty acids as biocompounds: their role in human metabolism, health and disease: a review. Part 2: fatty acid physiological roles and applications in human health and disease. *Biomed Pap Med Fac Univ Palacky Olomouc Czech Repub.* (2011) 155:195–218. doi: 10.5507/bp.2011.052
15. Wang D, Dubois RN. Prostaglandins and cancer. *Gut.* (2006) 55:115–22. doi: 10.1136/gut.2004.047100
16. Bousquenaud M, Fico F, Solinas G, Rüegg C, Santamaria-Martínez A. Obesity promotes the expansion of metastasis-initiating cells in breast cancer. *Breast Cancer Res.* (2018) 20:1–11. doi: 10.1186/s13058-018-1029-4
17. Dong L, Yuan Y, Opansky C, Chen Y, Barrantes IA, Wu S, et al. Diet-induced obesity links to ER positive breast cancer progression via LPA/PKD-1-CD36 signaling-mediated microvascular remodeling. *Oncotarget.* (2017) 8:22550–62. doi: 10.18632/oncotarget.15123
18. Iwase T, Sangai T, Nagashima T, Sakakibara M, Sakakibara J, Hayama S, et al. Impact of body fat distribution on neoadjuvant chemotherapy outcomes in advanced breast cancer patients. *Cancer Med.* (2016) 5:41–8. doi: 10.1002/cam4.571
19. Guenancia C, Ladoire S, Ghiringelli F, Rochette L, Vergely C, Cottin Y. Implications of excess weight in the cardiotoxicity of anthracyclines and trastuzumab in breast cancer. *Arch Cardiovasc Dis.* (2017) 110:69–71. doi: 10.1016/j.acvd.2016.12.004
20. Batatinha H, Souza C, Lima E, Alonso-Vale M, Cruz M, Da Cunha R, et al. Adipose tissue homeostasis is deeply disrupted by doxorubicin treatment. *Cancer Metab.* (2014) 2(Suppl. 1):P5. doi: 10.1186/2049-3002-2-S1-P5
21. Arunachalam S, Kim SY, Kim MS, Yi HK, Yun BS, Lee DY, et al. Adriamycin inhibits adipogenesis through the modulation of PPARγ and restoration of adriamycin-mediated inhibition of adipogenesis by PPARγ over-expression. *Toxicol Mech Methods.* (2012) 22:540–56. doi: 10.3109/15376516.2012.692110
22. Biondo LA, Lima EA, Souza CO, Cruz MM, Cunha RDC, Alons-Vale MI, et al. Impact of doxorubicin treatment on the physiological functions of white adipose tissue. *PLoS ONE.* (2016) 11:e0151548. doi: 10.1371/journal.pone.0151548
23. Cleary MP, Juneja SC, Phillips FC, Hu X, Grande JP, Maihle NJ. Leptin receptor-deficient MMTV-TGF-α/LeprdbLepr db female mice do not develop oncogene-Induced mammary tumors. *Exp Biol Med.* (2004) 229:182–93. doi: 10.1177/153537020422900207
24. Chu DT, Malinowska E, Jura M, Kozak LP. C57BL/6J mice as a polygenic developmental model of diet-induced obesity. *Physiol Rep.* (2017) 5:e13093. doi: 10.14814/phy2.13093
25. Reagan-Shaw S, Nihal M, Ahmad N. Dose translation from animal to human studies revisited. *FASEB J.* (2008) 22:659–61. doi: 10.1096/fj.07-9574LSF
26. Tomayko MM, Reynolds CP. Determination of subcutaneous tumor size in athymic (nude) mice. *Cancer Chemother Pharmacol.* (1989) 24:148–54. doi: 10.1007/BF00300234
27. Folch J, Lees M, Sloane Stanley GH. A simple method for the isolation and purification of total lipides from animal tissues. *J Biol Chem.* (1957) 226:497–509.
28. Hon G, Hassan M, van Rensburg SJ, Abel S, Marais DW, van Jaarsveld P, et al. Immune cell membrane fatty acids and inflammatory marker, C-reactive protein, in patients with multiple sclerosis. *Br J Nutr.* (2009) 102:1334–40. doi: 10.1017/S0007114509382185
29. Chimhashu T, Malan L, Baumgartner J, Jaarsveld PJ Van, Galetti V, Moretti D, et al. Sensitivity of fatty acid desaturation and elongation to plasma zinc concentration : a randomised controlled trial in Beninese children. *Random Control Trial.* (2018) 119:610–19. doi: 10.1017/S000711451700366X
30. Manni A, Richie JP, Schetter SE, Calcagnotto A, Trushin N, Aliaga C, et al. Stearoyl-CoA desaturase-1, a novel target of omega-3 fatty acids for reducing breast cancer risk in obese postmenopausal women. *Eur J Clin Nutr.* (2017) 71:762–5. doi: 10.1038/ejcn.2016.273
31. Petrus P, Edholm D, Rosqvist F, Dahlman I, Sundbom M, Arner P, et al. Depot-specific differences in fatty acid composition and distinct associations with lipogenic gene expression in abdominal adipose tissue of obese women. *Int J Obes.* (2017) 41:1295–8. doi: 10.1038/ijo.2017.106
32. Hu MB, Xu H, Zhu WH, Bai P De, Hu JM, Yang T, et al. High-fat diet-induced adipokine and cytokine alterations promote the progression of prostate cancer *in vivo* and *in vitro*. *Oncol Lett.* (2018) 15:1607–15. doi: 10.3892/ol.2017.7454
33. Incio J, Ligibel JA, McManus DT, Suboj P, Jung K, Kawaguchi K, et al. Obesity promotes resistance to anti-VEGF therapy in breast cancer by up-regulating IL-6 and potentially FGF-2. *Sci Transl Med.* (2018) 10:eaag0945. doi: 10.1126/scitranslmed.aag0945
34. Santander AM, Lopez-Ocejo O, Casas O, Agostini T, Sanchez L, Lamas-Basulto E, et al. Paracrine interactions between adipocytes and tumor cells recruit and modify macrophages to the mammary tumor microenvironment: the role of obesity and inflammation in breast adipose tissue. *Cancers.* (2015) 7:143–78. doi: 10.3390/cancers7010143
35. Cao JJ, Gregoire BR. A high-fat diet increases body weight and circulating estradiol concentrations but does not improve bone structural properties in ovariectomized mice. *Nutr Res.* (2016) 36:320–7. doi: 10.1016/j.nutres.2015.12.008
36. Thivat E, Thérondel S, Lapirot O, Abrial C, Gimbergues P, Gadéa E, et al. Weight change during chemotherapy changes the prognosis in non metastatic breast cancer for the worse. *BMC Cancer.* (2010) 10:648. doi: 10.1186/1471-2407-10-648
37. Lautenbach A, Budde A, Wrann CD, Teichmann B, Vieten G, Karl T, et al. Obesity and the associated mediators leptin, estrogen and IGF-I enhance the cell proliferation and early tumorigenesis of breast cancer cells. *Nutr Cancer.* (2009) 61:484–91. doi: 10.1080/01635580802610115
38. Khalid S, Hwang D, Babichev Y, Kolli R, Altamentova S, Koren S, et al. Evidence for a tumor promoting effect of high-fat diet independent of insulin resistance in HER2/Neu mammary carcinogenesis. *Breast Cancer Res Treat.* (2010) 122:647–59. doi: 10.1007/s10549-009-0586-8
39. Cowen S, McLaughlin S, Hobbs G, Coad J, Martin K, Olfert I, et al. High-fat, high-calorie diet enhances mammary carcinogenesis and local inflammation in MMTV-PyMT mouse model of breast cancer. *Cancers.* (2015) 7:1125–42. doi: 10.3390/cancers7030828
40. Guiu B, Petit JM, Bonnetain F, Ladoire S, Guiu S, Cercueil J-P, et al. Visceral fat area is an independent predictive biomarker of outcome after first-line bevacizumab-based treatment in metastatic colorectal cancer. *Gut.* (2010) 59:341–7. doi: 10.1136/gut.2009.188946
41. Stemmer K, Perez-Tilve D, Ananthakrishnan G, Bort A, Seeley RJ, Tschöp MH, et al. High-fat-diet-induced obesity causes an inflammatory and tumor-promoting microenvironment in the rat

kidney. *DMM Dis Model Mech*. (2012) 5:627–35. doi: 10.1242/dmm.009407
42. Gevorgyan A, Bregni G, Galli G, Ganzinelli M, Martinetti A, Lo Vullo S, et al. Body mass index and clinical benefit of fulvestrant in postmenopausal women with advanced breast cancer. *Tumori*. (2016) 102:e11–4. doi: 10.5301/tj.5000515
43. De Azambuja E, McCaskill-Stevens W, Francis P, Quinaux E, Crown JPA, Vicente M, et al. The effect of body mass index on overall and disease-free survival in node-positive breast cancer patients treated with docetaxel and doxorubicin-containing adjuvant chemotherapy: the experience of the BIG 02-98 trial. *Breast Cancer Res Treat*. (2010) 119:145–53. doi: 10.1007/s10549-009-0512-0
44. Karpinska A, Safranow K, Kładny J, Sulzyc-Bielicka V. The influence of obesity on results of at (doxorubicin plus docetaxel) neoadjuvant chemotherapy in locally advanced breast cancer patients. *Polish J Surg*. (2015) 87:231–7. doi: 10.1515/pjs-2015-0047
45. Lehuédé C, Li X, Dauvillier S, Vaysse C, Franchet C, Clement E, et al. Adipocytes promote breast cancer resistance to chemotherapy, a process amplified by obesity: role of the major vault protein (MVP). *Breast Cancer Res*. (2019) 21:1–7. doi: 10.1186/s13058-018-1088-6
46. Popko1 K, Gorska E, Stelmaszczyk-Emmel A, Plywaczewski R, Stoklosa A, Gorecka D, et al. European jouproinflammatory cytokines il-6 and tnf-α and the development of inflammation in obese subjects k.rnal of medical research. *Eur J Med Res*. (2010) 15(Suppl. II):120–2. doi: 10.1186/2047-783X-15-S2-120
47. Deng T, Lyon CJ, Bergin S, Caligiuri MA, Hsueh WA. Obesity, inflammation, and cancer. *Annu Rev Pathol*. (2016) 11:421–49. doi: 10.1146/annurev-pathol-012615-044359
48. Wang H, Yang X. Association between serum cytokines and progression of breast cancer in Chinese population. *Med*. (2017) 96:e08840. doi: 10.1097/MD.0000000000008840
49. Pérez-Hernández AI, Catalán V, Gómez-Ambrosi J, Rodríguez A, Frühbeck G. Mechanisms linking excess adiposity and carcinogenesis promotion. *Front Endocrinol*. (2014) 5:1–7. doi: 10.3389/fendo.2014.00065
50. Bougaret L, Delort L, Billard H, Le Huede C, Boby C, De la Foye A, et al. Adipocyte/breast cancer cell crosstalk in obesity interferes with the anti-proliferative efficacy of tamoxifen. *PLoS ONE*. (2018) 13:e0191571. doi: 10.1371/journal.pone.0191571
51. Surmacz E. Leptin and adiponectin: emerging therapeutic targets in breast cancer. *J Mammary Gland Biol Neoplasia*. (2013) 18:321–32. doi: 10.1007/s10911-013-9302-8
52. Rosendahl AH, Bergqvist M, Lettiero B, Kimbung S, Borgquist S. Adipocytes and obesity-related conditions jointly promote breast cancer cell growth and motility: associations with CAP1 for prognosis. *Front Endocrinol*. (2018) 9:689. doi: 10.3389/fendo.2018.00689
53. Zeidan B, Manousopoulou A, Garay-Baquero DJ, White CH, Larkin SET, Potter KN, et al. Increased circulating resistin levels in early-onset breast cancer patients of normal body mass index correlate with lymph node negative involvement and longer disease free survival: a multi-center POSH cohort serum proteomics study. *Breast Cancer Res*. (2018) 20:1–12. doi: 10.1186/s13058-018-0938-6
54. Assiri AMA, Kamel HFM, Hassanien MFR. Resistin, visfatin, adiponectin, and leptin: risk of breast cancer in pre- and postmenopausal saudi females and their possible diagnostic and predictive implications as novel biomarkers. *Dis Markers*. (2015) 2015:253519. doi: 10.1155/2015/253519
55. Sultana R, Kataki AC, Borthakur BB, Basumatary TK, Bose S. Imbalance in leptin-adiponectin levels and leptin receptor expression as chief contributors to triple negative breast cancer progression in Northeast India. *Gene*. (2017) 621:51–8. doi: 10.1016/j.gene.2017.04.021
56. Wang CH, Wang PJ, Hsieh YC, Lo S, Lee YC, Chen YC, et al. Resistin facilitates breast cancer progression via TLR4- mediated induction of mesenchymal phenotypes and stemness properties. *Oncogene*. (2018) 37:589–600. doi: 10.1038/onc.2017.357
57. Rodríguez AJ, Mastronardi C, Paz-Filho G. Leptin as a risk factor for the development of colorectal cancer. *Transl Gastrointest Cancer*. (2013) 2:211–22. doi: 10.3978/j.issn.2224-4778.2013.10.04
58. Lee JO, Kim N, Lee HJ, Lee YW, Kim SJ, Park SH, et al. Resistin, a fat-derived secretory factor, promotes metastasis of MDA-MB-231 human breast cancer cells through ERM activation. *Sci Rep*. (2016) 6:18923. doi: 10.1038/srep18923
59. Liu Z, Shi A, Song D, Han B, Zhang Z, Ma L, et al. Resistin confers resistance to doxorubicin-induced apoptosis in human breast cancer cells through autophagy induction. *Am J Cancer Res*. (2017) 7:574–83.
60. Behan JW, Avramis VI, Yun JP, Louie SG, Mittelman SD. Diet-induced obesity alters vincristine pharmacokinetics in blood and tissues of mice. *Pharmacol Res*. (2010) 61:385–90. doi: 10.1016/j.phrs.2010.01.007
61. Behan JW, Yun JP, Proektor MP, Ehsanipour EA, Arutyunyan A, Moses AS, et al. Adipocytes impair leukemia treatment in mice. *Cancer Res*. (2009) 69:7867–74. doi: 10.1158/0008-5472.CAN-09-0800
62. Cha YJ, Kim ES, Koo JS. Tumor-associated macrophages and crown-like structures in adipose tissue in breast cancer. *Breast Cancer Res Treat*. (2018) 170:15–25. doi: 10.1007/s10549-018-4722-1
63. Rezaee F, Dashty M. Role of Adipose Tissue in Metabolic System Disorder adipose tissue is the initiator of metabolic diseases. *J Diabetes Metab*. (2013). S13:008. doi: 10.4172/2155-6156.S13-008
64. Supriya R, Tam BT, Pei XM, Lai CW, Chan LW, Yung BY, et al. Doxorubicin induces inflammatory modulation and metabolic dysregulation in diabetic skeletal muscle. *Front Physiol*. (2016) 7:323. doi: 10.3389/fphys.2016.00323
65. Maillard V, Bougnoux P, Ferrari P, Jourdan ML, Pinault M, Lavillonnìre F, et al. N-3 and N-6 fatty acids in breast adipose tissue and relative risk of breast cancer in a case-control study in tours, France. *Int J Cancer*. (2002) 98:78–83. doi: 10.1002/ijc.10130
66. de Bree E, Mamalakis G, Sanidas E, Hatzis C, Askoxylakis I, Daskalakis M, et al. Adipose tissue fatty acid composition in greek patients with breast cancer versus those with benign breast tumors. *Anticancer Res*. (2013) 33:1667–72.
67. Mohammadzadeh F, Mosayebi G, Montazeri V, Darabi M, Fayezi S, Shaaker M, et al. Fatty acid composition of tissue cultured breast carcinoma and the effect of stearoyl-CoA desaturase 1 inhibition. *J Breast Cancer*. (2014) 17:136–42. doi: 10.4048/jbc.2014.17.2.136
68. Du T, Sikora MJ, Levine KM, Tasdemir N, Riggins RB, Wendell SG, et al. Key regulators of lipid metabolism drive endocrine resistance in invasive lobular breast cancer. *Breast Cancer Res*. (2018) 20:106. doi: 10.1186/s13058-018-1041-8
69. Iwamoto H, Abe M, Yang Y, Cui D, Seki T, Nakamura M, et al. Cancer lipid metabolism confers antiangiogenic drug resistance. *Cell Metab*. (2018) 28:104–17.e5. doi: 10.1016/j.cmet.2018.05.005
70. Veigel D, Wagner R, Stübiger G, Wuczkowski M, Filipits M, Horvat R, et al. Fatty acid synthase is a metabolic marker of cell proliferation rather than malignancy in ovarian cancer and its precursor cells. *Int J Cancer*. (2015) 136:2078–90. doi: 10.1002/ijc.29261
71. Yoon S, Lee MY, Park SW, Moon JS, Koh YK, Ahn YH, et al. Up-regulation of acetyl-CoA carboxylase α and fatty acid synthase by human epidermal growth factor receptor 2 at the translational level in breast cancer cells. *J Biol Chem*. (2007) 282:26122–31. doi: 10.1074/jbc.M702854200
72. Wang YY, Attané C, Milhas D, Dirat B, Dauvillier S, Guerard A, et al. Mammary adipocytes stimulate breast cancer invasion through metabolic remodeling of tumor cells. *JCI Insight*. (2017) 2:e87489. doi: 10.1172/jci.insight.87489
73. Antalis CJ, Uchida A, Buhman KK, Siddiqui RA. Migration of MDA-MB-231 breast cancer cells depends on the availability of exogenous lipids and cholesterol esterification. *Clin Exp Metastasis*. (2011) 28:733–41. doi: 10.1007/s10585-011-9405-9
74. Shyu P, Wong XFA, Crasta K, Thibault G. Dropping in on lipid droplets: insights into cellular stress and cancer. *Biosci Rep*. (2018) 38:BSR20180764. doi: 10.1042/BSR20180764
75. Steuwe C, Patel II, Ul-Hasan M, Schreiner A, Boren J, Brindle KM et al. CARS based label-free assay for assessment of drugs by monitoring lipid droplets in tumour cells. *J Biophotonics*. (2014) 7:906–13. doi: 10.1002/jbio.201300110
76. Zhao J, Zhi Z, Wang C, Xing H, Song G, Yu X, et al. Exogenous lipids promote the growth of breast cancer cells via CD36. *Oncol Rep*. (2017) 38:2105–15. doi: 10.3892/or.2017.5864
77. Kihara A. Very long-chain fatty acids: elongation, physiology and related disorders. *J Biochem*. (2012) 152:387–95. doi: 10.1093/jb/mvs105
78. Liu TW, Heden TD, Morris EM, Fritsche KL, Vieira VJ, John P, et al. High - fat diet alters serum fatty acid profiles in obesity prone rats : implications for *in vitro* studies. *Lipids*. (2015) 50:997–1008. doi: 10.1007/s11745-015-4061-5

79. Pierobon M, Frankenfeld CL. Obesity as a risk factor for triple-negative breast cancers: a systematic review and meta-analysis. *Breast Cancer Res Treat.* (2013) 137:307–14. doi: 10.1007/s10549-012-2339-3
80. Koti M, Siu A, Clément I, Bidarimath M, Turashvili G, Edwards A, et al. A distinct pre-existing inflammatory tumour microenvironment is associated with chemotherapy resistance in high-grade serous epithelial ovarian cancer. *Br J Cancer*. (2015) 112:1215–22. doi: 10.1038/bjc.2015.81
81. Mahon KL, Lin H-M, Castillo L, Lee BY, Lee-Ng M, Chatfield MD, et al. Cytokine profiling of docetaxel-resistant castration-resistant prostate cancer. *Br J Cancer*. (2015) 112:1340–8. doi: 10.1038/bjc.2015.74
82. Nieman KM, Romero IL, van Houten B, Lengyel E. Adipose tissue and adipocytes support tumorigenesis and metastasis. *Biochim Biophys Acta Mol Cell Biol Lipids*. (2013) 1831:1533–41. doi: 10.1016/j.bbalip.2013.02.010
83. Vyas D, Laput G, Vyas AK. Chemotherapy-enhanced inflammation may lead to the failure of therapy and metastasis. *Onco Targets Ther*. (2014) 7:1015–23. doi: 10.2147/OTT.S60114
84. Laurencikiene J, van Harmelen V, Nordström EA, Dicker A, Blomqvist L, Näslund E, et al. NF-κB is important for TNF-α-induced lipolysis in human adipocytes. *J Lipid Res.* (2007) 48:1069–77. doi: 10.1194/jlr.M600471-JLR200
85. Miyazaki M, Sampath H, Liu X, Flowers MT, Chu K, Dobrzyn A, et al. Stearoyl-CoA desaturase-1 deficiency attenuates obesity and insulin resistance in leptin-resistant obese mice. *Biochem Biophys Res Commun.* (2009) 380:818–22. doi: 10.1016/j.bbrc.2009.01.183
86. Milanski M, Degasperi G, Coope A, Morari J, Denis R, Cintra DE, et al. Saturated fatty acids produce an inflammatory response predominantly through the activation of TLR4 signaling in hypothalamus: implications for the pathogenesis of obesity. *J Neurosci.* (2009) 29:359–70. doi: 10.1523/JNEUROSCI.2760-08.2009
87. Lee JY, Zhao L, Youn HS, Weatherill AR, Tapping R, Feng L, et al. Saturated fatty acid activates but polyunsaturated fatty acid inhibits toll-like receptor 2 dimerized with toll-like receptor 6 or 1. *J Biol Chem*. (2004) 279:16971–9. doi: 10.1074/jbc.M312990200
88. Di Pasquale MG. The essentials of essential fatty acids. *J Diet Suppl.* (2009) 6:143–61. doi: 10.1080/19390210902861841
89. Currie E, Schulze A, Zechner R, Walther TC, Farese R V. Cellular fatty acid metabolism and cancer. *Cell Metab*. (2013) 18:153–61. doi: 10.1016/j.cmet.2013.05.017
90. Fritsche KL. The science of fatty acids and inflammation. *Adv Nutr.* (2015) 6:293S−301. doi: 10.3945/an.114.006940
91. de Lima Junior EA, Yamashita AS, Pimentel GD, de Sousa LGO, Santos RVT, Gonçalves CL, et al. Doxorubicin caused severe hyperglycaemia and insulin resistance, mediated by inhibition in AMPk signalling in skeletal muscle. *J Cachexia Sarcopenia Muscle.* (2016) 7:615–25. doi: 10.1002/jcsm.12104
92. Ebadi M, Field CJ, Lehner R, Mazurak VC. Chemotherapy diminishes lipid storage capacity of adipose tissue in a preclinical model of colon cancer. *Lipids Health Dis*. (2017) 16:247. doi: 10.1186/s12944-017-0638-8
93. Mehdizadeh A, Bonyadi M, Darabi M, Rahbarghazi R, Montazersaheb S, Velaei K, et al. Common chemotherapeutic agents modulate fatty acid distribution in human hepatocellular carcinoma and colorectal cancer cells. *Bioimpacts*. (2017) 7:31–9. doi: 10.15171/bi.2017.05
94. Ervin RB, Wang CY, Wright JD, Kennedy-Stephenson J. Dietary intake of selected minerals for the United States population: 1999-2000. *Adv Data*. (2004) 1–5.

Conflict of Interest: The authors declare that the research was conducted in the absence of any commercial or financial relationships that could be construed as a potential conflict of interest.

frontiers in Oncology

ORIGINAL RESEARCH
published: 10 July 2020
doi: 10.3389/fonc.2020.01123

Cytosolic NUAK1 Enhances ATP Production by Maintaining Proper Glycolysis and Mitochondrial Function in Cancer Cells

Emilia Escalona[1], *Marcelo Muñoz*[2], *Roxana Pincheira*[1], *Álvaro A. Elorza*[2]* and *Ariel F. Castro*[1]*

[1] Signal Transduction and Cancer Laboratory, Biochemistry and Molecular Biology Department, Faculty of Biological Sciences, Universidad de Concepción, Concepción, Chile, [2] Mitochondrial Medicine Laboratory, Institute of Biomedical Sciences, Faculty of Medicine and Faculty of Life Sciences, Universidad Andres Bello, Santiago, Chile

OPEN ACCESS

Edited by:
Stefano Falone,
University of L'Aquila, Italy

Reviewed by:
Olivier Peulen,
University of Liège, Belgium
Marco Fiorillo,
University of Salford, United Kingdom
Thomas N. Seyfried,
Boston College, United States

***Correspondence:**
Álvaro A. Elorza
alvaro.elorza@unab.cl
Ariel F. Castro
arcastro@udec.cl

Specialty section:
This article was submitted to Cancer Metabolism, a section of the journal Frontiers in Oncology

Received: 01 April 2020
Accepted: 04 June 2020
Published: 10 July 2020

Citation:
Escalona E, Muñoz M, Pincheira R, Elorza ÁA and Castro AF (2020) Cytosolic NUAK1 Enhances ATP Production by Maintaining Proper Glycolysis and Mitochondrial Function in Cancer Cells. Front. Oncol. 10:1123. doi: 10.3389/fonc.2020.01123

NUAK1 is an AMPK-related kinase located in the cytosol and the nucleus, whose expression associates with tumor malignancy and poor patient prognosis in several cancers. Accordingly, NUAK1 was associated with metastasis because it promotes cell migration and invasion in different cancer cells. Besides, NUAK1 supports cancer cell survival under metabolic stress and maintains ATP levels in hepatocarcinoma cells, suggesting a role in energy metabolism in cancer. However, the underlying mechanism for this metabolic function, as well as its link to NUAK1 subcellular localization, is unclear. We demonstrated that cytosolic NUAK1 increases ATP levels, which associates with increased mitochondrial respiration, supporting that cytosolic NUAK1 is involved in mitochondrial function regulation in cancer cells. NUAK1 inhibition led to the formation of "donut-like" structures, providing evidence of NUAK1-dependent mitochondrial morphology regulation. Additionally, our results indicated that cytosolic NUAK1 increases the glycolytic capacity of cancer cells under mitochondrial inhibition. Nuclear NUAK1 seems to be involved in the metabolic switch to glycolysis. Altogether, our results suggest that cytosolic NUAK1 participates in mitochondrial ATP production and the maintenance of proper glycolysis in cancer cells. Our current studies support the role of NUAK1 in bioenergetics, mitochondrial homeostasis, glycolysis and metabolic capacities. They suggest different metabolic outcomes depending on its subcellular localization. The identified roles of NUAK1 in cancer metabolism provide a potential mechanism relevant for tumor progression and its association with poor patient prognosis in several cancers. Further studies could shed light on the molecular mechanisms involved in the identified metabolic NUAK1 functions.

Keywords: NUAK1, cancer metabolism, cell bioenergetic, oxidative cells, glycolytic switch, seahorse assay, mitochondrial donut

INTRODUCTION

Cancer metabolism has become a trending topic in cancer research because it participates in tumorigenesis and cancer progression. Tumor cells are continuously exposed to wide metabolic changes, such as nutrient starvation, hypoxia, and microenvironment acidification (1, 2). Thus, tumor progression success depends on the capacity of cancer cells to adapt and surpass this metabolic challenge (2). Understanding the mechanisms and proteins involved in cancer cell's metabolic changes is critical for the development of new therapies.

NUAK1 is a serine/threonine kinase related by sequence homology to the catalytic α-subunits of the metabolic regulator AMPK (3). Multiple cancers overexpress NUAK1, such as hepatocarcinoma (4), colon cancer (5), glioma (6), and breast cancer within others (7, 8). NUAK1 shows stage-dependent expression in cancer tissues and associates with tumor malignancy and poor patient prognosis (6, 9–11). According to its association with cancer, NUAK1 plays a role in several processes related to tumor progression, including cell migration (12), invasion, and metastasis (13).

Additionally, NUAK1 plays a role in the survival of cancer cells (14, 15), protecting them from cell death induced by oxidative or metabolic stress. NUAK1 protected from metabolic stress through maintaining energy balance in MYC-driven cancer cells, which were unable to balance ATP levels, and mitochondrial function in the absence of NUAK1 (16). Also downstream of MYC, Calcium/PKCα-dependent activation of NUAK1 supported cell survival by engaging the AMPK-mTORC1 metabolic checkpoint (17). NUAK1 association with metabolism and survival seems to be independent of p53, the most frequently mutated and inactivated gene in cancer (18). Although there is a report suggesting that NUAK1 can regulate the p53 transcription factor, knock-down of NUAK1 provoked loss of ATP and cell death in p53-null hepatoma cells (16). Thus, NUAK1 might also be relevant in metabolism and tumor progression in a p53-independent context.

We recently showed that NUAK1 has nuclear and cytosolic subcellular locations regulated by active nuclear transport (19). Others and our studies indicate that NUAK1 distribution is cell- and context-specific, and might be associated with the clinical stage of cancer, displaying a cytosolic accumulation in late-stages histopathological samples (6, 10). Thus, NUAK1 may have specific functions according its subcellular localization. Consistent with a nuclear-associated function, NUAK1 was recently involved in promoting spliceosome activity (20). In association with its effect on cell migration, the cytosolic NUAK1 phosphorylates the myosin phosphatase targeting-1 (MYPT1), promoting cell detachment (12). However, it is unknown how NUAK1's effect on metabolism associates with its subcellular localization.

Here, we show that cytosolic NUAK1 increases the cellular bioenergetic state, mainly associated with mitochondrial respiration maintenance. Additionally, perturbations on NUAK1 function affect mitochondrial morphology. NUAK1 also shows a role in glycolysis, particularly in its nuclear localization. Our work suggests that the subcellular localization of NUAK1 is relevant to its specific metabolic effects.

MATERIALS AND METHODS

Cell Culture

Cancer cells lines HCT116 p53 null, kindly provided by Dr. B. Vogelstein (Johns Hopkins Medicine, USA) (21), and HeLa (ATCC® CCL-2™, Manassas, VA) were cultured in Dulbecco's modified Eagles's medium (DMEM) containing 4.5 g/l glucose, 2 mM L-glutamine, and 1 mM sodium pyruvate (Corning, New York, USA). MDA-MB-231 cells (ATCC® HTB-26) were cultured in DMEM containing 1 g/l glucose, 2 mM L-glutamine and 1 mM sodium pyruvate (HyClone, Logan, UT, USA) and MCF-7 cells (ATCC® HTB-22) were maintained in Minimal Essential Medium (MEM) with Earle's Balanced Salt Solution (EBSS) containing 1 g/l glucose, 2 mM L-glutamine and 1 mM sodium pyruvate (HyClone). All culture mediums were supplemented with 100 ug/ml streptomycin (HyClone), 100 U/ml penicillin (HyClone), 2.5 ug/ml Plasmocin (InvivoGen, San Diego, CA, USA), 10% fetal bovine serum (Biological Industries) and incubated at 37 °C in 5% CO_2. *Mycoplasma*-free cultures were frequently tested with EZ-PCR Mycoplasma Kit (Biological Industries, CT, USA). The hypoxic environment (1% O_2) was generated in a hypoxia chamber (STEMCELL Technologies, Vancouver, Canada).

Cell Transfection

Cells were transfected using Lipofectamine 3000 (ThermoFisher, Waltham, MA, USA) or Lipofectamine 2000 (for HeLa cells). For the overexpression of wild type NUAK1 and a nuclear-deficient NUAK1 mutant (19), we used pCMV-FLAG-hNUAK1 and pCMV-FLAG-hNUAK1-KR43/70AA (NUAK1cyt) plasmids, respectively, and the pCMV-2-FLAG plasmid as control. The pLKO system was used to silence NUAK1 expression (22). The shRNA for NUAK1: 5′- TGGCCGAGTGGTTGCTATAAA-3′ was purchased from Sigma-Aldrich (St. Louis, MO, USA).

Chemicals and Antibodies

Protease inhibitor and Phosphate inhibitor cocktails, 2-Deoxy-D-glucose, Oligomycin A, Carbonyl cyanide 4-(trifluoromethoxy)phenylhydrazone, Antimycin A and Rotenone were purchased from Sigma-Aldrich. HTH-01-015, a potent and selective NUAK1 inhibitor (23) was from Tocris (Bristol, UK). Fluorophores Tetramethylrhodamine Ethyl Ester, Perchlorate (TMRE), MitoTracker™ Green FM, and Hoechst 33,342 were from ThermoFisher. AccuRuler RGB plus protein ladder was purchased from MaestroGen Inc. (Hsinchu City, Taiwan). Anti-NUAK1 antibody (#4458) was from Cell Signaling (Danvers, MA, USA), and the anti-FLAG (M2) was from Sigma-Aldrich. Antibodies against β-Actin (AC-15), ATP5B (E-1), and TOM20 (F-10) were purchased from Santa Cruz Biotechnology (Dallas, TX, USA). Total OXPHOS Rodent WB Antibody Cocktail (ab110413) was from Abcam (Cambridge, United Kingdom). Goat Secondary antibodies anti-mouse IgG-HRP and anti-rabbit IgG-HRP conjugates were

purchased from Bio-Rad (Hercules, CA, USA). The anti-mouse Alexa-488 antibody (A11001) was from ThermoFisher.

Immunoblotting

Cell lines were lysed with modified NP-40 buffer (1%, NP-40, 25 mM Tris/HCl pH 7.4, 2.2 mM $MgCl_2$, 1 mM EDTA, NaCl 150 mM, 5% Glycerol). Total proteins from lysates were fractionated by SDS–polyacrylamide gel electrophoresis and transferred to PDVF membranes. Finally, membranes were incubated 3 min with ECL Western Blotting Detection Reagent (GE Healthcare, Amersham, UK). Immunolabeled proteins were visualized in Syngene PXi6 Documentation System (Frederick, MD, USA).

Immunofluorescence Microscopy

Cells grown on coverslips were prepared as previously described (19). After incubation with the FLAG and the secondary anti-mouse Alexa-488 antibodies, images were obtained with an LMS 780 spectral confocal system (Zeiss, Jena, Germany).

ATP Measurement

An equal number of cells were seeded in 96-well plates and 16 h later transfected. Twenty-four hours post-transfection of cells, ATP was measured by using the ATP Determination Kit (Invitrogen) according to the manufacturer's protocol. ATP levels were expressed as the percentage of their control group (arbitrary set to 100%) and normalized to the corresponding protein concentration.

Oxygen Consumption Rate (OCR) and Extracellular Acidification Rate (ECAR)

The mitochondrial respiratory activity and glycolysis status of live cells were measured by detection of cellular oxygen consumption rate (OCR) and extracellular acidification rate (ECAR), using a Seahorse XF24 (Agilent, Santa Clara, CA, USA). Briefly, 3 x 10^4 MCF-7 or MDA-MB-231 cells per well were plated on the XF24 culture plate and incubated at 37°C in 5% CO_2. The following day, the cells were incubated 1 h at 37 °C without CO_2 and washed 3 times with seahorse medium containing phenol red-free DMEM base (D5030, Sigma-Aldrich), 2 mM L-glutamine, and 1 mM pyruvate. The XF24 culture plate plus the cartridge pre-incubated with Seahorse XF Calibrant Solution (103059-000, Agilent) were mounted in the analyzer. OCR was recorded as pmolO_2/min, and ECAR was recorded as mpH/min. On the course of the assay, four sequential injections were performed after three readings in order to analyze OXPHOS and glycolytic parameters. For MCF-7 cells, it was sequentially injected to final concentration 5.5 mM glucose, 1.2 μM Oligomycin A, 0.5 μM FCCP, and finally 2 μM Rotenone with 2 μM Antimycin A. For MDA-MB-231 cells, it was used 5.5 mM glucose, 1 μM Oligomycin A, 1 μM FCCP, 1 μM Rotenone, and 1 μM Antimycin A. Right after the assay is ended, OCR and ECAR from each sample were normalized to the corresponding total protein concentration before calculation of metabolic parameters. Briefly, cells were lysed with SDS Lysis Buffer containing 20 mM HEPES, 2 mM EDTA, 0.5% Triton X-100, 0.1% SDS and 1 mM PMSF at 4°C. Proteins concentration was quantified by Bradford method. For OXPHOS parameters, we used normalized OCR and set the Non-Mitochondrial Oxygen Consumption (Non-MOC) as the minimum rate after Rotenone/antimycin A injection. Basal respiration was the last rate after glucose injection minus the Non-MOC; Maximal respiration was the maximum rate after FCCP injection minus the non-MOC; Proton Leak was the minimum rate after oligomycin injection minus the Non-MOC. ATP Production Coupled Respiration was the last rate before oligomycin injection minus the minimum rate after oligomycin injection, and Spare Respiratory Capacity was the maximal respiration minus the basal respiration. To analyze glycolysis, we used normalized ECAR. Glycolysis parameter was the maximum rate before oligomycin injection minus the last rate before glucose injection. Glycolytic capacity was the maximum rate after oligomycin injection minus the last rate before glucose injection, and glycolytic reserve was the glycolytic capacity minus the glycolysis parameter. All assays were done in triplicate and repeated three times.

Lactate Measurement

HCT116 p53-null cells (3.5 x 10^5) were plated in a 24-well plate and incubated overnight at 37 °C in 5% CO_2. The medium was replaced for phenol red-free medium, and cells were treated for 24 h. For recovering extracellular lactate, the supernatant was mixed with trichloroacetic acid 0.6N in 1:2 proportion in ice, mixed for 30 s, incubated at 4°C for 5 min and interfering proteins were precipitated and removed by centrifugation at 1500xG. Extracellular lactate concentration was calculated by measurement of NADH product obtained by a coupled-enzymatic method using L-lactate dehydrogenase (Sigma). NADH was detected by absorbance at 340 nm. Simultaneously, the cells were lysed with SDS Lysis Buffer, and protein concentration was measured by Bradford method. Results were expressed as μM lactate/μg protein. All assays were done in triplicate.

In vivo Microscopy

Cells were plated in a 35 mm imaging dish and incubated overnight at 37 °C in 5% CO_2. For the nuclear and mitochondrial staining, the cells were incubated with 200 nM Mitotracker Green and 5 μg/ml Hoechst 33,342 for 30 min in PBS at 37 °C in 5% CO_2. After washed the cells twice with PBS, 10 mM TMRE was added in a fresh culture medium. For the *in vivo* microscopy, the cells were maintained in the Chamlide chamber (Lice cell instrument, Seoul, Korea) and images were capture using Olympus FV1000 microscopy (Center Valley, PA, USA). The Z-stack was transformed into maximal intensity projection. The image analysis was performed using ImageJ software (24).

Statistical Analysis

Statistical analysis and graphics were performed with GraphPad Prism 6. Statistical significance was determined by unpaired Student's *t*-test or two-way ANOVA with Holm-Sidak correction. Differences were considered statistically significant if $p < 0.05$.

RESULTS

Cytosolic NUAK1 Enhances Cellular ATP in Cancer Cells

We have previously found that endogenous NUAK1 has a diverse subcellular localization depending on the cancer cell line, mostly located in the nucleus or the cytoplasm, or with an equilibrated distribution (19). From these previous studies, we choose cancer cells with high nuclear NUAK1 expression (HeLa and HCT116 p53-null cells) or with high cytosolic expression (MCF-7 cells). To initially investigate whether the metabolic function of NUAK1 associates with a specific subcellular location, we used a previously characterized nuclear-deficient NUAK1 mutant, from now on cytosolic NUAK1. Like the endogenous NUAK1 (19), immunocytochemistry assay showed that overexpressed wild type NUAK1 was mainly in the nucleus of HeLa cells, while the cytosolic NUAK1 showed the expected location (**Figure 1A**). Both wild type and cytosolic NUAK1 significantly increased ATP levels in HeLa cells; however, the cytosolic NUAK1 induced a higher ATP increment (**Figure 1B**). We found that only the cytosolic NUAK1 increases ATP levels in the colon HCT 116 p53-null cancer cells (**Figure 1C**), where endogenous NUAK1 is not detected in the cytoplasm (19). Although MFC-7 cells have high endogenous cytosolic NUAK1 expression (19), the expression of the cytosolic NUAK1 mutant could further increase the ATP levels, although to a lesser extent (**Figure 1D**). Altogether, our results suggest that the cytosolic NUAK1 associated with cancer cell bioenergetics.

NUAK1 Affects Mitochondrial Respiration Parameters and Mitochondrial Membrane Potential

The increase in cellular ATP could be due to alterations on either ATP consumption or ATP production. To discern between these two processes, we examined the mitochondrial responses by measuring the OCR under normal conditions or stimulation with pharmacological mitochondrial modulators. According to the above results, for these assays, we used MCF-7 cancer cells because they depend more on mitochondrial function for their bioenergetics demands (25). In addition, MCF-7 cells have high cytosolic NUAK1 expression, which is suitable to infer the role of the endogenous NUAK1. We used 10 μM HTH-01-015, a selective NUAK1 kinase inhibitor (23, 26). We found that NUAK1 inhibition significantly decreased maximal respiration (FCCP-stimulated) in MCF-7 cells; still, HTH-01-015 affected mitochondrial spare respiratory capacity, but no other mitochondrial respiration parameters (**Figure 2A**). The decrease in maximal respiration by NUAK1 inhibition was not accompanied by changes in mitochondrial protein expression (**Figure 2B**). Supporting that NUAK1 activity affects mitochondrial function, HTH-01-015 treatment (**Figure 2C**) and shRNA-mediated knock-down of NUAK1 expression (**Figure 2D**) significantly increased the mitochondrial membrane potential ($mt\Delta\Psi$).

Then, we analyzed the association of the increase of cellular ATP by the cytosolic NUAK1 in MCF-7 cells with mitochondrial respiration. According to the above results, the cytosolic NUAK1 increased maximal respiration (**Figure 3A**) and significantly decreased the $mt\Delta\Psi$ (**Figures 3B,C**), indicating that cytosolic NUAK1 induces ATP synthase activity (oligomycin-insensitive respiration showed no NUAK1-induced leaking). Besides, no significant changes in mitochondrial volume were observed (**Figure 3D**). To further confirm the role of the cytosolic NUAK1 in breast cancer cells, we used MDA-MB-231 cells, where NUAK1 only detected in the cytosolic fraction (19). Accordingly, we also found that NUAK1 inhibition significantly decreases maximal mitochondrial respiration and spare mitochondrial capacities (**Figure 3E**). In agreement with an exclusive cytosolic location of NUAK1 in MDA-MB-231 cells, the maximal respiration parameter was much higher than in MCF-7 cells and was strongly affected by NUAK1 inhibition. Altogether, our data suggest that the cytosolic NUAK1 enhances breast cancer cell bioenergetics by increasing the mitochondrial respiratory capacity.

The Downregulation of NUAK1 Induces Mitochondrial Morphology Alterations

Mitochondria are dynamic organelles, and their structures frequently reflect bioenergetics state or dysfunctions. Thus, to understand the NUAK1 function on mitochondria, we additionally investigated whether it affects mitochondria morphology, identifying networked, tubular, fragmented, and large and round mitochondria (**Figure 4A**). We observed that HTH-01-015 treatment drastically changed the mitochondria morphology of MCF-7 cells, from mainly networked and tubular to large and round mitochondrial structure (**Figures 4B,C**). Interestingly, mitotracker green images showed a mitochondrial structure known as "donut" rather than the typical punctate mitochondrion (**Figure 4B**). To validate that our morphological observations were specifically associated with the inhibition of NUAK1, we knocked-down NUAK1 in MCF-7 cells and performed mitochondria morphology analysis. The knock-down of NUAK1 also changed the mitochondrial morphology from networked to large and round shape (**Figures 4D,E**), but we observed less "donut" structures than the treatment with the inhibitor (**Figure 4D**). On the other hand, the overexpression of the cytosolic NUAK1 showed no significant impact on mitochondrial morphology (**Figure 2B**). These data suggest that NUAK1 activity maintains a suitable mitochondrial morphology. Interestingly, NUAK1 inhibition by HTH-01-015 showed a significant increase in mitochondrial volume (**Figure 4F**), whereas the NUAK1 knock-down showed no significant differences between groups (**Figure 4G**). This apparent discrepancy may be related to differences in the time points for the volume evaluation, measured at 4 h after HTH-01-015 treatment or at 24 h in NUAK1 knock-down cells. Summarizing, our data showed that NUAK1 is necessary for maintaining proper mitochondrial morphology in MCF-7 cells.

NUAK1 Is Involved in Glycolytic Capacity Regulation

Alterations in mitochondrial metabolism are usually accompanied by glycolysis regulation, allowing energy balance

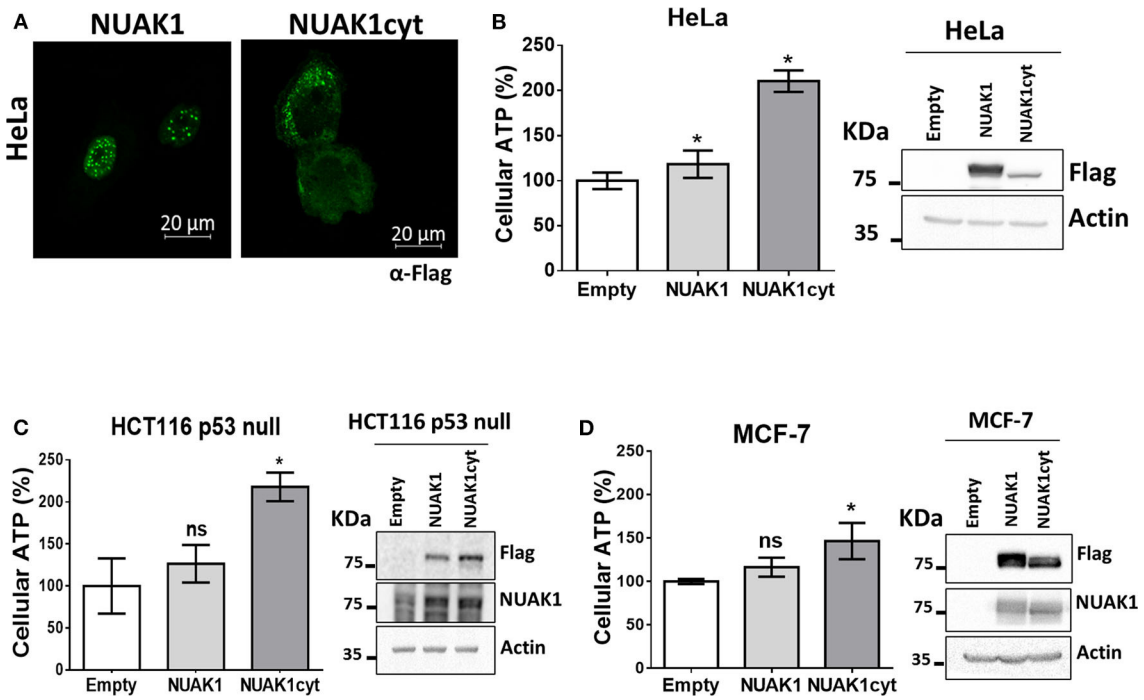

FIGURE 1 | Cytosolic NUAK1 increases cellular ATP in cancer cells. **(A)** Immunocytochemistry images of NUAK1 location in HeLa cells expressing FLAG-NUAK1 WT or FLAG-hNUAK1-KR43/70AA (NUAK1cyt) mutant. Cells were stained with FLAG-antibody, 630X zoom. ATP levels in **(B)** HeLa, **(C)** HCT116 p53-null and **(D)** MCF-7 cells 24 h post-transfection with FLAG-NUAK1 WT (gray bar) or FLAG-NUAK1cyt mutant vector (dark gray bar). Empty vector was used as control (white bar) and results were expressed as a percentage relative to the control group. The results are representative of three independent experiments ($n = 3$). Each bar represents the mean ± S.D, $^*p < 0.05$. On the right, immunoblots showing NUAK1 expression. NUAK1 was detected with FLAG antibody or a specific antibody against NUAK1. Actin was used as the loading control.

(27). To test this, we measured ECAR, which reflects the rate of lactic acid production by glycolysis. We found that the cytosolic NUAK1 did not significantly affect the glycolytic rate in MCF-7 cells (**Figure 5A**). However, NUAK1 inhibition significantly decreased their glycolytic capacity (**Figure 5B**). Although there was a small reproducible effect on the glycolytic rate, it was not significant. To confirm the cytosolic NUAK1 involvement in the glycolytic capacity, we evaluated it in MDA-MB-231 cells. We also found that NUAK1 inhibition significantly decreases glycolytic capacity (**Figure 5C**), suggesting that the cytosolic NUAK1 maintains these metabolic capacities. Since NUAK1 inhibition affected both mitochondrial and glycolytic capacity, we evaluated whether the ATP level remains balance in NUAK1-inhibited cells. We found that NUAK1 inhibition did not affect ATP in MCF-7 cells under normal conditions, where neither mitochondrial nor glycolytic functions were challenged (**Figure 5D**). To redirect cellular metabolism to glycolysis, we inhibited the mitochondria with oligomycin. **Figure 5D** shows that under this condition, HTH-01-015 significantly decreased cellular ATP, without affecting cell viability (data are not shown). Thus, associated with the decrease of glycolytic capacity, NUAK1 inhibition decreases cell energy in a condition of metabolic redirection from OXPHOS to glycolysis. Thereby, our findings suggest that cytosolic NUAK1 keeps ATP balance by maintaining the glycolytic capacity.

Nuclear NUAK1 Plays a Role in the Glycolytic Switch

Because of the low nuclear expression of NUAK1 in MCF7 cells, we could not discard that this nuclear NUAK1 is responsible for the small reproducible but not significant effect on the glycolytic rate in these cells (see **Figure 5B**). To evaluate it, we analyzed cells with high nuclear NUAK1 expression. Between the HeLa and the HCT116 p53-null cells, we choose the HCT116 p53-null cells because endogenous NUAK1 is only detected in the nucleus (19). In addition, we used the HCT116 p53-null cell model because NUAK1's role in cell survival has been related to the regulation of the p53 transcription factor (28), which is known to affect glycolysis (29). According to a p53-independent effect, shRNA-mediated knock-down of NUAK1 inhibited HCT116 p53-null cell survival under serum deprivation (data not shown). To directly evaluate an effect on glycolysis, we analyzed NUAK1-dependent lactate production. We found that NUAK1 knock-down (**Figure 6A**) decreased lactate production in HCT116 p53-null cells under basal conditions (**Figure 6B**) and blocked their metabolic switch to glycolysis under mitochondrial inhibition (**Figure 6B**). These results suggested that cells required nuclear NUAK1 for lactate production and glycolytic switch. Accordingly, wild type NUAK1, but not the cytosolic NUAK1, significantly increased lactate production under condition of mitochondrial inhibition by hypoxia or the oligomycin inhibitor

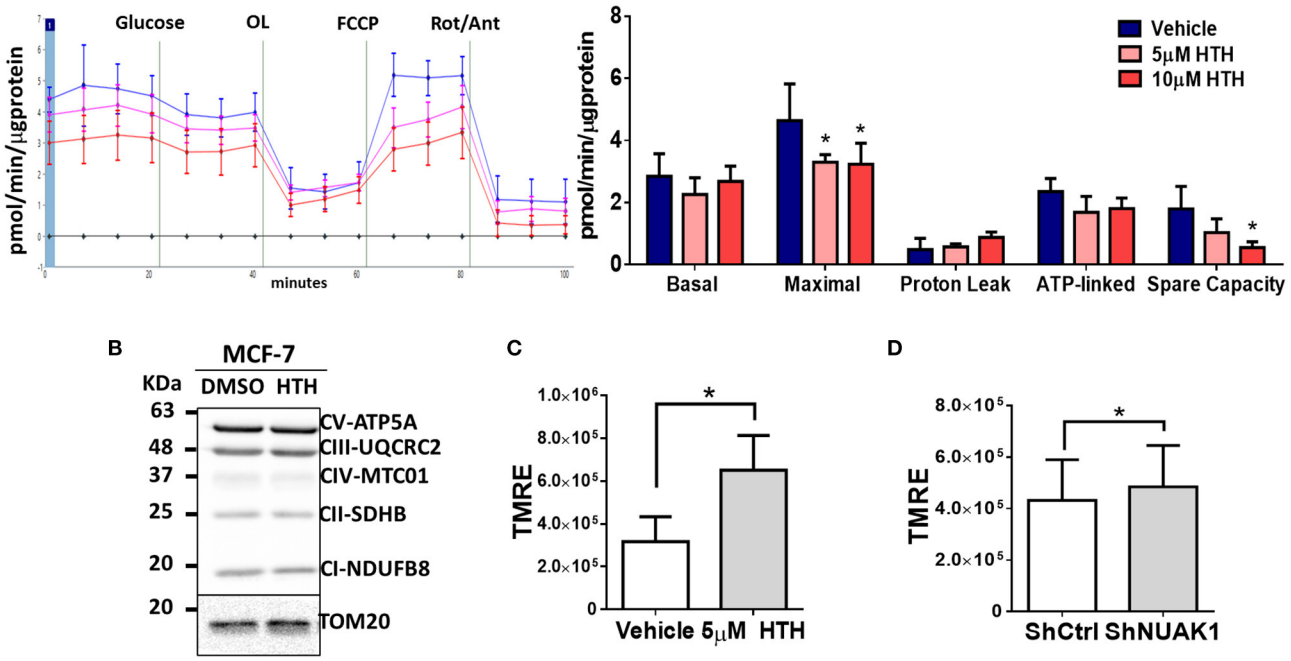

FIGURE 2 | NUAK1 allows proper mitochondrial function in breast cancer cells. **(A**,Left**)** Oxygen consumption rates of MCF-7 cells after 4 h incubation with 5 μM (pink curve) or 10 μM (red curve) HTH-01-015, or DMSO used as vehicle (blue curve), measured using the Seahorse XF24. At the times indicated, glucose, oligomycin (OL), FCCP, and Rotenone (Rot) with Antimycin A (Ant) were injected as described in the Methods section. (Right) Respiration parameters from the experiments on the *left*. Graph shows respiration parameters from MCF-7 cells with 5 μM (pink bar) or 10 μM (red bar) HTH-01-015, or DMSO (blue bar). All values were normalized to the corresponding protein concentration. OCR average ± SD from three independent experiments, $^*P < 0.05$. **(B)** Western blot showing OXPHOS complex proteins from MCF-7 cells after 4 h incubation with 5 μM HTH-01-015 or DMSO. TOM20 was used as the loading control. **(C)** Quantification of TMRE mean intensity from *in vivo* microscopy of MCF-7 cells treated for 4 h with 5 μM HTH-01-015 or vehicle ($n = 80$), $^*P < 0.05$. **(D)** Quantification of TMRE mean intensity from *in vivo* microscopy of NUAK1-silenced MCF-7 cells and control group ($n = 80$), $^*p < 0.05$.

in HCT116 p53-null cells (**Figure 6C**). Thus, nuclear NUAK1 increases glycolysis and is essential for the success of the glycolytic switch.

DISCUSSION

Our studies indicate that NUAK1 plays a role in the maintenance of glycolytic and respiratory capacities of cancer cells, suggesting that it affects the metabolic state and adaptation of tumors during cancer progression. Also, they suggest that the metabolic outcome depends on the NUAK1 subcellular distribution.

Constant ATP supply is essential for almost all cellular processes, including biomolecules synthesis, cytoskeleton remodeling or signaling phosphorylation (30). In this work, we found that the cytosolic NUAK1 upregulates mitochondrial ATP production, likely by inducing ATP synthase activity. Complete glucose oxidation coupled to TCA cycle and oxidative phosphorylation defines cancer cells susceptibility to apoptosis (31). Accordingly, NUAK1 promoted cell survival and inhibited apoptosis (14, 15); therefore, NUAK1's role in complete glucose oxidation by increased mitochondrial activity could also contribute to tumor viability. However, NUAK1 could also promote cancer cell survival under glucose deprivation (15). Other pathways than glucose oxidation could generate mitochondrial ATP, such as lactate metabolism, glutaminolysis, or fatty acid oxidation (30). Thus, NUAK1 may exert a more integrative regulation for the use of available substrates.

Our data also showed that cytosolic NUAK1 maintains and increases maximal mitochondrial respiration, suggesting that it increases the working capacity of the respiratory chain. Levels of expression of the respiratory complexes are usually associated with the working capacity of the respiratory chain. Because we could not detect any NUAK1-dependent increase in the respiratory complexes nor mitochondrial volumen, NUAK1's effect may be due to increased substrate availability. Nevertheless, we could not discard that NUAK1-dependent phosphorylation of respiratory complexes is responsible for an increase in the respiratory chain activity. Many kinases localize in the mitochondria and affect the mitochondrial function (32). By bioinformatics analysis, NUAK1 does not contain a typical mitochondrial localization signal. However, as reported for other kinases, NUAK1 may form part of a protein complex for translocation into the mitochondrial matrix space (32). This possibility deserves future studies.

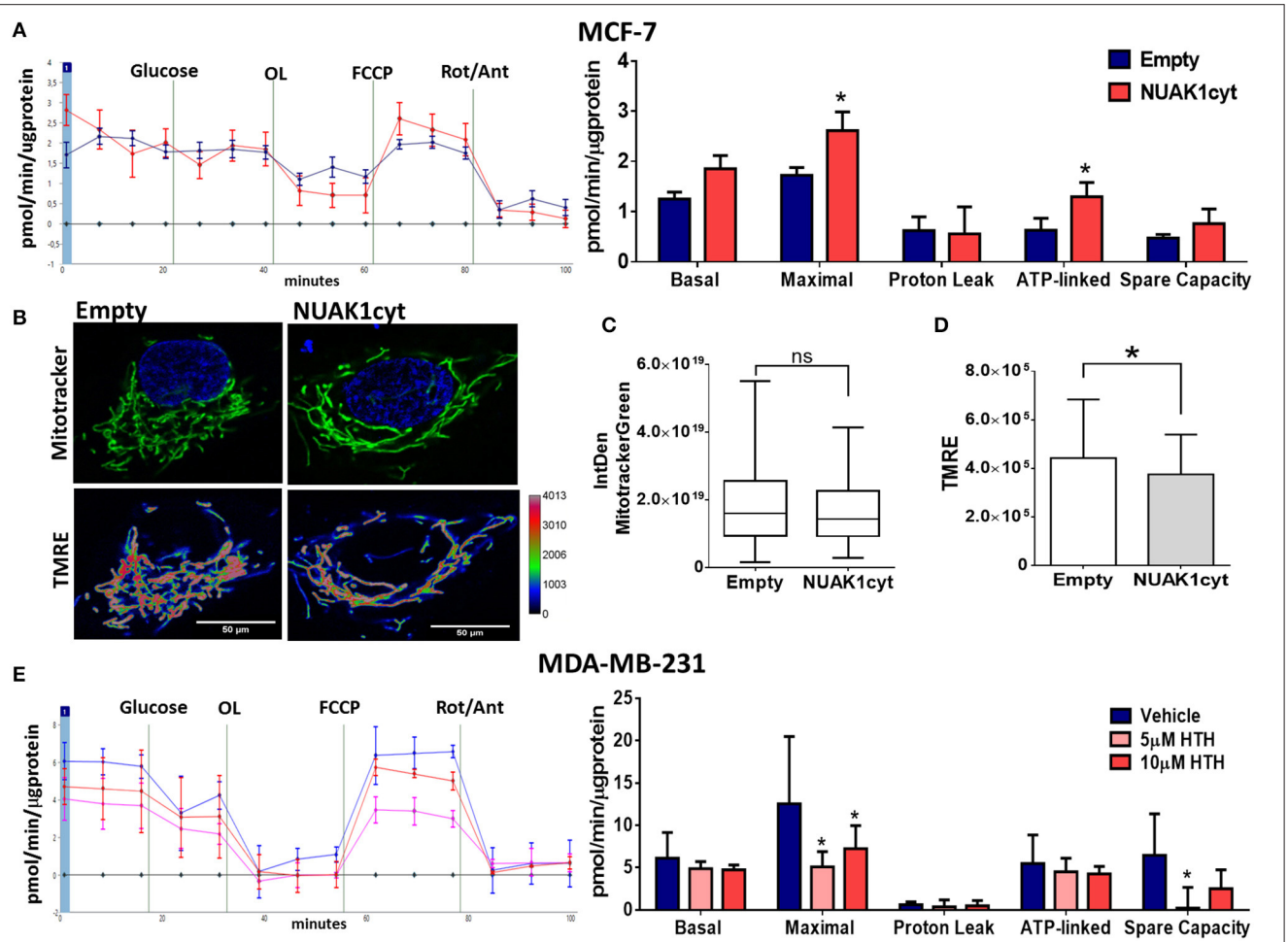

FIGURE 3 | Cytosolic NUAK1 expression is involved in mitochondrial function regulation in breast cancer cells. **(A**, Left**)** Oxygen consumption rates of MCF-7 cells 24 h post-transfection with FLAG-NUAK1cyt mutant (red curve) or empty vector (blue curve), measured using the Seahorse XF24. At the times indicated, glucose, oligomycin (OL), FCCP, and Rotenone (Rot) with Antimycin A (Ant) were injected as described in the Methods section. (Right) Respiration parameters from the experiments on the *left*. Graph shows respiration parameters from MCF-7 cells transfected with FLAG-NUAK1cyt mutant (red bar) or empty vector (blue bar). All values were normalized to the corresponding protein concentration. OCR average ± SD from 3 independent experiments, $^*p < 0.05$. **(B)** *in vivo* microscopy images of MCF-7 cells expressing FLAG-NUAK1cyt mutant or empty vector stained with mitotracker green (green), TMRE and Hoechst for nuclei (blue). Fluorescence intensity of TMRE is represented in pseudo color scale ("Rainbow RGB" in ImageJ software). 600X optical zoom plus 3X digital zoom. **(C)** Quantification of mitotracker green integrated density ($n = 90$). $^*p < 0.05$. **(D)** Plots of TMRE mean intensity quantification ($n = 90$). $^*p < 0.05$. **(E)** Same as in **(A)** for MDA-MB-231 cells. (Left) Oxygen consumption rates of MDA-MB-231 cells with 5 µM (pink curve) or 10 µM (red curve) HTH-01-015, or DMSO (blue curve). (Right) Respiration parameters from the experiments on the left. Graph shows respiration parameters from MDA-MB-231 cells with 5 µM (pink bar) or 10 µM (red bar) HTH-01-015, or DMSO (blue bar). All values were normalized to the corresponding protein concentration. OCR average ± SD from three independent experiments, $^*p < 0.05$.

Oxidative cells have high anabolic metabolism due to high protein and nucleotide biosynthesis, maintaining high mitochondrial biomass and activity (33). We were unable to find NUAK1 overexpression-induced changes in the mitochondrial volume; however, we cannot exclude that sustained NUAK1 overexpression, common in many cancers, could affect it. Studies have shown that within the heterogeneous cell population of a tumor, oxidative intratumoral cells are the most proliferative, invasive and resistant to chemotherapy and radiotherapy (34, 35). Thus, NUAK1-dependent metabolic effects may explain the aggressiveness of cancers associated with abnormal NUAK1 expression.

Cell energy remains balanced after mitochondrial inhibition due to the increase in glycolysis (27). When the mitochondria activity was pharmacologically inhibited, NUAK1-inhibited cells were unable to maintain ATP levels, indicating that NUAK1 maintains glycolytic ATP levels. However, we cannot discard some contribution from the glutaminolysis pathway. Because glutamine was present in all our experimental conditions, it is possible that this substrate is used as an alternative energy source, compensating for defects in OXPHOS through mitochondrial substrate-level phosphorylation (mSLP) (36–38).

Previous research showed that NUAK1 suppresses glucose uptake by negatively regulating insulin signaling and glycogen

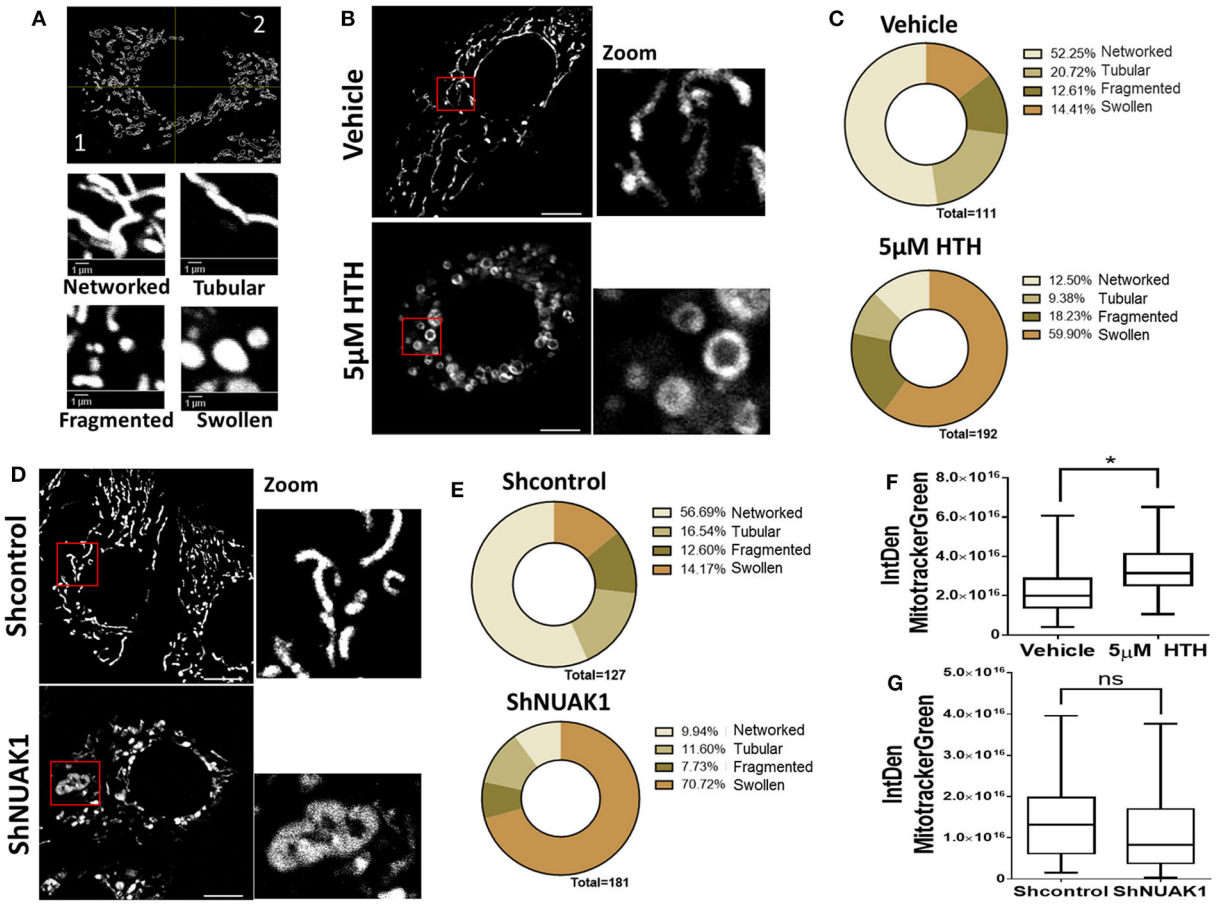

FIGURE 4 | Downregulation of N UAK1 function induces mitochondrial morphology alterations in MCF-7 cells. **(A)** *in vivo* microscopy of MCF-7 cells treated for 4 h with 5 μM HTH-01-015 or vehicle, stained with TMRE (red) and mitotracker green (green). Scale bar equal to 10 μm. 600X optical zoom plus 5X digital zoom. **(B)** Quantification of mitotracker green integrated density of MCF-7 cells treated with 5 μM HTH-01-015 or vehicle ($n = 80$), $^*p < 0.05$. **(C)** Representative image used for mitochondrial morphology quantification. Mitochondria were classified in networked, tubular, fragmented and swollen from two quadrants. **(D)** Mitochondrial morphology quantification of MCF-7 cells treated for 4 h with 5 μM HTH-01-015 and control cells. **(E)** *in vivo* microscopy of NUAK1 depleted MCF-7 cells and control group stained with TMRE (red) and mitotracker green (green). Scale bar equal to 10 μm. 600X optical zoom plus 5X digital zoom. **(F)** Quantification of mitotracker green integrated density of NUAK1 depleted MCF-7 cells and control cells ($n = 80$), $^*p < 0.05$. **(G)** Mitochondrial morphology quantification of NUAK1 depleted MCF-7 cells and control cells ($n = 80$), $^*p < 0.05$.

storage in the normal oxidative muscle (39). On the contrary, our data propose that the cytosolic NUAK1 maintains glycolytic capacity and the glycolysis-associated cell energy in the abnormal genetic and metabolic context of cancer. Glycolytic capacity may reflect increased activity of enzymes and more efficient expression of alternative isozymes, allowing cells to confront harsh conditions, such as hypoxia (27, 40). The four key points that raise the glycolysis rate are glucose import, hexokinase, phosphofructokinase, and lactate export (40). Several reports describe an increase in the expression of glycolytic enzymes in cancers. In particular, at least one isozyme catalyzing each of the four key points is elevated in human tumors (40). Our studies suggested that nuclear NUAK1 is necessary for the cellular glycolytic switch and the increase of extracellular lactate in a p53-null context. It was recently demonstrated that nuclear NUAK1 promotes spliceosome activity and regulates RNA synthesis (20). Thus, nuclear NUAK1 may transcriptionally affect the expression of enzymes controlling key points of glycolysis. Whether the effect of nuclear NUAK1 changes when p53 is present remains undefined.

It was shown that NUAK1 downregulation dramatically declines HEPG2 cells' tolerance to glucose starvation-induced hypoxia (41). Because metabolic changes in cancer cells are balanced between glycolysis and oxidative metabolism (27), the study indicated that NUAK1 keeps cells metabolically prepared to face microenvironmental energetic adversities. Accordingly, our studies suggest that NUAK1 promotes and maintains both the glycolytic and the oxidative phenotypes. Cytosolic NUAK1 affected both, the maximum rate of glycolysis and mitochondrial respiration. The maximum rate referred to the "metabolic capacity" of cells to respond to an acute increase in energy demand (27).

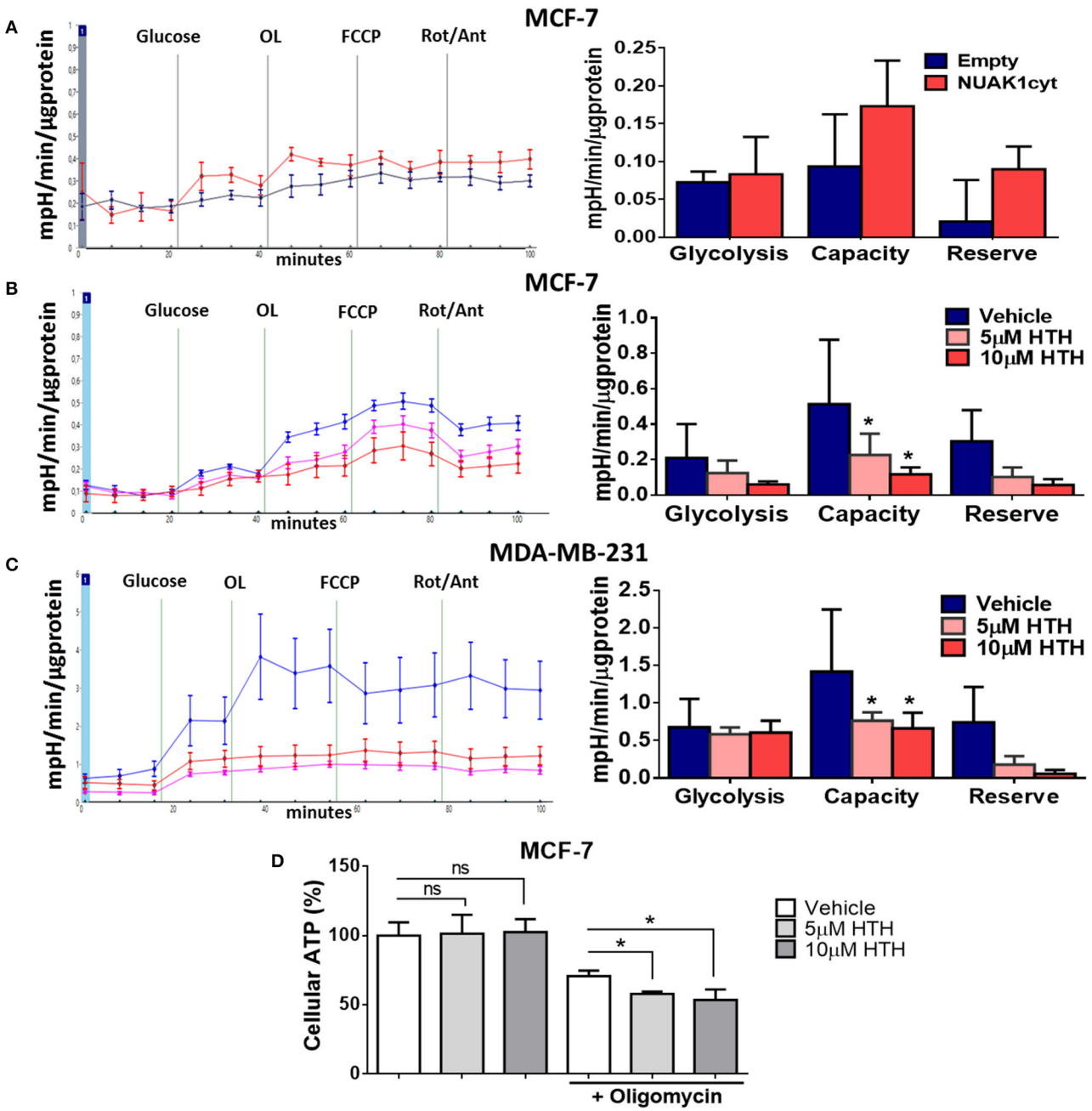

FIGURE 5 | Cytosolic NUAK1 plays a role in the regulation of glycolysis in breast cancer cells. **(A**, Left**)** Kinetic of extracellular acidification from MCF-7 cells 24 h post-transfection with FLAG-NUAK1cyt mutant (red curve) or empty vector (blue curve), measured using the Seahorse XF24. At the times indicated, glucose, oligomycin (OL), FCCP, and Rotenone (Rot) with Antimycin A (Ant) were injected as described in the Methods section. (Right) Glycolytic parameters evaluation from the experiments on the *left*. Graph shows MCF-7 cells with FLAG-NUAK1cyt mutant (red bar) or empty vector (blue bar). **(B)** Same as in **(A**, Left**)**. Kinetic of extracellular acidification from MCF-7 cells after 4 h of treatment with 5 µM HTH-01-015 (pink curve), 10 µM HTH-01-015 (red curve) or vehicle (blue curve). Right. Glycolytic parameters evaluation from the experiments on the *left*. Graph shows cells with 5 µM HTH-01-015 (pink bar), 10 µM HTH-01-015 (red bar) or vehicle (blue bar). **(C)** Same as in **(B)** for MDA-MD-231 cells. (Left) Kinetic of extracellular acidification from cells with 5 µM HTH-01-015 (pink curve), 10 µM HTH-01-015 (red curve) or vehicle (blue curve). (Right) Glycolytic parameters evaluation from the experiments on the *left*. Graph shows cells with 5 µM HTH-01-015 (pink bar), 10 µM HTH-01-015 (red bar) or vehicle (blue bar). All values were normalized to the corresponding protein concentration. **(A–C)** ECAR average ± SD from three independent experiments, $^*p < 0.05$. **(D)** ATP levels from MCF-7 cells treated 4 h with 5 µM HTH-01-015 (pink bar), 10 µM HTH-01-015 (red bar) or vehicle (blue bar). Also, all groups were incubated with 1 ug/ml oligomycin A. Results were expressed as a percentage relative to the control group. The results are representative of two independent experiments ($n = 3$). Each bar represents the mean ± S.D, $^*p < 0.05$.

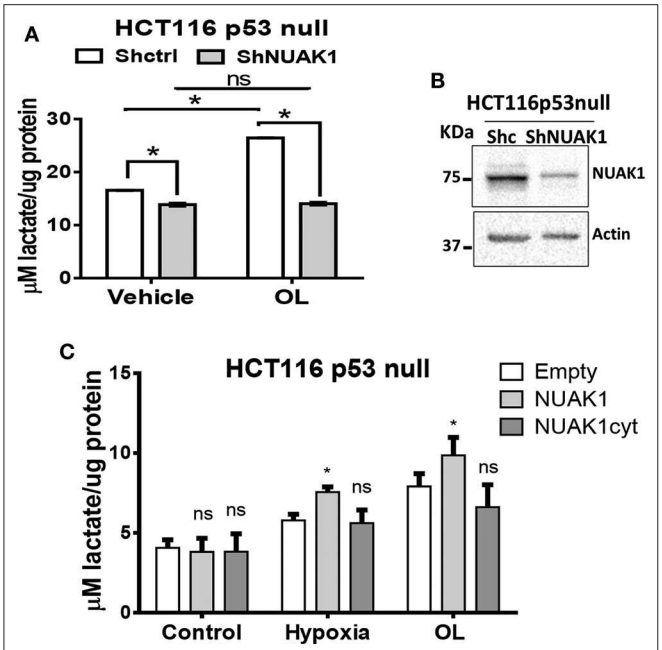

FIGURE 6 | Nuclear NUAK1 allows glycolysis switch in HCT116 p53 null cancer cells. **(A)** Lactate production evaluation in HCT116p53null cells transfected with shRNA NUAK1 (gray bar) and shRNA scramble as control (white bar). Extracellular lactate was evaluated under normal and 1 ug/ml oligomycin treatment conditions. The results were normalized to the corresponding protein concentration and each bar represents the mean ± S.D ($n = 3$), $^*p < 0.05$. **(B)** Western blot showing the NUAK1 silencing efficiency. Actin was used as the loading control. **(C)** Lactate production evaluation in HCT116p53null cells expressing FLAG-NUAK1 WT (gray bar) or FLAG-NUAK1cyt mutant (dark gray bar). Empty vector was used as the control group (white bar). Extracellular lactate was evaluated under normal condition, after 24 h of hypoxia or 24 h of 1 ug/ml oligomycin treatment. The results were normalized to the corresponding protein concentration and each bar represents the mean ± S.D ($n = 3$), $^*p < 0.05$.

We found that NUAK1 downregulation disrupts mitochondrial morphology. The ring-shaped mitochondria structures induced by NUAK1 inhibition are consistent with those known as "donut" shaped. Donut morphology appears after inhibition of respiratory chain function and under chemical uncoupling (42, 43) and involves the increase of mitochondrial calcium capture and mitochondrial ROS (mtROS) (43) and have pathophysiological significance (44). NUAK1 has been proposed as a key facilitator of the adaptive antioxidant response in colon cancer, playing a protective role against high oxidative stress (26). We have previously reported that oxidative stress retains NUAK1 in the cytosol (19). Although additional studies are needed, the increase of oxidative stress under NUAK1 inhibition may be responsible for the donut-shaped mitochondria.

Liu et al. (16) showed that NUAK1 expression was essential for the development of oncogenic MYC processes, such as maintaining ATP levels, glucose metabolism, TCA cycle, and oxidative phosphorylation. Some of our findings could be due to an effect of NUAK1 downstream of an oncogenic MYC context; however, addressing this possibility requires a detailed molecular study. Still, because NUAK1 protected cells from oncogenic MYC-induced metabolic stress and energy collapse, NUAK1 is also likely downstream of other oncogenes-induced metabolic stress, the hallmark of any cancer.

In summary, our findings show an association between metabolic NUAK1 functions and its subcellular distribution. We associated nuclear NUAK1 with the promotion of glycolysis. NUAK1 has been described as a predominantly nuclear protein in some cancer cells, where it promotes spliceosome activity and regulates RNA synthesis (20). Thus, glycolysis alterations could be an outcome of those NUAK1 nuclear functions. On the other hand, we associated the cytosolic NUAK1 with the maintenance of cellular ATP levels, suggesting that it increases ATP mitochondrial production under normal conditions. However, it can still maintain ATP from glycolysis source under mitochondrial dysfunction, without discarding some potential contribution of mSLP. NUAK1 showed different cell distribution in cancer samples, where cytosolic NUAK1 seems to be relevant in late-stages of cancer (6, 8, 10). Thereby, NUAK1 cell location could be relevant for metabolic adaptation along with tumor progression. Therefore, screening NUAK1 cell distribution in cancer tissues could help elucidate the metabolic state of tumors. Further studies could shed light on the molecular mechanisms associated with the identified metabolic NUAK1 functions and their implications on cancer cell metabolic adaptation during tumor progression.

DATA AVAILABILITY STATEMENT

The raw data supporting the conclusions of this article will be made available by the authors, without undue reservation.

AUTHOR CONTRIBUTIONS

EE, AE, and AC contributed to conception and design of the study. EE contributed to acquisition and analysis of the most data of this work, performed the statistical analysis, and wrote the first draft of the manuscript. MM took part of the microscopy images acquisition, seahorse assays, and performed mitochondria morphology analysis. AE programed and monitored seahorse and microscopy experiments. AC and RP wrote the final draft of the manuscript. AE, AC, and RP are the principal investigators of the FONDECYT grants that funded this work. All authors contributed to manuscript revision, read and approved the submitted version.

FUNDING

This work was supported by the Fondo Nacional de Desarrollo Científico y Tecnológico (FONDECYT) 1160731 and 1201215 (to AC), 1191172 (to RP), 1180983 (to AE), the grant P09-016-F from Millennium Institute on Immunology and Immunotherapy (to AE), and Ph.D. student grant to EE from Comisión Nacional de Investigación Científica y Tecnológica (CONICYT).

REFERENCES

1. Fouad YA, Aanei C. Revisiting the hallmarks of cancer. *Am J Cancer Res.* (2017) 7:1016–36.
2. DeBerardinis RJ, Chandel NS. Fundamentals of cancer metabolism. *Sci Adv.* (2016) 2:e1600200. doi: 10.1126/sciadv.1600200
3. Suzuki A, Kusakai G, Kishimoto A, Lu J, Ogura T, Lavin MF, et al. Identification of a novel protein kinase mediating Akt survival signaling to the ATM protein. *J Biol Chem.* (2003) 278:48–53. doi: 10.1074/jbc.M206025200
4. Cui J, Yu Y, Lu GF, Liu C, Liu X, Xu YX, et al. Overexpression of ARK5 is associated with poor prognosis in hepatocellular carcinoma. *Tumour Biol.* (2013) 34:1913–8. doi: 10.1007/s13277-013-0735-x
5. Kusakai G, Suzuki A, Ogura T, Miyamoto S, Ochiai A, Kaminishi M, et al. ARK5 expression in colorectal cancer and its implications for tumor progression. *Am J Pathol.* (2004) 164:987–95. doi: 10.1016/S0002-9440(10)63186-0
6. Lu S, Niu N, Guo H, Tang J, Guo W, Liu Z, et al. ARK5 promotes glioma cell invasion, and its elevated expression is correlated with poor clinical outcome. *Eur J Cancer.* (2013) 49:752–63. doi: 10.1016/j.ejca.2012.09.018
7. Chang XZ, Yu J, Liu HY, Dong RH, Cao XC. ARK5 is associated with the invasive and metastatic potential of human breast cancer cells. *J Cancer Res Clin Oncol.* (2012) 138:247–54. doi: 10.1007/s00432-011-1102-1
8. Chen P, Li K, Liang Y, Li L, Zhu X. High NUAK1 expression correlates with poor prognosis and involved in NSCLC cells migration and invasion. *Exp Lung Res.* (2013) 39:9–17. doi: 10.3109/01902148.2012.744115
9. Phippen NT, Bateman NW, Wang G, Conrads KA, Ao W, Teng PN, et al. NUAK1 (ARK5) is associated with poor prognosis in ovarian cancer. *Front Oncol.* (2016) 6:213. doi: 10.3389/fonc.2016.00213
10. Ye XT, Guo AJ, Yin PF, Cao XD, Chang JC. Overexpression of NUAK1 is associated with disease-free survival and overall survival in patients with gastric cancer. *Med Oncol.* (2014) 31:61. doi: 10.1007/s12032-014-0061-1
11. Kusakai G, Suzuki A, Ogura T, Kaminishi M, Esumi H. Strong association of ARK5 with tumor invasion and metastasis. *J Exp Clin Cancer Res.* (2004) 23:263–8.
12. Zagorska A, Deak M, Campbell DG, Banerjee S, Hirano M, Aizawa S, et al. New roles for the LKB1-NUAK pathway in controlling myosin phosphatase complexes and cell adhesion. *Sci Signal.* (2010) 3:ra25. doi: 10.1126/scisignal.2000616
13. Sun X, Gao L, Chien HY, Li WC, Zhao J. The regulation and function of the NUAK family. *J Mol Endocrinol.* (2013) 51:R15–22. doi: 10.1530/JME-13-0063
14. Suzuki A, Kusakai G, Kishimoto A, Shimojo Y, Miyamoto S, Ogura T, et al. Regulation of caspase-6 and FLIP by the AMPK family member ARK5. *Oncogene.* (2004) 23:7067–75. doi: 10.1038/sj.onc.1207963
15. Suzuki A, Kusakai G, Kishimoto A, Lu J, Ogura T, Esumi H. ARK5 suppresses the cell death induced by nutrient starvation and death receptors via inhibition of caspase 8 activation, but not by chemotherapeutic agents or UV irradiation. *Oncogene.* (2003) 22:6177–82. doi: 10.1038/sj.onc.1206899
16. Liu L, Ulbrich J, Muller J, Wustefeld T, Aeberhard L, Kress TR, et al. Deregulated MYC expression induces dependence upon AMPK-related kinase 5. *Nature.* (2012) 483:608–12. doi: 10.1038/nature10927
17. Monteverde T, Tait-Mulder J, Hedley A, Knight JR, Sansom OJ, Murphy DJ. Calcium signalling links MYC to NUAK1. *Oncogene*. (2017) 37:982–92. doi: 10.1038/onc.2017.394
18. Meek DW. Regulation of the p53 response and its relationship to cancer. *Biochem J.* (2015) 469:325–46. doi: 10.1042/BJ20150517
19. Palma M, Riffo EN, Suganuma T, Washburn MP, Workman JL, Pincheira R, et al. Identification of a nuclear localization signal and importin beta members mediating NUAK1 nuclear import inhibited by oxidative stress. *J Cell Biochem.* (2019) 120:16088–107. doi: 10.1002/jcb.28890
20. Cossa G, Roeschert I, Prinz F, Baluapuri A, Silveira Vidal R, Schulein-Volk C, et al. Localized inhibition of protein phosphatase 1 by NUAK1 promotes spliceosome activity and reveals a MYC-sensitive feedback control of transcription. *Mol Cell.* (2020) 77:1322–39.e11. doi: 10.1016/j.molcel.2020.01.008
21. Bunz F, Hwang PM, Torrance C, Waldman T, Zhang Y, Dillehay L, et al. Disruption of p53 in human cancer cells alters the responses to therapeutic agents. *J Clin Invest.* (1999) 104:263–9. doi: 10.1172/JCI6863
22. Moffat J, Grueneberg DA, Yang X, Kim SY, Kloepfer AM, Hinkle G, et al. A lentiviral RNAi library for human and mouse genes applied to an arrayed viral high-content screen. *Cell.* (2006) 124:1283–98. doi: 10.1016/j.cell.2006.01.040
23. Banerjee S, Buhrlage SJ, Huang HT, Deng X, Zhou W, Wang J, et al. Characterization of WZ4003 and HTH-01-015 as selective inhibitors of the LKB1-tumour-suppressor-activated NUAK kinases. *Biochem J.* (2014) 457:215–25. doi: 10.1042/BJ20131152
24. Schindelin J, Arganda-Carreras I, Frise E, Kaynig V, Longair M, Pietzsch T, et al. Fiji: an open-source platform for biological-image analysis. *Nat Methods.* (2012) 9:676–82. doi: 10.1038/nmeth.2019
25. Reda A, Refaat A, Abd-Rabou AA, Mahmoud AM, Adel M, Sabet S, et al. Role of mitochondria in rescuing glycolytically inhibited subpopulation of triple negative but not hormone-responsive breast cancer cells. *Sci Rep.* (2019) 9:13748. doi: 10.1038/s41598-019-50141-z
26. Port JLF, Muthalagu N, Raja M, Ceteci F, Monteverde T, Kruspig B, et al. Colorectal tumors require NUAK1 for protection from oxidative stress. *Cancer Discov*. (2018) 8:632–47. doi: 10.1158/2159-8290.CD-17-0533
27. Wu M, Neilson A, Swift AL, Moran R, Tamagnine J, Parslow D, et al. Multiparameter metabolic analysis reveals a close link between attenuated mitochondrial bioenergetic function and enhanced glycolysis dependency in human tumor cells. *Am J Physiol Cell Physiol.* (2007) 292:C125–36. doi: 10.1152/ajpcell.00247.2006
28. Hou X, Liu JE, Liu W, Liu CY, Liu ZY, Sun ZY. A new role of NUAK1: directly phosphorylating p53 and regulating cell proliferation. *Oncogene.* (2011) 30:2933–42. doi: 10.1038/onc.2011.19
29. Kawauchi K, Araki K, Tobiume K, Tanaka N. p53 regulates glucose metabolism through an IKK-NF-kappaB pathway and inhibits cell transformation. *Nat Cell Biol.* (2008) 10:611–8. doi: 10.1038/ncb1724
30. Kim SY. Cancer energy metabolism: shutting power off cancer factory. *Biomol Ther (Seoul)*. (2018) 26:39–44. doi: 10.4062/biomolther.2017.184
31. Santamaria G, Martinez-Diez M, Fabregat I, Cuezva JM. Efficient execution of cell death in non-glycolytic cells requires the generation of ROS controlled by the activity of mitochondrial H+-ATP synthase. *Carcinogenesis.* (2006) 27:925–35. doi: 10.1093/carcin/bgi315
32. Antico Arciuch VG, Alippe Y, Carreras MC, Poderoso JJ. Mitochondrial kinases in cell signaling: facts and perspectives. *Adv Drug Deliv Rev.* (2009) 61:1234–49. doi: 10.1016/j.addr.2009.04.025
33. Jose C, Bellance N, Rossignol R. Choosing between glycolysis and oxidative phosphorylation: a tumor's dilemma? *Biochim Biophys Acta.* (2011) 1807:552–61. doi: 10.1016/j.bbabio.2010.10.012
34. Nakajima EC, van Houten B. Metabolic symbiosis in cancer: refocusing the Warburg lens. *Mol Carcinog.* (2013) 52:329–37. doi: 10.1002/mc.21863
35. Kumar S, Sharife H, Kreisel T, Mogilevsky M, Bar-Lev L, Grunewald M, et al. Intra-tumoral metabolic zonation and resultant phenotypic diversification are dictated by blood vessel proximity. *Cell Metab.* (2019) 30:201–11.e6. doi: 10.1016/j.cmet.2019.04.003
36. Gao C, Shen Y, Jin F, Miao Y, Qiu X. Cancer stem cells in small cell lung cancer cell line h446: higher dependency on oxidative phosphorylation and mitochondrial substrate-level phosphorylation than non-stem cancer cells. *PLoS ONE.* (2016) 11:e0154576. doi: 10.1371/journal.pone.0154576
37. Chen Q, Kirk K, Shurubor YI, Zhao D, Arreguin AJ, Shahi I, et al. Rewiring of glutamine metabolism is a bioenergetic adaptation of human cells with mitochondrial DNA mutations. *Cell Metab.* (2018) 27:1007–1025 e5. doi: 10.1016/j.cmet.2018.03.002
38. Chinopoulos C. Acute sources of mitochondrial NAD(+) during respiratory chain dysfunction. *Exp Neurol.* (2020) 327:113218. doi: 10.1016/j.expneurol.2020.113218
39. Inazuka F, Sugiyama N, Tomita M, Abe T, Shioi G, Esumi H. Muscle-specific knock-out of NUAK family SNF1-like kinase 1 (NUAK1) prevents high fat diet-induced glucose intolerance. *J Biol Chem.* (2012) 287:16379–89. doi: 10.1074/jbc.M111.302687
40. Tanner LB, Goglia AG, Wei MH, Sehgal T, Parsons LR, Park JO, et al. Four key steps control glycolytic flux in mammalian cells. *Cell Syst.* (2018) 7:49–62.e8. doi: 10.1016/j.cels.2018.06.003
41. Suzuki A, Kusakai G, Shimojo Y, Chen J, Ogura T, Kobayashi M, et al. Involvement of transforming growth factor-beta 1 signaling in hypoxia-induced tolerance to glucose starvation. *J Biol Chem.* (2005) 280:31557–63. doi: 10.1074/jbc.M503714200

42. Miyazono Y, Hirashima S, Ishihara N, Kusukawa J, Nakamura KI, Ohta K. Uncoupled mitochondria quickly shorten along their long axis to form indented spheroids, instead of rings, in a fission-independent manner. *Sci Rep.* (2018) 8:350. doi: 10.1038/s41598-017-18582-6
43. Ahmad T, Aggarwal K, Pattnaik B, Mukherjee S, Sethi T, Tiwari BK, et al. Computational classification of mitochondrial shapes reflects stress and redox state. *Cell Death Dis.* (2013) 4:e461. doi: 10.1038/cddis.2012.213
44. Picard M, McEwen BS. Mitochondria impact brain function and cognition. *Proc Natl Acad Sci USA*. (2014) 111:7–8. doi: 10.1073/pnas.1321881111

Conflict of Interest: The authors declare that the research was conducted in the absence of any commercial or financial relationships that could be construed as a potential conflict of interest.

frontiers in Oncology

ORIGINAL RESEARCH
published: 31 July 2020
doi: 10.3389/fonc.2020.01185

Inhibition of Fatty Acid Synthase Upregulates Expression of CD36 to Sustain Proliferation of Colorectal Cancer Cells

*James Drury[1], Piotr G. Rychahou[2,3], Daheng He[2], Naser Jafari[1], Chi Wang[2], Eun Y. Lee[4], Heidi L. Weiss[2], Bernard Mark Evers[2,3] and Yekaterina Y. Zaytseva[1,2]**

[1] Department of Toxicology and Cancer Biology, University of Kentucky, Lexington, KY, United States, [2] Markey Cancer Center, University of Kentucky, Lexington, KY, United States, [3] Department of Surgery, University of Kentucky, Lexington, KY, United States, [4] Department of Pathology and Laboratory Medicine, University of Kentucky, Lexington, KY, United States

OPEN ACCESS

Edited by:
Stefano Falone,
University of L'Aquila, Italy

Reviewed by:
Puttur Devi Prasad,
Augusta University, United States
Shivendra Vikram Singh,
St. Jude Children's Research Hospital, United States
Vadivel Ganapathy,
Texas Tech University Health Sciences Center, United States

***Correspondence:**
Yekaterina Y. Zaytseva
yyzayt2@uky.edu

Specialty section:
This article was submitted to Cancer Metabolism, a section of the journal Frontiers in Oncology

Received: 21 April 2020
Accepted: 11 June 2020
Published: 31 July 2020

Citation:
Drury J, Rychahou PG, He D, Jafari N, Wang C, Lee EY, Weiss HL, Evers BM and Zaytseva YY (2020) Inhibition of Fatty Acid Synthase Upregulates Expression of CD36 to Sustain Proliferation of Colorectal Cancer Cells. Front. Oncol. 10:1185. doi: 10.3389/fonc.2020.01185

Fatty acid synthase, a key enzyme of *de novo* lipogenesis, is an attractive therapeutic target in cancer. The novel fatty acid synthase inhibitor, TVB-3664, shows anti-cancer activity in multiple cancers including colorectal cancer; however, it is unclear whether uptake of exogeneous fatty acids can compensate for the effect of fatty acid synthase inhibition. This study demonstrates that inhibition of fatty acid synthase selectively upregulates fatty acid translocase (CD36), a fatty acid transporter, in multiple colorectal cancer models including colorectal cancer cells with shRNA mediated knockdown of fatty acid synthase and genetically modified mouse tissues with heterozygous and homozygous deletion of fatty acid synthase. Furthermore, human colorectal cancer tissues treated with TVB-3664 show a significant and selective upregulation of CD36 mRNA. shRNA-mediated knockdown of CD36 and inhibition of CD36 via sulfosuccinimidyl oleate, a chemical inhibitor of CD36, decreased cell proliferation *in vitro* and reduced tumor growth in subcutaneous xenograft models. Isogenic cell populations established from patient derived xenografts and expressing high levels of CD36 show a significantly increased ability to grow tumors *in vivo*. The tumor-promoting effect of CD36 is associated with an increase in the levels of pAkt and survivin. Importantly, combinatorial treatment of primary and established colorectal cancer cells with TVB-3664 and sulfosuccinimidyl oleate shows a synergistic effect on cell proliferation. In summary, our study demonstrates that upregulation of CD36 expression is a potential compensatory mechanism for fatty acid synthase inhibition and that inhibition of CD36 can improve the efficacy of fatty acid synthase-targeted therapy.

Keywords: lipogenesis, anticancer activity, FASN-targeted therapy, fatty acid metabolism, TVB inhibitors

INTRODUCTION

Colorectal cancer (CRC) is the leading cause of non-smoking related cancer deaths in the world (1). Altered fatty acid metabolism is a hallmark of cancer and a potential target for therapeutic intervention (2–4).

Fatty Acid Synthase (FASN), a key enzyme of *de novo* lipogenesis, is significantly upregulated in CRC and promotes tumor growth and metastasis (5–7). Novel FASN inhibitors developed by Sagimet Biosciences show anti-cancer activity in lung, prostate, ovarian, and colon cancer models *in vitro* and *in vivo* (8–10), and are currently being tested in phase I/II clinical trials (11–13). Our studies show anti-tumor activity of TVB inhibitors in primary CRC cells and CRC patient-derived xenograft (PDX) models (10, 14).

While most tumors exhibit a shift toward FA synthesis, they can also scavenge lipids from their environment (4). Fatty Acid Translocase (CD36), a multifunctional glycoprotein, has an important role in fatty acid metabolism as a fatty acid receptor and transporter (15, 16). CD36 translocates to the plasma membrane, where an extracellular domain of the protein binds low density lipoproteins and transports them across the plasma membrane into the cytosol, thus playing a critical role in metabolism of extracellular fatty acids (15–17). CD36 is subject to various types of post-translational modifications. Glycosylation, ubiquitination, and palmitoylation are involved in regulating CD36 stability and the rate of fatty acid uptake (18). Recent studies have shown that CD36 is highly expressed and enhances the progression of solid malignancies such as breast, ovarian, gastric, and glioblastoma cancers (19–22). Silencing CD36 in human prostate cancer cells reduces fatty acid uptake and cellular proliferation (23). Furthermore, the presence of CD36 positive metastasis initiating cells correlates with a poorer prognosis in glioblastoma and oral carcinoma (21, 24). The contribution of CD36 to CRC progression has not yet been investigated.

Since cancer cells utilize both endogenously-synthesized lipids and exogeneous fatty acids (25), and our published data indicate that an enhanced uptake of dietary fatty acids may be a potential mechanism of resistance to FASN inhibitors (10), the goal of this study was to evaluate the interconnection between these two pathways.

We found that CD36 is significantly overexpressed in CRC and that there is a correlation between expression of FASN and CD36 in primary human CRC specimens. We demonstrate that a decrease in FASN expression is associated with selective induction of CD36 and that this phenomenon is consistent among multiple cancer models. Pharmacological and shRNA-mediated inhibition of CD36 decreases proliferation of primary CRC cells *in vitro* and inhibits tumor growth *in vivo*. We also show that CD36 overexpression is associated with upregulation of survivin, a protein linked to apoptosis resistance, metastasis, bypass of cell cycle checkpoints, and resistance to therapy (26, 27). Consistent with our *in vitro* data, we show that $CD36^{high}$-expressing cells, isolated from CRC PDXs, have a significantly higher level of survivin as compared to $CD36^{low}$-expressing cells from the same tumor. Our results also demonstrate that combined inhibition of FASN and CD36 has a synergetic effect on inhibition of cellular proliferation suggesting that combination treatment may be a potential therapeutic strategy for CRC.

Together, our findings demonstrate the tightly regulated interconnection between *de novo* lipid synthesis and CD36-mediated lipid uptake in CRC progression during targeted inhibition of FASN, suggesting that inhibition of CD36 may be necessary to improve the efficacy of FASN-targeted therapy.

MATERIALS AND METHODS

CRC Cell Lines

Established cell lines HCT116, HT29, and HT29LuM3 were maintained in McCoy's 5A medium supplemented with 10% FBS (Sigma-Aldrich, St. Louis, MO) and 1% penicillin–streptomycin. Primary colon cancer patient Pt 93 and Pt 130 cultures were isolated and established from PDX tumors as previously described (1). Cells were maintained as monolayer culture in DMEM supplemented with 10% FBS (Sigma-Aldrich, St. Louis, MO) and 1% penicillin–streptomycin. Primary Pt 93 and Pt 130 colon cancer cells were authenticated as unique human cell lines (Genetica). Established CRC cell lines were authenticated using STR DNA profiling (Genetica, Cincinnati, OH). Stable CD36 knockdown HCT116, HT29, and HT29LuM3 cell lines were established using CD36 shRNAs from Sigma-Aldrich (TRCN000005699, TRCN0000057000, and TRCN0000057001). Cells were selected with 10 mg/mL puromycin. Knockdown was confirmed via quantitative real-time PCR (qRT-PCR) after cell selection and prior performing animal experiments. Overexpression cell lines were established by transfecting HCT116 cells with either pCMV-Spark-CD36 (Sino Biological Inc., NM 001001547.2), td-Tomato-CD36 (Addgene, Plasmid #58077).

Tissue Microarray Analysis—Immunohistochemistry

Immunoreactivity scores of CD36 (antibody sc-7309, Santa Cruz Biotechnology) and FASN (antibody #3180, Cell signaling) expression were analyzed in matched normal colon mucosa and tumor tissues from patients diagnosed with Stage I–IV CRC who had surgery at UK Chandler Medical Center (TMA ID BH15991A, $n = 56$) by a GI pathologist (EYL) blinded as to tumor stage. The final immunoreactivity score was determined by multiplication of the values for staining intensity (0, no staining; 1, weak; 2, moderate; 3, strong staining) and the values for percentage of positive tumor cells (0, no positive cells; 1, 0–10%; 2, 11–50%; 3, 51–100% positive).

Tissue Collection

Tissues were obtained from consented patients with Stage II–IV CRC who had undergone surgery at UK Medical Center (IRB #16-0439-P2H). 6–8-week-old NSG mice (NOD.Cg-Prkdc Il2rg /SzJ) from The Jackson Laboratory (Bar Harbor, ME) were used for PDX models. All procedures were performed using protocols approved by the UK Animal Care and Use Committee. Briefly, CRC tissues (2–5 mm) obtained from CRC patients of both sexes were implanted subcutaneously into their flanks in a small pocket surgically created under the skin. Established tumors

were designated as generation 0 (G0). Tumor tissues from G0 were minced and mixed with Matrigel to ensure homogeneous distribution of tissues among mice and allow implantation of an equal volume of tumor tissues into the flank. Tumor tissues were resected when they reached an appropriate size and digested as previously described (1). For evaluation of CD36 expression in PDX models, we utilized tissue samples from Pt 2402 PDX model established from a patient diagnosed with metastatic adenocarcinoma (lung) consistent with colon primary tumor (1). Pt 2402 PDX tumors were grown to ∼200 mm^3 then tissues were collected and lysed for analysis via western blot.

Flow Cytometry

Individual cells from PDX model Pt 2402 were stained for CD36 with fluorescent antibody (Abcam ab23680). Stained cells were sorted via flow cytometry and the top 10% of GFP positive CD36 expressing cells ($CD36^{high}$) and the bottom 10% of GFP negative cells ($CD36^{low}$) were sorted separately from the rest of the tumor cell population. $CD36^{high}$ and $CD36^{low}$ were mixed with 100 μL of 30% Matrigel and subcutaneously injected into NSG mice. Tumor growth was monitored for three months. Samples were taken from subsequent tumors for western blot analysis and immunohistochemistry and the remaining tumor tissue was re-sorted for CD36.

Fatty Acid Uptake

HCT116, NTC, and FASN shRNA cells were plated at 10,000 cells/well on an 8-well coverslip u-slide (Ibidi #80826) and treated with CD36 neutralizing antibody (Cayman Chemical #1009893) for 24 h. After incubation with neutralizing antibody, cells were then treated with fluorescent FA analog BODIPY FL (Thermo Fisher #D3822) for 10 min in serum free McCoy's 5A medium supplemented with 10% fatty acid free BSA. Cells were washed twice with PBS and fixed with PBS containing 5% formalin for 20 min at 37°C. Cell were then imaged via confocal microscopy using a Nikon A1 Confocal Microscope.

Cell Proliferation Assay

CRC cell lines were plated onto 24 well-plates at a concentration of 30,000 cells per well. Cells were given DMEM medium for Pt 93 and Pt 130 and McCoy's 5A medium for HCT116 with and without FBS to simulate starvation conditions. Cells were also treated with or without 100 μM SSO (Cayman Chemical) or 0.2 μM TVB-3664 or both. TVB-3664 was provided by Sagimet Biosciences (Menlo Park, CA). SSO was purchased from Cayman Chemical (Ann Arbor, MI). Cells were incubated at 37°C for 6 days. After the incubation period, cells were trypsinized, and collected individually based on well and condition of treatment. Cells were counted using a Vi-Cell XR Cell Viability Analyzer (Beckman Coulter). HCT116, NTC, and CD36 shRNA(#2 and #4), cells were plated onto 24 well-plates at a concentration of 30,000 cells per well. Cells were cultured in McCoy's 5A medium with and without fetal bovine serum for 72 h and counted as described above.

Quantitative Real-Time PCR

Total RNA was isolated using a RNeasy mini kit (QIAGEN). cDNA was synthesized using a high capacity cDNA reverse transcription kit (Applied Biosystems). QRT-PCR was carried out using a TaqMan Gene Expression Master Mix (#4369016) according to manufacture protocol and TaqMan probes for human CD36 (ID Hs00354519 m1), human FASN (ID Hs01005622 m1), human FATP3 (ID Hs00354519 m1), human FATP4 (Hs00192700 m1), and human GAPDH (#4333764F; Applied Biosystems).

Subcutaneous Xenografts

NU/NU mice were injected subcutaneously with 1.0×10^6 cells of HCT116 NTC (non-targeted control, $n = 7$), shCD36 #2 ($n = 6$), or shCD36 #4 ($n = 7$) in 100 μL PBS and tumor growth was monitored. Tumor size was measured via calipers every 3 days and tumor volume was calculated using the formula: $TV = width^2 \times length/0.52$. When NTC tumor growth reached ∼200 mm^3, all mice were sacrificed, and tumor weight was taken via digital scale. NU/NU mice were injected subcutaneously with 2.0×10^6 cells of NTC ($n = 5$) and shCD36 #4 ($n = 5$) in 100 μL PBS for HT29 and HT29 LuM3 xenografts experiments.

Genetically Modified Mice

C57BL/6J mice with LoxP-flanked FASN alleles were obtained from Clay Semenkovich, MD at Washington University, and FASN/VillinCre and FASN/Apc/VillinCre mouse colonies were established by mating these mice with C57BL/6J Villin/Cre and C57BL/6J Apc/Cre mice in Dr. Zaytseva's laboratory.

RESULTS

CD36 Protein Is Overexpressed in CRC

Upregulation of lipid metabolism is a common characteristic of many solid malignancies, and frequently, enhanced *de novo* lipogenesis occurs concomitantly with enhanced import of lipids from the extracellular space (3, 28). In our previously published study we showed that FASN is significantly overexpressed in primary tumor tissues as compared to matched normal colon mucosa using tissue microarray analysis (TMA) (29). Using the same TMA, we assessed the expression of CD36 levels in tumor tissues and found that expression was significantly higher as compared to normal colon mucosa as determined by statistical evaluation of immunoreactivity scores. We noted that the expression of CD36 is predominantly cytosolic in primary CRC tumors (**Figures 1A,B**). Interestingly, statistical analysis via Spearman Correlation showed a positive correlation between expression of CD36 and FASN in primary CRC tumor tissues, but it was not statistically significant (Spearman $r = 0.21743$, $n = 56$). We have also detected an increase in expression of CD36 in CRC metastasis to liver and lung (**Figure 1C**).

Using The Cancer Genome Atlas (TCGA) data, we also analyze FASN and CD36 mRNA expression. Consistent with protein data, the level of FASN mRNA is significantly higher in tumor tissues as compared to normal mucosa (**Supplementary Figure 1A**). In contrast, we found that the level of CD36 mRNA is significantly lower in cancer tissues

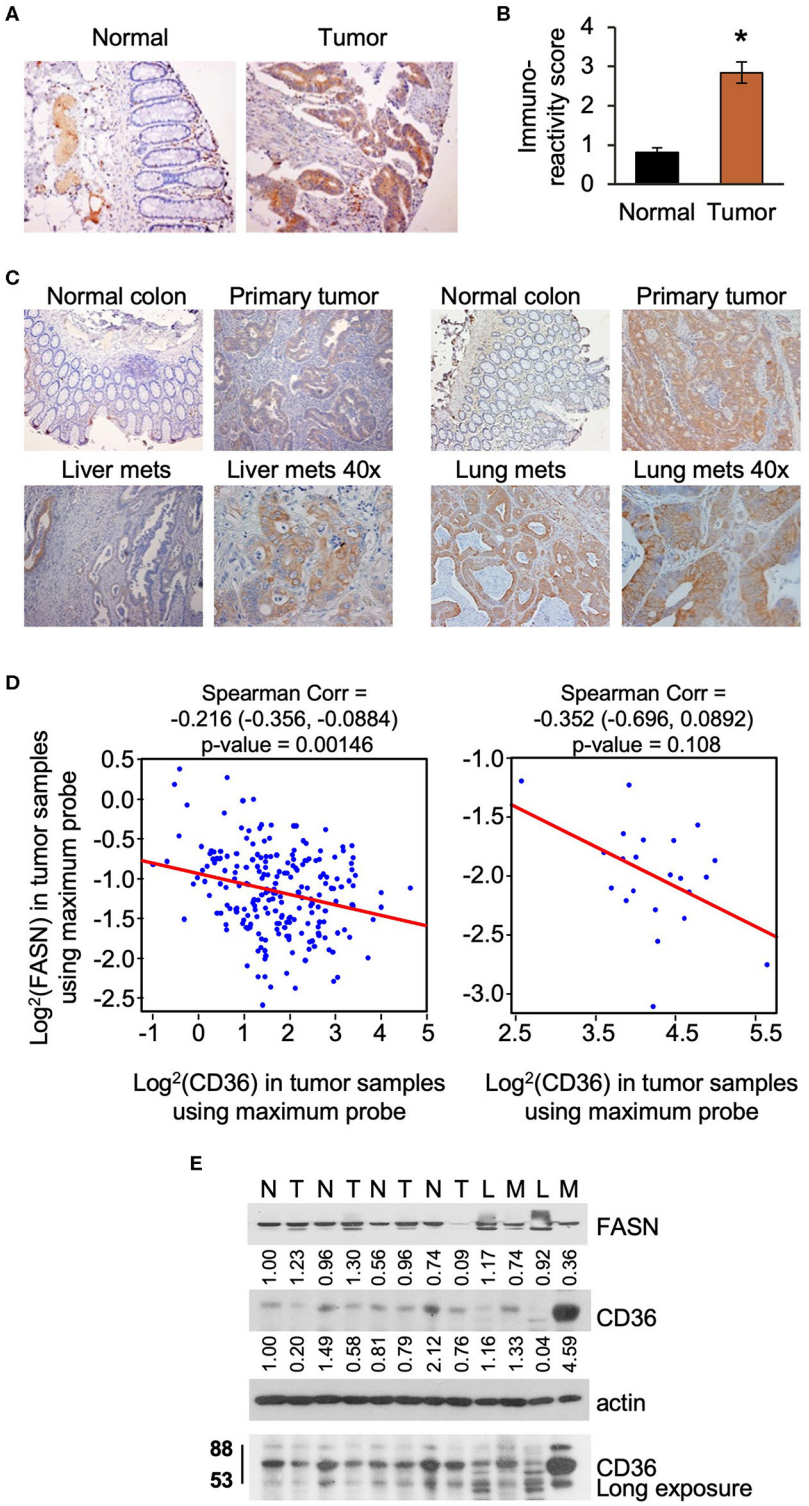

FIGURE 1 | CD36 is overexpressed in human CRC. **(A,B)** Immunoreactivity score of CD36 expression was analyzed in matched normal colon mucosa and tumor tissues from patients diagnosed with Stage I–IV CRC (TMA: $n = 56$, $^*p < 0.001$ vs. normal tissue). **(C)** CD36 staining in matched normal colon mucosa, primary CRC, and CRC metastasis to liver and lung [representative images are shown; liver ($n = 12$) and lung metastasis ($n = 5$)]. **(D)** Correlations between FASN and CD36 was determined based on RNASeq data of CRC patient samples ($n = 22$ of normal tissues and $n = 215$ of tumors) from The Cancer Genome Atlas. **(E)** Expression of FASN and CD36 in human normal colon mucosa and tumor tissues. N, normal mucosa; T, primary tumor; L, normal liver tissue; M, liver metastasis.

as compared to normal tissues (**Supplementary Figure 1B**). Interestingly, according to data analysis from The Human Protein Atlas, the high mRNA expression of CD36 ($n = 131$) is associated with poor prognosis in CRC with 5-year survival of 53% of patients as compared to 5-year survival of 64% of patients with low CD36 mRNA expression ($n = 466$) (30). Statistical analysis of correlation between FASN and CD36 revealed a significant negative correlation between FASN and CD36 mRNA levels in tumor tissues, but not in normal tissues (**Figure 1D**).

To further delineate the association between expression of FASN and CD36, we analyzed the expression of these proteins in fresh human normal colon mucosa, primary CRC tissues, and metastasis (**Figure 1E**). The predicted molecular mass of CD36 protein is 53kD. However, due to the post-transcriptional modifications including extensive protein glycosylation, it is widely reported as ∼80–88 kD protein (16, 18, 31). This size will be shown for all *in vitro* and *in vivo* data in this manuscript. In the analyzed tissues sample set, the expression of FASN is higher in primary tumors as compared to normal mucosa in most cases. Due to FASN being expressed in healthy liver tissue, it is not suprizing to see that its expression is higher in the normal liver as compared to liver metastasis. CD36 expression seems to be higher or the same in primary tumors as compared to normal colon mucosa. However, expression of CD36, particularly in its glycosylated form, is much higher in liver metastasis as compared to normal liver or normal colon mucosa (**Figure 1E**).

To further analyze CD36 in CRC we analyzed tissues from PDX models, which retain the intratumorally clonal heterogeneity and tumor microenvironment of the parent tumor through passages in mice (10, 32). We analyzed the expression of CD36 in nine PDXs established from primary tumors and CRC metastasis (10), and found that CD36 (88kD) is mostly associated with PDX established from metastatic tumors with the exception of Pt 2568, which was established from primary CRC tumor (10) (**Supplementary Figure 1C**).

Together, these data demonstrate that CD36 is upregulated and exhibits multiple post-translational modificatios in CRC and that a significant inverse correlation exists between mRNA expression of FASN and CD36 in primary human CRC.

FASN Selectively Regulates Expression of CD36

To test whether alterations in FASN expression affect FA uptake, we assessed the expression of major FA transporters (FATPs and CD36) in HCT116 NTC and FASN shRNA CRC cells and found that FASN selectively upregulates mRNA expression of CD36, but not other FAs transporters (**Figure 2A**). To confirm that FASN selectively upregulates CD36, we treated fresh CRC human tissue slices with TVB-3664 and assessed the expression of FA transporters, including CD36. Consistent with our *in vitro* data, in all three CRC cases (**Supplementary Table 1**), we observed that CD36 mRNA expression increased at least two-fold and as much as four-fold when tissues were treated with TVB-3664. No changes were observed in expression of the other FA transporters tested (**Figure 2B**).

To further elucidate whether the level of endogenous fatty acid synthesis affects the expression of CD36, we next treated primary CRC cells from Pt 93 and Pt 130 with TVB-3664 for six days at a concentration of 0.2 μM as previously described (10). Inhibition of FASN led to an increase in CD36 mRNA and protein expression in both cell lines (**Figure 2C**). Consistently, shRNA-mediated knockdown of FASN in HCT116 and HT29 cell lines led to an increase in CD36 expression in normal and hypoxic conditions in both cell lines (**Figure 2D**, **Supplementary Figure 2A**). Interestingly, shRNA-mediated knockdown of CD36 does not affect FASN expression, suggesting a one-dimensional relationship between the two proteins (**Supplementary Figure 2B**).

The adenomatous polyposis coli (APC) gene product is mutated in the vast majority of human CRC and deletion of the APC gene leads to intestinal tumor formation in mice (33). In agreement with *in vitro* data, the analysis of intestinal tumors from mice with hetero- and homozygous deletions of FASN on C57BL/6-Apc/Cre background showed that deletion of FASN significantly upregulates CD36 expression (**Figures 2E,F**). Collectively, these data suggest that inhibition of FASN leads to selective upregulation of CD36 expression.

Inhibition of FASN Leads to CD36 Translocation to Plasma Membrane

Confocal imaging of primary Pt 93 CRC cells, control, and treated with TVB-3664, shows that CD36 protein expression is upregulated and primarily localized to the plasma membrane when FASN is inhibited by TVB-3664 (**Figure 2G**). To confirm these data, primary CRC cells from Pt 93 and Pt 130 were treated with 0.2 μM TVB-3664 for 6 days in normal or serum-starved conditions and labeled with CD36-FITC antibody. Flow cytometry analysis was performed; the results confirmed that inhibition of FASN activity by TVB-3664 led to an increase in membrane-associated CD36 when compared to control cells in both cell lines in normal and serum-starved conditions (**Figure 2H**).

To confirm that this upregulation and translocation of CD36 to the plasma membrane was related to FA metabolism, a FA uptake assay was performed. HCT116, NTC, and FASN shRNA cells were plated and treated with BODIPY FL and imaged using confocal microscopy. We observed that FASN knockdown increases FA uptake as indicated by an increase in BODIPY FL staining (**Figure 2I**). Furthermore, to test that this increase in FAs within the cell was due to CD36 upregulation, we treated NTC and FASN shRNA cells with neutralizing antibody for CD36. As shown in **Figure 2I**, blocking CD36 has a minimum effect in NTC cells, but significantly decreases BODIPY FL uptake in FASN shRNA cells, further confirming that inhibition of FASN increases FA uptake via upregulation of CD36.

Inhibition of CD36 Reduces CRC Cell Proliferation *in vitro*

We have previously shown that stable knockdown and pharmacological inhibition of FASN are associated with a decrease in cellular proliferation and tumor growth (7, 10). However, the observed effects *in vivo* were not as prominent as the effects *in vitro*, suggesting the potential compensatory effects of diet and exogeneous FA uptake on tumor growth (7, 10). To test whether blocking fatty-acid uptake via CD36 has an effect on CRC cell proliferation, primary CRC cells,

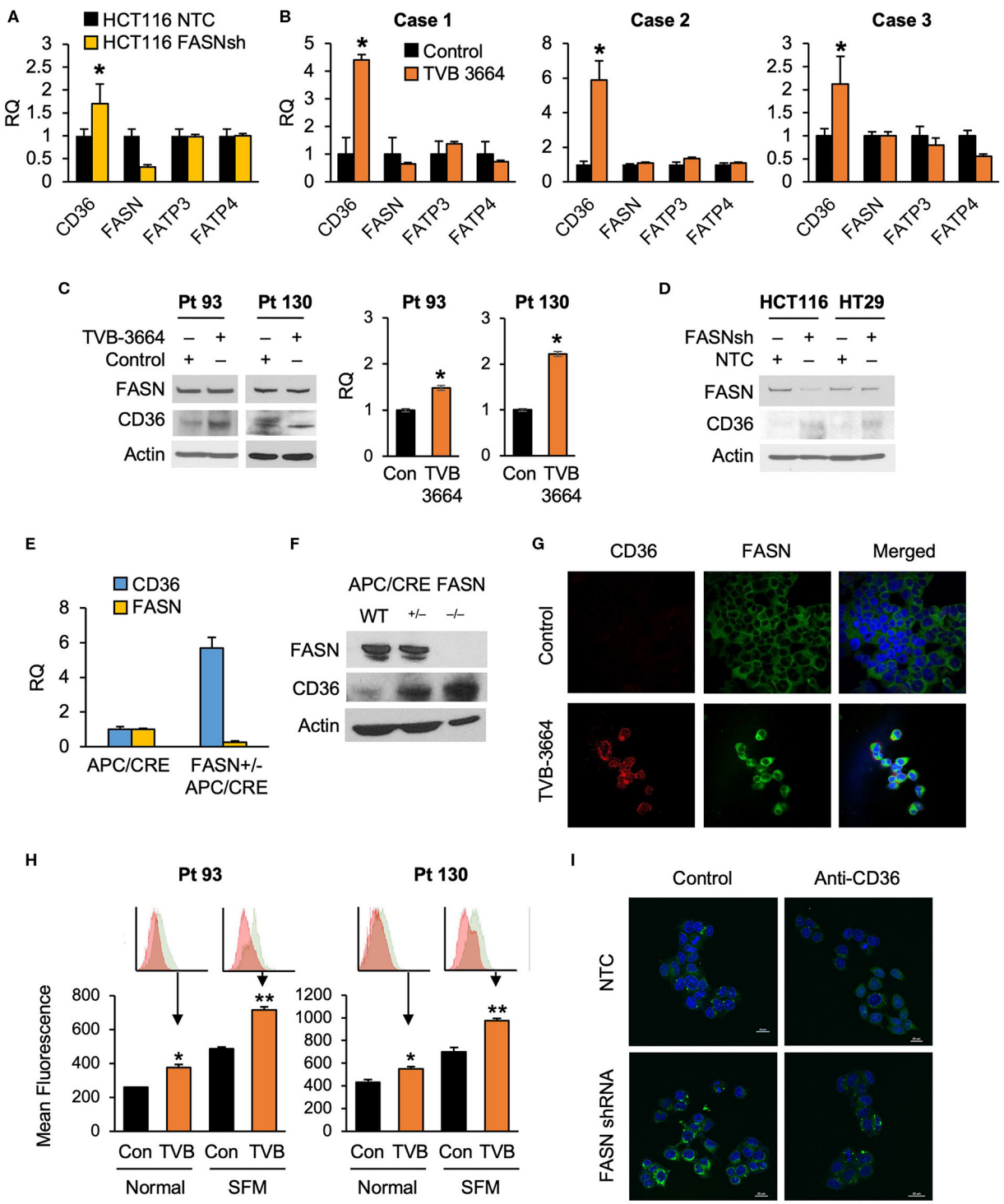

FIGURE 2 | Expression of CD36 is selectively regulated by the level of *de novo* fatty acid synthesis in CRC. **(A)** shRNA-mediated knockdown of FASN leads to upregulation of CD36 mRNA expression in HCT116 cells (*$p < 0.05$). **(B)** TVB-3664 treatment of CRC tissue slices (18 h) selectively upregulates CD36 mRNA expression (*$p < 0.05$). **(C)** TVB-3664 treatment of Pt 93 and Pt 130 primary CRC cells increases CD36 mRNA and protein expression. **(D)** shRNA mediated knockdown of FASN increases CD36 protein expression in HCT116 and HT29 cells. **(E)** Relative mRNA expression of FASN and CD36 in intestinal tumors collected from APC/Cre and FASN$^{+/-}$/APC/Cre mice. **(F)** FASN and CD36 protein expression in intestinal mucosa collected from Apc/Cre and Apc/Cre mice with hetero- and homo-zygous deletion of FASN. **(G,H)** Inhibition of FASN increases membrane-associated expression of CD36. **(G)** Confocal images of FASN and CD36 in control and 0.2 μM TVB-3664 treated (6 days) Pt 93 primary CRC cells. **(H)** Flow cytometry analysis of Pt 93 and Pt 130 primary CRC cells treated with 0.2 μM TVB-3664 (6 days) in normal and serum free media conditions. Mean fluorescence for CD36 is shown for representative data from three different experiments (**$p < 0.01$, *$p < 0.05$). **(I)** FA uptake in HCT116, NTC, and FASN shRNA. Cells were pre-treated with anti-CD36 antibody or vehicle for 24 h and then treated with BODIPY FL for 10 min.

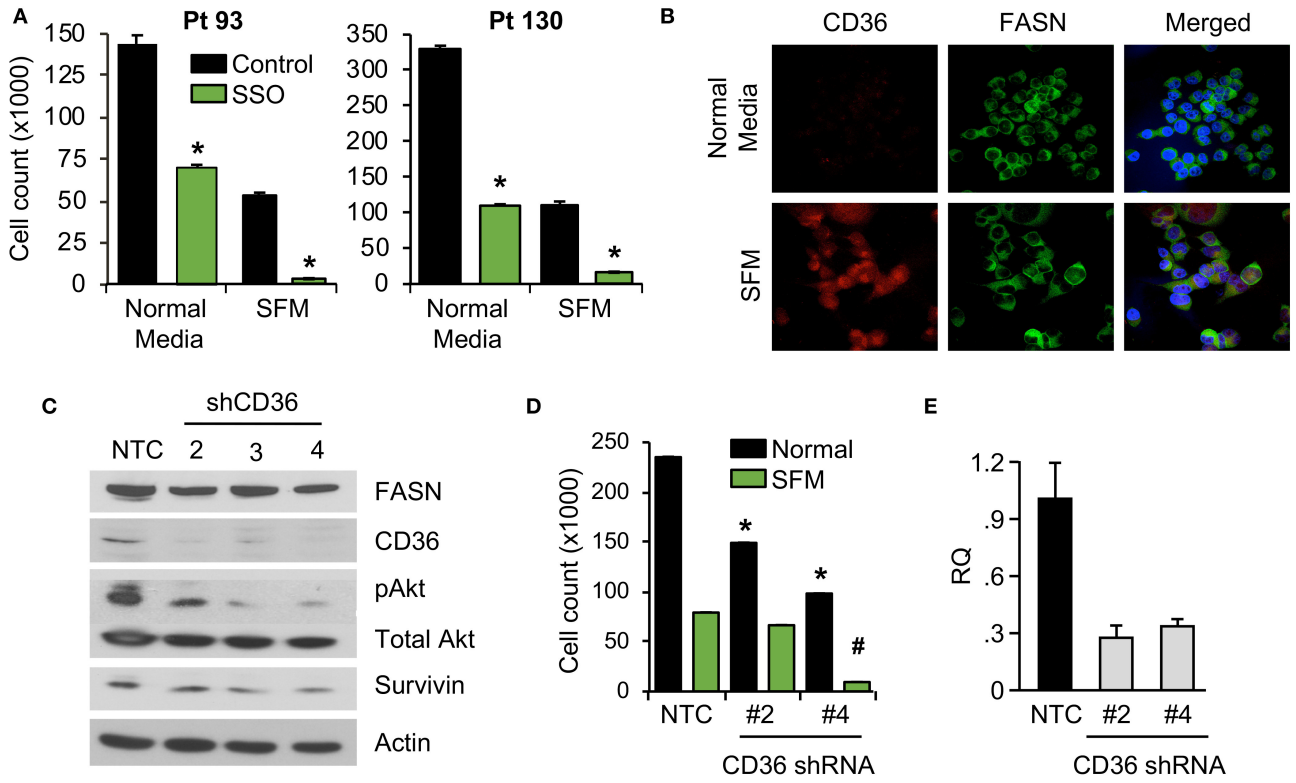

FIGURE 3 | Inhibition of CD36 is associated with decreased cellular proliferation. **(A)** Primary Pt 93 and Pt 130 CRC cells treated with 100 μM SSO for 6 days. Cellular proliferation assays were performed via cell count. Representative data from three experiments is shown (*$p < 0.05$). **(B)** Confocal images of FASN and CD36 in Pt 93 cells in normal and serum free media (6 days). **(C)** Expression of proteins associated with apoptosis and survival in HCT116 transfected with CD36 shRNAs and analyzed via western blot. **(D)** Cellular proliferation assay with HCT116, NTC, and CD36 shRNA (*$p < 0.05$ for normal medium, $^{\#}p <$ for SFM). **(E)** qRT-PCR confirmation of CD36 knockdown using CD36 shRNA #2 (73%) and CD36 shRNA #4 (67%).

Pt 93 and Pt 130, were treated with the chemical CD36 inhibitor sulfosuccinimidyl oleate (SSO), which binds to CD36 via Lys164 in the hydrophobic cavity thereby impairing CD36-mediated fatty acid uptake (18, 34), at 100 μM in both normal and serum free medium (SFM) conditions. Under both conditions, primary CRC cells treated with SSO exhibited decreased cellular proliferation. Interestingly, sensitivity of both cell lines to SSO increased in SFM (**Figure 3A**). To evaluate differences in CD36 expression in normal and SFM, we performed confocal microscopy on Pt 93 cells cultured in normal and SFM conditions. We found that starvation of CRC cells leads to upregulation of CD36, which could explain an increase in sensitivity to SSO treatment (**Figure 3B**).

To assess the effect of CD36 overexpression on apoptotic markers we performed an Apoptosis Antibody Array. Data showed that overexpression of CD36 decreased caspase-3 cleavage and increased expression of survivin, a protein overexpressed in most transformed cell lines and malignancies and associated with poor clinical outcome (**Supplementary Figure 3A**) (27, 35). Consistently, western blot analysis of control and SSO-treated Pt 130 and Pt 93 primary CRC cells showed an increase in cleaved caspase-3 in both cell lines. A decrease in expression of survivin was observed in Pt 130 cells only (**Supplementary Figure 3B**). Consistent with pharmacological inhibition of CD36, shRNA-mediated knockdown of CD36 lead to a significant decrease in cellular proliferation and expression of survivin and pAkt in HCT116 cells (**Figures 3C–E**). Furthermore, shRNA-mediated knockdown of CD36 inhibits colony formation in the HT29 cell line (**Supplementary Figure 3C**). Together, these data demonstrate that CD36 promotes cellular proliferation in CRC.

Inhibition and Knockdown of CD36 Reduces Xenograft Tumor Growth *in vivo*

To further investigate the role of CD36 in CRC tumor growth, HCT116 subcutaneous xenografts were treated with vehicle or SSO daily for 5 weeks. SSO treatment lead to significant decreases in tumor volume compared to vehicle control with no observable SSO toxicity as indicated by unchanged animal weight (**Figure 4A**). Furthermore, consistent with *in vitro* data, analysis of tumor tissues treated with SSO show a decrease in survivin mRNA (**Figure 4B**). FASN mRNA expression does not change with inhibition of CD36, further supporting the notion of a one directional relationship between the two proteins. Interestingly, SSO treatment led to an increase in CD36 mRNA suggesting that

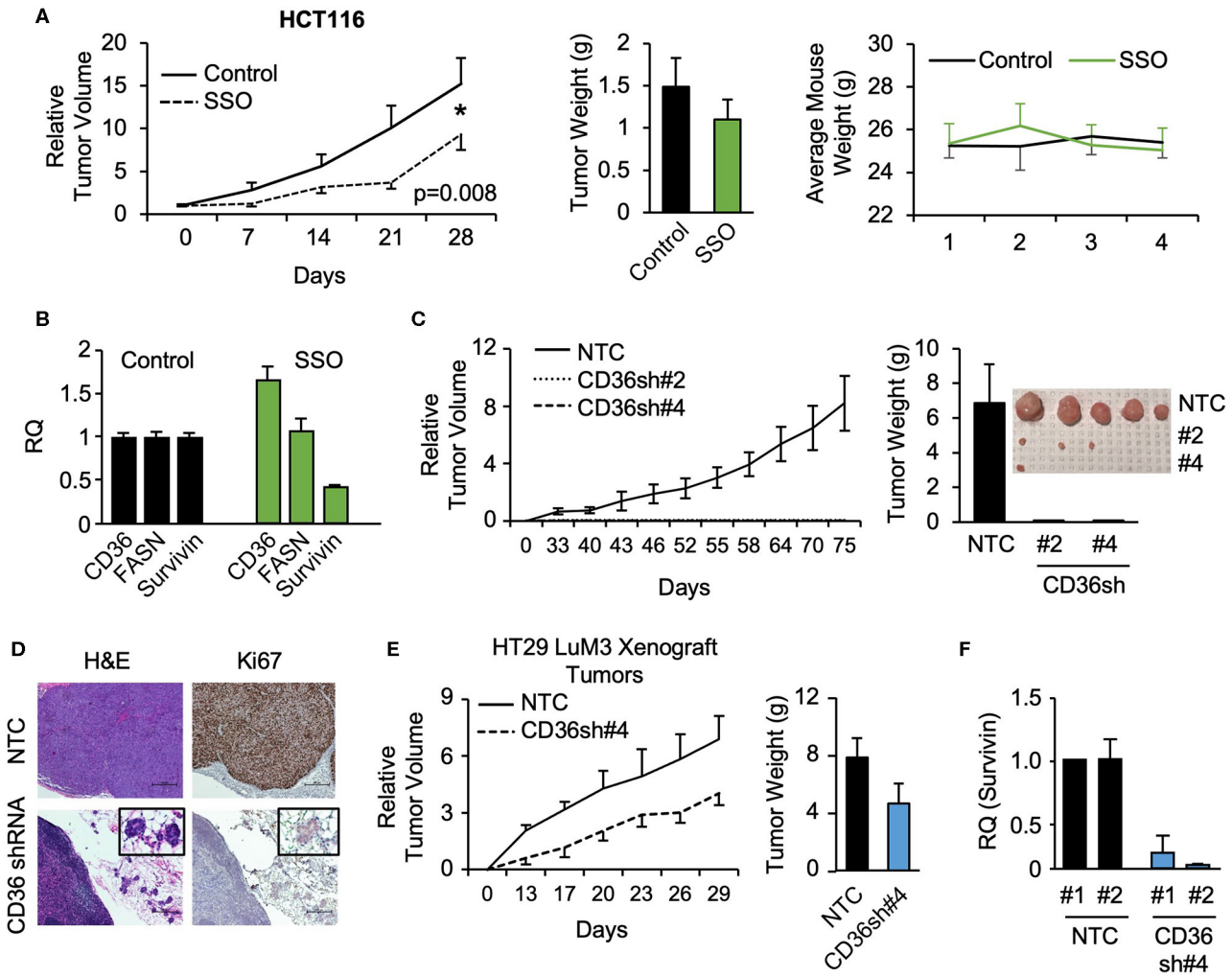

FIGURE 4 | SSO treatment and CD36 knockdown inhibit tumor growth *in vivo*. **(A)** Tumor volume, tumor weight, and mouse weight of control and SSO treated (20 mg/kg) mice are shown. SSO was dissolved in 10% PEG and administered in 200 μl dosages via oral gavage daily. 1.0×10^6 cells were injected into NU/NU mice. Treatment was initiated when tumors reached ~100 mm^3 (day 0). **(B)** RT-PCR analysis of HCT116 tumors showing the effect of SSO treatment on CD36, FASN, and survivin mRNA expression. **(C)** Tumor volume of HCT116 NTC and CD36 shRNA #2 and #4 xenografts is shown. 1.0×10^6 cells were injected into NU/NU mice and tumor growth was measured every 3 days. **(D)** H&E and Ki67 staining of HCT116 NTC and CD36 shRNA tumors. **(E)** Tumor volume and tumor weight of HT29 LuM3 NTC and CD36 shRNA #4 xenografts are shown. **(F)** mRNA expression of survivin in HT29 LuM3 xenografts (analysis of tumors from 2 mice per group is show).

the potential compensation for the lack of functional CD36 was due to antagonistic action of SSO (**Figure 4B**).

To further investigate the role of CD36 in CRC tumor growth, the CRC cell lines, HCT116, HT29, and HT29 LuM3 [an HT29 cell line that was trained to efficiently metastasize to lung via *in vivo* selection process (36)], were established as subcutaneous xenografts. Interestingly, *in vivo* selection led to an increase in CD36 expression in HT29 LuM3 as compared to parental HT29 cells (**Supplementary Figure 4A**). HCT116, HT29, and HT29 LuM3 cells (NTC and shRNA-mediated CD36 knockdown cell lines) were injected subcutaneously into Nu/Nu mice and tumor growth was measured. Knockdown of CD36 in HCT116 cells markedly attenuated the growth of xenograft tumors compared to NTC (**Figure 4C**, **Supplementary Figure 4B**). In the case of CD36 shRNA #2 and CD36 shRNA #4 cells, we were able to identify microtumors at the site of injections. Tumor tissues were stained for Ki67, a known marker for tumor cell proliferation and growth (37). Ki67 expression was greatly reduced in CD36 knockdown tumors as compared to control (**Figure 4D**). In contrast to HCT116 cells, CD36 knockdown in HT29 did not significantly affect tumor growth, suggesting that this cell line may not be dependent on CD36 due to considerably lower CD36 expression as compared to HCT116 cells (**Supplementary Figures 4A,C,D**). However, CD36 knockdown using CD36 shRNA #4 in HT29 LuM3 cells, which have higher levels of CD36 expression as well as higher metastatic potential (36) (**Supplementary Figure 4A**), lead to a more prominent inhibition of tumor growth and a decrease in

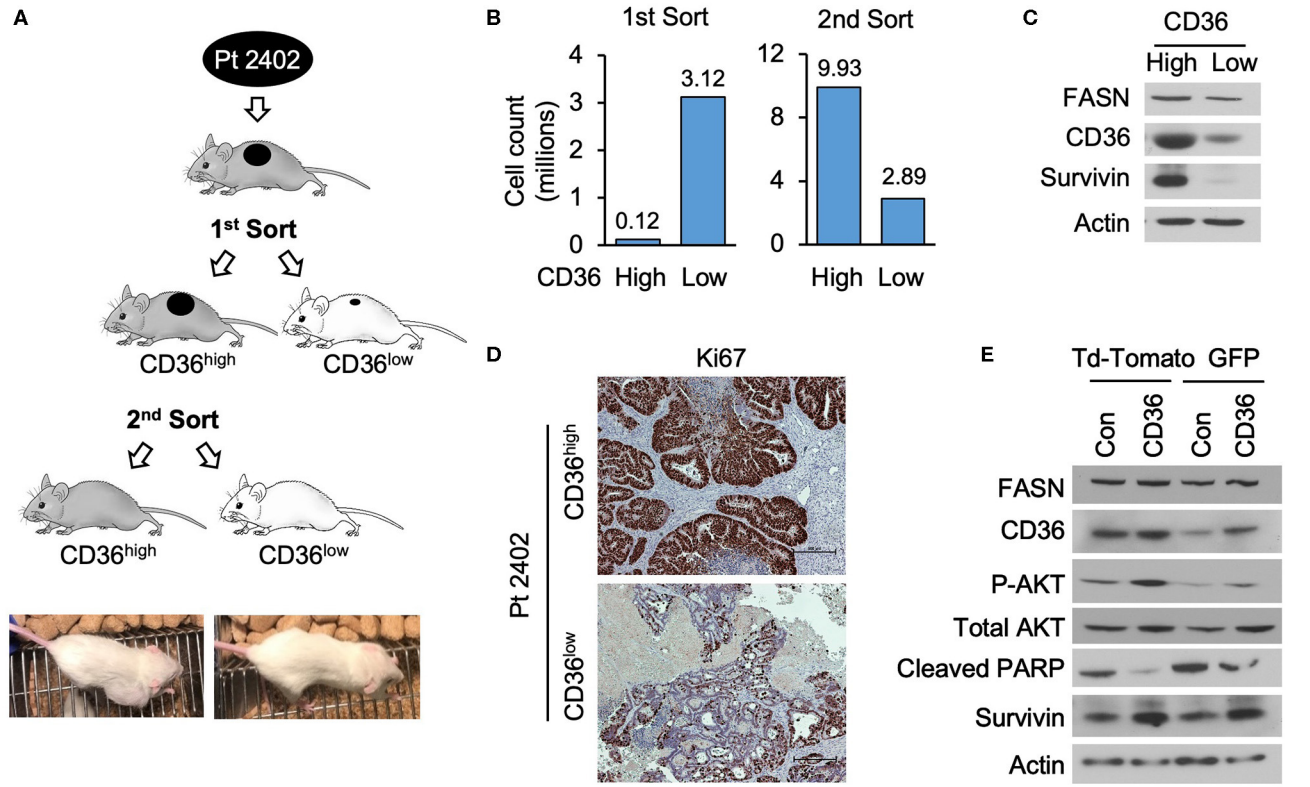

FIGURE 5 | High expression of CD36 is associated with an increase in pAkt and survivin in CRC. **(A)** Diagram of Pt 2402 propagation after flow cytometry sorting for CD36^{high} and CD36^{low} cells. **(B)** Numbers of CD36^{high} and CD36^{low} Pt 2402 cells for first and second flow cytometry sorts. **(C)** Protein expression levels of FASN, CD36, and survivin in CD36^{high} and CD36^{low} Pt 2402 primary cells from first flow cytometry sort. **(D)** IHC staining for Ki67 in Pt 2402 CD36^{high} and CD36^{low} tumors. **(E)** Protein expression levels of FASN, CD36, pAkt, cleaved PARP, and survivin in HCT116 CRC cells, control, and CD36 overexpression.

tumor weight (**Figure 4E**). Moreover, consistent with our *in vitro* data, qRT-PCR analysis of tumor tissues demonstrates a decrease in survivin expression when CD36 is knocked down in HT29 LuM3 tumors (**Figure 4F**). Thus, these data further support the role of CD36 in promoting CRC tumor growth.

High Expression of CD36 Is Associated With an Increase in Survivin in CRC

To further establish that CD36 promotes cellular proliferation via upregulation of pro-survival pathways, we utilized a PDX tumor model, Pt 2402, which was established from a CRC metastasis to the lung (10) and is positive for CD36 expression (see **Supplementary Figure 1C**). Tumor tissue from first generation Pt 2402 PDX was inoculated into NOD/SCID mice and grown to ∼1 cm^3 volume. The tumor was excised, digested as previously described to a single cell suspension (29), stained with CD36-FITC and sorted via flow cytometry. The top 10% of the brightest green fluorescent protein (GFP) positive cells (117,000 cells), designated CD36^{high}, and the bottom 10% of GFP negative cells (3,120,000 cells), designated CD36^{low}, were sorted separately, placed in Matrigel, and sequentially implanted into NOD/SCID mice and allowed to grow. The tumor established from CD36^{high} cells grew much larger compared to the CD36^{low} tumor (tumor volume 2,419.64 vs. 53.57mm^3, respectively; **Figures 5A,B**). Western blot analysis of tumor tissues from CD36^{high} and CD36^{low} cells showed an increase in survivin expression in the CD36^{high} tumors in comparison to the CD36^{low} tumors (**Figure 5C**). Interestingly, similar to our data obtained from TMA analysis, we observed that FASN was higher in CD36^{high} cells as compared to CD36^{low} cells, further supporting a potential interconnection between these two proteins (**Figure 5C**). Ki67 staining of Pt 2402 CD36^{high} and CD36^{low} tumors showed a significant reduction in Ki67 expression in the CD36^{low} tumors compared to CD36^{high} (**Figure 5D**).

To confirm that an increase in CD36 expression is associated with an increase in survivin expression, we overexpressed CD36 in the established HCT116 CRC cell line. Western blot analysis of HCT116 cells demonstrated CD36 overexpression leads to an increase in expression of survivin and activation of Akt, an upstream translational regulator of survivin in CRC (38), as well as a decrease in cleaved-PARP (**Figure 5E**). Therefore, taken together, our data suggest that upregulation of pAkt and survivin are potential mechanisms by which CD36 promotes CRC cell proliferation and tumor growth.

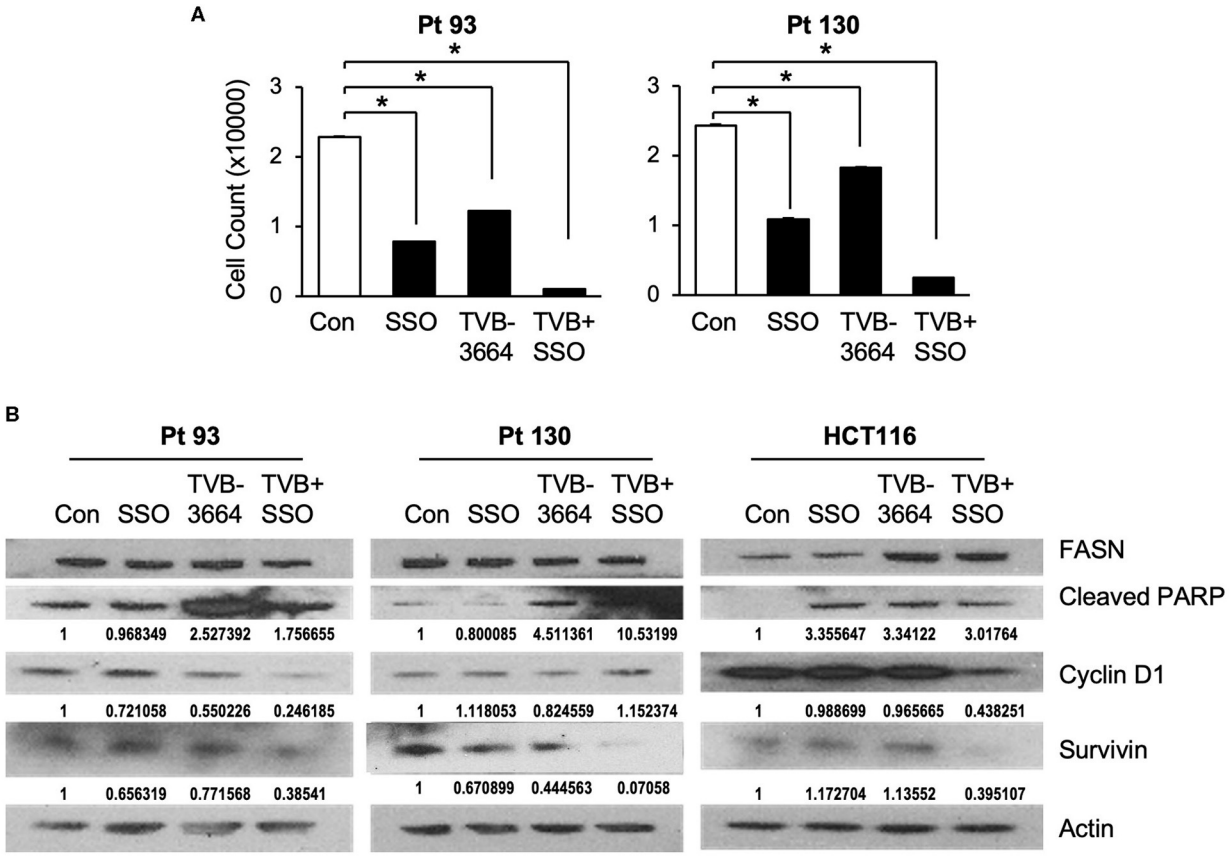

FIGURE 6 | Inhibition of CD36 and FASN have a synergetic effect in reducing cell proliferation. **(A)** Pt 93, Pt 130, and HCT116 cells were treated with SSO and TVB-3664 alone or in combination for 6 days and cell number was counted. Representative data from three experiments is shown (*$p < 0.05$). **(B)** Western blot analysis of cells treated with TVB-3664, SSO, or TVB-3664 and SSO in combination.

Inhibition of FASN and CD36 in Combination Reduce Primary CRC Cell Proliferation *in vitro*

Both *de novo* synthesized and exogenous FA play important roles in carcinogenesis (28, 39), To extend our findings that FASN inhibition upregulates the expression of CD36 and to further test whether inhibition of CD36 can improve the efficacy of TVB-3664, primary CRC cells from Pt 93 and Pt 130 were treated with CD36 inhibitor SSO and FASN inhibitor TVB-3664, alone or in combination, in both normal and serum-starved media. Cellular proliferation was significantly reduced in both SSO- and TVB-3664-treated cells and was further significantly reduced in cells that received combination treatment (**Figure 6A**). Western blot analysis of CRC cells treated with a combination of TVB-3664 and SSO shows that combination treatment significantly reduces expression of survivin in Pt 130 and HCT116 cell lines but not in Pt 93 cell line as compared to control or single agent treatment alone (**Figure 6B**). Combination treatment was also associated with reduced expression of cyclin D1 in Pt 93 and HCT116 cell lines. Interestingly, cyclin D1 in Pt 130 cells increased expression in combination treatments. This suggests a different mode of action and sensitivity to SSO and TVB-3664 in Pt 130 when compared to other CRC cell lines. Collectively, these data suggest that inhibition of both FA synthesis and FA uptake may be a potential therapeutic strategy for CRC. However, further studies are necessary to evaluate the effect of combinational treatment *in vivo*.

DISCUSSION

Our previous studies demonstrate that the effect of FASN inhibition on cellular proliferation *in vitro* does not always translate to the same effect on tumor growth *in vivo* (7, 10). Despite a significant decrease in cellular proliferation in primary CRC cell lines treated with TVB-3664, the efficacy of TVB-3664 in PDX models was much lower, suggesting a potential compensatory impact of diet on the effect of FASN inhibitors (10, 14). Therefore, the goal of this study was to delineate the effect of FASN inhibition on exogeneous FA uptake and elucidate the effect of FA uptake on sustaining cellular proliferation.

Here, for the first time, we report that inhibition of FASN leads to a selective upregulation of CD36 expression. CD36 enhances FA uptake and FA oxidation, and plays a critical role in cancer cell growth and metastasis (20, 21, 24, 40, 41). Consistent with reports that CD36 is upregulated in breast cancer and glioblastoma (42), we found that CD36 is highly expressed in CRC as compared to normal mucosa. Tumor stroma is deficient in CD36 expression (43). High stromal content in fresh primary CRC tumors can potentially explain why fresh CRC tissue analysis shows inconsistent results for CD36 expression in primary CRC as compare to normal colon. Based on tissue analysis, we found that high expression of CD36 is primarily associated with CRC metastasis, suggesting that metastatic tumors are more dependent on FA uptake as compared to primary CRC. Our findings are supported by multiple studies showing the involvement of CD36 in metastatic disease (24, 44, 45). Interestingly, even though we have identified a positive correlation between the protein expression of FASN and CD36 using TMA analysis, based on TCGA data, there is a significant inverse correlation between these two proteins at the mRNA levels. Indeed, we found that inhibition of FASN selectively upregulates CD36 mRNA and protein expression, but not expression of other FA transporters in multiple models including CRC cells, tumor xenografts, genetically modified mice and in human tissues. Interestingly, we did not note any significant changes in FASN expression when the expression of CD36 was altered, suggesting that the level of *de novo* lipid synthesis is not regulated by FA uptake via CD36 in our modes. Current understanding of the regulation of CD36 expression is rather limited (46), and how CD36 expression is regulated in cancer, and in particular in CRC, is not known. Several transcriptional activators have been implicated in regulation of CD36 expression including peroxisome proliferator-activated receptors (PPARs), CCAAT/enhancer-binding protein, and HIF-1 (16). Ongoing studies in our laboratory are investigating CD36 expression in different cell types in primary and metastatic CRC and potential mechanisms of CD36 regulation by FASN.

It has been reported that siRNA-mediated inhibition of CD36 decreases cellular proliferation in MCF-7 breast cancer cells (19). Additionally, CD36 has pro-tumorigenic and progression properties in glioblastoma stem cells (21). In agreement with these data, our study shows that chemical inhibition and stable knockdown of CD36 via shRNA in established and primary CRC cells decrease cellular proliferation. Consistent with data using a specific small molecule CD36 inhibitor, 2-methylthio-1,4-napthoquinone (MTN), in glioblastoma stem cells (21), inhibition of CD36 with SSO is associated with a decrease in activation of pAkt. We have also showed that CD36 regulates survivin, a member of the inhibitor of apoptosis (IAP) family that is highly expressed in most cancer and associated with a poor prognosis (47). The pro-survival role of CD36 in CRC is further supported by data showing that Pt 2402 $CD36^{high}$ cells have a much higher propensity to establish xenograft tumors, which grow significantly faster and express higher levels of survivin, in comparison to $CD36^{low}$ cells.

Interestingly, in a previously published study in oral carcinoma, the effect of CD36 inhibition was associated with inhibition of metastasis, but not with growth of primary oral cancers (24). In contrast to these findings, our study suggests a critical role of CD36 in CRC proliferation and tumor growth *in vivo* with both chemical inhibition via SSO as well as shRNA-mediated knockdown of CD36 in xenografts using multiple established cell lines.

Novel FASN inhibitors, TVBs, have demonstrated anticancer activity in multiple preclinical models (3), and TVB-2640 is currently in a number of clinical trials, including one at the University of Kentucky's Markey Cancer Center (https://www.cancer.gov/about-cancer/treatment/clinical-trials/search/v?id=NCI-2016-01710&r=1). Thus, it is crucial to identify and understand potential resistance mechanisms to FASN-targeted therapy. The current study demonstrates that inhibition of FASN leads to upregulation of CD36 expression and its translocation to the plasma membrane. One of the primary roles of CD36, when located within the cell membrane, is the transport of FAs (15, 16). Therefore, this upregulation of membrane bound CD36 and, consequently, an increase in FA uptake, could be a potential mechanism of resistance to FASN inhibition. Importantly, our data demonstrate that the combined inhibition of CD36 and FASN has a synergistic effect on inhibition of cellular proliferation as well as survivin and cyclin D1, further suggests that targeting FA uptake may be a potential therapeutic approach to increase the efficacy of FASN inhibitors.

We previously reported that the level of FASN expression determines the sensitivity of tumors to TVBs compounds (10). Consistently throughout this study, we observed that the higher expression of CD36 in HT29 LuM3 cells (36) as compared to parental HT29 cells, makes these cells more sensitive to CD36 inhibition via CD36 shRNA and inhibits xenograft tumor growth to a higher extent as compared to HT29 xenografts. Furthermore, the mutational and metabolic profiles of tumors determine tumor cell response to multiple therapies including metabolic inhibitors (48, 49). Different genetic profiles and metabolic features can explain the varying levels of response of cell lines to FASN and CD36 inhibition. Pt 93 and Pt 130 cells have KRAS and V600E BRAF mutations. The Pt 130 cell line also carries an FGFR mutation (10). The HCT116 cell line is a KRAS mutant, but BRAF wild type as compared to HT29 which has a V600E BRAF mutation but KRAS wild type (50). In addition, TVB-3664 seems to have more efficacy in activating PARP cleavage as compared to SSO, suggesting that inhibition of lipid synthesis leads to activation of apoptosis through distinct pathways other than those related to the inhibition of FA uptake. Our ongoing studies in the laboratory are focused on identifying the mutational and metabolic features of tumors that would determine their sensitivity to lipid metabolism targeted therapies.

Multiple studies suggest that fatty acid metabolism in adipose tissue is a major contributor to the etiology of obesity and diabetes (51). Obesity is associated with chronic elevation of free fatty acids, which promote insulin resistance and contribute to the development of systemic hyperglycemia (52). Interestingly, FASN expression is directly linked to obesity and type 2 diabetes (53) and CD36 protein expression is upregulated in both obese patients and type 2 diabetics (54). Therefore, the findings from this study support the idea that targeting both FASN and CD36 in combination may have therapeutic potential not only in cancer but also in metabolic disorders such as obesity and diabetes.

This report is the first to describe the functional importance of CD36 and its indolent role in fatty acid metabolism in the setting of CRC. It is also the first to describe the interconnection between FASN and CD36 and provides a strong rationale for further investigation into the interconnection of *de novo* lipogenesis and FA uptake that could potentially lead to the development of new therapeutic strategies for CRC and other solid malignancies, and potentially some metabolic disorders as well.

DATA AVAILABILITY STATEMENT

The raw data supporting the conclusions of this article will be made available by the authors, without undue reservation.

ETHICS STATEMENT

The animal study was reviewed and approved by UK Animal Care and Use Committee, University of Kentucky. The studies involving human participants were reviewed and approved by UK Medical Center (IRB #16-0439-P2H), University of Kentucky. The patients/participants provided their written informed consent to participate in this study.

AUTHOR CONTRIBUTIONS

JD designed and performed experiments, wrote the methods, and drafted the manuscript. PR contributed to experimental design, data acquisition and interpretation, and reviewed the manuscript. NJ contributed to data acquisition. EL performed TMA scoring and tissue evaluation. HW performed statistical analysis. DH and CW performed analysis of TCGA data. BE contributed to experimental design and reviewed the manuscript. YZ contributed to experimental design, data acquisition and interpretation, and co-wrote the manuscript. All authors contributed to the article and approved the submitted version.

FUNDING

National Institutes of Health (P20 GM121327 to YZ, R01 CA208343 to BE, T32 ES07266 to JD); Markey Cancer Center shared resource facilities (Biospecimen Procurement and Translational Pathology SRF, Flow Cytometry and Immune Monitoring SRF, Biostatistics and Bioinformatics SRF) are partially supported by National Cancer Institute (P30 CA177558 to BE).

ACKNOWLEDGMENTS

The Markey Cancer Center's Research Communications Office assisted with preparation of this manuscript.

SUPPLEMENTARY MATERIAL

The Supplementary Material for this article can be found online at: https://www.frontiersin.org/articles/10.3389/fonc.2020.01185/full#supplementary-material

REFERENCES

1. Ferlay J, Shin HR, Bray F, Forman D, Mathers C, Parkin DM. Estimates of worldwide burden of cancer in 2008: GLOBOCAN (2008). *Int J Cancer.* (2010) 127:2893–917. doi: 10.1002/ijc.25516
2. Pavlova NN, Thompson CB. The emerging hallmarks of cancer metabolism. *Cell Metab.* (2016) 23:27–47. doi: 10.1016/j.cmet.2015.12.006
3. Buckley D, Duke G, Heuer TS, O'Farrell M, Wagman AS, McCulloch W, et al. Fatty acid synthase - modern tumor cell biology insights into a classical oncology target. *Pharmacol Ther.* (2017) 177:23–31. doi: 10.1016/j.pharmthera.2017.02.021
4. Currie E, Schulze A, Zechner R, Walther TC, Farese RV, Jr. Cellular fatty acid metabolism and cancer. *Cell Metab.* (2013) 18:153–61. doi: 10.1016/j.cmet.2013.05.017
5. Kim JT, Liu C, Zaytseva YY, Weiss HL, Townsend CM Jr, Evers BM, et al. Neurotensin, a novel target of Wnt/beta-catenin pathway, promotes growth of neuroendocrine tumor cells. *Int J Cancer.* (2015) 136:1475–81. doi: 10.1002/ijc.29123
6. Zaytseva YY, Elliott VA, Rychahou P, Mustain WC, Kim JT, Valentino J, et al. Cancer cell-associated fatty acid synthase activates endothelial cells and promotes angiogenesis in colorectal cancer. *Carcinogenesis.* (2014) 35:1341–51. doi: 10.1093/carcin/bgu042
7. Zaytseva YY, Rychahou PG, Gulhati P, Elliott VA, Mustain WC, O'Connor K, et al. Inhibition of fatty acid synthase attenuates CD44-associated signaling and reduces metastasis in colorectal cancer. *Cancer Res.* (2012) 72:1504–17. doi: 10.1158/0008-5472.CAN-11-4057
8. Heuer TS, Ventura R, Mordec K, Lai J, Fridlib M, Buckley D, et al. FASN inhibition and taxane treatment combine to enhance anti-tumor efficacy in diverse xenograft tumor models through disruption of tubulin palmitoylation and microtubule organization and FASN inhibition-mediated effects on oncogenic signaling and gene expression. *EBioMedicine.* (2017) 16:51–62. doi: 10.1016/j.ebiom.2016.12.012
9. Ventura R, Mordec K, Waszczuk J, Wang Z, Lai J, Fridlib M, et al. Inhibition of *de novo* palmitate synthesis by fatty acid synthase induces apoptosis in tumor cells by remodeling cell membranes, inhibiting signaling pathways, and reprogramming gene expression. *EBioMedicine.* (2015) 2:806–22. doi: 10.1016/j.ebiom.2015.06.020
10. Zaytseva YY, Rychahou PG, Le AT, Scott TL, Flight RM, Kim JT, et al. Preclinical evaluation of novel fatty acid synthase inhibitors in primary colorectal cancer cells and a patient-derived xenograft model of colorectal cancer. *Oncotarget.* (2018) 9:24787–800. doi: 10.18632/oncotarget.25361
11. O'Farrell M, Crowley R, Heuer TS, Buckley D, Rubino CM, McCulloch W, et al. Abstract 2675: biomarker and PK/PD analyses of first in class FASN inhibitor TVB-2640 in a first-in-human phase 1 study in solid tumor patients. *AACR.* (2015) 75(Suppl):2675. doi: 10.1158/1538-7445.AM2015-2675
12. Dean EJ, Falchook GS, Patel MR, Brenner AJ, Infante JR, Arkenau H-T, et al. Abstract 2512: Preliminary activity in the first in human study of the first-in-class fatty acid synthase (FASN) inhibitor, TVB-2640. *J Clin Oncol.* (2016) 34(15_suppl):2512. doi: 10.1200/JCO.2016.34.15_suppl.2512
13. National Cancer Institute. *FASN Inhibitor TVB-2640 in Treating Patients with Colon or Other Cancers That Can Be Removed by Surgery.* National Institutes of Health (2017). Available online at: https://www.cancer.gov/about-cancer/treatment/clinical-trials/search/v?id=NCI-2016-01710&r=1
14. Jafari N, Drury J, Morris AJ, Onono FO, Stevens PD, Gao T, et al. *De novo* fatty acid synthesis-driven sphingolipid metabolism promotes metastatic potential of colorectal cancer. *Mol Cancer Res.* (2019) 17:140–52. doi: 10.1158/1541-7786.MCR-18-0199
15. Pepino MY, Kuda O, Samovski D, Abumrad NA. Structure-function of CD36 and importance of fatty acid signal transduction in fat metabolism. *Annu Rev Nutr.* (2014) 34:281–303. doi: 10.1146/annurev-nutr-071812-161220

16. Glatz JFC, Luiken J. Dynamic role of the transmembrane glycoprotein CD36 (SR-B2) in cellular fatty acid uptake and utilization. *J Lipid Res.* (2018) 59:1084–93. doi: 10.1194/jlr.R082933
17. Glatz JF, Luiken JJ, Bonen A. Membrane fatty acid transporters as regulators of lipid metabolism: implications for metabolic disease. *Physiol Rev.* (2010) 90:367–417. doi: 10.1152/physrev.00003.2009
18. Luiken JJ, Chanda D, Nabben M, Neumann D, Glatz JF. Post-translational modifications of CD36 (SR-B2): implications for regulation of myocellular fatty acid uptake. *Biochim Biophys Acta.* (2016) 1862:2253–8. doi: 10.1016/j.bbadis.2016.09.004
19. Zhao J, Zhi Z, Wang C, Xing H, Song G, Yu X, et al. Exogenous lipids promote the growth of breast cancer cells via CD36. *Oncol Rep.* (2017) 38:2105–15. doi: 10.3892/or.2017.5864
20. Ladanyi A, Mukherjee A, Kenny HA, Johnson A, Mitra AK, Sundaresan S, et al. Adipocyte-induced CD36 expression drives ovarian cancer progression and metastasis. *Oncogene.* (2018) 37:2285–301. doi: 10.1038/s41388-017-0093-z
21. Hale JS, Otvos B, Sinyuk M, Alvarado AG, Hitomi M, Stoltz K, et al. Cancer stem cell-specific scavenger receptor CD36 drives glioblastoma progression. *Stem Cells.* (2014) 32:1746–58. doi: 10.1002/stem.1716
22. Pan J, Fan Z, Wang Z, Dai Q, Xiang Z, Yuan F, et al. CD36 mediates palmitate acid-induced metastasis of gastric cancer via AKT/GSK-3β/β-catenin pathway. *J Exp Clin Cancer Res.* (2019) 38:52. doi: 10.1186/s13046-019-1049-7
23. Watt MJ, Clark AK, Selth LA, Haynes VR, Lister N, Rebello R, et al. Suppressing fatty acid uptake has therapeutic effects in preclinical models of prostate cancer. *Sci Transl Med.* (2019) 11:eaau5758. doi: 10.1126/scitranslmed.aau5758
24. Pascual G, Avgustinova A, Mejetta S, Martin M, Castellanos A, Attolini CS, et al. Targeting metastasis-initiating cells through the fatty acid receptor CD36. *Nature.* (2017) 541:41–5. doi: 10.1038/nature20791
25. Menendez JA, Lupu R. Fatty acid synthase and the lipogenic phenotype in cancer pathogenesis. *Nat Rev Cancer.* (2007) 7:763–77. doi: 10.1038/nrc2222
26. Altieri DC. Targeting survivin in cancer. *Cancer Lett.* (2013) 332:225–8. doi: 10.1016/j.canlet.2012.03.005
27. Garg H, Suri P, Gupta JC, Talwar GP, Dubey S. Survivin: a unique target for tumor therapy. *Cancer Cell Int.* (2016) 16:49. doi: 10.1186/s12935-016-0326-1
28. DeBerardinis RJ, Chandel NS. Fundamentals of cancer metabolism. *Sci Adv.* (2016) 2:e1600200. doi: 10.1126/sciadv.1600200
29. Jafari N, Drury J, Morris AJ, Onono FO, Stevens PD, Gao T, et al. *De novo* fatty acid synthesis driven sphingolipid metabolism promotes metastatic potential of colorectal cancer. *Mol Cancer Res.* (2018) 78(Suppl):1437. doi: 10.1158/1538-7445.AM2018-1437
30. Uhlen M, Fagerberg L, Hallstrom BM, Lindskog C, Oksvold P, Mardinoglu A, et al. Proteomics. Tissue-based map of the human proteome. *Science.* (2015) 347:1260419. doi: 10.1126/science.1260419
31. Silverstein RL, Febbraio M. CD36, a scavenger receptor involved in immunity, metabolism, angiogenesis, and behavior. *Sci Signal.* (2009) 2:re3. doi: 10.1126/scisignal.272re3
32. Julien S, Merino-Trigo A, Lacroix L, Pocard M, Goere D, Mariani P, et al. Characterization of a large panel of patient-derived tumor xenografts representing the clinical heterogeneity of human colorectal cancer. *Clin Cancer Res.* (2012) 18:5314–28. doi: 10.1158/1078-0432.CCR-12-0372
33. Cheung AF, Carter AM, Kostova KK, Woodruff JF, Crowley D, Bronson RT, et al. Complete deletion of Apc results in severe polyposis in mice. *Oncogene.* (2010) 29:1857–64. doi: 10.1038/onc.2009.457
34. Coort SL, Willems J, Coumans WA, van der Vusse GJ, Bonen A, Glatz JF, et al. Sulfo-N-succinimidyl esters of long chain fatty acids specifically inhibit fatty acid translocase (FAT/CD36)-mediated cellular fatty acid uptake. *Mol Cell Biochem.* (2002) 239:213–9. doi: 10.1007/978-1-4419-9270-3_27
35. Sommer KW, Schamberger CJ, Schmidt GE, Sasgary S, Cerni C. Inhibitor of apoptosis protein (IAP) survivin is upregulated by oncogenic c-H-Ras. *Oncogene.* (2003) 22:4266–80. doi: 10.1038/sj.onc.1206509
36. Rychahou P, Bae Y, Reichel D, Zaytseva YY, Lee EY, Napier D, et al. Colorectal cancer lung metastasis treatment with polymer-drug nanoparticles. *J Control Release.* (2018) 275:85–91. doi: 10.1016/j.jconrel.2018.02.008
37. Sahin AA, Ro JY, Brown RW, Ordonez NG, Cleary KR, el-Naggar AK, et al. Assessment of Ki-67-derived tumor proliferative activity in colorectal adenocarcinomas. *Mod Pathol.* (1994) 7:17–22.
38. Ye Q, Cai W, Zheng Y, Evers BM, She QB. ERK and AKT signaling cooperate to translationally regulate survivin expression for metastatic progression of colorectal cancer. *Oncogene.* (2014) 33:1828–39. doi: 10.1038/onc.2013.122
39. Cao D, Song X, Che L, Li X, Pilo MG, Vidili G, et al. Both *de novo* synthetized and exogenous fatty acids support the growth of hepatocellular carcinoma cells. *Liver Int.* (2017) 37:80–9. doi: 10.1111/liv.13183
40. Cheng C, Geng F, Cheng X, Guo D. Lipid metabolism reprogramming and its potential targets in cancer. *Cancer Commun (Lond).* (2018) 38:27. doi: 10.1186/s40880-018-0301-4
41. Clezardin P, Frappart L, Clerget M, Pechoux C, Delmas PD. Expression of thrombospondin (TSP1) and its receptors (CD36 and CD51) in normal, hyperplastic, and neoplastic human breast. *Cancer Res.* (1993) 53:1421–30.
42. Liang Y, Han H, Liu L, Duan Y, Yang X, Ma C, et al. CD36 plays a critical role in proliferation, migration and tamoxifen-inhibited growth of ER-positive breast cancer cells. *Oncogenesis.* (2018) 7:98. doi: 10.1038/s41389-018-0107-x
43. Wang J, Li Y. CD36 tango in cancer: signaling pathways and functions. *Theranostics.* (2019) 9:4893–908. doi: 10.7150/thno.36037
44. Enciu AM, Radu E, Popescu ID, Hinescu ME, Ceafalan LC. Targeting CD36 as biomarker for metastasis prognostic: how far from translation into clinical practice? *Biomed Res Int.* (2018) 2018:7801202. doi: 10.1155/2018/7801202
45. Pascual G, Dominguez D, Benitah SA. The contributions of cancer cell metabolism to metastasis. *Dis Model Mech.* (2018) 11:dmm032920. doi: 10.1242/dmm.032920
46. Showkat M, Beigh MA, Andrabi KI. mTOR signaling in protein translation regulation: implications in cancer genesis and therapeutic interventions. *Mol Biol Int.* (2014) 2014:686984. doi: 10.1155/2014/686984
47. Altieri DC. Survivin, cancer networks and pathway-directed drug discovery. *Nat Rev Cancer.* (2008) 8:61–70. doi: 10.1038/nrc2293
48. Luengo A, Gui DY, Vander Heiden MG. Targeting metabolism for cancer therapy. *Cell Chem Biol.* (2017) 24:1161–80. doi: 10.1016/j.chembiol.2017.08.028
49. Parca L, Pepe G, Pietrosanto M, Galvan G, Galli L, Palmeri A, et al. Modeling cancer drug response through drug-specific informative genes. *Sci Rep.* (2019) 9:15222. doi: 10.1038/s41598-019-50720-0
50. Ahmed D, Eide PW, Eilertsen IA, Danielsen SA, Eknaes M, Hektoen M, et al. Epigenetic and genetic features of 24 colon cancer cell lines. *Oncogenesis.* (2013) 2:e71. doi: 10.1038/oncsis.2013.35
51. Park J, Morley TS, Kim M, Clegg DJ, Scherer PE. Obesity and cancer–mechanisms underlying tumour progression and recurrence. *Nat Rev Endocrinol.* (2014) 10:455–65. doi: 10.1038/nrendo.2014.94
52. Hellmann J, Zhang MJ, Tang Y, Rane M, Bhatnagar A, Spite M. Increased saturated fatty acids in obesity alter resolution of inflammation in part by stimulating prostaglandin production. *J Immunol.* (2013) 191:1383–92. doi: 10.4049/jimmunol.1203369
53. Berndt J, Kovacs P, Ruschke K, Kloting N, Fasshauer M, Schon MR, et al. Fatty acid synthase gene expression in human adipose tissue: association with obesity and type 2 diabetes. *Diabetologia.* (2007) 50:1472–80. doi: 10.1007/s00125-007-0689-x
54. Balaban S, Lee LS, Schreuder M, Hoy AJ. Obesity and cancer progression: is there a role of fatty acid metabolism? *Biomed Res Int.* (2015) 2015:274585. doi: 10.1155/2015/274585

Conflict of Interest: The authors declare that the research was conducted in the absence of any commercial or financial relationships that could be construed as a potential conflict of interest.

frontiers | Frontiers in Oncology

TYPE Review
PUBLISHED 17 February 2023
DOI 10.3389/fonc.2023.1060112

OPEN ACCESS

EDITED BY
Carlos Pérez-Plasencia,
National Autonomous University of Mexico, Mexico

REVIEWED BY
Bernd Heinrich,
National Institutes of Health (NIH), United States
Mohamed S. Abdel-Hakeem,
Emory University, United States

*CORRESPONDENCE
Sascha Kahlfuss
sascha.kahlfuss@med.ovgu.de
Dimitrios Mougiakakos
dimitrios.mougiakakos@med.ovgu.de

SPECIALTY SECTION
This article was submitted to Cancer Metabolism, a section of the journal Frontiers in Oncology

RECEIVED 02 October 2022
ACCEPTED 11 January 2023
PUBLISHED 17 February 2023

CITATION
Jantz-Naeem N, Böttcher-Loschinski R, Borucki K, Mitchell-Flack M, Böttcher M, Schraven B, Mougiakakos D and Kahlfuss S (2023) TIGIT signaling and its influence on T cell metabolism and immune cell function in the tumor microenvironment. *Front. Oncol.* 13:1060112. doi: 10.3389/fonc.2023.1060112

TIGIT signaling and its influence on T cell metabolism and immune cell function in the tumor microenvironment

Nouria Jantz-Naeem[1], Romy Böttcher-Loschinski[2], Katrin Borucki[3], Marisa Mitchell-Flack[4], Martin Böttcher[2,5], Burkhart Schraven[1,5], Dimitrios Mougiakakos[2,5]* and Sascha Kahlfuss[1,5,6,7]*

[1]Institute of Molecular and Clinical Immunology, Medical Faculty, Otto-von-Guericke University Magdeburg, Magdeburg, Germany, [2]Department of Hematology and Oncology, University Hospital Magdeburg, Otto-von-Guericke University Magdeburg, Magdeburg, Germany, [3]Institute of Clinical Chemistry, Department of Pathobiochemistry, Medical Faculty, Otto-von-Guericke University Magdeburg, Magdeburg, Germany, [4]Department of Oncology, The Bloomberg~Kimmel Institute for Cancer Immunotherapy, Johns Hopkins University School of Medicine, Baltimore, MD, United States, [5]Health Campus Immunology, Infectiology and Inflammation (GCI), Medical Faculty, Otto-von-Guericke University Magdeburg, Magdeburg, Germany, [6]Institute of Medical Microbiology and Hospital Hygiene, Medical Faculty, Otto-von-Guericke University Magdeburg, Magdeburg, Germany, [7]Center for Health and Medical Prevention (CHaMP), Otto-von-Guericke-University, Magdeburg, Germany

One of the key challenges for successful cancer therapy is the capacity of tumors to evade immune surveillance. Tumor immune evasion can be accomplished through the induction of T cell exhaustion *via* the activation of various immune checkpoint molecules. The most prominent examples of immune checkpoints are PD-1 and CTLA-4. Meanwhile, several other immune checkpoint molecules have since been identified. One of these is the T cell immunoglobulin and ITIM domain (TIGIT), which was first described in 2009. Interestingly, many studies have established a synergistic reciprocity between TIGIT and PD-1. TIGIT has also been described to interfere with the energy metabolism of T cells and thereby affect adaptive anti-tumor immunity. In this context, recent studies have reported a link between TIGIT and the hypoxia-inducible factor 1-α (HIF1-α), a master transcription factor sensing hypoxia in several tissues including tumors that among others regulates the expression of metabolically relevant genes. Furthermore, distinct cancer types were shown to inhibit glucose uptake and effector function by inducing TIGIT expression in $CD8^+$ T cells, resulting in an impaired anti-tumor immunity. In addition, TIGIT was associated with adenosine receptor signaling in T cells and the kynurenine pathway in tumor cells, both altering the tumor microenvironment and T cell-mediated immunity against tumors. Here, we review the most recent literature on the reciprocal interaction of TIGIT and T cell metabolism and specifically how TIGIT affects anti-tumor immunity. We believe understanding this interaction may pave the way for improved immunotherapy to treat cancer.

KEYWORDS

T cells, metabolism, cancer, therapy, microenviroment

1 Introduction

1.1 Reciprocal metabolic interaction of tumor cells and T cells within the tumor microenvironment

Tumors are notorious for evading surveillance of the immune system *via* T cell hyporesponsiveness and dysfunction (1, 2). In particular, limited nutrient availability, in particular the scarcity of glucose (3) and tryptophan (4, 5) which are required for normal cell functionality, in the tumor microenvironment (TME) due to competition can impair $CD8^+$ cytotoxic T cells (CTL) proliferation, survival, and effector function (4–6). In this context, tumor cells have been shown to express the enzyme indoleamine 2,3-dioxygenase (IDO), which on the one hand depletes tryptophan, a critical amino acid needed for T cell proliferation (4, 5), and on the other hand produces kynurenine, a T cell suppressive metabolic 'waste' product (7). It is noteworthy that the role of effector $CD4^+$ T cells during anti-tumor immunity is not as well resolved as it is for $CD8^+$ T cells (8). In addition, hypoxia within the TME can diminish anti-tumor activity directly by inhibiting NK cell-mediated killing (9), or by inducing T cell apoptosis through inhibition of CCR7 expression *via* the A2A receptor signaling pathway (10). Hypoxia has also been demonstrated to upregulate immune checkpoint proteins such as PD-L1 on tumor cells (11–13). Additionally, metabolites produced by tumor cells can promote tumor immune evasion. In this regard, adenosine, a byproduct of the enzymatic breakdown of adenosine 5'-triphosphate (ATP) *via* the ectonucleotidases CD39 and CD73, promotes tumor growth, survival, and metastasis and also impairs $CD8^+$ T cell signaling and function (14–18). Furthermore, acidification of the TME through the generation of lactic acid by the tumor itself impairs respiration, chemotaxis, and cytokine production of CTLs (6, 19). Altogether, the TME is a unique metabolic niche that consists of several mechanisms to escape immune surveillance by impairing T cell metabolism and effector function.

1.2 The role of T cell and tumor cell metabolism for anti-tumor immunity

For T cells to be able to undergo essential processes such as proliferation, growth and differentiation, they need to metabolically adapt to their new requirements, a process also referred to as metabolic reprogramming (20, 21). Naïve T cells mainly make use of fatty acid oxidation, while activated T cells tend to shift from the energetically more favorable oxidative phosphorylation (OXPHOS) to the Warburg metabolism (22–24) to fulfill their need for various metabolic resources. In order to facilitate this kind of metabolic reprogramming during T cell activation, several different signaling cascades and transcription factors come into play. IL-2, a classical growth factor cytokine, and the ligation of costimulatory proteins will enable the metabolic transition to glycolysis by increasing the expression of nutrient transporters and activation of mTOR, a key metabolic regulator (25–27). Together with c-Myc, a protein that activates the transcription of metabolic genes essential for T cell activation (28), mTOR induces the increased expression of glucose transporter 1 (GLUT1) and CD98, a protein responsible for transporting amino acids into the cell (29). To summarize, it can be stated that the metabolic profile of T cells will determine their functional state.

There is increasing appreciation for the fact that a metabolic interplay between tumor and immune cells exists in the TME (30, 31). Further, there is evidence that immune checkpoint proteins themselves have an effect on T cell metabolism, reviewed comprehensively by Lim et al. (32). Kleffel et al. (33) have demonstrated that melanoma cell intrinsically expressed PD-1 upregulates the Akt/mTOR signaling pathway in cancer cells. In another study by Chang et al. (31), tumor PD-L1 expression promoted glycolysis and the activation of Akt/mTOR in tumor cells, while simultaneously suppressing the activity of mTOR in T cells by competing for glucose. The blocking of PD-L1, PD-1 and CTLA-4 resulted in altered concentrations of extracellular glucose (31). This is noteworthy as acidosis in the TME can limit the anti-tumor activity of CTL, as well as suppress their proliferation and cytokine production (34). It is plausible to assume that several immune checkpoint proteins can promote glycolysis in tumor cells, therefore creating a nutrient competitive scenario between tumor cells and immune cells within the TME.

1.3 Immune checkpoints in T cell immunity

To elicit a successful immune response against tumors, T cells need to become fully activated. This activation depends on two distinct signals. The first signal represents the engagement of the T cell receptor (TCR) by cognate peptide:MHC class I or II complexes (pMHC) presented by antigen presenting cells (APCs) (35). The second signal involves the co-stimulation *via* B7 proteins on APCs that interact with cluster of differentiation (CD)28 expressed on the surface of T cells (36, 37). Unchecked and/or persistent activation of T cells could lead to aberrant inflammation causing severe damage to host tissue. Because of this, it is necessary that T cell activation is closely regulated by co-stimulatory and co-inhibitory proteins, referred to as immune checkpoints (38).

In the past 10 years, the development of novel immunotherapies has been enormously successful especially within the areas of chimeric antigen receptor (CAR) T cells (39), bispecific antibodies capable of binding two targets simultaneously (40), and immune checkpoint inhibitors (ICI) (41). However, despite the enormous success of ICIs, many patients show or acquire resistance to treatment with ICIs (42). Consequently, the latter has resulted in a need for the identification of novel immune checkpoints such as lymphocyte activation gene-3 (LAG3) (43), V-domain Ig suppressor of T cell activation (VISTA) (44), B and T cell attenuator (BTLA) (45), B7 homolog 3 protein (B7-H3) (46), T cell immunoglobulin and mucin-domain containing-3 (TIM3) (47) and T cell immunoglobulin and ITIM domain (TIGIT) (48). These proteins each have distinct ligands and suppress T cell function through several mechanisms to ensure there is proper regulation of the T cell response. In the following paragraphs, we will briefly introduce several immune checkpoints by structure and function. Figure 1 details these

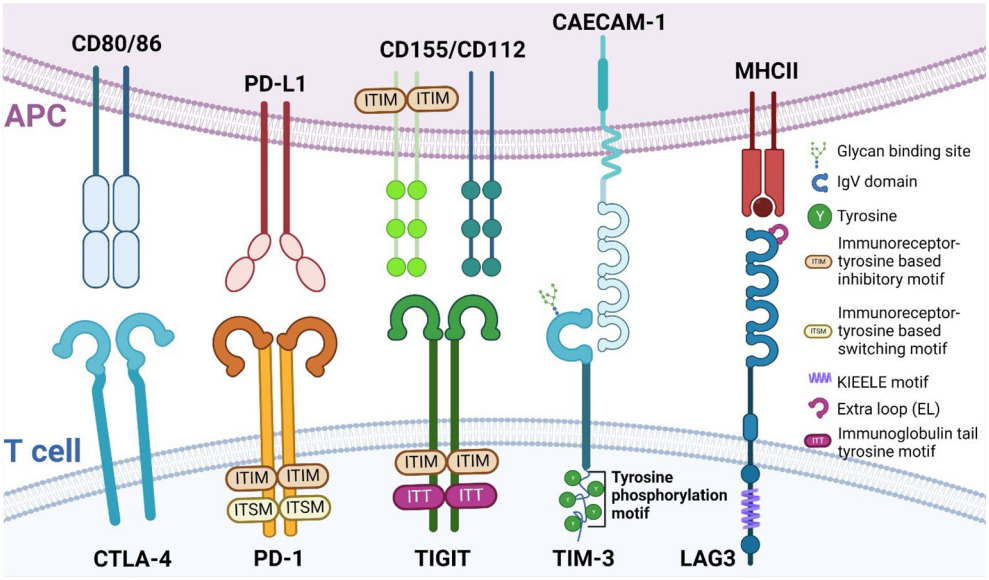

FIGURE 1
Structure of different immune checkpoints. Immune checkpoints and their structure expressed on T cells (bottom) and their respective ligands expressed on APCs (top). Depicted here are CTLA-4, PD-1, TIGIT, TIM-3 and LAG3. APC, antigen presenting cell; CTLA-4, Cytotoxic T lymphocyte antigen 4; PD-1, Programmed Death-1; TIGIT, T cell immunoglobulin and ITIM domain; TIM-3, T cell immunoglobulin domain and mucin domain 3; LAG3, lymphocyte activation gene-3.

structural differences and similarities between the different immune checkpoints.

1.3.1 PD-1

Programmed Death-1 (PD-1) is a type I transmembrane protein that is expressed in several immune cells, such as T, B, and NK cells. Structurally, it is composed of an extracellular immunoglobulin-like binding domain, a transmembrane region and a cytoplasmic domain containing an immunoreceptor tyrosine-based inhibitory motif (ITIM) and an immunoreceptor tyrosine-base switch motif (ITSM) (49). Engagement of PD-L1 with its receptor results in T cell dysfunction, exhaustion, and production of the immunosuppressive cytokine IL10 within the tumor (50). With the FDA approval for Nivolumab and Pembrolizumab, the potential of blocking PD-1 was realized and successfully applied to improve patient outcomes.

1.3.2 CTLA-4

Cytotoxic T lymphocyte antigen 4 (CTLA-4), also known as CD152, and CD28 are homologous receptors expressed on T cells. While structurally similar, they mediate opposing functions in T cell activation (51–54). Blockade of CTLA-4, such as with Ipilimumab (55), results in the amelioration of the immune response against tumors.

1.3.3 LAG3

LAG3 and CD4 share very similar structures in that they both have four extracellular Ig-like domains (56, 57). Interestingly, LAG3 has a 100-fold higher binding affinity with MHC class II (MHCII) compared to CD4, which is why MHCII is presumed to be the ligand for LAG3 (43) and why LAG3 may be a negative competitor of CD4 (58–62).

1.3.4 TIM3

Contrary to other immune checkpoint proteins, TIM3 does not consist of classical inhibitory signaling motifs such as ITIMS, but instead contains five conserved tyrosine residues (47). Two of these residues can be phosphorylated by Src kinases and are essential for downstream signal transduction (63, 64). Thus far, four distinct ligands, both soluble and surface-bound, have been found to interact with the IgV domain of TIM3 (phosphatidylserine (PtdSer), high-mobility group box-1 protein (HMGB1), carcinoembryonic antigen-related cell adhesion molecule 1 (CAECAM-1) and galectin-9 (Gal-9)) (65). It is noteworthy to mention that PD-1 and TIM-3 can share ligands, as is the case with Gal-9 (66). Tumor-infiltrating dendritic cells (DC) highly express TIM3, which can compete with nucleic acid binding to its ligand high-mobility group protein B1 (HMGB1), reducing anti-tumor immunity otherwise mediated by nucleic acids (67). TIM3 also works to inhibit T cells *via* interaction with the ligand Caecam1 (68).

1.3.5 TIGIT

T cell immunoglobulin and ITIM domain (TIGIT) was first identified in 2009 as an inhibitory immune checkpoint by Yu et al. (48). TIGIT has an extracellular immunoglobulin variable region, a transmembrane domain, as well as a cytoplasmic portion that contains an ITIM and an immunoglobulin tail tyrosine (ITT)-like phosphorylation motif (48), by which it delivers its inhibitory signals. TIGIT expression is restricted to lymphocyte and is found mainly on memory T cells and regulatory T cells (Tregs) as well as on NK cells (48, 69). Niebel et al. (70) have suggested that the expression of TIGIT mRNA is regulated *via* the methylation of the *TIGIT* gene. TIGIT binds to poliovirus receptor (PVR), also known as CD155 (71) with the highest binding affinity, as well as PVR ligand (PVRL) 2, also

known as CD112 or Nectin-2 and PVRL3, also known as CD113 or Nectin-3 with lower affinity (71). Similar to CTLA-4/B7/CD28 pathway (72), TIGIT achieves its inhibitory effects by competing with other ligands such as CD266 or CD96 (73). The hypothesis that TIGIT inhibits T cell proliferation has been tested by several groups (74–76) and they reported a direct inhibitory effect.

Concerning the immunosuppressive effect of TIGIT, several mechanisms may explain its function. Among them, TIGIT signaling has been shown to inhibit NK cell degranulation and cytotoxicity (69, 77), where Stanietsky et al. (69) have demonstrated that this inhibitory effect is mediated directly *via* the ITIM of TIGIT. Additionally, TIGIT prevents CD226 signaling in T cells by preventing the homodimerization of the protein (78). CD226 transmits an activating signal and consequently induces the aggregation of LFA-1, an important integrin involved in T cell migration as well as cytotoxicity (79), where aggregation of integrins affects their conformation and the interaction with their ligand (80). The Treg response has also been reported to be modulated by TIGIT (78, 81). In these studies, TIGIT$^+$ Tregs express higher levels of classical Treg genes, such as the transcription factor forkhead box P3 (FoxP3), and the surface molecules CD25 and CTLA-4. The engagement of TIGIT further leads to the secretion of IL10, a hallmark immunosuppressive cytokine, which selectively dampens T helper (Th)1 and Th17 immune responses (78). In certain types of cancer such as follicular lymphoma, TIGIT is strongly expressed by intratumoral Tregs as well as memory CD8$^+$ T cells. Here, high numbers of TIGIT-expressing tumor infiltrating lymphocytes have been correlated with a poor survival rate (82). As such, TIGIT may in the future be used as a prognostic marker, since elevated expression in T and NK cells predicts negative clinical outcomes (83–90). Based on these findings, TIGIT has become the subject of increased research as a target for cancer therapy, especially in combination with other ICIs, such as PD-1 inhibitors (91).

We here set out to review the literature of the past 20 years on the reciprocal interaction of TIGIT and the T cell metabolism, how it affects anti-tumor immunity, and how a better understanding of this interaction can pave the way for improved immunotherapy to treat cancer.

2 Main review

2.1 Interaction of TIGIT and the metabolic TME

2.1.1 Inhibition of glucose metabolism in T cells

A recent study by Shao et al. (92) focused on the role of TIGIT in patients with colorectal cancer and revealed that upregulated TIGIT expression in CD3$^+$ T cells correlated with poor survival. In this study the authors found that T cells expressing TIGIT had impaired proliferation, cytokine production, glucose uptake, and glycolytic function. Investigations by He et al. (86) demonstrated that TIGIT$^+$ CD8$^+$ T cells are impaired in their effector function, allowing for the hypothesis that immune escape in gastric cancer is at least in part mediated by the upregulation of TIGIT. These TIGIT$^+$ CD8$^+$ T cells had significantly reduced expression of glycolysis genes, including *GLUT1* as well as (hexokinase) *HK1* and *HK2*, which resulted in impaired glucose uptake and glycolysis (Figure 2). Aside from cancer, another study by Calvet-Mirabent et al. (93) has shown the relevance of the connection between glucose metabolism and TIGIT as an immune checkpoint in HIV infection. In their study, the authors utilized dual blockade of PD-1 and TIGIT, as well as employed the pro-glycolytic drug Metformin, and investigated the functional properties of CD8$^+$ T cells from HIV-1 patients. Significant positive correlations were observed between the increase in maximum glycolytic activity after TCR activation and the percentages of single-positive TIGIT cells, while co-expression of PD-1 and TIGIT resulted in lower glycolysis rates. Further, treatment with Metformin together with dual blockade of the two checkpoints restored cytotoxic activity of CD8$^+$ T cells (93). Thus, TIGIT seems to be capable to alter T cell function *via* the inhibition of glycolysis.

2.1.2 Hypoxia

Hypoxia is widely accepted to be a critical mechanism responsible for the resistance of tumor cells to radio-, chemo-, and immunotherapy (94–97). As the volume of a tumor increases, increasing numbers of cells need to be supplied with blood and oxygen, which requires additional vascularization of the tumor tissue. Without this additional supply of blood and oxygen, a state of hypoxia sets in (98). It is well established that the transcription factor hypoxia-inducible factor 1α (HIF-1α) regulates the expression of immune checkpoint proteins such as PD-L1 and CD73 (99, 100). HIF-1α is a master regulator of the cell's response to hypoxia (101). Under normoxic conditions, the activity of HIF-1α is repressed by proteasomal degradation *via* the oxygen-dependent prolyl hydroxylase domain (PHD) and the von Hippel-Lindau (VHL) protein (102). During tumor development, HIF-1α is pivotal to the cells' metabolic adaptation to their surroundings, as growth success under metabolic duress strongly depends upon the cell's ability to shift from oxidative phosphorylation (OXPHOS) to the more inefficient glycolytic metabolism for ATP generation. This is accomplished by HIF-1α-regulated genes encoding enzymes for glycolysis, such as the glucose transporters *GLUT1* and *GLUT3*, *HK1*, and *HK2* as well as phosphoglycerate kinase 1 (*PGK1*) (103). HIF-1α further regulates the expression of vascular endothelial growth factor (VEGF) (104), which enables neovascularization of tumors.

So far, one study has recently addressed the synergy between TIGIT and HIF-1α (105). In this study, Fathi et al. demonstrated that simultaneous blocking of both TIGIT and HIF-1α results in a significant reduction of tumor cell invasion, decreased colony formation, and inhibited angiogenesis (105). Both matrix metalloproteinases (MMP) 2 and MMP9 as well as *VEGF* mRNA expression levels were decreased under the dual blockade. Additionally, expression of the anti-apoptotic protein B-cell lymphoma (BCL)2 was downregulated, whereas mRNA expression of the pro-apoptotic protein Bcl-2-associated X protein (BAX) was upregulated. What remains unclear is if and how, precisely, these two proteins interact with one another. Since a correlation between TIGIT and HIF1a was demonstrated by Fathi et al., further research is required to unravel the precise mechanisms of relation of the two proteins in T cells, especially when considering that HIF1a increases the expression of other immune checkpoints such as PD-L1 (11–13).

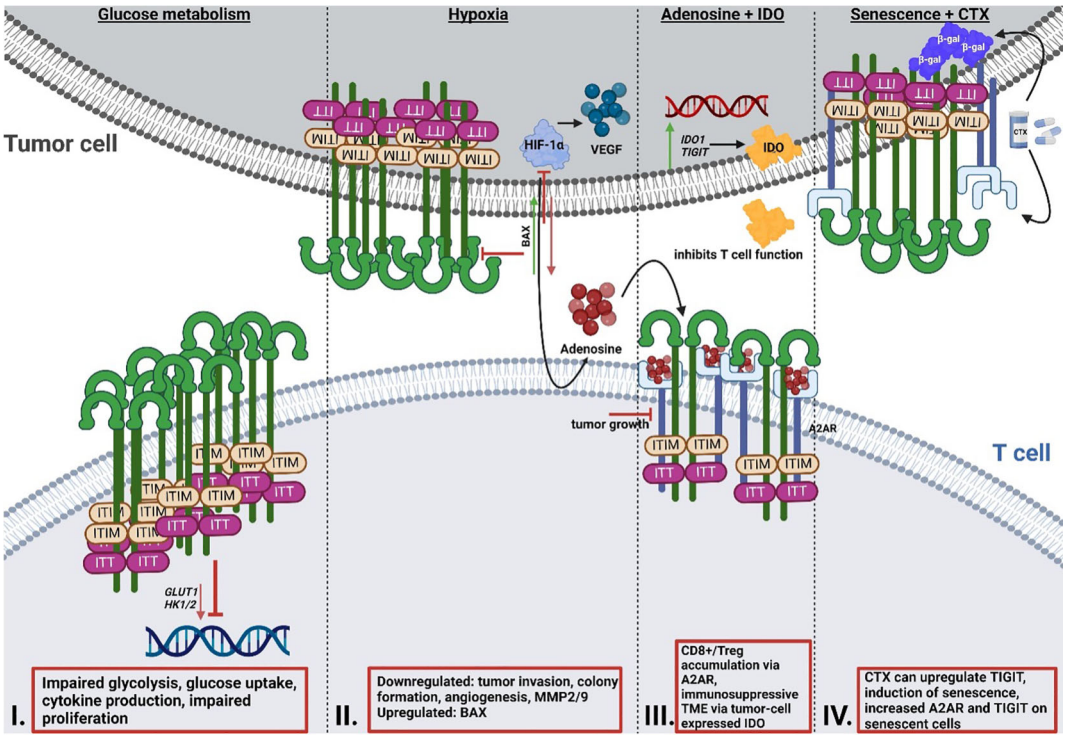

FIGURE 2
Reciprocal interaction of TIGIT signaling and T cell metabolism. **I**: Effect of TIGIT on glucose metabolism. Cancer cells inhibit T cell metabolism *via* enhancing the upregulation of TIGIT, resulting in impaired glycolysis gene expression of *GLUT1* and *HK1/2*, glucose uptake and glycolysis, and reduced proliferation. **II**: Effect of TIGIT on hypoxia and hypoxia sensing. HIF1-α regulates the expression of immune checkpoints and the expression of VEGF, which mediates tumor neovascularization. Simultaneous blocking of HIF1-α and TIGIT results in reduced tumor invasion and colony formation, as well as impaired angiogenesis and reduced MMP2/9 expression. Dual blockade leads to induction of pro-apoptotic BAX. **III**: Interaction of TIGIT and adenosine signaling and IDO. A2AR regulates the accumulation of CD8+ T cells and Tregs. Altered metabolism and hypoxia result in increased adenosine in the TME. Deletion of A2AR leads to tumor rejection in mice. IDO is highly expressed by tumor cells and generates an immunosuppressive TME. Many cancer cells overexpress *IDO1* and *TIGIT* simultaneously. **IV**: Interaction of chemotherapy and senescence and TIGIT. Chemotherapy regimens can result in the upregulation of TIGIT. A2AR is increased on the surface of senescent cells, with simultaneous upregulation of TIGIT. TIGIT, T cell immunoglobulin and ITIM domain; HK, hexokinase; GLUT1, glucose transporter 1; HIF1-α; hypoxia-inducible factor 1 alpha; MMP, matrix metalloproteinase; BAX, Bcl-2-associated X protein; IDO, indoleamine-pyrrole 2,3-dioxygenase; TME, tumor microenvironment.

2.1.3 Adenosine

Originally, adenosine receptors (ARs) were categorized into A1 or A2 ARs, depending on whether they have an inhibitory or stimulatory effect on cyclic adenosine monophosphate (cAMP) in the brain (106). Currently, ARs are categorized into four subtypes, A1, A2A, A2B and A3 (107). The majority of A2ARs are distributed in organs of the respiratory system, heart and lung, as well as in the central nervous system (CNS), and the immune system (108, 109). The adenosine receptor A2A (ADORA2) plays an important role in protecting tissues from immune-mediated damage following noninfectious inflammation, as well as in regulating the accumulation of $CD8^+$ T cells and NK cells (110, 111). An altered metabolism, increased expression of CD73 as well as hypoxia (112) in the tumor can lead to higher adenosine levels in the TME (111, 113) *via* signaling through the A2A adenosine receptors (114). In this context, Ohta et al. (111) investigated the effect of A2A receptor deficiency on anti-tumor immunity mediated by $CD8^+$ T cells and observed that genetic deletion of the A2A receptor results in tumor rejection in mice. Additionally, A2A receptor antagonists considerably delayed tumor growth *via* anti-tumor $CD8^+$ T cells. Ohta et al. (115) have shown that immunosuppressive Tregs were induced by increased levels of extracellular adenosine, as mediated *via* A2AR stimulation. As of yet, only very few studies (116, 117) have investigated in detail the correlation between the A2A receptor and TIGIT so far. Brauneck et al. (116) investigated the correlation between the A2A receptor and TIGIT on NK cells and showed that NK-cell mediated killing of acute myeloid leukemia (AML) cells could be ameliorated by co-blockade of TIGIT and A2AR, or of TIGIT and CD39, indicating a link between the two proteins. Another study by Muhammad et al. (117) revealed that the stimulation of the A2A receptor is necessary for the emergence of TIGIT-positive Tregs in mice and that this axis is impaired in uveitis patients. This study appears to have identified a subset of TIGIT+ Tregs that are functionally dependent on the expression of the A2A receptor.

2.1.4 IDO

IDO1 plays a pivotal role in the conversion of tryptophan to kynurenine (118). IDO1 is highly expressed in tumor cells and contributes to the establishment of a local immunosuppressive TME by enabling immune tolerance (119). It has been demonstrated that IDO1 inhibition induced a robust anti-tumor immune response in a mouse model when employed both as a single agent (120–127), or in combination with chemotherapeutic drugs (121, 128), highlighting the potential of IDO1 as a therapeutic target.

A recent study by Robertson et al. (129) has shown that CD8+ T cell tumor infiltrates from uveal melanoma (UM) overexpress the genes

encoding for both IDO1 and TIGIT. As previously mentioned, IDO is known to limit T cell function and induce mechanisms of tolerance (130, 131). Stålhammer et al. (83) have demonstrated that not only the number of IDO^+ cells in tumor tissues of UM appear higher than in normal choroid tissues, but that the same is true for $TIGIT^+$ cells. Importantly, the number of IDO^+ cells correlated with the number of $TIGIT^+$ cells in tumor cores and full tumor sections (83). The association of TIGIT expression with IDO and PD-L1 has also been observed in the tumor core of glioblastoma (GBM) (132), underlining the necessity to further study the correlation between these proteins.

2.1.5 Chemotherapy and senescence

TIGIT has recently been described as a marker for senescence due to its higher expression in aged T cells (133). The blocking of TIGIT results in improved functional capacity of senescent T cells as demonstrated by Song et al. (133), Chew et al. (134) and Kong et al. (84). The latter study also demonstrated that TIGIT expression on $CD8^+$ T cells is not only elevated in acute myeloid leukemia (AML) patients, but that high TIGIT levels also correlate with primary refractory disease, as well as leukemia relapse following allogenic stem cell transplantation. TIGIT-high $CD8^+$ T cells presented as functionally impaired and exhausted, whereas TIGIT blockade rescued functionality and anti-tumor response, highlighting TIGIT blockade as a potential therapeutic approach for leukemia.

Cancer treatment options in terms of chemotherapy are varied and often rely on combinatorial therapies. Some common agents used for different types of cancer are 5-Fluorouracil, an antimetabolite, DNA intercalators such as oxaliplatin and taxanes that target microtubules (135). A recent study by Davern et al. (136) revealed certain chemotherapy regimens give rise to an immune-resistant phenotype *via* the upregulation of inhibitory immune checkpoint ligands, among them TIGIT, in oesophageal adenocarcinoma (OAC). The study aimed to elucidate the effect of OAC chemotherapy approaches on the induction of a senescent-like state in cancer cells as senescent cancer cells are involved in conferring treatment resistance and promoting a microenvironment conducive to tumor growth *via* secretion of several pro-inflammatory markers, referred to as senescence-associated phenotype (SASP) (136).Using ß-galactosidase (ß-gal), an enzyme involved in the process of producing galactosylated proteins, as a marker for senescence, the authors demonstrated that the number of senescent-like cells increased significantly following chemotherapy, prompting the question whether immune checkpoints were expressed on these senescent cells or even upregulated following the treatment. The immune checkpoint TIM-3 was significantly upregulated in OE33 cells, whereas TIGIT was significantly upregulated in the SK-GT-4 cells. We know that immune checkpoints are essential for immune evasion, and if these immune checkpoints are present on senescent OAC cells, this may represent a drugable target for future therapies. Returning to another protein already addressed in this review, the adenosine receptor A2A was significantly increased on the surface of senescent-like SK-GT-4 cells, which were also shown to have increased TIGIT expression following a chemotherapy regimen. While senescent cells do have an activated glucose metabolism, they at the same time display an unbalanced lipid metabolism, which results in an altered expression of lipid metabolic enzymes, ultimately culminating in senescence induction and thereby limited functionality (137). Senescent T cells also demonstrate loss of cell surface CD28 (138–140), a protein required for lipid raft formation, IL-2 gene transcription and T cell activation. Since CD28 has also been linked to metabolic fitness of a T cell (141), the loss of this protein due to senescence can dramatically affect T cell functionality (142). Liu et al. (137) have demonstrated that the prevention of T cell senescence resulted in enhanced anti-tumor immunity, therefore maybe providing another point of potential therapeutic application.

Interestingly, TIGIT has also been shown to be intrinsically expressed in murine colorectal cell lines (143). To elucidate the functional effect of this intrinsic TIGIT, Zhou et al. (143) deleted the protein using CRISPR/Cas9 and observed that knockout resulted in significantly impaired tumor growth, together with increased IFNy secretion and cytotoxicity by NK cells, indicating that tumor cell-intrinsic TIGIT has a considerable effect on tumor growth and may present a potential therapeutic target.

2.2 Current status of anti-TIGIT therapeutics in clinical studies

As of August 2021, several anti-TIGIT antibodies were registered in preclinical and active clinical trials (clinicaltrials.org, anti-TIGIT). For example, two antibodies had progressed to the Phase III status (Tiragolumab (144), Ociperlimab (145)) and two were active in Phase II trials Vibostolimab, Domvanalimab) (146, 147), all of which also in combination with Atelizumab (anti-PD-L1), Pembrolizumab (anti-PD-1) and other agents. Additionally, a bispecific antibody targeting both PD-1 and TIGIT (HLX301, NCT05102214) simultaneously is under current clinical review. As discussed, TIGIT expression has been observed, among others, with PD-L1 in the tumor core (132), hinting at some kind of link between these two proteins. Currently, an anti-TIGIT candidate in combination with an anti-PD-1 antibody is being evaluated for the application for recurrent glioblastoma (148). Furthermore, increased levels of extracellular adenosine, as mediated by A2AR stimulation (114), have been shown to have a detrimental effect on anti-tumor activity (111, 115–117). Etrumadenant, an A2AR antagonist, is currently being investigated in a clinical trial in combination with Domvanalimab and Zimbrelimab (anti-PD-1) (149). It is noteworthy that the majority of the anti-TIGIT antibodies in clinical trials currently are fully human and demonstrate good tolerance by patients, also in combination with anti-PD-1 and anti-PD-L1 antibodies (150). As previously discussed in this review, TIGIT monotherapy does not result in significantly altered disease outcomes, underlining this as a potential caveat of TIGIT as a therapeutic target and highlighting the necessity for a combinatorial approach with other agents. Immune checkpoint therapy using Ipilimumab and Nivolumab as the most prominent agents has proved successful, and, taken together with the low efficacy of anti-TIGIT monotherapy, prompts the question which cohort of patients could additionally benefit from either a monotherapy or a combinatorial treatment.

2.3 The potential of PD-1, CTLA-4 and other negative regulators as biomarkers

Predictive biomarkers are essential to evaluate the outcome of therapeutic approaches, or at least, to provide an indication before

commencement of the therapy regimen. Especially in the case of highly multifactorial diseases such as cancer and autoimmunity, such biomarkers should ideally indicate whether a monotherapy or a combinatorial approach is necessary. Here, the induction of negative regulators results in the suppression of, among other mediators, cell death mechanisms (151). Specifically these negative regulators of cell death signaling, such as heat shock proteins (HSP) (152), the Bcl-2 family (153), the PI3K/Akt/mTOR pathway (154) and others, as reviewed in detail by Razaghi et al. in (155), have found clinical application as prognostic biomarkers. In summary, negative regulators of cell death signaling appear to have great potential and present clinical application as prognostic biomarkers, raising the question whether this is also the case for the immune checkpoint proteins. When considering anti-PD-1 or anti-PD-L1 therapy, using (over-)expression of PD-L1 as biomarker appears plausible. In this context, Teng et al. (156) came up with a classification that describes PD-L1 positive tumors with infiltrating lymphocytes as a type 1 TME, proposing it to be the most likely to respond to immune checkpoint blockade. However, also PD-L1 negative tumors have been shown to be able to respond positively to antibodies targeting the PD-1/PD-L1 axis (157, 158). This consequently raises the concern that the predictive value of PD-1 and PD-L1 as biomarkers may not be optimal and universally valid across all patients, as intrapatient and even intratumor heterogeneity has been observed (159).

Other studies have hinted at the possible prognostic power of CLTA-4 expression. Here, Liu et al. (160) have demonstrated that, in some cancers, patients with higher CTLA-4 expression had a shorter overall survival than those with lower expression. However, an association between the expression levels of PD-1 and CTLA-4 and tumor-infiltrating cells exists (160). Liu et al. point out that the expression of these two immune checkpoint proteins varies across different cancers and that many cancer types demonstrate PD-1 and CTLA-4 mutations, leading to their abnormal expression, which may be used as a prognostic biomarker.

Whether TIGIT can be used in a similar manner remains to be investigated and demonstrated. Since TIGIT in its effects appears to be functionally and mechanistically tethered to other negative immune regulators such as PD-1, TIGIT alone may not prove a reliable and unambiguous prognostic biomarker. To assess the protein's capacity of serving as a prognostic factor, large amounts of correlation data from different kinds of cancers, across different genders, ages and perhaps even ethnicities are necessary, providing information on its function and mechanistics on its own and together with other proteins that TIGIT is known to interact with. It may well be possible that a combination of factors, such as presence of PD-1, TIGIT and senescence markers will be able to form a prognostic unit of response to and success of immunotherapy in different cancers.

3 Discussion

While the exact role of TIGIT within the TME is still not fully elucidated, the apparent synergy between TIGIT and HIF-1α as well as PD-1 (161) does allow for the assumption that this protein does not simply have a redundant role. Based upon the literature reviewed here, blockade or targeting of TIGIT alone does not appear to have a major effect on either the progression or even curative approaches in different oncologic diseases. It is rather the combination of TIGIT blockade together with blocking of another checkpoint, such as PD-1. The fact that a synergy exists between the two is well documented and accepted to the point that several clinical trials aiming to block both proteins simultaneously are currently ongoing (162). The challenge of such a therapy, even if successful, lies in the fact that not all cancers are PD-L1 positive, thereby restricting the potential applications from the beginning. Another potential caveat is that the precise mechanism of the synergistic effects observed between the two checkpoint proteins is not fully understood, and as such it may prove difficult to design effective and individualized therapies without fully understanding the mechanistic foundations of the observed effects.

In terms of metabolism, it can be hypothesized that presence or overexpression of TIGIT poses a metabolic barrier to T cell function. Data by Gilmour et al. (163) suggest that the co-expression of TIGIT with VISTA may lead to an altered metabolic phenotype of CTL. It was been detailed in the introductory section of this review that several other immune checkpoint proteins, such as

PD-1 and CTLA-4 appear to have an effect on glycolysis of tumor cells, and thereby on the ability of immune cells to perform glycolysis due to nutrient competition within the TME. Limited nutrient ability, such as the scarcity of glucose, will lead to impaired T cell function and therefore an impaired anti-tumor response of those T cells. It is therefore crucial to further investigate the potential direct and indirect effects of TIGIT on the metabolism of T cells and other immune cells in the context of anti-tumor immunity.

It is well-known that hypoxia plays a major role in creating hostile microenvironments that are toxic to immune cells yet conducive to tumor growth. So far, only one study has investigated the direct interaction between HIF-1α and TIGIT. It remains an open question whether a potential three-way synergy might exist between blocking not only TIGIT and PD-1, but also HIF-1α. Along this line, it would be important to assess whether a co-blockade of TIGIT and HIF-1α is as effective as the blockade of TIGIT and PD-1 as a therapeutic possibility for those cancers which are not PD-L1 positive.

The interplay between TIGIT and adenosine as well as the A2A receptor makes for another interesting point of further investigation. The genetic deletion of the A2A receptor in mice resulted in tumor rejection (162), allowing for the hypothesis that some connection may also exist between these proteins. Additionally, it is known that hypoxia leads to higher adenosine levels in the TME, prompting the question whether the TIGIT-A2AR-HIF-1α axis could provide another possible three-way blockade for therapeutic purposes. The A2A receptor was additionally observed to be upregulated on the surface senescent cancer cells, which at the same time showed increased TIGIT expression following some chemotherapy regimens.

The potential of TIGIT expression as a biomarker has been suggested, although for this, larger association studies are needed. Future experiments should aim to elucidate the connection between TIGIT and other immune checkpoints, particularly those involved in the immune response against cancers which do not express PD-L1, as well as the interplay with HIF-1α and the A2A receptor. Perhaps this will lead to a better understanding of the exact mechanisms governing the synergistic inhibitory effects of combination treatments. Taken together, TIGIT appears to have a therapeutic potential, especially in the context of combinatorial therapies and alleviating the metabolic barrier that immune checkpoint proteins are able to pose, that should

not be overlooked and disregarded for further research, both of basic and translational nature.

Author contributions

NJ-N and SK designed the study. NJ-N performed literature search. NJ-N and SK drafted the manuscript. NJ-N designed Figures 1 and 2. RB-L, KB, MM-F, MB, BS and DM provided critical input throughout the work and corrected the manuscript. SK and BS together with DM supervised the work. All authors contributed to the article and approved the submitted version.

Funding

This work was supported by grants of the state of Saxony-Anhalt (SI2 and SI3) to BS and the Deutsche Forschungsgemeinschaft (DFG, German Research Foundation) – 361210922/GRK2408 – (Project 12) to SK. For the latter, a monthly academic individual plan (to sascha.kahlfuss@med.ovgu.de) was purchased.

Acknowledgments

Figures 1 and 2 were created with BioRender.com.

Conflict of interest

The authors declare that the research was conducted in the absence of any commercial or financial relationships that could be construed as a potential conflict of interest.

Publisher's note

References

1. Crespo J, Sun H, Welling TH, Tian Z, Zou W. T Cell anergy, exhaustion, senescence, and stemness in the tumor microenvironment. *Curr Opin Immunol* (2013) 25:214–21. doi: 10.1016/j.coi.2012.12.003

2. Wherry EJ. T Cell exhaustion. *Nat Immunol* (2011) 12:492–9. doi: 10.1038/ni.2035

3. Palmer CS, Ostrowski M, Balderson B, Christian N, Crowe SM. Glucose metabolism regulates T cell activation, differentiation, and functions. *Front Immunol* (2015) 6:1. doi: 10.3389/fimmu.2015.00001

4. Munn DH, Mellor AL. Indoleamine 2,3 dioxygenase and metabolic control of immune responses. *Trends Immunol* (2013) 34:137–43. doi: 10.1016/j.it.2012.10.001

5. Munn DH, Shafizadeh E, Attwood JT, Bondarev I, Pashine A, Mellor AL. Inhibition of T cell proliferation by macrophage tryptophan catabolism. *J Exp Med* (1999) 189:1363–72. doi: 10.1084/jem.189.9.1363

6. Fischer K, Hoffmann P, Voelkl S, Meidenbauer N, Ammer J, Edinger M, et al. Inhibitory effect of tumor cell–derived lactic acid on human T cells. *Blood* (2007) 109:3812–9. doi: 10.1182/blood-2006-07-035972

7. Siska PJ, Jiao J, Matos C, Singer K., Berger RS, Dettmer K, et al. Kynurenine induces T cell fat catabolism and has limited suppressive effects *in vivo*. *EBioMedicine* (2021) 74:103734. doi: 10.1016/j.ebiom.2021.103734

8. Schreiber S, Hammers CM, Kaasch AJ, Schraven B, Dudeck A, Kahlfuss S. Metabolic interdependency of Th2 cell-mediated type 2 immunity and the tumor microenvironment. *Front Immunol* (2021) 12:632581. doi: 10.3389/fimmu.2021.632581

9. Sarkar S, Germeraad WT, Rouschop KM, Steeghs EM, van Gelder M, Bos GM, et al. Hypoxia induced impairment of NK cell cytotoxicity against multiple myeloma can be overcome by IL-2 activation of the NK cells. *PloS One* (2013) 8:e64835. doi: 10.1371/journal.pone.0064835

10. Sun J, Zhang Y, Yang M, Zhang Y, Xie Q, Li Z, et al. Hypoxia induces T-cell apoptosis by inhibiting chemokine c receptor 7 expression: the role of adenosine receptor A(2). *Cell Mol Immunol* (2010) 7:77–82. doi: 10.1038/cmi.2009.105

11. Barsoum IB, Smallwood CA, Siemens DR, Graham CH. A mechanism of hypoxia-mediated escape from adaptive immunity in cancer cells. *Cancer Res* (2014) 74:665–74. doi: 10.1158/0008-5472.CAN-13-0992

12. Palsson-McDermott EM, Dyck L, Zaslona Z, Menon D, McGettrick AF, Mills KHG, et al. Pyruvate kinase M2 is required for the expression of the immune checkpoint PD-L1 in immune cells and tumors. *Front Immunol* (2017) 8:1300. doi: 10.3389/fimmu.2017.01300

13. Jayaprakash P, Ai M, Liu A, Budhani P, Bartkowiak T, Sheng J, et al. Targeted hypoxia reduction restores T cell infiltration and sensitizes prostate cancer to immunotherapy. *J Clin Invest.* (2018) 128:5137–49. doi: 10.1172/JCI96268

14. Allard B, Longhi MS, Robson SC, Stagg J. The ectonucleotidases CD39 and CD73: novel checkpoint inhibitor targets. *Immunol Rev* (2017) 276:121–44. doi: 10.1111/imr.12528

15. d'Almeida SM, Kauffenstein G, Roy C, Basset L, Papargyris L, Henrion D, et al. The ecto-ATPDase CD39 is involved in the acquisition of the immunoregulatory phenotype by m-CSF-macrophages and ovarian cancer tumor-associated macrophages: Regulatory role of IL-27. *Oncoimmunology* (2016) 5:e1178025. doi: 10.1080/2162402X.2016.1178025

16. Gourdin N, Bossennec M, Rodriguez C, Vigano S, Machon C, Jandus C, et al. Autocrine adenosine regulates tumor polyfunctional CD73(+)CD4(+) effector T cells devoid of immune checkpoints. *Cancer Res* (2018) 78:3604–18. doi: 10.1158/0008-5472.CAN-17-2405

17. Li L, Wang L, Li J, Fan Z, Yang L, Zhang Z, et al. Metformin-induced reduction of CD39 and CD73 blocks myeloid-derived suppressor cell activity in patients with ovarian cancer. *Cancer Res* (2018) 78:1779–91. doi: 10.1158/0008-5472.CAN-17-2460

18. Linnemann C, Schildberg FA, Schurich A, Diehl L, Hegenbarth SI, Endl E, et al. Adenosine regulates CD8 T-cell priming by inhibition of membrane-proximal T-cell receptor signalling. *Immunology* (2009) 128(1 Suppl):e728–37. doi: 10.1111/j.1365-2567.2009.03075.x

19. Calcinotto A, Filipazzi P, Grioni M, Iero M, De Milito A, Ricupito A, et al. Modulation of microenvironment acidity reverses anergy in human and murine tumor-infiltrating T lymphocytes. *Cancer Res* (2012) 72:2746–56. doi: 10.1158/0008-5472.CAN-11-1272

20. Peng HY, Lucavs J, Ballard D, Das JK, Kumar A, Wang L, et al. Metabolic reprogramming and reactive oxygen species in T cell immunity. *Front Immunol* (2021) 12:652687. doi: 10.3389/fimmu.2021.652687

21. Balyan R, Gautam N, Gascoigne NRJ. The ups and downs of metabolism during the lifespan of a T cell. *Int J Mol Sci* (2020) 21(21):7972. doi: 10.3390/ijms21217972

22. Gubser PM, Bantug GR, Razik L, Fischer M, Dimeloe S, Hoenger G, et al. Rapid effector function of memory CD8+ T cells requires an immediate-early glycolytic switch. *Nat Immunol* (2013) 14:1064–72. doi: 10.1038/ni.2687

23. Cham CM, Gajewski TF. Glucose availability regulates IFN-gamma production and p70S6 kinase activation in CD8+ effector T cells. *J Immunol* (2005) 174:4670–7. doi: 10.4049/jimmunol.174.8.4670

24. Chang CH, Curtis JD, Maggi LB Jr., Faubert B, Villarino AV, O'Sullivan D, et al. Posttranscriptional control of T cell effector function by aerobic glycolysis. *Cell* (2013) 153:1239–51. doi: 10.1016/j.cell.2013.05.016

25. Frauwirth KA, Riley JL, Harris MH, Parry RV, Rathmell JC, Plas DR, et al. The CD28 signaling pathway regulates glucose metabolism. *Immunity* (2002) 16(6):769–77. doi: 10.1016/s1074-7613(02)00323-0

26. Jones RG, Thompson CB. Revving the engine: signal transduction fuels T cell activation. *Immunity* (2007) 27(2):173–8. doi: 10.1016/j.immuni.2007.07.008

27. Wieman HL, Wofford JA, Rathmell JC. Cytokine stimulation promotes glucose uptake *via* phosphatidylinositol-3 kinase/Akt regulation of Glut1 activity and trafficking. *Mol Biol Cell* (2007) 18(4):1437–46. doi: 10.1091/mbc.e06-07-0593

28. Wang R, Dillon CP, Shi LZ, Milasta S, Carter R, Finkelstein D, et al. The transcription factor myc controls metabolic reprogramming upon T lymphocyte activation. *Immunity* (2011) 35(6):871–82. doi: 10.1016/j.immuni.2011.09.021

29. Geltink RIK, Kyle RL, Pearce EL. Unraveling the complex interplay between T cell metabolism and function. *Annu Rev Immunol* (2018) 36:461–88. doi: 10.1146/annurev-immunol-042617-053019

30. Ghesquière B, Wong BW, Kuchnio A, Carmeliet P. Metabolism of stromal and immune cells in health and disease. *Nature* (2014) 511(7508):167–76. doi: 10.1038/nature13312

31. Chang CH, Qiu J, O'Sullivan D, Buck MD, Noguchi T, Curtis JD, et al. Metabolic competition in the tumor microenvironment is a driver of cancer progression. *Cell* (2015) 162(6):1229–41. doi: 10.1016/j.cell.2015.08.016

32. Lim S, Phillips JB, Madeira da Silva L, Zhou M, Fodstad O, Owen LB, et al. Interplay between immune checkpoint proteins and cellular metabolism. *Cancer Res* (2017) 77(6):1245–9. doi: 10.1158/0008-5472.CAN-16-1647

33. Kleffel S, Posch C, Barthel SR, Mueller H, Schlapbach C, Guenova E, et al. Melanoma cell-intrinsic PD-1 receptor functions promote tumor growth. *Cell* (2015) 162(6):1242–56. doi: 10.1016/j.cell.2015.08.052

34. Fischer K, Hoffmann P, Voelkl S, Meidenbauer N, Ammer J, Edinger M, et al. Inhibitory effect of tumor cell-derived lactic acid on human T cells. *Blood* (2007) 109 (9):3812–9. doi: 10.1182/blood-2006-07-035972

35. Sharpe AH. Mechanisms of costimulation. *Immunol Rev* (2009) 229:5–11. doi: 10.1111/j.1600-065X.2009.00784.x

36. Bour-Jordan H, Bluestone JA. CD28 function: A balance of costimulatory and regulatory signals. *J Clin Immunol* (2002) 22(1):1–7. doi: 10.1023/a:1014256417651

37. Esensten JH, Helou YA, Chopra G, Weiss A, Bluestone JA. CD28 costimulation: From mechanism to therapy. *Immunity* (2016) 44(5):973–88. doi: 10.1016/j.immuni.2016.04.020

38. Chen L. Co-Inhibitory molecules of the B7-CD28 family in the control of T-cell immunity. *Nat Rev Immunol* (2004) 4:336–47. doi: 10.1038/nri1349

39. Yu S, Li A, Liu Q, Li T, Yuan X, Han X, et al. Chimeric antigen receptor T cells: A novel therapy for solid tumors. *J Hematol Oncol* (2017) 10:78. doi: 10.1186/s13045-017-0444-9

40. Yu S, Li A, Liu Q, Yuan X, Xu H, Jiao D, et al. Recent advances of bispecific antibodies in solid tumors. *J Hematol Oncol* (2017) 10:155. doi: 10.1186/s13045-017-0522-z

41. Ballas ZK. The 2018 Nobel prize in physiology or medicine: an exemplar of bench to bedside in immunology. *J Allergy Clin Immunol* (2018) 142:1752–3. doi: 10.1016/j.jaci.2018.10.021

42. Yi M, Yu S, Qin S, Liu Q, Xu H, Zhao W, et al. Gut microbiome modulates efficacy of immune checkpoint inhibitors. *J Hematol Oncol* (2018) 11:47. doi: 10.1186/s13045-018-0592-6

43. Andrews LP, Marciscano AE, Drake CG, Vignali DA. LAG3 (CD223) as a cancer immunotherapy target. *Immunol Rev* (2017) 276:80–96. doi: 10.1111/imr.12519

44. Wang L, Rubinstein R, Lines JL, Wasiuk A, Ahonen C, Guo Y, et al. VISTA, a novel mouse ig superfamily ligand that negatively regulates T cell responses. *J Exp Med* (2011) 208:577–92. doi: 10.1084/jem.20100619

45. Yu X, Zheng Y, Mao R, Su Z, Zhang J. BTLA/HVEM signaling: milestones in research and role in chronic hepatitis b virus infection. *Front Immunol* (2019) 10:617. doi: 10.3389/fimmu.2019.00617

46. Chapoval AI, Ni J, Lau JS, Wilcox RA, Flies DB, Liu D, et al. B7-H3: A costimulatory molecule for T cell activation and IFN-gamma production. *Nat Immunol* (2001) 2:269–74. doi: 10.1038/85339

47. Monney L, Sabatos CA, Gaglia JL, Ryu A, Waldner H, Chernova T, et al. Th1-specific cell surface protein Tim-3 regulates macrophage activation and severity of an autoimmune disease. *Nature* (2002) 415:536–41. doi: 10.1038/415536a

48. Yu X, Harden K, Gonzalez LC, Francesco M, Chiang E, Irving B, et al. The surface protein TIGIT suppresses T cell activation by promoting the generation of mature immunoregulatory dendritic cells. *Nat Immunol* (2009) 10:48–57. doi: 10.1038/ni.1674

49. Sharpe AH, Wherry EJ, Ahmed R, Freeman GJ. The function of programmed cell death 1 and its ligands in regulating autoimmunity and infection. *Nat Immunol* (2007) 8:239–45. doi: 10.1038/ni1443

50. Sun Z, Fourcade J, Pagliano O, Chauvin JM, Sander C, Kirkwood JM. IL10 and PD-1 cooperate to limit the activity of tumor-specific CD8+ T cells. *Cancer Res* (2015) 75:1635–44. doi: 10.1158/0008-5472.CAN-14-3016

51. Rowshanravan B, Halliday N, Sansom DM. CTLA-4: A moving target in immunotherapy. *Blood* (2018) 131(1):58–67. doi: 10.1182/blood-2017-06-741033

52. Schwartz JC, Zhang X, Fedorov AA, Nathenson SG, Almo SC. Structural basis for co-stimulation by the human CTLA-4/B7-2 complex. *Nature* (2001) 410(6828):604–8. doi: 10.1038/35069112

53. Stamper CC, Zhang Y, Tobin JF, Erbe DV, Ikemizu S, Davis SJ, et al. Crystal structure of the B7-1/CTLA-4 complex that inhibits human immune responses. *Nature* (2001) 410(6828):608–11. doi: 10.1038/35069118

54. Collins AV, Brodie DW, Gilbert RJ, Iaboni A, Manso-Sancho R, Walse B, et al. The interaction properties of costimulatory molecules revisited. *Immunity* (2002) 17(2):201–10. doi: 10.1016/S1074-7613(02)00362-X

55. Romano E, Kusio-Kobialka M, Foukas PG, Baumgaertner P, Meyer C, Ballabeni P, et al. Ipilimumab-dependent cell-mediated cytotoxicity of regulatory T cells ex vivo by nonclassical monocytes in melanoma patients. *Proc Natl Acad Sci U S A.* (2015) 112 (19):6140–5. doi: 10.1073/pnas.1417320112

56. Triebel F, Jitsukawa S, Baixeras E, Roman-Roman S, Genevee C, Viegas-Pequignot E, et al. LAG-3, a novel lymphocyte activation gene closely related to CD4. *J Exp Med* (1990) 171:1393–405. doi: 10.1084/jem.171.5.1393

57. Mastrangeli R, Micangeli E, Donini S. Cloning of murine LAG-3 by magnetic bead-bound homologous probes and PCR (gene-capture PCR). *Anal Biochem* (1996) 241:93–102. doi: 10.1006/abio.1996.0382

58. Wang J, Sanmamed MF, Datar I, Su TT, Ji L, Sun J, et al. Fibrinogen-like protein 1 is a major immune inhibitory ligand of LAG-3. *Cell* (2019) 176:334–347.e12. doi: 10.1016/j.cell.2018.11.010

59. Huard B, Gaulard P, Faure F, Hercend T, Triebel F. Cellular expression and tissue distribution of the human LAG-3-encoded protein, an MHC class II ligand. *Immunogenetics* (1994) 39:213–7. doi: 10.1007/BF00241263

60. Workman CJ, Rice DS, Dugger KJ, Kurschner C, Vignali DAA. Phenotypic analysis of the murine CD4-related glycoprotein, CD223 (LAG-3). *Eur J Immunol* (2002) 32:2255–63. doi: 10.1002/1521-4141(200208)32:8<2255::AID-IMMU2255>3.0.CO;2-A

61. Huard B, Prigent P, Tournier M, Bruniquel D, Triebel F. CD4/major histocompatibility complex class II interaction analyzed with CD4- and lymphocyte activation gene-3 (LAG-3)-Ig fusion proteins. *Eur J Immunol* (1995) 25:2718–21. doi: 10.1002/eji.1830250949

62. Workman C, Vignali D. The CD4-related molecule, LAG-3 (CD223), regulates the expansion of activated T cells. *Eur J Immunol* (2003) 33:970–9. doi: 10.1002/eji.200323382

63. Das M, Zhu C, Kuchroo VK. Tim-3 and its role in regulating anti-tumor immunity. *Immunol Rev* (2017) 276:97–111. doi: 10.1111/imr.12520

64. van de Weyer PS, Muehlfeit M, Klose C, Bonventre JV, Walz G, Kuehn EW. A highly conserved tyrosine of Tim-3 is phosphorylated upon stimulation by its ligand galectin-9. *Biochem Biophys Res Commun* (2006) 351:571–6. doi: 10.1016/j.bbrc.2006.10.079

65. Liu F, Liu Y, Chen Z. Tim-3 expression and its role in hepatocellular carcinoma. *J Hematol Oncol* (2018) 11:126. doi: 10.1186/s13045-018-0667-4

66. Yang R, Sun L, Li CF, Wang YH, Yao J, Li H, et al. Galectin-9 interacts with PD-1 and TIM-3 to regulate T cell death and is a target for cancer immunotherapy. *Nat Commun* (2021) 12(1):832. doi: 10.1038/s41467-021-21099-2

67. Chiba S, Baghdadi M, Akiba H, Yoshiyama H, Kinoshita I, Dosaka-Akita H, et al. Tumor-infiltrating DCs suppress nucleic acid-mediated innate immune responses through interactions between the receptor TIM-3 and the alarmin HMGB1. *Nat Immunol* (2012) 13:832–42. doi: 10.1038/ni.2376

68. Huang YH, Zhu C, Kondo Y, Anderson AC, Gandhi A, Russell A, et al. CEACAM1 regulates TIM-3-mediated tolerance and exhaustion. *Nature* (2015) 517:386–90. doi: 10.1038/nature13848

69. Stanietsky N, Simic H, Arapovic J, Toporik A, Levy O, Novik A, et al. The interaction of TIGIT with PVR and PVRL2 inhibits human NK cell cytotoxicity. *Proc Natl Acad Sci U S A.* (2009) 106:17858–63. doi: 10.1073/pnas.0903474106

70. Niebel D, Fröhlich A, Zarbl R, Fietz S, de Vos L, Vogt TJ, et al. DNA Methylation regulates TIGIT expression within the melanoma microenvironment, is prognostic for overall survival, and predicts progression-free survival in patients treated with anti-PD-1 immunotherapy. *Clin Epigenetics.* (2022) 14(1):50. doi: 10.1186/s13148-022-01270-2

71. Anderson AC, Joller N, Kuchroo VK. Lag-3, Tim-3, and TIGIT Co-inhibitory receptors with specialized functions in immune regulation. *Immunity* (2016) 17:989–1004. doi: 10.1016/j.immuni.2016.05.001

72. Le Mercier I, Lines JL, Noelle RJ. Beyond CTLA-4 and PD-1, the generation z of negative checkpoint regulators. *Front Immunol* (2015) 6:418. doi: 10.3389/fimmu.2015.00418

73. Dougall WC, Kurtulus S, Smyth MJ, Anderson AC. TIGIT and CD96: New checkpoint receptor targets for cancer immunotherapy. *Immunol Rev* (2017) 276:112–20. doi: 10.1111/imr.12518

74. Levin SD, Taft DW, Brandt CS, Bucher C, Howard ED, Chadwick EM, et al. Vstm3 is a member of the CD28 family and an important modulator of T-cell function. *Eur J Immunol* (2011) 41:902–15. doi: 10.1002/eji.201041136

75. Lozano E, Dominguez-Villar M, Kuchroo V, Hafler DA. The TIGIT/CD226 axis regulates human T cell function. *J Immunol* (2012) 188:3869–75. doi: 10.4049/jimmunol.1103627

76. Joller N, Hafler JP, Brynedal B, Kassam N, Spoerl S, Levin SD, et al. Cutting edge: TIGIT has T cell-intrinsic inhibitory functions. *J Immunol* (2011) 186:1338–42. doi: 10.4049/jimmunol.1003081

77. Stanietsky N, Rovis TL, Glasner A, Seidel E, Tsukerman P, Yamin R, et al. Mouse TIGIT inhibits NK-cell cytotoxicity upon interaction with PVR. *Eur J Immunol* (2013) 43:2138–50. doi: 10.1002/eji.201243072

78. Johnston RJ, Comps-Agrar L, Hackney J, Yu X, Huseni M, Yang Y, et al. The immunoreceptor TIGIT regulates antitumor and antiviral CD8(+) T cell effector function. *Cancer Cell* (2014) 26:923–37. doi: 10.1016/j.ccell.2014.10.018

79. Shibuya K, Lanier LL, Phillips JH, Ochs HD, Shimizu K, Nakayama E, et al. Physical and functional association of LFA-1 with DNAM-1 adhesion molecule. *Immunity* (1999) 11:615–23. doi: 10.1016/S1074-7613(00)80136-3

80. Reyes R, Monjas A, Yánez-Mó M, Cardeñes B, Morlino G, Gilsanz A, et al. Different states of integrin LFA-1 aggregation are controlled through its association with tetraspanin CD9. *Biochim Biophys Acta* (2015) 1853(10 Pt A):2464–80. doi: 10.1016/j.bbamcr.2015.05.018

81. Fuhrman CA, Yeh WI, Seay HR, Saikumar Lakshmi P, Chopra G, Zhang L, et al. Divergent phenotypes of human regulatory T cells expressing the receptors TIGIT and CD226. *J Immunol* (2015) 195:145–55. doi: 10.4049/jimmunol.1402381

82. Yang ZZ, Kim HJ, Wu H, Jalali S, Tang X, Krull J, et al. TIGIT expression is associated with T-cell suppression and exhaustion and predicts clinical outcome and anti-PD-1 response in follicular lymphoma. *Clin Cancer Res* (2020) 26(19):5217–31. doi: 10.1158/1078-0432.CCR-20-0558

83. Stålhammar G, Seregard S, Grossniklaus HE. Expression of immune checkpoint receptors indoleamine 2,3-dioxygenase and T cell ig and ITIM domain in metastatic versus nonmetastatic choroidal melanoma. *Cancer Med* (2019) 8(6):2784–92. doi: 10.1002/cam4.2167

84. Kong Y, Zhu L, Schell TD, Zhang J, Claxton DF, Ehmann WC, et al. T-Cell immunoglobulin and ITIM domain (TIGIT) associates with CD8+ T-cell exhaustion and poor clinical outcome in AML patients. *Clin Cancer Res* (2016) 22:3057–66. doi: 10.1158/1078-0432.CCR-15-2626

85. Chauvin JM, Pagliano O, Fourcade J, Sun Z, Wang H, Sander C, et al. TIGIT and PD-1 impair tumor antigen-specific CD8(+) T cells in melanoma patients. *J Clin Investig* (2015) 125:2046–58. doi: 10.1172/JCI80445

86. He W, Zhang H, Han F, Chen X, Lin R, Wang W, et al. CD155T/TIGIT signaling regulates CD8(+) T-cell metabolism and promotes tumor progression in human gastric cancer. *Cancer Res* (2017) 77:6375–88. doi: 10.1158/0008-5472.CAN-17-0381

87. Lucca LE, Lerner BA, Park C, DeBartolo D, Harnett B, Kumar VP, et al. Differential expression of the T-cell inhibitor TIGIT in glioblastoma and MS. *Neurol Neuroimmunol. Neuroinflamm.* (2020) 7. doi: 10.1212/NXI.0000000000000712

88. Ostroumov D, Duong S, Wingerath J, Woller N, Manns MP, Timrott K, et al. Transcriptome profiling identifies TIGIT as a marker of T cell exhaustion in liver cancer. *Hepatology* (2021) 73(4):1399–418. doi: 10.1002/hep.31466

89. Xu D, Zhao E, Zhu C, Zhao W, Wang C, Zhang Z, et al. TIGIT and PD-1 may serve as potential prognostic biomarkers for gastric cancer. *Immunobiology* (2020) 225:151915. doi: 10.1016/j.imbio.2020.151915

90. Duan X, Liu J, Cui J, Ma B, Zhou Q, Yang X, et al. Expression of TIGIT/CD155 and correlations with clinical pathological features in human hepatocellular carcinoma. *Mol Med Rep* (2019) 20:3773–81. doi: 10.3892/mmr.2019.10641

91. Solomon BL, Garrido-Laguna I. TIGIT: A novel immunotherapy target moving from bench to bedside. *Cancer Immunol Immunother.* (2018) 67:1659–67. doi: 10.1007/s00262-018-2246-5

92. Shao Q, Wang L, Yuan M, Jin X, Chen Z, Wu C. TIGIT induces (CD3+) T cell dysfunction in colorectal cancer by inhibiting glucose metabolism. *Front Immunol* (2021) 12:688961. doi: 10.3389/fimmu.2021.688961

93. Calvet-Mirabent M, Sánchez-Cerrillo I, Martín-Cófreces N, Martínez-Fleta P, de la Fuente H, Tsukalov I, et al. Antiretroviral therapy duration and immunometabolic state determine efficacy of ex vivo dendritic cell-based treatment restoring functional HIV-specific CD8+ T cells in people living with HIV. *EBioMedicine* (2022) 81:104090. doi: 10.1016/j.ebiom.2022.104090

94. Harris AL. Hypoxia–a key regulatory factor in tumour growth. *Nat Rev Cancer* (2002) 2:38–47. doi: 10.1038/nrc704

95. Shannon AM, Bouchier-Hayes DJ, Condron CM, Toomey D. Tumour hypoxia, chemotherapeutic resistance and hypoxia-related therapies. *Cancer Treat Rev* (2003) 29:297–307. doi: 10.1016/S0305-7372(03)00003-3

96. Daniel SK, Sullivan KM, Labadie KP, Pillarisetty VG. Hypoxia as a barrier to immunotherapy in pancreatic adenocarcinoma, clin. *Transl Med* (2019) 8:10. doi: 10.1186/s40169-019-0226-9

97. Semenza GL. HIF-1 mediates metabolic responses to intratumoral hypoxia and oncogenic mutations. *J Clin Invest.* (2013) 123(9):3664–71. doi: 10.1172/JCI67230

98. Li Y, Zhao L, Li XF. Hypoxia and the tumor microenvironment. *Technol Cancer Res Treat* (2021) 20. doi: 10.1177/15330338211036304

99. Wu Q, Zhou W, Yin S, Zhou Y, Chen T, Qian J, et al. Blocking triggering receptor expressed on myeloid cells-1-positive tumor-associated macrophages induced by hypoxia reverses immunosuppression and anti-programmed cell death ligand 1 resistance in liver cancer. *Hepatology* (2019) 70(1):198–214. doi: 10.1002/hep.30593

100. Lequeux A, Noman MZ, Xiao M, Sauvage D, Van Moer K, Viry E, et al. Impact of hypoxic tumor microenvironment and tumor cell plasticity on the expression of immune checkpoints. *Cancer Lett* (2019) 458:13–20. doi: 10.1016/j.bbcan.2018.07.002

101. Wang GL, Jiang BH, Rue EA, Semenza GL. Hypoxia-inducible factor 1 is a basic-helix-loop-helix-PAS heterodimer regulated by cellular O2 tension. *Proc Natl Acad Sci U S A.* (1995) 92(12):5510–4. doi: 10.1073/pnas.92.12.5510

102. Samanta D, Semenza GL. Metabolic adaptation of cancer and immune cells mediated by hypoxia-inducible factors. *Biochim Biophys Acta Rev Cancer.* (2018) 1870 (1):15–22. doi: 10.1016/j.bbcan.2018.07.002

103. Dengler VL, Galbraith M, Espinosa JM. Transcriptional regulation by hypoxia inducible factors. *Crit Rev Biochem Mol Biol* (2014) 49:1–15. doi: 10.3109/10409238.2013.838205

104. Forsythe JA, Jiang BH, Iyer NV, Agani F, Leung SW, Koos RD, et al. Activation of vascular endothelial growth factor gene transcription by hypoxia-inducible factor 1. *Mol Cell Biol* (1996) 16:4604–13. doi: 10.1111/j.1471-4159.1979.tb05236.x

105. Fathi M, Bahmanpour S, Barshidi A, Rasouli H, Karoon Kiani F, Mahmoud Salehi Khesht A, et al. Simultaneous blockade of TIGIT and HIF-1α induces synergistic anti-tumor effect and decreases the growth and development of cancer cells. *Int Immunopharmacol.* (2021) 101(Pt A):108288. doi: 10.1016/j.intimp.2021.108288

106. Van Calker D, Muller M, Hamprecht B. Adenosine regulates *via* two different types of receptors, the accumulation of cyclic AMP in cultured brain cells. *J Neurochem* (1979) 33:999–1005. doi: 10.1111/j.1471-4159.1979.tb05236.x

107. Fredholm BB, IJzerman AP, Jacobson KA, Klotz KN, Linden J. International union of pharmacology. XXV. nomenclature and classification of adenosine receptors. *Pharmacol Rev* (2001) 53(4):527–52. doi: 10.1016/j.pneurobio.2007.07.005

108. Fredholm BB, Arslan G, Halldner L, Kull B, Schulte G, Wasserman W. Structure and function of adenosine receptors and their genes. *Naunyn. Schmiedebergs. Arch Pharmacol* (2000) 362:364–74. doi: 10.1007/s002100000313

109. Fredholm BB, Chern Y, Franco R, Sitkovsky M. Aspects of the general biology of adenosine A2A signaling. *Prog Neurobiol* (2007) 83:263–76. doi: 10.1016/j.pneurobio.2007.07.005

110. Sitkovsky MV, Hatfield S, Abbott R, Belikoff B, Lukashev D, Ohta A. Hostile, hypoxia-A2-adenosinergic tumor biology as the next barrier to overcome for tumor immunologists. *Cancer Immunol Res* (2014) 2:598–605. doi: 10.1161/01.RES.81.2.154

111. Ohta A, Gorelik E, Prasad SJ, Ronchese F, Lukashev D, Wong MK, et al. A2A adenosine receptor protects tumors from antitumor T cells. *Proc Natl Acad Sci U.S.A.* (2006) 103:13132–7. doi: 10.1016/j.ccell.2016.06.025

112. Decking UK, Schlieper G, Kroll K, Schrader J. Hypoxia-induced inhibition of adenosine kinase potentiates cardiac adenosine release. *Circ Res* (1997) 81(2):154–64. doi: 10.1161/01.res.81.2.154

113. Young A, Ngiow SF, Barkauskas DS, Sult E, Hay C, Blake SJ, et al. Co-Inhibition of CD73 and A2AR adenosine signaling improves anti-tumor immune responses. *Cancer Cell* (2016) 30:391–403. doi: 10.3389/fimmu.2012.00190

114. Hatfield SM, Kjaergaard J, Lukashev D, Belikoff B, Schreiber TH, Sethumadhavan S, et al. Systemic oxygenation weakens the hypoxia and hypoxia inducible factor 1α-dependent and extracellular adenosine-mediated tumor protection. *J Mol Med (Berl).* (2014) 92(12):1283–92. doi: 10.1007/s00109-014-1189-3

115. Ohta A, Kini R, Ohta A, Subramanian M, Madasu M, Sitkovsky M. The development and immunosuppressive functions of CD4(+) CD25(+) FoxP3(+) regulatory T cells are under influence of the adenosine-A2A adenosine receptor pathway. *Front Immunol* (2012) 3:190. doi: 10.3389/fimmu.2012.00190

116. Brauneck F, Seubert E, Wellbrock J, Schulze Zur Wiesch J, Duan Y, Magnus T, et al. Combined blockade of TIGIT and CD39 or A2AR enhances NK-92 cell-mediated cytotoxicity in AML. *Int J Mol Sci* (2021) 22(23):12919. doi: 10.3390/ijms222312919

117. Muhammad F, Wang D, McDonald T, Walsh M, Drenen K, Montieth A, et al. TIGIT$^+$ A2Ar-dependent anti-uveitic treg cells are a novel subset of tregs associated with resolution of autoimmune uveitis. *J Autoimmun* (2020) 111:102441. doi: 10.1016/j.jaut.2020.102441

118. Löb S, Königsrainer A, Rammensee HG, Opelz G, Terness P. Inhibitors of indoleamine-2,3-dioxygenase for cancer therapy: can we see the wood for the trees? *Nat Rev Cancer* (2009) 9:445–52. doi: 10.1038/nm934

119. Vacchelli E, Aranda F, Eggermont A, Sautès-Fridman C, Tartour E, Kennedy EP, et al. Trial watch: IDO inhibitors in cancer therapy. *OncoImmunology* (2014) 3:e957994. doi: 10.1038/nm1196

120. Uyttenhove C, Pilotte L, Théate I, Stroobant V, Colau D, Parmentier N, et al. Evidence for a tumoral immune resistance mechanism based on tryptophan degradation by indoleamine 2,3-dioxygenase. *Nat Med* (2003) 9:1269–74. doi: 10.1002/ijc.10645

121. Muller AJ, DuHadaway JB, Donover PS, Sutanto-Ward E, Prendergast GC. Inhibition of indoleamine 2,3-dioxygenase, an immunoregulatory target of the cancer suppression gene Bin1, potentiates cancer chemotherapy. *Nat Med* (2005) 11:312–19. doi: 10.1038/nm1196

122. Friberg M, Jennings R, Alsarraj M, Dessureault S, Cantor A, Extermann M, et al. Indoleamine 2,3-dioxygenase contributes to tumor cell evasion of T cell-mediated rejection. *Int J Cancer* (2002) 101:151–55. doi: 10.1002/ijc.10645

123. Hoffman RM. Tumor growth control with IDO-silencing salmonella-letter. *Cancer Res* (2013) 73:4591. doi: 10.1158/0008-5472.CAN-12-4719

124. Manuel ER, Diamond DJ. A road less traveled paved by IDO silencing: harnessing the antitumor activity of neutrophils. *Oncoimmunology* (2013) 2:e23322. doi: 10.4161/onci.23322

125. Zheng X, Koropatnick J, Chen D, Velenosi T, Ling H, Zhang X, et al. Silencing IDO in dendritic cells: a novel approach to enhance cancer immunotherapy in a murine breast cancer model. *Int J Cancer* (2013) 132:967–77. doi: 10.1002/ijc.27710

126. Blache CA, Manuel ER, Kaltcheva TI, Wong AN, Ellenhorn JD, Blazar BR, et al. Systemic delivery of salmonella typhimurium transformed with IDO shRNA enhances intratumoral vector colonization and suppresses tumor growth. *Cancer Res* (2012) 72:6447–56. doi: 10.1158/0008-5472.CAN-12-0193

127. Wang D, Saga Y, Mizukami H, Sato N, Nonaka H, Fujiwara H, et al. Indoleamine-2,3-dioxygenase, an immunosuppressive enzyme that inhibits natural killer cell function, as a useful target for ovarian cancer therapy. *Int J Oncol* (2012) 40:929–34. doi: 10.1016/j.ccell.2017.07.003

128. Hou DY, Muller AJ, Sharma MD, DuHadaway J, Banerjee T, Johnson M, et al. Inhibition of indoleamine 2,3-dioxygenase in dendritic cells by stereoisomers of 1-methyl-tryptophan correlates with antitumor responses. *Cancer Res* (2007) 67:792–801. doi: 10.1016/j.it.2012.10.001

129. Robertson AG, Shih J, Yau C, Gibb EA, Oba J, Mungall KL, et al. Integrative analysis identifies four molecular and clinical subsets in uveal melanoma. *Cancer Cell* (2017) 32(204–220):e215. doi: 10.1097/PPO.0b013e3181eb3343

130. Munn DH, Mellor AL. Indoleamine 2,3 dioxygenase and metabolic control of immune responses. *Trends Immunol* (2012) 34:137–43. doi: 10.3390/jpm10030112

131. Soliman H, Mediavilla-Varela M, Antonia S. Indoleamine 2,3-dioxygenase: is it an immune suppressor? *Cancer J* (2010) 16:354–9. doi: 10.1111/acel.12716

132. Rahimi Koshkaki H, Minasi S, Ugolini A, Trevisi G, Napoletano C, Zizzari IG, et al. Immunohistochemical characterization of immune infiltrate in tumor microenvironment of glioblastoma. *J Pers Med* (2020) 10(3):112. doi: 10.3390/jpm10030112

133. Song Y, Wang B, Song R, Hao Y, Wang D, Li Y, et al. T-Cell immunoglobulin and ITIM domain contributes to $CD8^+$ T-cell immunosenescence. *Aging Cell* (2018) 17(2): e12716. doi: 10.1111/acel.12716

134. Chew GM, Fujita T, Webb GM, Burwitz BJ, Wu HL, Reed JS, et al. TIGIT marks exhausted T cells, correlates with disease progression, and serves as a target for immune restoration in HIV and SIV infection. *PloS Pathog* (2016) 12(1):e1005349. doi: 10.1371/journal.ppat.1005349

135. Holzheimer R, Mannick JA, Zuckschwerdt. *Surgical treatment: Evidence-based and problem-oriented*. (2001). doi: 10.1126/scitranslmed.aaz6314

136. Davern M, Donlon NE, Sheppard A, Connell FO, Hayes C, Bhardwaj A, et al. Chemotherapy regimens induce inhibitory immune checkpoint protein expression on stem-like and senescent-like oesophageal adenocarcinoma cells. *Transl Oncol* (2021) 14 (6):101062. doi: 10.1016/j.tranon.2021.101062

137. Liu X, Hartman CL, Li L, Albert CJ, Si F, Gao A, et al. Reprogramming lipid metabolism prevents effector T cell senescence and enhances tumor immunotherapy. *Sci Transl Med* (2021) 13:eaaz6314. doi: 10.1046/j.1365-2567.1996.d01-689.x

138. Effros RB, Boucher N, Porter V, Zhu X, Spaulding C, Walford RL, et al. Decline in CD28+ T cells in centenarians and in long-term T cell cultures: A possible cause for both *in vivo* and *in vitro* immunosenescence. *Exp Gerontol.* (1994) 29(6):601–9. doi: 10.1016/0531-5565(94)90073-6

139. Fagnoni FF, Vescovini R, Mazzola M, Bologna G, Nigro E, Lavagetto G, et al. Expansion of cytotoxic CD8+ CD28- T cells in healthy ageing people, including centenarians. *Immunology* (1996) 88(4):501–7. doi: 10.1046/j.1365-2567.1996.d01-689.x

140. Weng NP, Akbar AN, Goronzy J. CD28(-) T cells: Their role in the age-associated decline of immune function. *Trends Immunol* (2009) 30(7):306–12. doi: 10.1016/j.it.2009.03.013

141. Thompson CB, Lindsten T, Ledbetter JA, Kunkel SL, Young HA, Emerson SG, et al. CD28 activation pathway regulates the production of multiple T-cell-derived lymphokines/cytokines. *Proc Natl Acad Sci U S A.* (1989) 86(4):1333–7. doi: 10.1073/pnas.86.4.1333

142. Klein Geltink RI, O'Sullivan D, Corrado M, Bremser A, Buck MD, Buescher JM, et al. Mitochondrial priming by CD28. *Cell* (2017) 171(2):385–397.e11. doi: 10.1016/j.cell.2017.08.018

143. Zhou XM, Li WQ, Wu YH, Han L, Cao XG, Yang XM, et al. Intrinsic expression of immune checkpoint molecule TIGIT could help tumor growth *in vivo* by suppressing the function of NK and $CD8^+$ T cells. *Front Immunol* (2018) 9:2821. doi: 10.3389/fimmu.2018.02821

144. Search of: Tiragolumab - List Results - ClinicalTrials.gov.

145. Search of: ociperlimab - List Results - ClinicalTrials.gov.

146. Search of: vibostolimab - List Results - ClinicalTrials.gov.

147. Search of: domvanalimab - List Results - ClinicalTrials.gov.

148. AB154 Combined With AB122 for Recurrent Glioblastoma - Full Text View - ClinicalTrials.gov.

149. Safety and Efficacy of Zimberelimab (AB122) in Combination With Domvanalimab (AB154) and Etrumadenant (AB928) in Patients With Previously Treated Non-Small Cell Lung Cancer - Full Text View - ClinicalTrials.gov.

150. Rotte A, Sahasranaman S, Budha N. Targeting TIGIT for immunotherapy of cancer: Update on clinical development. *Biomedicines* (2021) 9(9):1277. doi: 10.3390/biomedicines9091277

151. Hata AN, Engelman JA, Faber AC. The BCL2 family: Key mediators of the apoptotic response to targeted anticancer therapeutics. *Cancer Discovery* (2015) 5(5):475–87. doi: 10.1158/2159-8290.CD-15-0011

152. Khalil AA, Kabapy NF, Deraz SF, Smith C. Heat shock proteins in oncology: diagnostic biomarkers or therapeutic targets? *Biochim Biophys Acta* (2011) 1816(2):89–104. doi: 10.1016/j.bbcan.2011.05.001

153. Del Gaizo Moore V, Letai A. BH3 profiling–measuring integrated function of the mitochondrial apoptotic pathway to predict cell fate decisions. *Cancer Lett* (2013) 332 (2):202–5. doi: 10.1016/j.canlet.2011.12.021

154. Owonikoko TK, Khuri FR. Targeting the PI3K/AKT/mTOR pathway: Biomarkers of success and tribulation. *Am Soc Clin Oncol Educ Book* (2013) 10.1200/EdBook_AM.2013.33.e395. doi: 10.14694/EdBook_AM.2013.33.e395

155. Razaghi A, Heimann K, Schaeffer PM, Gibson SB. Negative regulators of cell death pathways in cancer: perspective on biomarkers and targeted therapies. *Apoptosis* (2018) 23(2):93–112. doi: 10.1007/s10495-018-1440-4

156. Teng MW, Ngiow SF, Ribas A, Smyth MJ. Classifying cancers based on T-cell infiltration and PD-L1. *Cancer Res* (2015) 75(11):2139–45. doi: 10.1158/0008-5472.CAN-15-0255

157. Larkin J, Chiarion-Sileni V, Gonzalez R, Grob JJ, Cowey CL, Lao CD, et al. Combined nivolumab and ipilimumab or monotherapy in untreated melanoma. *N Engl J Med* (2015) 373(1):23–34. doi: 10.1056/NEJMoa1504030

158. Mahoney KM, Atkins MB. Prognostic and predictive markers for the new immunotherapies. *Oncol (Williston Park).* (2014) 28 Suppl 3:39–48. doi: 10.3389/fimmu.2020.02048

159. Mansfield AS, Murphy SJ, Peikert T, Yi ES, Vasmatzis G, Wigle DA, et al. Heterogeneity of programmed cell death ligand 1 expression in multifocal lung cancer. *Clin Cancer Res* (2016) 22(9):2177–82. doi: 10.1158/1078-0432.CCR-15-2246

160. Liu JN, Kong XS, Huang T, Wang R, Li W, Chen QF. Clinical implications of aberrant PD-1 and CTLA4 expression for cancer immunity and prognosis: A pan-cancer study. *Front Immunol* (2020) 11:2048. doi: 10.3389/fimmu.2020.02048

161. Ma L, Gai J, Qiao P, Li Y, Li X, Zhu M, et al. A novel bispecific nanobody with PD-L1/TIGIT dual immune checkpoint blockade. *Biochem Biophys Res Commun* (2020) 531 (2):144–51. doi: 10.1016/j.bbrc.2020.07.072

162. Chauvin JM, Zarour HM. TIGIT in cancer immunotherapy. *J Immunother Cancer.* (2020) 8(2):e000957. doi: 10.1136/jitc-2020-000957

163. Gilmour C, Yoo S-K, Chan T, Wang L. The co-expression of VISTA and TIGIT on cytotoxic T cells defines subpopulation with altered immunometabolism [abstract]. in: Abstracts: AACR virtual special conference: Tumor immunology and immunotherapy; 2021 Oct 5-6. Philadelphia (PA): AACR. *Cancer Immunol Res* (2022) 10(1 Suppl). doi: 10.1002/hep.30593

frontiers | Frontiers in Oncology

TYPE Review
PUBLISHED 10 May 2023
DOI 10.3389/fonc.2023.1175532

OPEN ACCESS

EDITED BY
Martin Böttcher,
Otto-von-Guericke University Magdeburg, Germany

REVIEWED BY
Mario Jolicoeur,
Polytechnique Montréal, Canada
Mark Woodford,
Upstate Medical University, United States

*CORRESPONDENCE
Vivek Verma
vermav@umn.edu

RECEIVED 27 February 2023
ACCEPTED 25 April 2023
PUBLISHED 10 May 2023

CITATION
Mortazavi Farsani SS and Verma V (2023) Lactate mediated metabolic crosstalk between cancer and immune cells and its therapeutic implications.
Front. Oncol. 13:1175532.
doi: 10.3389/fonc.2023.1175532

Lactate mediated metabolic crosstalk between cancer and immune cells and its therapeutic implications

Seyedeh Sahar Mortazavi Farsani [1] and Vivek Verma [1,2]*

[1]Section of Cancer Immunotherapy and Immune Metabolism, The Hormel Institute, University of Minnesota, Austin, MN, United States, [2]Masonic Cancer Center, University of Minnesota, Minneapolis, MN, United States

Metabolism is central to energy generation and cell signaling in all life forms. Cancer cells rely heavily on glucose metabolism wherein glucose is primarily converted to lactate even in adequate oxygen conditions, a process famously known as "the Warburg effect." In addition to cancer cells, Warburg effect was found to be operational in other cell types, including actively proliferating immune cells. According to current dogma, pyruvate is the end product of glycolysis that is converted into lactate in normal cells, particularly under hypoxic conditions. However, several recent observations suggest that the final product of glycolysis may be lactate, which is produced irrespective of oxygen concentrations. Traditionally, glucose-derived lactate can have three fates: it can be used as a fuel in the TCA cycle or lipid synthesis; it can be converted back into pyruvate in the cytosol that feeds into the mitochondrial TCA; or, at very high concentrations, accumulated lactate in the cytosol may be released from cells that act as an oncometabolite. In immune cells as well, glucose-derived lactate seems to play a major role in metabolism and cell signaling. However, immune cells are much more sensitive to lactate concentrations, as higher lactate levels have been found to inhibit immune cell function. Thus, tumor cell-derived lactate may serve as a major player in deciding the response and resistance to immune cell-directed therapies. In the current review, we will provide a comprehensive overview of the glycolytic process in eukaryotic cells with a special focus on the fate of pyruvate and lactate in tumor and immune cells. We will also review the evidence supporting the idea that lactate, not pyruvate, is the end product of glycolysis. In addition, we will discuss the impact of glucose-lactate-mediated cross-talk between tumor and immune cells on the therapeutic outcomes after immunotherapy.

KEYWORDS

Warburg effect, cancer, lactate, glycolysis, immunotherapy, metabolism, TCA cycle, mitochondria

Introduction

Animal cells, particularly the actively dividing cancer cells rely heavily on glucose as a source of energy for their survival and for generation of macromolecules required for their proliferation (1). Similarly, the fate of immune cells, their ability to get activated and their effector functions are tightly coupled with the glucose metabolism, especially during the acute phase of antigen mediated activation (2). Because cancer and immune cells rely on similar fuel types for their proliferation and activation, there is an acute competition between the two cell types for nutrients (3). Ultimately, the nutrient availability, optimal utilization of available nutrients, and presence of appropriate metabolic machinery to support the nutrient utilization decides the outcomes of cell metabolism (4). Hence, a thorough understanding of the regulators of metabolism in cancer and immune cells, especially in the context of complex environment of tumors is important for generation of appropriate immune functions and for institution of adequate anti-cancer therapies.

Continuum of metabolism as the driver of cell functions

The term life refers to the ability of an organism or a cell to grow, reproduce, and demonstrate functional activity and continued change preceding death (5). These life processes are supported by the sum of chemical changes termed metabolism that take place inside an organism at cell and molecular levels, leading to generation of energy or building blocks required for sustenance of life (6). Metabolism not only provides the energy and building blocks for cellular growth but also ensures protection against stress factors such as osmotic changes, xenobiotics, and oxidative stress (7). Metabolism has evolved to support cell function and activity by either generating or breaking down the building blocks, based on which the metabolism can be respectively termed anabolic or catabolic. In anabolic metabolism, utilizing simpler building blocks such as glucose, free fatty acids and amino acids, cells synthesize complex molecules such as glycogen, fatty acids, and proteins which are required for generation of cellular building blocks (8). On the contrary, catabolism refers to the breakdown of complex cellular molecules into their simpler forms. Hence, anabolism and catabolism represent two opposite ends of the metabolic spectrum (9). In particular, the central carbon metabolism that represents the six carbon fixation pathways, ensures conversion of carbon and energy sources such as sugars into precursor of metabolism which are used to generate entire biomass of the cells in addition to the generation of free energy, redox power, and precursor metabolites required for biosynthesis (Figure 1). Depending upon the cellular/organismal complexity, the amount of cell's genetic and proteomic machinery involved in regulating metabolism varies. Metabolism is usually the largest constituent of the proteome with approximately 50% of the proteome being allocated to metabolism in yeast. In humans the fraction of proteome associated with cell metabolism is lower as a larger fraction of the proteome is allocated to cell signaling, cytoskeleton proteins, chaperones, and the spliceosome (10). However, consistently within the metabolic spectrum, the glycolytic enzymes are allocated a larger fraction of the proteome than the TCA cycle (10) with about 15-20% being allocated alone to glycolysis in humans (11). The high catalytic efficiency, small size, and high abundance of enzymes in the central carbon metabolism are consistent with the central role this part of metabolism plays in ensuring constant provision of energy, primarily in the form of ATP, in handling electron flows by balancing the co-factors NADH and NADPH, and in providing precursors for cellular growth (12). Thus, the flux through the central carbon metabolism typically exceeds the flux through other metabolic pathways by a factor of 10 or more. With these multiple roles, the central carbon metabolism must be highly connected with the other parts of metabolism (12). This implies that a perturbation of almost any part of metabolism results in a global response in which a large number of enzymes have to alter their function in order to maintain homeostasis or generate a particular cell function such as effector functions in T cells (13). This explains why almost any change in cellular physiology has a metabolic fingerprint, i.e., changes in a certain part of metabolism. Thus, it is safe to say that metabolic perturbations have a global impact on cell function and physiology (13). In this review, we critically analyze the intricately associated central carbon metabolism in cancer and immune cells with special reference to glycolysis and lactate metabolism. We provide evidence that glucose derived lactate may be a significant driver of mitochondrial metabolism in CD8 T cells and that lactate driven cross talk between tumor and immune cells shapes the response to therapies. We also discuss the potential of targeting central carbon metabolism as an avenue for enhancement of anti-cancer therapies.

Regulation of glycolysis

Central carbon metabolism plays an important role in metabolic networking and is composed of the flow of carbon from nutrients into biomass. Central carbon metabolism is composed of the glycolytic pathway, the citric acid cycle, the pentose phosphate pathway (PPP), and six known carbon fixation pathways (14). Of these, carbon fixation pathways are the most fundamental pathways that take place inside the mesophyll cells of plants that help to bring CO_2 into the anabolic phase of cell metabolism (15). Sugars, primarily glucose, fuels the glycolytic pathway in animal cells whereby through a series of enzymatic reactions these sugars are broken down into pyruvate which is then either fed into the mitochondrial TCA cycle for electron reduction and ATP generation or is converted into lactate in the cytoplasm. The PPP shunts carbons back into the glycolytic or gluconeogenic pathways and is a major regulator of the cellular reduction-oxidation (redox), homeostasis and biosynthesis. Glycolysis and citric acid cycle (also called tricarboxylic acid (TCA) cycle) are the most intricately associated and well-defined energy generating pathways in eukaryotic cells. In glycolysis glucose, through a

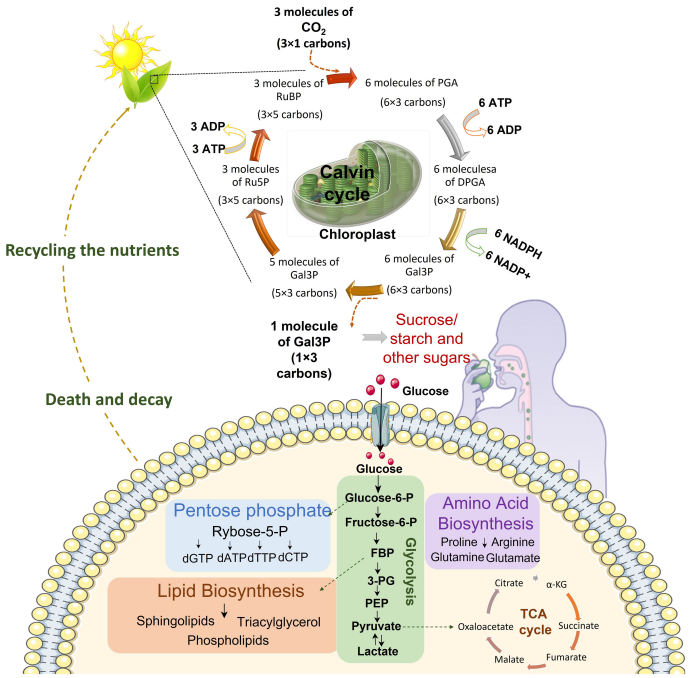

FIGURE 1
Continuum of energy flow. Central carbon metabolism is responsible to lead carbon from nutrients into biomass. The first source of carbon is atmospheric CO_2. Plants utilize sunlight, CO_2 and H_2O to trigger chloroplast factory. In the chloroplast sunlight dependent reactions prepare NADPH and ATP for Calvin cycle which finally produces comestible source of carbons including sucrose, sugar and starch. These food sources would be broken down to glucose in the body. Cells uptake glucose and metabolize it in glycolysis pathway which prepare energy and various metabolites for nucleotide synthesis, lipid biosynthesis, amino acid biosynthesis and mitochondrial TCA cycle for electron reduction and energy generation. After death decay, nutrients be recycled for plants in the soil. (DPGA: Diphosphoglycerate, FBP: Fructose 1,6-bisphosphate, 3PG: 3-Phosphoglyceric acid, Gal3P: Glyceraldehyde-3-phosphate, PEP: Phosphoenolpyruvate, PGA: Phosphoglyceric acid, RuBP: Ribulose 1,5-biphosphate, Ru5P: Ribulose-5-phosphate).

multistep reaction is converted into pyruvate which is then transformed either into lactate that is secreted to outside of the cell or gets converted into oxaloacetate (OAA) or acetyl-CoA that feeds into TCA cycle inside the cell (Figure 1). In the presence of adequate amounts of oxygen, cytoplasmic glycolysis is connected to the mitochondrial respiratory chain that enables oxidative phosphorylation (OXPHOS) by transport of electrons through the proteins of the respiratory chain (16). This electron transport generates a proton gradient which is necessary for ATP synthesis. Ideally, when glycolysis and OXPHOS are coupled, one mole of glucose produces up to 36 moles of ATP. However, under the conditions of limited oxygen availability, OXPHOS reactions are impaired, and there is a compensatory upregulation in the glycolytic activity that helps to fulfill the increased energy demands (17). Even if the oxygen concentrations are high, if the demand for ATP increases suddenly, such as under acute cell expansion phase after antigenic stimulation of immune cells, aerobic glycolysis is enhanced rapidly since mitochondrial activity is not sufficient to supply the required amount of ATP. Moreover, intermediate metabolites of glycolysis are precursors for the biosynthesis of pentose phosphates, hexosamines, glycerophospholipids and amino acids, so that glycolysis can fuel various anabolic pathways whenever required. Hence, an upregulated glycolytic pathway not only supplies ATP under acute energy shortage conditions, but also provides intermediates for cell biomass synthesis.

Glycolysis is regulated at three points, each serving a different function. Hexokinase (HK), phosphofructokinase (PFK) and pyruvate kinase (PK) are the three rate-limiting enzymes regulating the glycolytic flux. HK controls the entry of glucose into the glycolytic pathway by producing glucose-6-phosphate (G6P), which also acts as an allosteric inhibitor of HK. HK exists in 4 isoenzyme types (HK1-4) with HK1 and HK3 being ubiquitously expressed while HK4 being restricted to liver and pancreas. HK1-3 are associated with the outer mitochondrial membrane and are shown to play a critical role in maintaining aerobic glycolysis in cancer cells. High affinity HK2 is mainly expressed in tissues with high energy demand such as tumors. In particular, HK2 has been shown to act as a bridge between cell metabolism and cellular longevity primarily by preventing the mitochondrial death pathways (18). Surprisingly, HK2 has been found to be dispensable for T cell based immunity (19) thus pitching HK2 as a putative differential target in tumor cells that heavily rely on HK2 for their energy and biosynthetic demands (20). High expression of HK2 in tumor and associated mesenchymal stromal cells inhibit glucose uptake in T cells preventing their activation. The second point of glycolysis regulation is the entry point of fructose-6-phosphate into glycolytic cycle by phosphofructokinase (PFK). PFK exists as a tetramer and has two isoforms, PFK1 and PFK2. PFK1 catalyzes the conversion of fructose-6-phosphate to fructose-1,6-bisphosphate while PFK2

catalyzes the conversion of fructose-6-phosphate to fructose-2,6-bisphosphate. Fructose-2,6-bisphosphate is a stimulator of PFK1 by its ability to increase the affinity of PFK1 for fructose-6-phosphate and to decrease the ability of ATP to inhibit the reaction (21). When the rate of PFK1 is slowed, G6P accumulates and is routed toward glycogen synthesis or the pentose phosphate pathway (PPP). PFK-1 is allosterically regulated by effectors such as fructose-2,6-biphosphate (FBP) or adenosine monophosphate (AMP). Oncogene activation including Ras and Src leads to reduced regulation of PFK1 activity by elevated levels of FBP that acts as a natural activator of PFK1 (22, 23) leading to enhanced glucose uptake and its conversion into downstream substrates, preferably lactate that can be shunted into various biosynthetic pathways. There is limited evidence regarding the role of PFK in immune cells. In CD4 T-helper cells from rheumatoid arthritis patients, deficiency of PFK was found to impair the ATP generation and autophagy, making the cells prone to apoptosis and senescence (24). In addition, PFK seems to have a significant role in regulatory T cells, as calcium regulated protein kinase-4 (CaMK4) controlled PFK-platelet type (PFKP) was found to enhance the regulatory role of these cells (25). Finally, in an irreversible reaction pyruvate kinase (PK) controls the conversion of phosphoenol pyruvate (PEP) into pyruvate or to gluconeogenesis. Pyruvate kinase exists in four isozyme forms: PKL (liver), PKR (red blood cells), PKM1 (muscle and brain) and PKM2 (early fetal tissue and actively growing cells such as tumor cells and immune cells). PKM2 can exist in two isozyme forms, the tetrameric and the dimeric form, both of which are constituted of the same monomeric units. Tetrameric PKM2 (tet-PKM2) localizes in the cytoplasm and is the enzymatically active form while the dimeric PKM2 (di-PKM2) localizes in the nucleus and is transcriptionally active form. There are several allosteric stimulators that induce tetrameric form including F1,6-BP that help to prevent a metabolic roadblock when upstream PFK is active. In fasting conditions, pyruvate kinase is allosterically inhibited by ATP and alanine (mostly mobilized from muscle) decreasing the concentrations of tet-PKM2 that prevents PEP that is needed for gluconeogenesis from being converted directly back to pyruvate. The role of PKM2 in immune cells is not well defined and only recently has started to be appreciated. Angiari et al. show that the tetramerization of PKM2 prevents CD4 T cell activation. Most effect was on generation of Tregs and Th17 cells thus preventing the induction of autoimmune diseases (26). Similarly, PKM2 in macrophages has been shown to prevent generation of proinflammatory phenotype thus helping in prevention of autoimmune disorders (27). However, the role of PKM2 in cytotoxic CD8 T cells is still under debate.

Pyruvate generated as a result of glycolysis can have multiple fates in the cytoplasm. Pyruvate can be effluxed from the cell, or is converted into alanine by alanine aminotransferase, or by the process of gluconeogenesis reactions is converted into oxaloacetate or malate, or may be transported into the mitochondria where it is converted to acetyl-CoA for its utilization in the TCA cycle. Interestingly, none of these steps occur at a rate that can match the conversion of pyruvate into lactate, making lactate the inevitable and ultimate metabolite of glycolytic pathway (Figure 2). Pyruvate is the precursor of lactate and under certain conditions can exclusively be the source of energy inside the cells. Pyruvate is transported into mitochondria by MPC1 and MPC2 heterodimers (28, 29). In the inter-mitochondrial membrane, it gets converted into acetyl-CoA that is funneled into TCA cycle. Pyruvate alters epigenome in CD4 T cells during activation by altering the cell genome (30). In the same line, inhibition of mitochondrial transfer of pyruvate by blocking MPC1 and MPC2 has been shown to mold the CD8 T cells into memory phenotype thus supporting the observation that enhanced availability of pyruvate and its oxidation through mitochondria supports effector functions (31). Moreover, pyruvate metabolism may support antitumor signaling in CD8 T Cells by upregulating succinate uptake through its receptor (32).

Pyruvate is converted into lactate by lactate-dehydrogenase (LDH). LDH is a tetrameric enzyme composed of two protein subunits. The tetramer can be assembled by combination of the M (muscle) form (encoded from Ldh-A gene) or the H (heart) form (product of the Ldh-B gene) producing five separate isozymes: M_4 (LDH5), M_3H_1 (LDH_4), M_2H_2 (LDH3), M_1H_3 (LDH2), and H_4 (LDH1) (33). These isozymes have different kinetic properties with respect to substrate affinity and inhibition among these isozymes. LDH activity depends on the metabolic switch to anaerobic respiration. LDH is modulated by three types of regulations, namely, allosteric modulation (34), substrate-level regulation (35), and transcriptional regulation (36). The relative availability and concentration of substrates regulate the activity of LDH. The enzyme becomes more active during high availability of its substrates. The demand for ATP compared to aerobic ATP supply causes the accumulation of ADP, AMP, and free phosphates (Pi). Glycolytic flux leads to the production of pyruvate that exceeds the metabolic capacity of pyruvate dehydrogenase and other shuttle enzymes that metabolize pyruvate. This process channelizes the flux of pyruvate and NAD+ through LDH, subsequently generating lactate and NADH (37).

The anecdote of Warburg effect

The ability of pyruvate to get converted into lactate even under aerobic conditions has been established as a universal phenomenon. Importantly, aerobic glycolysis was traditionally considered to be a negative cellular phenomenon that contributed to cell exhaustion partly by nutrient depletion and partly by accumulation of acidic byproduct such as lactate (38). Pyruvate can be converted into lactate quickly by lactate dehydrogenase (LDH) and lactate is the final product of glycolysis that was thought to be produced as a waste material by the tumor or the tumor associated stromal cells (39). However, over a period of time several published reports demonstrate that lactate can serve as a significant source of energy inside cells. In fact, in CD8 cells, lactate has been shown to be the preferred substrate albeit in a narrow range of concentrations. Importantly, tumor infiltrating cytotoxic CD8 T cells have been shown to be dependent on lactate metabolism to sustain their antitumor function (40). It has bene shown that mitochondria are capable of transporting lactate across the inner membrane and oxidizing it (41). Lactate transport into the mitochondrial matrix

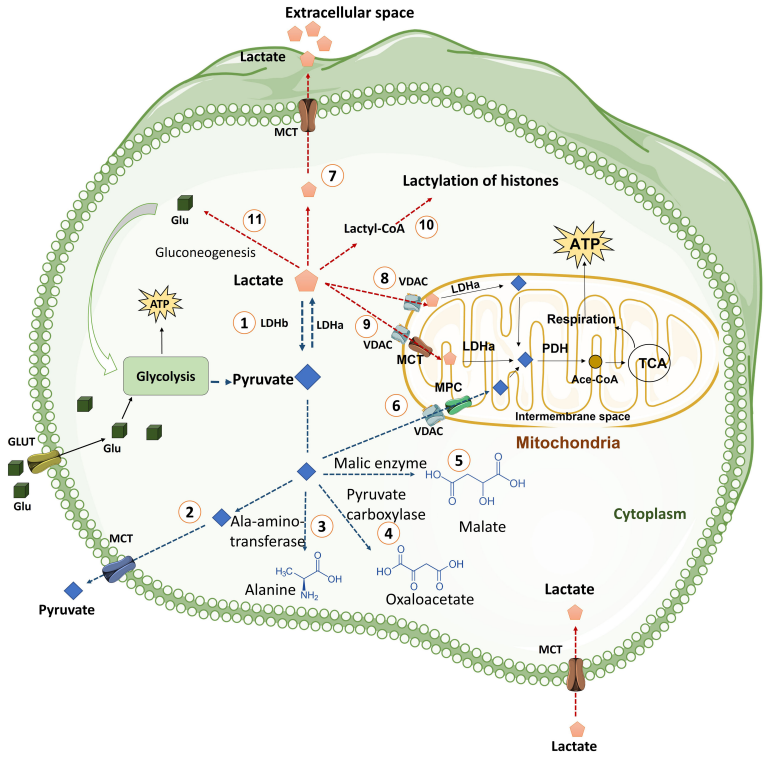

FIGURE 2
The fate of pyruvate and Lactate in the cells. Cells uptake glucose molecules *via* GLT and use them in glycolysis pathway. Glycolysis prepares ATP and some other intermediate metabolites for cells. Pyruvate derived from glycolysis has several fates including: (1) Conversion pyruvate to lactate *via* LDHa enzyme quickly. This reaction is reversible by LDHb. (2) Exporting pyruvate from cells by MCT transporter, which is located in plasma membrane, to extracellular space. (3) Generation of alanine amino acid from pyruvate *via* Ala-amino-transferase enzyme. (4) Conversion of pyruvate to oxaloacetate by pyruvate carboxylase enzyme. (5) Generation of Malate from pyruvate in a reaction mediated by malic enzyme. (6) Transporting of pyruvate into mitochondria by VDAC in the mitochondrial outer membrane and MPC transporter in the mitochondrial inner membrane. Pyruvate in mitochondria is converted to Ace.CoA by PDH and used in TCA cycle. TCA cycle generates NADH and $FADH_2$ for mitochondria respiration process in the inner membrane of mitochondria that produces more ATP for cells. Lactate derived from glycolysis has also various fates including: (7) Releasing lactate from cells into extracellular space by MCT transporters (MCT1 and MCT4). (8) Transporting lactate into Intermembrane space, by VDAC channel, where lactate can be converted to pyruvate by LDHa. (9) Entering lactate into the mitochondrial matrix where lactate can be converted to pyruvate by LDHa. (10) Lactate can be converted into lactyl-CoA and is involved in the lactylation of histones in the nucleus. (11) Lactate is converted to glucose through gluconeogenesis and glucose goes back to glycolysis. (Ace. CoA: Acetyl coenzyme A, GLT: Glucose transporter, LDH: Lactate dehydrogenase, MCT: Monocarboxylate transporter, MPC: Mitochondrial pyruvate carrier, PDH: Pyruvate dehydrogenase, PEP: phosphoenolpyruvate, PEPS: phosphoenolpyruvate synthetase, TCA cycle: Tricarboxylic acid cycle, VDAC: Voltage-dependent anion channel).

would simultaneously deliver both pyruvate and cytosolic reducing equivalents from the cytosol into the mitochondrial matrix (42). There are some other evidences suggesting that LDH and monocarboxylate transporter (MCT)1 are colocalized in the inner mitochondrial membrane facilitating the transport of lactate into the mitochondria (43). Excessive lactate production and rapid lactate transport in cancer cells depend primarily on the upregulation of hypoxia-inducible factor-1α (HIF-1α) and c-Myc (44, 45). Continuous activation of HIF-1α and c-Myc causes aberrant expression of multiple glycolytic enzymes and monocarboxylate transporters (MCTs), including lactate dehydrogenase A (LDHA), MCT1, and MCT4 (46). Lactate in the TME not only induces lactic acidosis, but also shuttles among cell populations, including cancer cells, tumor-associated stromal cells, tumor-associated macrophages (TAMs), and tumor-infiltrating lymphocytes (TILs) (47, 48). Cancer cells export lactate to the extracellular space *via* MCTs (49) that makes many unpleasant consequences in tumor microenvironment (TME) (38). High level of lactate decreases pH in TME which triggers increase of angiogenesis, proteolytic activity, metastatic, and resistance to anti-cancer therapies (50). High lactate in TME also makes cancer prognosis more difficult (48). Recently, in breast cancer cells lactate has been shown to regulate malignancy by reprogramming energy metabolism and by altering cell signaling *via* binding of lactate to G-protein-coupled receptor 81 (GPR81) (51). In addition to its effect in cancer cells, an indirect effect of interaction between lactate and GPR81 is to reduce the expression of MHCII on APCs in the TME that tend to mitigate the generation of immune response and promote immune escape (52). The use of lactate or alternate molecules such as glutamine as an energy source may not only depend upon the activation of various signaling pathways but also on the anatomical location of tumor cells. For example, tumor cells located deep in the TME away from blood supply may use glutamine as a source of energy for glycolysis and produce huge amount of lactate, whereas cancer cells near blood vessels (in normoxic condition), such as in lung tumor, prefer to oxidize lactate and obtain energy by TCA cycle (53). The presence of various physiologic carbon sources (PCSs) such as lactate, acetate,

glutamate, citrate, and pyruvate in extracellular environment strongly impact the uptake and utilization of glucose by CD8 T cells. Enough amount of PCSs in the cell culture media decreases glucose contribution to the TCA cycle and interestingly, enhances effector function, such as production of IFN-γ (40). The role of glutamine mediated cell metabolism is intriguing in this regard. Glutamine participates in TCA cycle and in the synthesis of nucleotides, glutathione, and other non-essential amino acids. In fact, despite being a non-essential amino acid, it is considered essential for tumor cell metabolism as its deprivation suppresses tumor cell growth and induces cell killing. Interestingly, glutamine supports mitochondrial metabolism when glucose derived pyruvate is converted into lactate. However, in the current review, we are going to limit our discussion to the effect of lactate metabolism in immune cells and its impact on immune mediated anti-cancer responses.

Effect of lactate in different immune cell populations

Glycolytic pathway, through the active or passive participation of its metabolites controls the function of various immune cells. Active participation refers to direct effect of various metabolites on the cell function and physiology while passive control is by relative abundance, or lack of thereof, of various metabolites, particularly the glucose and lactate which may be required for energy generation or cell signaling. In this section we discuss the implications of metabolite alterations, especially increased lactate concentrations on various immune cell populations.

Lymphocytes

T cells in the TME have been found to lose their antitumor activity because of either glucose deprivation (54), or presence of high levels of lactate. The presence of high levels of lactate (which is mostly tumor derived) disrupts the transmembrane concentration gradients thus preventing the secretion of intracellular lactate by activated and proliferating immune cells. This leads to decreased intracellular pH and shutting down of the homeostasis cell machinery tipping the balance towards cell dysfunctionality. Accumulation of lactate in T cells is mediated by the high expression of MCT1 lactate transporters after TCR engagement that increases lactate uptake into the cells (48). In the tumor-immune microenvironment, the effect of lactate on immune cells can be highly complex and hard to decipher, which is further confounded by acidic protons, a co-product of glycolysis. In one study, Mendler et al. showed that lactate acidosis impaired the TCR-triggered induction of p38/JNK signaling required for IFNγ production but not the MEK1/ERK signaling required for granule movement (55). In another study, lactate has been shown to reduce pyruvate carboxylase mediated replenishment of TCA cycle intermediates leading to inhibition of anaplerotic pathways (32). In yet another study, inhibition of lactate dehydrogenase, in combination with IL-21 was found to reduce the lactate concentrations while increasing the stemness and anti-tumor ability of CD8 T cells (56). In contrast to these studies, lactate has been shown to increase the stemness of CD8 T cells leading to augmentation of anti-tumor immunity (57). In this study, using mouse models of colon cancer, subcutaneous administration of lactate but not glucose was found to inhibit tumor growth in a CD8 T cell-dependent manner. This reduction in tumor growth was associated with an increased proportion of $TFC1^{+}CD8$ T cells, as revealed by single cell transcriptomics analysis (57). Mechanistically, lactate inhibits histone deacetylase activity, which results in an increased acetylation at H3K27 of the *Tcf7* super enhancer locus, leading to increased *Tcf7* gene expression. In addition, *in vitro*, lactate pre-treated $CD8^{+}$ T cells were also found to efficiently inhibit tumor growth upon adoptive transfer to tumor-bearing mice. However, one limitation of in-vitro studies is the exposure of immune cells to super-physiological conditions where nutrients are available in excess compared to physiological conditions (58) that may alter the outcomes of cell activation. Indeed, CD8 T cells activated under *in vivo* conditions were found to utilize glucose though oxidative metabolism with flow of glucose derived carbon into anabolic phase compared to *in vitro* activation that showed hallmarks of aerobic glycolysis (59). Hence, the observations from various studies should be analyzed with caution as metabolite utilization and cell activation events may be highly context dependent.

Regulatory T cells

The effects of lactate on Treg cells in TME are also in favor of cancer progression. It has been shown that lactate can preserve Treg cell immune-suppressive functions by upregulation of FOXP3 (60), and MCT1 (61). In a recent study, Gu et al. showed that tumor derived lactate regulates Tregs by lactylation of MOESIN at Lys72 residue enhancing the TGBβ mediated signaling *via* TGFβ-RI (62). The more the expression of FOXP3, the more OXPHOS, NAD^{+} oxidation and adaptation of Treg cells to low-glucose and high-lactate conditions (60). Additionally, MCT1 mediated lactate influx and intracellular lactate metabolism are important for tumor-infiltrating Treg cells to sustain their suppressive activity (63), while high glucose levels dampen their function and stability (64). A summary of the effects of glycolysis, lactate and OXPHOS on cancer and immune cells are described in Figure 3.

Natural killer cells

In addition to T cells, NK cell activity is also directly and indirectly affected by high level of lactate (65). Lactate acidosis restricts the cytolytic functions of natural killer (NK) cells by inhibition of nuclear factor of activated T cells (NFAT), reducing IFNγ production and downregulation of peroxisome proliferator-activated receptor g (PPARg) (66).Tumor derived lactate has also been shown to inhibit cytotoxic NK cell activity by inhibiting the

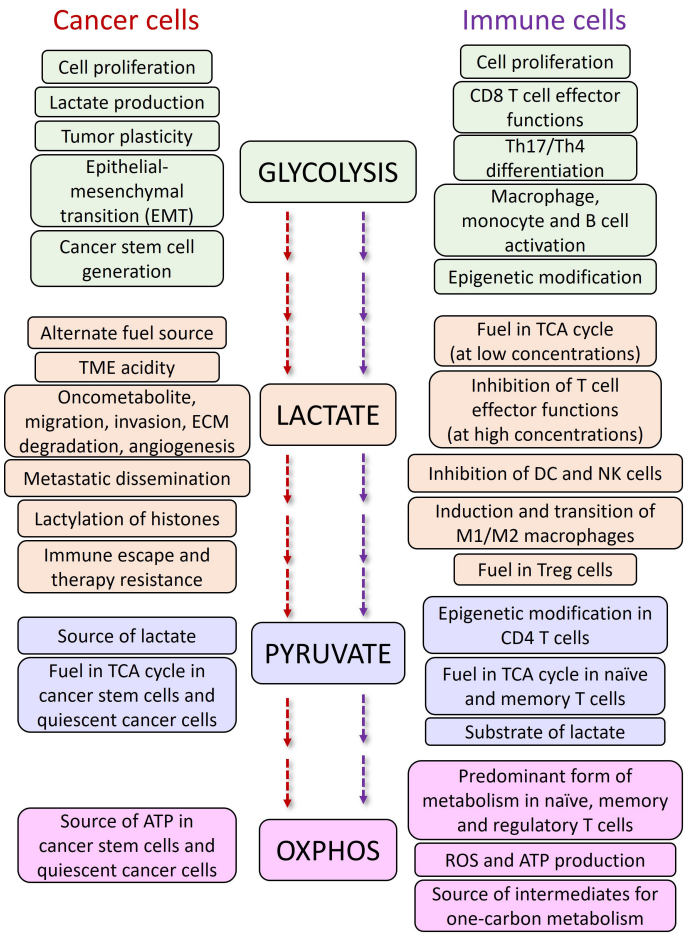

FIGURE 3
The functions of glycolysis and OXPHOS pathways and, lactate and pyruvate metabolites in cancer and immune cells.

production of perforin and granzyme or indirectly by enhancing the numbers of myeloid derived suppressor cells that suppress the functionality of NK cells (67). Interestingly, tissue resident NK cells from liver have been found to have increased sensitivity to lactate that impairs the mitochondrial functions leading to cell apoptosis (65). Hence, lactate in NK cells seems to have a multipronged strategy all culminating in suppression of NK cell activity.

Monocytes, dendritic cells and macrophages

There are two different reports about the effect of lactic acidosis on monocytes: Lactate induces monocyte differentiation to immunosuppressive dendritic cells or macrophages (68, 69), but huge amount of lactate may also delays the differentiation of monocytes into dendritic cells (70). Lactate also indirectly can be sensed by G-protein-coupled receptor 81 (GPR81, also termed hydroxycarboxylic acid receptor 1 or HCAR1) on the surface of plasmacytoid dendritic cells (pDCs). This interaction triggers calcineurin phosphatase signaling, leading to enhancement of free cytosolic Ca^{2+} and deduction of pDC function (71). Additionally, MCT1-mediated lactate influx partially contributes to the inhibition of pDC activation (72). Tumor derived lactate also increases M2 macrophage polarization mediated by ERK-STAT3 signaling pathway (73), HIF-1a stabilization (74), and G-protein-coupled receptor 132 (GPR132) activity (75). Lactate binding to the surface GPR132 in macrophages leads to induction of cyclic AMP (cAMP) and cAMP early repressor (ICER), thus increasing the expression of arginine-metabolizing enzyme arginase 1 (ARG1), VEGF (76), and HIF-1a (77), and the production of pro-angiogenic phenotype of macrophages (78). Lactate acidosis also reduces the function of M1 macrophages by downregulation of IL-6, iNOS, and CCL2 (79). Epigenetic modification mediated by high levels of intracellular lactate are also demonstrated in macrophages. Lactate inhibits NAD^+-independent histone deacetylase and enhances histone lysine residue lactylation in macrophages (80). Histone lactylation level has been shown to have a direct correlation with oncogenic factors generation in M2 macrophages (81). In addition to its signaling effects, lactate acts as a direct Carbon source in tumor associated macrophages (TAMs), directly derogating the $MHCII^{hi}$ TAM subset thus stimulating the T cell suppression by transcriptionally stabilizing the $MHCII^{lo}$ TAM subset (82).

Targeting glycolysis in solid tumors for therapy enhancement

Given the central role of glucose mediated metabolism in cancer and immune cells (3), to use glycolysis inhibitors to impede the growth and spread of cancer cells, which could potentially help to improve the efficacy of cancer immunotherapy treatments are being developed (83, 84). Both, the process of glucose utilization and the production of lactate through glycolysis are high in cancer cells, resulting in higher turnaround of the proteins, enzymes, and metabolites passing through the pathway, thus making these proteins lucrative targets for the diagnosis and treatment of various cancers (85). There are various drugs which target glucose transferase1 (GLUT1) such as BAY-876, ritonavir, genistein, STF-31 and WZB117. These drugs inhibit glucose uptake into cancer cells and lead to cell death. After uptake of glucose, it is phosphorylated in a rate limiting reaction by hexokinase (HK), making HK another target for cancer therapy. Several drugs have been developed for inhibition of this enzyme, such as 2-deoxy-D-glucose (2-DG) and 3-BrPA. Another glycolytic enzyme with potential for targeting in cancer treatment is PFK which creates fructose-1,6-bisphosphate from substrate fructose-6-phosphate. The main PFK inhibitors include 3-(3-pyridinyl)-1-(4-pyridinyl)-2-propen-1-one (3PO), 1-(4-pyridinyl)-3-(2-quinolinyl)-2-propen-1-one (PFK15), PFK158, YN1, and N4A. Since lactate has important effects in favor of tumor growth including acidification of tumor microenvironment and triggering immune suppressive signals, various inhibitor compounds targeting LDH such as galloflavin (86), FX-11, gossypol (87, 88), NCI-006 (89), N-hydroxyindole-based inhibitors (90) and pyrazole based inhibitors (91)have been developed (Figure 4). However, recent demonstration of solid tumors downregulating the energetically expensive tissue specific functions such as glycolysis to allow uncontrolled growth despite a limited supply of ATP (92) should add a word of caution while choosing the drug targets. Moreover, targeting of lactate transporters with drugs such as cinnamate and AZD3965 can stop cancer cell proliferation (93, 94).

As explained before, lactate transporter inhibition diminishes cancer cells proliferation. On the other hand, inhibiting MCT protects immune cells from the risk of intracellular lactate accumulation. It has also been shown that knockout of MCT1 represses the function of immunosuppressive Treg cells and make the tumor environment conducive for antitumor immunity (61).

In addition to lactate, the accumulation of succinate is detected in the tumor microenvironment of some tumors. Tumor derived succinate impedes degranulation and cytokine (such as interferon-γ (IFN-γ)) secretion in both CD4 and CD8 T cells. In this situation T cells uptake more succinate (partly by MCT1) and accumulation of succinate into the cells inhibits succinyl coenzyme A synthetase activity and consequently, glucose flux through the tricarboxylic acid cycle is disturbed (95).

There are only a few studies that explored the combination of glycolysis metabolism targeted therapy with cancer immunotherapy.

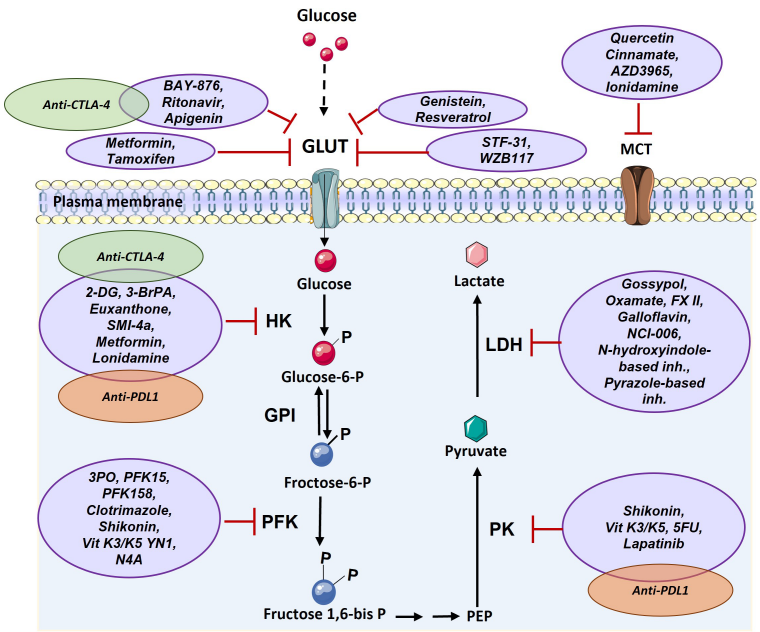

FIGURE 4
Targeting glucose transporter, critical glycolytic enzymes, and lactate transporter in cancer therapy. GLUT can be targeted *via* various components such as Ritonavir, Apigenin, Metformin, Tamoxifen, Genistein, Resveratrol, STF-31, and WZB117. HK enzyme can be inhibited by 2-DG, 3-BrPA, Euxanthone, SMI-4a, Metformin, Lonidamine. PFK enzyme is targeted by 3PO, PFK15, PFK158, Clotrimazole, Shikonin, Vit K3/K5 YN1, and N4A. PK enzyme can be inhibited by Shikonin, Vit K3/K5, 5FU, and Lapatinib. LDH enzyme is targeted by Gossypol, Oxamate, FX II, Galloflavin, NCI-006, N-hydroxyindole-based inhibitors, Pyrazole-based inhibitors and MCT transporter can be inhibited by Quercetin, Cinnamate, AZD3965, and Ionidamine. There are a few combination therapy with metabolism targeting and immunotherapy that are shown by green (anti-CTLA-4) and orange (anti-PD1) (2-DG: 2-Deoxy- d-glucose, 3-BrPA: 3-bromopyruvate, 5FU: Fluorouracil, GLUT: Glucose Transporter, GPI: Glucose-6-phosphate isomerase, HK: Hexokinase, LDH: Lactate dehydrogenase, MCT: Monocarboxylate Transporter, PEP: Phosphoenolpyruvate, PFK: phosphofructokinase, PK: Pyruvate kinase, Vit K: Vitamin K).

Genetic inhibition of glycolysis in tumor cells has been found to augment checkpoint blocker therapy (96). Accordingly, combination of 2-DG, BAY-876, and chloroquine and a glycolysis inhibitor nano-drug (D/B/CQ@ZIF-8@CS) has been shown to improve anti-CTLA-4 immunotherapy by reducing Treg metabolic fitness (97). Combination of Lonidamine, with anti-PD-1 therapy also has been shown to improve the therapeutic outcomes in glioblastoma mice model (98). The efficiency of anti-PD-1/PD-L1 therapy is also increased in pancreatic ductal adenocarcinoma cells (PDAC) which have deletion of PKM2 (99) implying strategies downregulating PKM2 in PDAC may synergize with ICI using anti-PD1/PD-L1.

Various therapeutic interventions may have differential effects on the ability of immune cells, particularly the effector T cells to migrate, infiltrate, and kill the tumor cells (96). Application of inhibitors of glycolysis or transport molecules such as MCT and GLUT may result in decreased lactate levels in the TME that would tend to alleviate the lactate mediated immune suppression and may also enhance immune cell infiltration (100). However, given the complexity of the TME and presence of tumor and immune cells in close proximation, it will be important to devise strategies for differential targeting of tumor and immune cells. One alternate can be ex-vivo treatment of immune cells for increasing the efficacy of adoptive cell therapy or CAR-T cell therapy. For example, culturing cytotoxic T cells or CAR-T cells under hypoxic conditions (101), or reducing culture conditions (102), or in the presence of appropriate inhibitors such as adenosine receptor inhibitors (103) seem to enhance the anti-tumor potential of these cells.

Conclusion

Glycolysis is central to cell metabolism. However, its role goes far beyond the energy channel of cells. Various metabolites passing through the glycolytic pathway not only help in ATP synthesis but also in generation of reducing powers such as NAD. These reducing powers and other intermediates generated during the process of glycolysis are involved in cell signaling. Interestingly, these intermediates seem to be utilized differentially in tumor and immune cells. Thus, a thorough understanding of the regulatory factors that control a continued flow of energy and of various metabolites in cancer and immune cells will be helpful in devising differential targeting strategies. Such differential targeting strategies will be especially important in complex tumor microenvironment wherein tumor and immune cells reside in close contact, and it is difficult to target one cell type over the other. For example, lactate has been traditionally recognized as a tumor cell derived waste product and an oncometabolite that contributes to suppression of immune functions. However, it has become amply clear that in addition to being an immune suppressant, lactate also functions as an energy source in immune cells as at low concentrations, lactate can fuel the TCA cycle and can be used preferentially through TCA cycle. Hence, the role of metabolites of the glycolytic pathway, particularly the lactate is highly context dependent and may potentially be used for enhancement of the efficiency of cancer immunotherapy.

Author contributions

SM and VV conceptualize and wrote the manuscript. Both authors confirm reading and approving the contents of the present manuscript. All authors contributed to the article and approved the submitted version.

Funding

VV acknowledge receiving the ACS-IRG Grant# 129819-IRG-21-049-61-IRG134 that in part enabled generation of this manuscript.

Conflict of interest

The authors declare that the research was conducted in the absence of any commercial or financial relationships that could be construed as a potential conflict of interest.

Publisher's note

All claims expressed in this article are solely those of the authors and do not necessarily represent those of their affiliated organizations, or those of the publisher, the editors and the reviewers. Any product that may be evaluated in this article, or claim that may be made by its manufacturer, is not guaranteed or endorsed by the publisher.

References

1. Poulsen RC, Knowles HJ, Carr AJ, Hulley PA. Cell differentiation versus cell death: extracellular glucose is a key determinant of cell fate following oxidative stress exposure. *Cell Death Dis* (2014) 5:e1074. doi: 10.1038/cddis.2014.52

2. Palmer CS, Ostrowski M, Balderson B, Christian N, Crowe SM. Glucose metabolism regulates T cell activation, differentiation, and functions. *Front Immunol* (2015) 6:1. doi: 10.3389/fimmu.2015.00001

3. Kao KC, Vilbois S, Tsai CH, Ho PC. Metabolic communication in the tumour-immune microenvironment. *Nat Cell Biol* (2022) 24:1574–83. doi: 10.1038/s41556-022-01002-x

4. Zhao S, Peralta RM, Avina-Ochoa N, Delgoffe GM, Kaech SM. Metabolic regulation of T cells in the tumor microenvironment by nutrient availability and diet. *Semin Immunol* (2021) 52:101485. doi: 10.1016/j.smim.2021.101485

5. Stewart EJ, Madden R, Paul G, Taddei F. Aging and death in an organism that reproduces by morphologically symmetric division. *PloS Biol* (2005) 3:e45. doi: 10.1371/journal.pbio.0030045

6. Wilson DF, Matschinsky FM. Metabolic homeostasis in life as we know it: its origin and thermodynamic basis. *Front Physiol* (2021) 12:658997. doi: 10.3389/fphys.2021.658997

7. Jiang S, Liu H, Li C. Dietary regulation of oxidative stress in chronic metabolic diseases. *Foods* (2021) 10(8):1854. doi: 10.3390/foods10081854

8. Ponisovskiy MR. Cancer metabolism and the warburg effect as anabolic process outcomes of oncogene operation. *Crit Rev Eukaryot Gene Expr* (2010) 20:325–39. doi: 10.1615/CritRevEukarGeneExpr.v20.i4.40

9. Deberardinis RJ, Chandel NS. Fundamentals of cancer metabolism. *Sci Adv* (2016) 2:e1600200. doi: 10.1126/sciadv.1600200

10. Liebermeister W, Noor E, Flamholz A, Davidi D, Bernhardt J, Milo R, et al. Visual account of protein investment in cellular functions. *Proc Natl Acad Sci USA* (2014) 111(23):8488–93. doi: 10.1073/pnas.1314810111

11. Yu R, Campbell K, Pereira R, Bjorkeroth J, Qi Q, Vorontsov E, et al. Nitrogen limitation reveals large reserves in metabolic and translational capacities of yeast. *Nat Commun* (2020) 11:1881. doi: 10.1038/s41467-020-15749-0

12. Noor E, Eden E, Milo R, Alon U. Central carbon metabolism as a minimal biochemical walk between precursors for biomass and energy. *Mol Cell* (2010) 39:809–20. doi: 10.1016/j.molcel.2010.08.031

13. Fendt SM, Buescher JM, Rudroff F, Picotti P, Zamboni N, Sauer U. Tradeoff between enzyme and metabolite efficiency maintains metabolic homeostasis upon perturbations in enzyme capacity. *Mol Syst Biol* (2010) 6:356. doi: 10.1038/msb.2010.11

14. Keibler MA, Wasylenko TM, Kelleher JK, Iliopoulos O, Vander Heiden MG, Stephanopoulos G. Metabolic requirements for cancer cell proliferation. *Cancer Metab* (2016) 4:16. doi: 10.1186/s40170-016-0156-6

15. Momayyezi M, Borsuk AM, Brodersen CR, Gilbert ME, Theroux-Rancourt G, Kluepfel DA, et al. Desiccation of the leaf mesophyll and its implications for CO(2) diffusion and light processing. *Plant Cell Environ* (2022) 45:1362–81. doi: 10.1111/pce.14287

16. Da Veiga Moreira J, Schwartz L, Jolicoeur M. Targeting mitochondrial singlet oxygen dynamics offers new perspectives for effective metabolic therapies of cancer. *Front Oncol* (2020) 10:573399. doi: 10.3389/fonc.2020.573399

17. Xu Y, Xue D, Bankhead A3rd, Neamati N. Why all the fuss about oxidative phosphorylation (OXPHOS)? *J Med Chem* (2020) 63:14276–307. doi: 10.1021/acs.jmedchem.0c01013

18. Roberts DJ, Miyamoto S. Hexokinase II integrates energy metabolism and cellular protection: akting on mitochondria and TORCing to autophagy. *Cell Death Differ* (2015) 22:248–57. doi: 10.1038/cdd.2014.173

19. Mehta MM, Weinberg SE, Steinert EM, Chhiba K, Martinez CA, Gao P, et al. Hexokinase 2 is dispensable for T cell-dependent immunity. *Cancer Metab* (2018) 6:10. doi: 10.1186/s40170-018-0184-5

20. Patra KC, Wang Q, Bhaskar PT, Miller L, Wang Z, Wheaton W, et al. Hexokinase 2 is required for tumor initiation and maintenance and its systemic deletion is therapeutic in mouse models of cancer. *Cancer Cell* (2013) 24:213–28. doi: 10.1016/j.ccr.2013.06.014

21. Yi W, Clark PM, Mason DE, Keenan MC, Hill C, Goddard WA3rd, et al. Phosphofructokinase 1 glycosylation regulates cell growth and metabolism. *Science* (2012) 337:975–80. doi: 10.1126/science.1222278

22. Bosca L, Mojena M, Ghysdael J, Rousseau GG, Hue L. Expression of the v-src or v-fps oncogene increases fructose 2,6-bisphosphate in chick-embryo fibroblasts. novel mechanism for the stimulation of glycolysis by retroviruses. *Biochem J* (1986) 236:595–9. doi: 10.1042/bj2360595

23. Kole HK, Resnick RJ, Van Doren M, Racker E. Regulation of 6-phosphofructo-1-kinase activity in ras-transformed rat-1 fibroblasts. *Arch Biochem Biophys* (1991) 286:586–90. doi: 10.1016/0003-9861(91)90084-V

24. Yang Z, Fujii H, Mohan SV, Goronzy JJ, Weyand CM. Phosphofructokinase deficiency impairs ATP generation, autophagy, and redox balance in rheumatoid arthritis T cells. *J Exp Med* (2013) 210:2119–34. doi: 10.1084/jem.20130252

25. Scherlinger M, Pan W, Hisada R, Boulougoura A, Yoshida N, Vukelic M, et al. Phosphofructokinase p fine-tunes T regulatory cell metabolism, function, and stability in systemic autoimmunity. *Sci Adv* (2022) 8:eadc9657. doi: 10.1126/sciadv.adc9657

26. Angiari S, Runtsch MC, Sutton CE, Palsson-Mcdermott EM, Kelly B, Rana N, et al. Pharmacological activation of pyruvate kinase M2 inhibits CD4(+) T cell pathogenicity and suppresses autoimmunity. *Cell Metab* (2020) 31:391–405.e398. doi: 10.1016/j.cmet.2019.10.015

27. Palsson-Mcdermott EM, Curtis AM, Goel G, Lauterbach MA, Sheedy FJ, Gleeson LE, et al. Pyruvate kinase M2 regulates hif-1alpha activity and IL-1beta induction and is a critical determinant of the warburg effect in LPS-activated macrophages. *Cell Metab* (2015) 21:65–80. doi: 10.1016/j.cmet.2014.12.005

28. Bricker DK, Taylor EB, Schell JC, Orsak T, Boutron A, Chen YC, et al. A mitochondrial pyruvate carrier required for pyruvate uptake in yeast, drosophila, and humans. *Science* (2012) 337:96–100. doi: 10.1126/science.1218099

29. Herzig S, Raemy E, Montessuit S, Veuthey JL, Zamboni N, Westermann B, et al. Identification and functional expression of the mitochondrial pyruvate carrier. *Science* (2012) 337:93–6. doi: 10.1126/science.1218530

30. Phan AT, Goldrath AW, Glass CK. Metabolic and epigenetic coordination of T cell and macrophage immunity. *Immunity* (2017) 46:714–29. doi: 10.1016/j.immuni.2017.04.016

31. Wenes M, Jaccard A, Wyss T, Maldonado-Perez N, Teoh ST, Lepez A, et al. The mitochondrial pyruvate carrier regulates memory T cell differentiation and antitumor function. *Cell Metab* (2022) 34:731–746.e739. doi: 10.1016/j.cmet.2022.03.013

32. Elia I, Rowe JH, Johnson S, Joshi S, Notarangelo G, Kurmi K, et al. Tumor cells dictate anti-tumor immune responses by altering pyruvate utilization and succinate signaling in CD8(+) T cells. *Cell Metab* (2022) 34:1137–1150.e1136. doi: 10.1016/j.cmet.2022.06.008

33. Thabault L, Liberelle M, Koruza K, Yildiz E, Joudiou N, Messens J, et al. Discovery of a novel lactate dehydrogenase tetramerization domain using epitope mapping and peptides. *J Biol Chem* (2021) 296:100422. doi: 10.1016/j.jbc.2021.100422

34. Pasti AP, Rossi V, Di Stefano G, Brigotti M, Hochkoeppler A. Human lactate dehydrogenase a undergoes allosteric transitions under pH conditions inducing the dissociation of the tetrameric enzyme. *Biosci Rep* (2022) 42(1):BSR20212654. doi: 10.1042/BSR20212654

35. Valvona CJ, Fillmore HL, Nunn PB, Pilkington GJ. The regulation and function of lactate dehydrogenase a: therapeutic potential in brain tumor. *Brain Pathol* (2016) 26:3–17. doi: 10.1111/bpa.12299

36. Jungmann RA, Huang D, Tian D. Regulation of LDH-a gene expression by transcriptional and posttranscriptional signal transduction mechanisms. *J Exp Zool* (1998) 282:188–95. doi: 10.1002/(SICI)1097-010X(199809/10)282:1/2<188::AID-JEZ21>3.0.CO;2-P

37. Farhana A, Lappin SL. Biochemistry, lactate dehydrogenase. In: *StatPearls*. Treasure Island (FL (2022).

38. Wang JX, Choi SYC, Niu X, Kang N, Xue H, Killam J, et al. Lactic acid and an acidic tumor microenvironment suppress anticancer immunity. *Int J Mol Sci* (2020) 21(21):8363. doi: 10.3390/ijms21218363

39. Li X, Yang Y, Zhang B, Lin X, Fu X, An Y, et al. Lactate metabolism in human health and disease. *Signal Transduct Target Ther* (2022) 7:305. doi: 10.1038/s41392-022-01151-3

40. Kaymak I, Luda KM, Duimstra LR, Ma EH, Longo J, Dahabieh MS, et al. Carbon source availability drives nutrient utilization in CD8(+) T cells. *Cell Metab* (2022) 34:1298–1311.e1296. doi: 10.1016/j.cmet.2022.07.012

41. Chen YJ, Mahieu NG, Huang X, Singh M, Crawford PA, Johnson SL, et al. Lactate metabolism is associated with mammalian mitochondria. *Nat Chem Biol* (2016) 12:937–43. doi: 10.1038/nchembio.2172

42. Glancy B, Kane DA, Kavazis AN, Goodwin ML, Willis WT, Gladden LB. Mitochondrial lactate metabolism: history and implications for exercise and disease. *J Physiol* (2021) 599:863–88. doi: 10.1113/JP278930

43. Hashimoto T, Hussien R, Brooks GA. Colocalization of MCT1, CD147, and LDH in mitochondrial inner membrane of L6 muscle cells: evidence of a mitochondrial lactate oxidation complex. *Am J Physiol Endocrinol Metab* (2006) 290:E1237–1244. doi: 10.1152/ajpendo.00594.2005

44. Lum JJ, Bui T, Gruber M, Gordan JD, Deberardinis RJ, Covello KL, et al. The transcription factor HIF-1alpha plays a critical role in the growth factor-dependent regulation of both aerobic and anaerobic glycolysis. *Genes Dev* (2007) 21:1037–49. doi: 10.1101/gad.1529107

45. Masoud GN, Li W. HIF-1alpha pathway: role, regulation and intervention for cancer therapy. *Acta Pharm Sin B* (2015) 5:378–89. doi: 10.1016/j.apsb.2015.05.007

46. Brown TP, Ganapathy V. Lactate/GPR81 signaling and proton motive force in cancer: role in angiogenesis, immune escape, nutrition, and warburg phenomenon. *Pharmacol Ther* (2020) 206:107451. doi: 10.1016/j.pharmthera.2019.107451

47. Certo M, Tsai CH, Pucino V, Ho PC, Mauro C. Lactate modulation of immune responses in inflammatory versus tumour microenvironments. *Nat Rev Immunol* (2021) 21:151–61. doi: 10.1038/s41577-020-0406-2

48. Wang ZH, Peng WB, Zhang P, Yang XP, Zhou Q. Lactate in the tumour microenvironment: from immune modulation to therapy. *EBioMedicine* (2021) 73:103627. doi: 10.1016/j.ebiom.2021.103627

49. Payen VL, Mina E, Van Hee VF, Porporato PE, Sonveaux P. Monocarboxylate transporters in cancer. *Mol Metab* (2020) 33:48–66. doi: 10.1016/j.molmet.2019.07.006

50. Corbet C, Feron O. Tumour acidosis: from the passenger to the driver's seat. *Nat Rev Cancer* (2017) 17:577–93. doi: 10.1038/nrc.2017.77

51. Ishihara S, Hata K, Hirose K, Okui T, Toyosawa S, Uzawa N, et al. The lactate sensor GPR81 regulates glycolysis and tumor growth of breast cancer. *Sci Rep* (2022) 12:6261. doi: 10.1038/s41598-022-10143-w

52. Lundo K, Trauelsen M, Pedersen SF, Schwartz TW. Why warburg works: lactate controls immune evasion through GPR81. *Cell Metab* (2020) 31:666–8. doi: 10.1016/j.cmet.2020.03.001

53. Hensley CT, Faubert B, Yuan Q, Lev-Cohain N, Jin E, Kim J, et al. Metabolic heterogeneity in human lung tumors. *Cell* (2016) 164:681–94. doi: 10.1016/j.cell.2015.12.034

54. Lim AR, Rathmell WK, Rathmell JC. The tumor microenvironment as a metabolic barrier to effector T cells and immunotherapy. *Elife* (2020) 9:e55185. doi: 10.7554/eLife.55185

55. Mendler AN, Hu B, Prinz PU, Kreutz M, Gottfried E, Noessner E. Tumor lactic acidosis suppresses CTL function by inhibition of p38 and JNK/c-jun activation. *Int J Cancer* (2012) 131:633–40. doi: 10.1002/ijc.26410

56. Hermans D, Gautam S, Garcia-Canaveras JC, Gromer D, Mitra S, Spolski R, et al. Lactate dehydrogenase inhibition synergizes with IL-21 to promote CD8(+) T cell stemness and antitumor immunity. *Proc Natl Acad Sci USA* (2020) 117:6047–55. doi: 10.1073/pnas.1920413117

57. Feng Q, Liu Z, Yu X, Huang T, Chen J, Wang J, et al. Lactate increases stemness of CD8 + T cells to augment anti-tumor immunity. *Nat Commun* (2022) 13:4981. doi: 10.1038/s41467-022-32521-8

58. Cantor JR, Abu-Remaileh M, Kanarek N, Freinkman E, Gao X, Louissaint AJr., et al. Physiologic medium rewires cellular metabolism and reveals uric acid as an endogenous inhibitor of UMP synthase. *Cell* (2017) 169:258–272.e217. doi: 10.1016/j.cell.2017.03.023

59. Ma EH, Verway MJ, Johnson RM, Roy DG, Steadman M, Hayes S, et al. Metabolic profiling using stable isotope tracing reveals distinct patterns of glucose utilization by physiologically activated CD8(+) T cells. *Immunity* (2019) 51:856–870.e855. doi: 10.1016/j.immuni.2019.09.003

60. Angelin A, Gil-De-Gomez L, Dahiya S, Jiao J, Guo L, Levine MH, et al. Foxp3 reprograms T cell metabolism to function in low-glucose, high-lactate environments. *Cell Metab* (2017) 25:1282–1293.e1287. doi: 10.1016/j.cmet.2016.12.018

61. Watson MJ, Vignali PDA, Mullett SJ, Overacre-Delgoffe AE, Peralta RM, Grebinoski S, et al. Metabolic support of tumour-infiltrating regulatory T cells by lactic acid. *Nature* (2021) 591:645–51. doi: 10.1038/s41586-020-03045-2

62. Gu J, Zhou J, Chen Q, Xu X, Gao J, Li X, et al. Tumor metabolite lactate promotes tumorigenesis by modulating MOESIN lactylation and enhancing TGF-beta signaling in regulatory T cells. *Cell Rep* (2022) 39:110986. doi: 10.1016/j.celrep.2022.110986

63. Multhoff G, Vaupel P. Lactate-avid regulatory T cells: metabolic plasticity controls immunosuppression in tumour microenvironment. *Signal Transduct Target Ther* (2021) 6:171. doi: 10.1038/s41392-021-00598-0

64. Villa M, O'sullivan D, Pearce EL. Glucose makes t(reg) lose their temper. *Cancer Cell* (2021) 39:460–2. doi: 10.1016/j.ccell.2021.03.001

65. Dodard G, Tata A, Erick TK, Jaime D, Miah SMS, Quatrini L, et al. Inflammation-induced lactate leads to rapid loss of hepatic tissue-resident NK cells. *Cell Rep* (2020) 32:107855. doi: 10.1016/j.celrep.2020.107855

66. Xie D, Zhu S, Bai L. Lactic acid in tumor microenvironments causes dysfunction of NKT cells by interfering with mTOR signaling. *Sci China Life Sci* (2016) 59:1290–6. doi: 10.1007/s11427-016-0348-7

67. Husain Z, Huang Y, Seth P, Sukhatme VP. Tumor-derived lactate modifies antitumor immune response: effect on myeloid-derived suppressor cells and NK cells. *J Immunol* (2013) 191:1486–95. doi: 10.4049/jimmunol.1202702

68. Gottfried E, Kunz-Schughart LA, Ebner S, Mueller-Klieser W, Hoves S, Andreesen R, et al. Tumor-derived lactic acid modulates dendritic cell activation and antigen expression. *Blood* (2006) 107:2013–21. doi: 10.1182/blood-2005-05-1795

69. Sangsuwan R, Thuamsang B, Pacifici N, Allen R, Han H, Miakicheva S, et al. Lactate exposure promotes immunosuppressive phenotypes in innate immune cells. *Cell Mol Bioeng* (2020) 13:541–57. doi: 10.1007/s12195-020-00652-x

70. Nasi A, Rethi B. Disarmed by density: a glycolytic break for immunostimulatory dendritic cells? *Oncoimmunology* (2013) 2:e26744. doi: 10.4161/onci.26744

71. Monti M, Vescovi R, Consoli F, Farina D, Moratto D, Berruti A, et al. Plasmacytoid dendritic cell impairment in metastatic melanoma by lactic acidosis. *Cancers (Basel)* (2020) 12(8):2085. doi: 10.3390/cancers12082085

72. Raychaudhuri D, Bhattacharya R, Sinha BP, Liu CSC, Ghosh AR, Rahaman O, et al. Lactate induces pro-tumor reprogramming in intratumoral plasmacytoid dendritic cells. *Front Immunol* (2019) 10:1878. doi: 10.3389/fimmu.2019.01878

73. Papa S, Choy PM, Bubici C. The ERK and JNK pathways in the regulation of metabolic reprogramming. *Oncogene* (2019) 38:2223–40. doi: 10.1038/s41388-018-0582-8

74. Taylor CT, Scholz CC. The effect of HIF on metabolism and immunity. *Nat Rev Nephrol* (2022) 18:573–87. doi: 10.1038/s41581-022-00587-8

75. Chen P, Zuo H, Xiong H, Kolar MJ, Chu Q, Saghatelian A, et al. Gpr132 sensing of lactate mediates tumor-macrophage interplay to promote breast cancer metastasis. *Proc Natl Acad Sci USA* (2017) 114:580–5. doi: 10.1073/pnas.1614035114

76. Colegio OR, Chu NQ, Szabo AL, Chu T, Rhebergen AM, Jairam V, et al. Functional polarization of tumour-associated macrophages by tumour-derived lactic acid. *Nature* (2014) 513:559–63. doi: 10.1038/nature13490

77. Zhang L, Li S. Lactic acid promotes macrophage polarization through MCT-HIF1alpha signaling in gastric cancer. *Exp Cell Res* (2020) 388:111846. doi: 10.1016/j.yexcr.2020.111846

78. Kes MMG, Van Den Bossche J, Griffioen AW, Huijbers EJM. Oncometabolites lactate and succinate drive pro-angiogenic macrophage response in tumors. *Biochim Biophys Acta Rev Cancer* (2020) 1874:188427. doi: 10.1016/j.bbcan.2020.188427

79. Dichtl S, Lindenthal L, Zeitler L, Behnke K, Schlosser D, Strobl B, et al. Lactate and IL6 define separable paths of inflammatory metabolic adaptation. *Sci Adv* (2021) 7: eabg3505. doi: 10.1126/sciadv.abg3505

80. Zhang D, Tang Z, Huang H, Zhou G, Cui C, Weng Y, et al. Metabolic regulation of gene expression by histone lactylation. *Nature* (2019) 574:575–80. doi: 10.1038/s41586-019-1678-1

81. Zhou HC, Xin-Yan Y, Yu WW, Liang XQ, Du XY, Liu ZC, et al. Lactic acid in macrophage polarization: the significant role in inflammation and cancer. *Int Rev Immunol* (2022) 41:4–18. doi: 10.1080/08830185.2021.1955876

82. Geeraerts X, Fernandez-Garcia J, Hartmann FJ, De Goede KE, Martens L, Elkrim Y, et al. Macrophages are metabolically heterogeneous within the tumor microenvironment. *Cell Rep* (2021) 37:110171. doi: 10.1016/j.celrep.2021.110171

83. Caslin HL, Abebayehu D, Abdul Qayum A, Haque TT, Taruselli MT, Paez PA, et al. Lactic acid inhibits lipopolysaccharide-induced mast cell function by limiting glycolysis and ATP availability. *J Immunol* (2019) 203:453–64. doi: 10.4049/jimmunol.1801005

84. Rostamian H, Khakpoor-Koosheh M, Jafarzadeh L, Masoumi E, Fallah-Mehrjardi K, Tavassolifar MJ, et al. Restricting tumor lactic acid metabolism using dichloroacetate improves T cell functions. *BMC Cancer* (2022) 22:39. doi: 10.1186/s12885-021-09151-2

85. Varghese E, Samuel SM, Liskova A, Samec M, Kubatka P, Busselberg D. Targeting glucose metabolism to overcome resistance to anticancer chemotherapy in breast cancer. *Cancers (Basel)* (2020) 12(8):2252. doi: 10.3390/cancers12082252

86. Manerba M, Vettraino M, Fiume L, Di Stefano G, Sartini A, Giacomini E, et al. Galloflavin (CAS 568-80-9): a novel inhibitor of lactate dehydrogenase. *ChemMedChem* (2012) 7:311–7. doi: 10.1002/cmdc.201100471

87. Vander Jagt DL, Deck LM, Royer RE. Gossypol: prototype of inhibitors targeted to dinucleotide folds. *Curr Med Chem* (2000) 7:479–98. doi: 10.2174/0929867003375119

88. Yu Y, Deck JA, Hunsaker LA, Deck LM, Royer RE, Goldberg E, et al. Selective active site inhibitors of human lactate dehydrogenases A4, B4, and C4. *Biochem Pharmacol* (2001) 62:81–9. doi: 10.1016/S0006-2952(01)00636-0

89. Oshima N, Ishida R, Kishimoto S, Beebe K, Brender JR, Yamamoto K, et al. Dynamic imaging of LDH inhibition in tumors reveals rapid *In vivo* metabolic rewiring and vulnerability to combination therapy. *Cell Rep* (2020) 30:1798–1810.e1794. doi: 10.1016/j.celrep.2020.01.039

90. Granchi C, Roy S, Giacomelli C, Macchia M, Tuccinardi T, Martinelli A, et al. Discovery of n-hydroxyindole-based inhibitors of human lactate dehydrogenase isoform a (LDH-a) as starvation agents against cancer cells. *J Med Chem* (2011) 54:1599–612. doi: 10.1021/jm101007q

91. Rai G, Brimacombe KR, Mott BT, Urban DJ, Hu X, Yang SM, et al. Discovery and optimization of potent, cell-active pyrazole-based inhibitors of lactate dehydrogenase (LDH). *J Med Chem* (2017) 60:9184–204. doi: 10.1021/acs.jmedchem.7b00941

92. Bartman CR, Weilandt DR, Shen Y, Lee WD, Han Y, Teslaa T, et al. Slow TCA flux and ATP production in primary solid tumours but not metastases. *Nature* (2023) 614:349–57. doi: 10.1038/s41586-022-05661-6

93. Murray CM, Hutchinson R, Bantick JR, Belfield GP, Benjamin AD, Brazma D, et al. Monocarboxylate transporter MCT1 is a target for immunosuppression. *Nat Chem Biol* (2005) 1:371–6. doi: 10.1038/nchembio744

94. Ovens MJ, Davies AJ, Wilson MC, Murray CM, Halestrap AP. AR-C155858 is a potent inhibitor of monocarboxylate transporters MCT1 and MCT2 that binds to an intracellular site involving transmembrane helices 7-10. *Biochem J* (2010) 425:523–30. doi: 10.1042/BJ20091515

95. Gudgeon N, Munford H, Bishop EL, Hill J, Fulton-Ward T, Bending D, et al. Succinate uptake by T cells suppresses their effector function *via* inhibition of mitochondrial glucose oxidation. *Cell Rep* (2022) 40:111193. doi: 10.1016/j.celrep.2022.111193

96. Renner K, Bruss C, Schnell A, Koehl G, Becker HM, Fante M, et al. Restricting glycolysis preserves T cell effector functions and augments checkpoint therapy. *Cell Rep* (2019) 29:135–150.e139. doi: 10.1016/j.celrep.2019.08.068

97. Luo Y, Li Y, Huang Z, Li X, Wang Y, Hou J, et al. A nanounit strategy disrupts energy metabolism and alleviates immunosuppression for cancer therapy. *Nano Lett* (2022) 22:6418–27. doi: 10.1021/acs.nanolett.2c02475

98. Guo D, Tong Y, Jiang X, Meng Y, Jiang H, Du L, et al. Aerobic glycolysis promotes tumor immune evasion by hexokinase2-mediated phosphorylation of IkappaBalpha. *Cell Metab* (2022) 34:1312–1324.e1316. doi: 10.1016/j.cmet.2022.08.002

99. Xia Q, Jia J, Hu C, Lu J, Li J, Xu H, et al. Tumor-associated macrophages promote PD-L1 expression in tumor cells by regulating PKM2 nuclear translocation in pancreatic ductal adenocarcinoma. *Oncogene* (2022) 41:865–77. doi: 10.1038/s41388-021-02133-5

100. Haas R, Smith J, Rocher-Ros V, Nadkarni S, Montero-Melendez T, D'acquisto F, et al. Lactate regulates metabolic and pro-inflammatory circuits in control of T cell migration and effector functions. *PloS Biol* (2015) 13:e1002202. doi: 10.1371/journal.pbio.1002202

101. Gropper Y, Feferman T, Shalit T, Salame TM, Porat Z, Shakhar G. Culturing CTLs under hypoxic conditions enhances their cytolysis and improves their anti-tumor function. *Cell Rep* (2017) 20:2547–55. doi: 10.1016/j.celrep.2017.08.071

102. Ghassemi S, Nunez-Cruz S, O'connor RS, Fraietta JA, Patel PR, Scholler J, et al. Reducing ex vivo culture improves the antileukemic activity of chimeric antigen receptor (CAR) T cells. *Cancer Immunol Res* (2018) 6:1100–9. doi: 10.1158/2326-6066.CIR-17-0405

103. Beavis PA, Henderson MA, Giuffrida L, Mills JK, Sek K, Cross RS, et al. Targeting the adenosine 2A receptor enhances chimeric antigen receptor T cell efficacy. *J Clin Invest* (2017) 127:929–41. doi: 10.1172/JCI89455

frontiers | Frontiers in Oncology

TYPE Mini Review
PUBLISHED 19 May 2023
DOI 10.3389/fonc.2023.1186539

OPEN ACCESS

EDITED BY
Benny Abraham Kaipparettu,
Baylor College of Medicine, United States

REVIEWED BY
Luigi Ippolito,
University of Florence, Italy

*CORRESPONDENCE
Elitsa A. Ananieva
elitsa.ananieva-stoyanova@dmu.edu

RECEIVED 14 March 2023
ACCEPTED 03 May 2023
PUBLISHED 19 May 2023

CITATION
Wetzel TJ, Erfan SC, Figueroa LD, Wheeler LM and Ananieva EA (2023) Crosstalk between arginine, glutamine, and the branched chain amino acid metabolism in the tumor microenvironment. *Front. Oncol.* 13:1186539. doi: 10.3389/fonc.2023.1186539

Crosstalk between arginine, glutamine, and the branched chain amino acid metabolism in the tumor microenvironment

Tanner J. Wetzel, Sheila C. Erfan, Lucas D. Figueroa, Leighton M. Wheeler and Elitsa A. Ananieva*

Ananieva Laboratory, Biochemistry and Nutrition Department, Des Moines University, Des Moines, IA, United States

Arginine, glutamine, and the branched chain amino acids (BCAAs) are a focus of increased interest in the field of oncology due to their importance in the metabolic reprogramming of cancer cells. In the tumor microenvironment (TME), these amino acids serve to support the elevated biosynthetic and energy demands of cancer cells, while simultaneously maintaining the growth, homeostasis, and effector function of tumor-infiltrating immune cells. To escape immune destruction, cancer cells utilize a variety of mechanisms to suppress the cytotoxic activity of effector T cells, facilitating T cell exhaustion. One such mechanism is the ability of cancer cells to overexpress metabolic enzymes specializing in the catabolism of arginine, glutamine, and the BCAAs in the TME. The action of such enzymes supplies cancer cells with metabolic intermediates that feed into the TCA cycle, supporting energy generation, or providing precursors for purine, pyrimidine, and polyamine biosynthesis. Armed with substantial metabolic flexibility, cancer cells redirect amino acids from the TME for their own advantage and growth, while leaving the local infiltrating effector T cells deprived of essential nutrients. This review addresses the metabolic pressure that cancer cells exert over immune cells in the TME by up-regulating amino acid metabolism, while discussing opportunities for targeting amino acid metabolism for therapeutic intervention. Special emphasis is given to the crosstalk between arginine, glutamine, and BCAA metabolism in affording cancer cells with metabolic dominance in the TME.

KEYWORDS

glutamine, arginine, leucine, isoleucine, valine, TME, metabolism

1 Introduction

Recent advances in our understanding of the interactions between cancer and immune cells strongly suggest the outcome of the anti-tumor T cell response is dictated by the nutrient availability and the flexibility of cancer and T cell metabolism (1–3). Cancer cells remodel their metabolism to escape immune surveillance in the TME creating nutrient-

depleted TME with dysfunctional and exhausted T cells (4, 5). Amino acid deprivation is one of the signatures of nutrient-deprived TME.

Arginine, glutamine, and the BCAAs are needed to support the increased biosynthetic and bioenergetic demands of the growing tumor and the incoming tumor infiltrating lymphocytes (TILs) (6–8). These amino acids interconnect at several metabolic steps. Breakdown of BCAAs to branched chain keto acids (BCKAs) releases glutamate, which is the precursor for glutamine (9). Glutamine is converted into ornithine, which is the precursor of arginine (10). Arginine and ornithine are precursors for polyamine synthesis, which is upregulated in cancer and immune cells (11). The depletion of glutamine, arginine or the BCAAs in the TME, alone or in combination, may impact the ability of TILs to eliminate cancer cells. However, TILs and cancer cells share similar requirements for these amino acids, creating a practical conundrum regarding nutrient-based cancer treatments (12, 13). This review provides an overview of glutamine, arginine and the BCAAs based on recent discoveries in the context of TME and the challenges associated with future therapeutic approaches.

2 Overview of arginine

2.1 Arginine uptake and metabolism in mammalian cells

Dietary intake and protein degradation are the main sources of arginine for growing children. Postnatally, humans synthesize arginine via the intestinal-renal axis. This interorgan process includes the synthesis of citrulline by the small intestines and its absorption by the kidneys where citrulline is converted to arginine by argininosuccinate synthase 1 (ASS1) and lyase (ASL) (14). Once released in the circulation, arginine enters cells preferentially via cationic amino acid transporters (CATs) existing in eight different isoforms, each with different tissue distribution (Figure 1) (15). Inside the cells, arginine is incorporated into new protein, or used for polyamine and collagen synthesis, or as an activator of the mammalian target of rapamycin (mTOR) (Figure 1) (16). Thus, arginine availability is crucial for maintaining physiological cell function.

Arginine catabolism includes the urea cycle and nitric oxide (NO) production. The urea cycle comprises five enzymatic reactions that occur within the liver. Carbamoyl phosphate synthetase 1 (CPS1) incorporates ammonia into carbamoyl phosphate followed by formation of citrulline by ornithine transcarbamoylase (OTC), and argininosuccinate by ASS1. Arginine is then produced by ASL followed by hydrolysis by arginase 1 (Arg1) to urea and ornithine (16). Arg1 is a cytosolic enzyme expressed in the liver; however, humans express mitochondrial arginase, Arg2, in most tissues (17). During NO synthesis, nitric oxide synthases (NOS) catalyze the oxidation of arginine to NO and citrulline (Figure 1) (18). Mammals have three NOS isoforms, NOS1-3. NOS2 is the inducible and prevalent isoform in immune cells (iNOS) (19). The mononuclear myeloid-derived suppressor cells (M-MDSCs) rely on iNOS to drive immunosuppression (20). High expression of iNOS in M-MDSCs cells releases NO, which is converted into reactive oxygen species (ROS) causing DNA damage and promoting tumor growth (21).

2.2 Cancer and immune cells have high demands for arginine

Arginine is conditionally essential in patients with severe trauma, compromised immune system, or cancer cachexia. Under these disease states, the demand for arginine exceeds its endogenous production (22, 23).

Defective arginine synthesis (arginine auxotrophy) is a common occurrence in cancer cells. It primarily associates with a deficiency in ASS1 (24). To persist in the TME, $CD4^+$ and $CD8^+$ T cells must maintain adequate arginine concentrations. Arg2-deficient $CD8^+$ T cells display enhanced cytotoxic activity against murine melanoma B16-OVA and colon adenocarcinoma MC38-OVA (25). The Arg2-deficent $CD8^+$ T cells have improved effector function as seen by increased perforin, granzyme, IFN-γ and IL-2 (25). Alternatively, Arg2-specific human $CD8^+$ T cells recognize Arg2-expressing regulatory T cells (Tregs), suggesting a naturally existing immunomodulatory potential of $CD8^+$ T cells to remove immune suppression by targeting Tregs with high Arg2 expression (26). Similarly, Arg1-specific T cells target Arg1-expressing myeloid cells (27). In another study, bone marrow derived dendritic cells (BMDCs) and peritoneal macrophages synthesize arginine via ASL and ASS1 and supply $CD4^+$ T cells with arginine (28). Studies with colorectal cancer patients failed to support the hypothesis that supplementation with arginine reduces the frequency of immunosuppressive M-MDSCs and polymorphonuclear myeloid-derived suppressor cells (PMN-MDSCs) but increases the frequency of $CD4^+$ T cells. Thus, while arginine deficiency contributes to immunosuppression, systemic arginine supplementation alone does not restore immune system activity (29).

The rest of the urea cycle enzymes, CPS1 and OTC are studied to a lesser extent in cancer and immune cells (30). Cancer cells upregulate CPS1 to prevent ammonia buildup. A small-molecule inhibitor of CPS1 (H3B-120) that blocks CPS1 activity in human hepatocytes might be valuable for future therapeutic approaches (31). In contrast to CPS1, OTC is downregulated in cancer cells leading to accumulation of ammonia. Cancer cells can recycle ammonia for amino and nucleic acid synthesis (32). Lastly, a virus-induced metabolic reprogramming of mouse liver, results in transcriptional repression of the OTC and ASS1 genes leading to decreased arginine but increased ornithine concentrations in the circulation, which in turn suppresses virus-specific $CD8^+$ T cells (33).

3 Overview of glutamine

3.1 Glutamine metabolism and transport in mammalian cells

Glutamine is the most abundant non-essential amino acid within human plasma. It contributes to nucleic acid (34) and

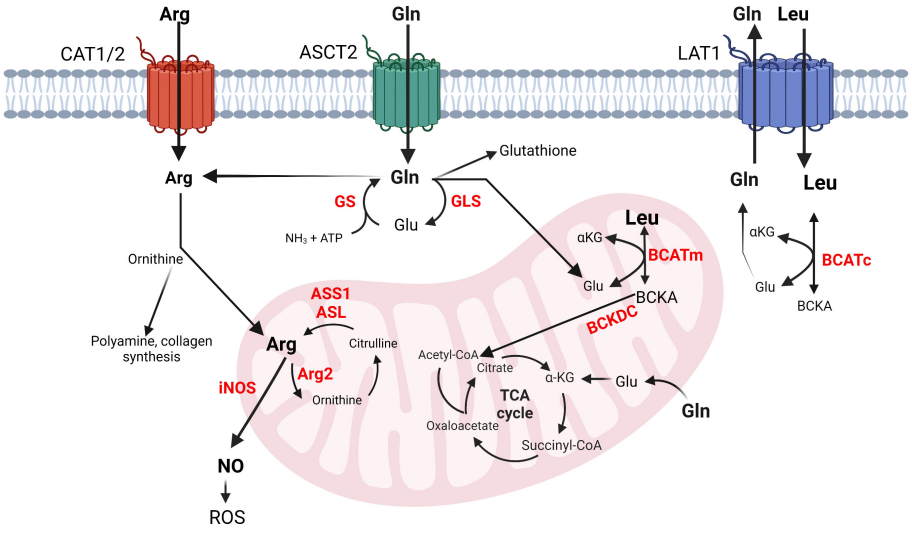

FIGURE 1
Simplified schematics of glutamine, arginine and BCAA metabolic interconnections in cancer and immune cells. Left to right: Arginine transportation is assisted by CAT. Arginine can be converted into ornithine, polyamines, collagen, or nitric oxide (NO). Glutamine enters the cells via ASCT2 and is converted into glutamate, glutathione, arginine, or nucleotides (not shown) or it may exit the cells via LAT1, which transfers leucine in exchange for glutamine. Leucine is converted into its corresponding BCKA in the cytosol or in the mitochondria. Arginine and glutamine (not shown) can be also synthesized in mitochondria. Glutamine and the BCAAs contribute to energy production by feeding into the TCA cycle. The metabolism of BCAAs is illustrated with leucine. The enzyme names are given in red. arginine, Arg, glutamine; Gln, glutamate; Glu, glutamine synthase; GS, glutaminase; GLS, arginosuccinate synthase 1; ASS1, arginosuccinate lyase; ASL, inducible nitric oxide synthase; iNOS, arginase 2; Arg2, leucine; Leu, α-ketoglutarate; αKG, cytosolic and mitochondrial branched chain aminotransferase BCATc and BCATm, branched chain keto acids; BCKAs, reactive oxygen species; ROS.

protein synthesis (35), cellular response to ROS (36), and energy production through the TCA cycle (37). It is conditionally essential for proliferating cells during high demand, where endogenous synthesis is insufficient to support cellular homeostasis (38). Glutamine synthase (GS) generates glutamine from glutamate and ammonia (34). This reaction facilitates interorgan ammonium and glutamate transport, prevents toxic encephalopathy and blood acidification (35). Glutamine hydrolysis to glutamate and ammonia is facilitated, in part, by glutaminase-1 (GLS-1) in the kidney and glutaminase-2 (GLS-2) in the liver. Different transport systems specialize in assisting glutamine import and export by the cells. Among them are the sodium-dependent transporter ASCT2 (Solute Carrier 1a5, Slc1a5) and the sodium-independent antiporter Slc3a2 that work together with Slc7a5 (also known as L-type amino acid transporter 1, LAT1) to exchange glutamine for leucine (Figure 1). These transporters have vast tissue distribution, but most notably they are overexpressed in immune and cancer cells (12, 36, 37).

3.2 Cancer and immune cells reliance on glutamine

Cancer reliance on glutamine is established in tumors throughout the body, including pancreatic (39), prostate (40), breast (41), and liver (42) cancers. Increased expression of ASCT2 and GLS are found in squamous cell carcinoma, adenocarcinoma, and neuroendocrine lung tumors (43). Such increases in the expression of ASCT2 and GLS are linked to tumors with aberrant oncogene c-MYC (40, 44). With a growing dependence on exogenous glutamine, tumor cells exhibit “glutamine addiction”. Glutamine addiction prevents cells from relying on endogenous glutamine synthesis and leads to cell death in glutamine free environments (45).

Similarly, immune cells rely on glutamine to sustain homeostasis and execute proper functions. A blockage of glutamine metabolism by DON (6-diazo-5-oxy-L-norleucine), or its modified prodrug JHU-083, causes a shift of $CD8^+$ T cells towards a long-lived memory state and increases their tumor infiltration potential and survival in the TME (46–48). A loss of GLS halts Th17 differentiation but promotes the expression of Tbet and stimulates Th1 and $CD8^+$ T cells. A long-term loss of GLS correlates with an impaired Th17 immune response, yet a transient loss of GLS promotes Th17, but restricts Th1 and $CD8^+$ T cell effector differentiation (49). In a glutamine-depleted environment, activated $CD8^+$ T cells produce significantly less IFN-γ and TNF-α (50). Selective GLS inhibition by CB-839, Telaglenastat, impairs the clonal expansion and activation of $CD8^+$ T cells in the context of combinatorial anti-PD-1 treatment (51). In glutamine-addicted clear cell renal cell carcinoma (ccRCC), tumor-associated macrophages (TAMs) shift to M2 (immunosuppressive phenotype) promoting a pro-tumor environment. Such TAMs produce IL-23 in the context of hypoxia (HIF-α activation), activating Tregs (52). Taken together, glutamine metabolism plays an important role in T cell activation and function.

4 Overview of the branched chain amino acids

4.1 BCAA metabolism and transport in mammalian cells

The BCAAs (leucine, isoleucine, and valine) are supplemented through the diet to mammalian cells. BCAAs make up ~35% of the essential amino acids in the blood (53). The BCAAs are important nutrients under physiological and pathological conditions (54). They are nitrogen donors to glutamate and alanine and stimulate protein synthesis in the muscle (55). In the brain, the BCAAs maintain the glutamate-glutamine interconversions by engaging in "glutamate-BCAA" cycles between neurons and astrocytes (56). BCAAs trigger insulin release from the pancreatic β-islets; however, chronically elevated plasma BCAAs are a common clinical finding in patients with Type 2 Diabetes and Cardiovascular Disease (56, 57).

BCAAs travel across the plasma membranes utilizing the heterodimeric transporter Slc7a5/Slc3a2. As stated earlier, this transporter works in antiport with Slc1a5 where glutamine efflux proceeds BCAA influx (6, 58). Once inside the cells, BCAAs are incorporated into protein or subjected to degradation by the cytosolic branched chain aminotransferase, BCATc (6). Alternately, the BCAAs enter the mitochondria, assisted by the Scl24a44 transporter, to become subjected to degradation by the mitochondrial BCATm (59). BCATc and BCATm catalyze the reversible transamination of the BCAAs to their corresponding BCKAs, which are subjected to irreversible oxidative decarboxylation by the mitochondrial branched chain alpha-ketoacid dehydrogenase complex (BCKDC). Following this step, each BCAA commits to their unique degradation pathways releasing propionyl-CoA, acetoacetate, or acetyl-CoA that feed into the TCA cycle or other pathways (Figure 1) (60).

4.2 BCAAs support cancer growth but they are also essential for proper immune function

BCAAs are important for sustainable tumor growth. The growing tumor obtains BCAAs from the circulation or the tissues surrounding it. Positive association between elevated plasma BCAAs and the risk of colorectal adenoma and pancreatic adenocarcinoma are reported in human patients but controversial in animal studies (61–65). High plasma concentrations of BCAAs, due to disruption in BCAA metabolism, or dietary supplementation with BCAAs, are associated with delayed onset of lymphoma, or suppression of breast cancer in mice (63, 64). In contrast, mice subjected to a diet high in BCAAs, have increased incidences of pancreatic ductal adenocarcinoma (PDAC) (66). Elevated BCAA metabolism at the BCAT step is implicated in the onset of many cancers including glioblastoma (53) myeloid leukemia (54) lymphoma (50) lung (55), gastric (56), pancreatic (57) and breast cancers (58).

To a lesser extent, BCAAs and their metabolism are studied in immune cells. Leucine is indispensable for T cell activation as insufficient leucine prevents clonal expansion to Th1, Th17 and $CD8^+$ T cells (37). Mice deficient of Slc3a2 in $Foxp3^+$ Tregs, generate a low number of $Foxp3^+$ Tregs and fail to suppress intestinal inflammation (67). $CD4^+$ T cells, deficient in BCATc or BCATm, have higher glycolytic capacity, improved oxygen consumption and increased capacity to secrete IFNγ (6, 68). Studies with BCATc in human macrophages identified a non-catalytic role for BCATc in the metabolic events associated with fragmented TCA cycle (69, 70). It remains to be further established whether the non-enzymatic function of BCATc represents a universal mechanism to regulate cellular metabolism.

5 Discussion

5.1 The interconnected network between arginine, glutamine and the BCAAs in TME

Rapidly dividing cancer cells are forced to reprogram their metabolism to ensure long term survival and metastatic growth. Their major opponents, the effector Th1 and $CD8^+$ T cells, must also reprogram metabolism to embrace the harsh TME. However, these functionally unrelated cells have similar demands for nutrients, including amino acids (71, 72).

Numerous reports have demonstrated uptake of glutamine, arginine, and the BCAAs is upregulated in cancer and activated Th1 and $CD8^+$ T cells (6, 73–75). There is a high redundancy in transport preference for these amino acids, making current approaches to target amino acid uptake particularly challenging (6, 76). Ovarian cancer cells, $CD4^+$ and $CD8^+$ memory T cells, and M0 macrophages overexpress the arginine CAT1 transporter. Silencing CAT1 in the ovarian cancer cells significantly reduces the concentration of arginine but lowers the concentrations of BCAAs (77). The uptake of glutamine by human breast HCC1806 cancer cells, deficient in ASCT2, is sensitive to the inhibition of leucine uptake when LAT1 is targeted by JPH203 (78). This suggests that LAT1 plays a role as a rescue transporter for glutamine. In breast cancer biopsies, high LAT1 expression is associated with invasive breast cancer where LAT1 overexpression positively correlates with the expression of the estrogen receptor (ER) and the programmed death ligand-1 (PD-L1) (79). LAT1 is highly expressed in malignant skin lesions (80) and in cells from patients with skin disorders (81). Increased LAT1 expression is observed in keratinocytes and dermal infiltrating lymphocytes of patients with psoriasis, where LAT1 expression is upregulated by IL-23 and IL-1b (81). Thus, scientific evidence exists to support the notion of high reliance of malignant and non-malignant cells on amino acid transporters specializing in the uptake of arginine, glutamine, and the BCAAs. Because these transporters exert overlapping functions, their targeting may impact the uptake of more than one amino acid in clinical trials.

Most of arginine, glutamine and the BCAAs are delivered to the TME for incorporation in new protein. However, 20-25% are

degraded or used to stimulate signal transduction cascades, such as mTOR pathway (72). Such distribution is necessary to supply the cells with fuel and precursor metabolites for purine, pyrimidine, or polyamine biosynthesis (Figure 2) (82–85). The intracellular concentrations of these amino acids, however, fluctuate based on shared metabolic precursors and enzymatic reactions. A global deletion of BCATm leads to a reduction in lymphoma burden, which correlates with elevated concentrations of BCAAs, but reduced concentrations of glutamine (64). In a non-small cell lung carcinoma (NSCLC), nitrogen derived from BCAA transamination supports glutamine and nucleotide synthesis via the glutamine-purine-pyrimidine axis. However, such reliance on nitrogen from BCAAs is not observed in PDAC (86). In contrast, BCATc selective inhibition, but not changes in the BCAAs, results in upregulation of genes involved in the transport of glutamate and the conversion of glutamate into glutathione in human macrophages (70). Similarly, mouse embryonic fibroblasts, grown in a glutamine-depleted environment, show a significant increase in arginine, but not in BCAAs. The arginine levels balance off, while the levels of BCAAs increase when *TP53* is deleted. The authors thus identified the tumor suppressor p53 as an important transcriptional regulator of arginine uptake during a pro-survival response to glutamine-induced metabolic stress (87). In the TME, restricting glutamine or glutamine-dependent purine and pyrimidine synthesis shifts $CD4^+$ T cells toward Tregs but this shift is abolished if GS is inhibited. GS is described as de-repressed under low glutamine, or nucleotide starvation (88). Arginine is a precursor of polyamines and targeting enzymes such as Arg1, can impact the synthesis of polyamines in the TME. Polyamines exert immunosuppressive effects, promoting tumor growth (83). Arg1 is overexpressed in dendritic cells and represents one of the immune checkpoints in the TME (11). Dendritic cells may deprive the TME of arginine causing T cell exhaustion (83).

Lastly, arginine, glutamine and the BCAAs activate complex 1 of mTOR in cancer and immune cells. Nutrient sensing via mTOR is essential for growth and survival; however, in the context of TME, this is yet another mechanism cancer and immune cells exploit to compete for nutrients (Figure 2). mTOR signaling is dysregulated in cancer cells, while T cell function requires upregulation of mTOR (89–91). While leucine is the most potent activator of mTOR as reviewed in (6), glutamine and arginine are other stimulators of mTOR signaling. mTOR sensing may occur via Rag-GTPase-dependent and independent pathways and may engage different protein targets (92, 93). Leucine-driven activation of mTOR includes GATOR1-2, Sestrin2, and SAR1B and follows the Rag-GTPase dependent mechanism (94, 95). Arginine cannot bind Sestrin 2 or SAR1B but requires a lysosomal membrane protein SLC38A9 (96). Glutamine synergizes asparagine to activate mTOR signaling via Rag-GTPase independent mechanism (93). In summary, cancer and immune cells co-exist in the TME in a bidirectional metabolic relationship, influenced by the fluctuations in arginine, glutamine and the BCAAs.

5.2 Targeting arginine, glutamine and the BCAAs for cancer therapy

Because arginine, glutamine and the BCAAs are required for growth of cancer and immune cells, targeted deprivation or supplementation of these amino acids may lead to undesirable

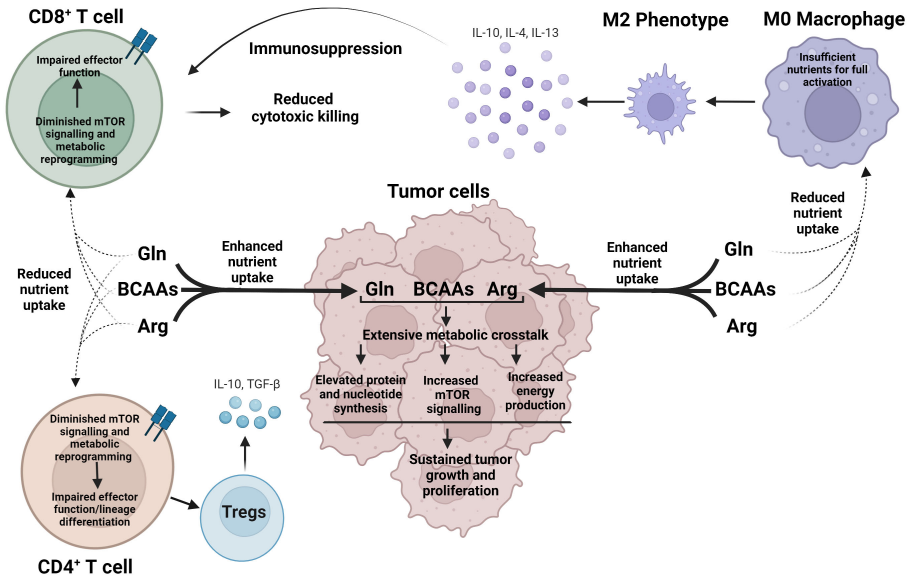

FIGURE 2
Cancer cells exert metabolic dominance over immune cells within the TME to avoid detection and destruction. In a nutrient-depleted TME, cancer cells preferentially uptake arginine, glutamine, and BCAAs, which undergo vast, interconnected metabolic pathways to produce essential biosynthetic precursors to support rapid cancer growth, as well as activate mTOR signaling. Oppositely, reduced nutrient uptake of arginine, glutamine, and the BCAAs voids $CD4^+$ and $CD8^+$ T cells of essential nutrients and diminishes mTOR signaling leading to impaired effector function and aberrant lineage commitment. As a result, immune cells, such as M2 macrophages and Tregs cells, are generated, which in turn release immunosuppressive cytokines, promoting an environment for cancer growth. Arg, arginine; Gln, glutamine; BCAAs Branched chain amino acids.

therapeutic effects (97). Selectively limiting the availability of these amino acids in tumor cells while supplying them to immune cells may help overcome this obstacle. Indeed, pharmacological inhibition of glutamine uptake by the ASCT2 inhibitor, V-9302, blocks glutamine uptake in triple negative breast cancer cells but not in $CD8^+$ T cells. The $CD8^+$ T cells adapt by upregulating a Na^+/Cl^- dependent neutral and cationic amino acid transporter $ATB^{0,+}$ (98). A similar approach is used in keratinocytes from patients with psoriasis, where deleting LAT1 controls skin inflammation, while $CD4^+$ T cells use alternative amino acid transporters (LAT2 and LAT3) (81). Lastly, pro-drugs, such as DRP104, target GLS-1 in tumors and cause $CD8^+$ T cell-dependent tumor regression (94) Such approaches could potentially unleash the immune cells in destroying cancer cells in the TME.

The endurance of the chimeric antigen receptor T (CAR-T) cells in hematological and solid malignancies can be affected by amino-acid depleted TME. Induced expression of ASS1 in re-engineered CAR-T cells increases their proliferation without compromising their function (99).

A combinatorial therapy including multivesicular liposome technology, designed to supply arginine to melanoma tumors, and selective suppression of the CAT2 transporter, leads to arginine starvation of tumor cells but promotes the infiltration of $CD8^+$ T cells in the TME (100). Similarly, a local therapy using nanoparticles to deliver poly(L-arginine) and hyaluronic acid to tumor-associated macrophages successfully induces tumor-suppressive M1 phenotype and leads to an increased iNOS expression in these cells (101).

Although still in their infancy, nanomaterials or liposome-based technologies could be expanded to deliver glutamine and BCAAs to $CD8^+$ and $CD4^+$T cells in the TME. In addition, new generations of CAR-T cells could be designed to competitively intake arginine, glutamine and BCAAs from the TME. Under such a scenario, systemic side effects should be minimal and can address the low therapeutic efficacy of the conventional cancer therapies.

Author contributions

TW and EA designed the mini review. TW prepared the glutamine overview and Figures 1, 2. SE prepared the arginine overview. LW and LF prepared the BCAA overview. EA compiled and edit the different sections. All authors contributed to the article and approved the submitted version.

Acknowledgement

The digital illustrations in Figure 1 and Figure 2 were created using Biorender.

Conflict of interest

The authors declare that the research was conducted in the absence of any commercial or financial relationships that could be construed as a potential conflict of interest.

Publisher's note

References

1. Delgoffe GM. Filling the tank: keeping antitumor T cells metabolically fit for the long haul. *Cancer Immunol Res* (2016) 4(12):1001–6. doi: 10.1158/2326-6066.CIR-16-0244

2. DePeaux K, Delgoffe GM. Metabolic barriers to cancer immunotherapy. *Nat Rev Immunol* (2021) 21(12):785–97. doi: 10.1038/s41577-021-00541-y

3. Lim AR, Rathmell WK, Rathmell JC. The tumor microenvironment as a metabolic barrier to effector T cells and immunotherapy. *Elife*. (2020) 9. doi: 10.7554/eLife.55185

4. Kim SK, Cho SW. The evasion mechanisms of cancer immunity and drug intervention in the tumor microenvironment. *Front Pharmacol* (2022) 13:868695. doi: 10.3389/fphar.2022.868695

5. Aktar N, Yueting C, Abbas M, Zafar H, Paiva-Santos AC, Zhang Q, et al. Understanding of immune escape mechanisms and advances in cancer immunotherapy. *J Oncol* (2022) 2022:8901326. doi: 10.1155/2022/8901326

6. Wetzel TJ, Erfan SC, Ananieva EA. The emerging role of the branched chain aminotransferases, BCATc and BCATm, for anti-tumor T-cell immunity. *Immunometabolism* (2023) 5(1):e00014. doi: 10.1097/IN9.0000000000000014

7. Endicott M, Jones M, Hull J. Amino acid metabolism as a therapeutic target in cancer: a review. *Amino Acids* (2021) 53(8):1169–79. doi: 10.1007/s00726-021-03052-1

8. Lieu EL, Nguyen T, Rhyne S, Kim J. Amino acids in cancer. *Exp Mol Med* (2020) 52(1):15–30. doi: 10.1038/s12276-020-0375-3

9. Holeček M. Branched-chain amino acids in health and disease: metabolism, alterations in blood plasma, and as supplements. *Nutr Metab* (2018) 15:33. doi: 10.1186/s12986-018-0271-1

10. Watford M. Glutamine metabolism and function in relation to proline synthesis and the safety of glutamine and proline supplementation. *J Nutr* (2008) 138(10):2003s–7s. doi: 10.1093/jn/138.10.2003S

11. Martí ILAA, Reith W. Arginine-dependent immune responses. *Cell Mol Life Sci* (2021) 78(13):5303–24. doi: 10.1007/s00018-021-03828-4

12. Wei Z , Liu X, Cheng C, Yu W, Yi P. Metabolism of amino acids in cancer. *Front Cell Dev Biol* (2020) 8:603837. doi: 10.3389/fcell.2020.603837

13. Kelly B, Pearce EL. Amino assets: how amino acids support immunity. *Cell Metab* (2020) 32(2):154–75. doi: 10.1016/j.cmet.2020.06.010

14. Marini JC, Agarwal U, Robinson JL, Yuan Y, Didelija IC, Stoll B, et al. The intestinal-renal axis for arginine synthesis is present and functional in the neonatal pig. *Am J Physiol Endocrinol Metab* (2017) 313(2):E233–e42. doi: 10.1152/ajpendo.00055.2017

15. Werner A, Pieh D, Echchannaoui H, Rupp J, Rajalingam K, Theobald M, et al. Cationic amino acid transporter-1-Mediated arginine uptake is essential for chronic lymphocytic leukemia cell proliferation and viability. *Front Oncol* (2019) 9:1268. doi: 10.3389/fonc.2019.01268

16. Morris SMJr. Arginine metabolism revisited *J Nutr* (2016) 146(12):2579s–86s doi: 10.3945/jn.115.226621

17. Grzywa TM, Sosnowska A, Matryba P, Rydzynska Z, Jasinski M, Nowis D, et al. Myeloid cell-derived arginase in cancer immune response. *Front Immunol* (2020) 11:938. doi: 10.3389/fimmu.2020.00938

18. Stuehr DJ. Enzymes of the l-arginine to nitric oxide pathway. *J Nutr* (2004) 134 (10 Suppl):2748S–51S. doi: 10.1093/jn/134.10.2748S

19. Morris SMJr. Arginine: master and commander in innate immune responses *Sci Signal* (2010) 3(135):pe27 doi: 10.1126/scisignal.3135pe27

20. Ekmekcioglu S, Grimm EA, Roszik J. Targeting iNOS to increase efficacy of immunotherapies. *Hum Vaccin Immunother.* (2017) 13(5):1105–8. doi: 10.1080/21645515.2016.1276682

21. Wu Y, Yi M, Niu M, Mei Q, Wu K. Myeloid-derived suppressor cells: an emerging target for anticancer immunotherapy. *Mol Cancer.* (2022) 21(1):184. doi: 10.1186/s12943-022-01657-y

22. Tabe Y, Lorenzi PL, Konopleva M. Amino acid metabolism in hematologic malignancies and the era of targeted therapy. *Blood.* (2019) 134(13):1014–23. doi: 10.1182/blood.2019001034

23. Arribas-López E, Zand N, Ojo O, Snowden MJ, Kochhar T. The effect of amino acids on wound healing: a systematic review and meta-analysis on arginine and glutamine. *Nutrients.* (2021) 13(8):2498. doi: 10.3390/nu13082498

24. Delage B, Fennell DA, Nicholson L, McNeish I, Lemoine NR, Crook T, et al. Arginine deprivation and argininosuccinate synthetase expression in the treatment of cancer. *Int J Cancer.* (2010) 126(12):2762–72. doi: 10.1002/ijc.25202

25. Martí i Líndez AA, Dunand-Sauthier I, Conti M, Gobet F, Núñez N, Hannich JT, et al. Mitochondrial arginase-2 is a cell–autonomous regulator of CD8+ T cell function and antitumor efficacy. *JCI Insight* (2019) 4(24):e132975. doi: 10.1172/jci.insight.132975

26. Perez-Penco M, Weis-Banke SE, Schina A, Siersbæk M, Hübbe ML, Jørgensen MA, et al. TGFβ-derived immune modulatory vaccine: targeting the immunosuppressive and fibrotic tumor microenvironment in a murine model of pancreatic cancer. *J Immunother Cancer* (2022) 10(12):e005491. doi: 10.1136/jitc-2022-005491

27. Martinenaite E, Ahmad SM, Bendtsen SK, Jørgensen MA, Weis-Banke SE, Svane IM, et al. Arginase-1-based vaccination against the tumor microenvironment: the identification of an optimal T-cell epitope. *Cancer Immunol Immunother.* (2019) 68 (11):1901–7. doi: 10.1007/s00262-019-02425-6

28. Crowther RR, Schmidt SM, Lange SM, McKell MC, Robillard MC, Zhao J, et al. Cutting edge: l-arginine transfer from antigen-presenting cells sustains CD4(+) T cell viability and proliferation. *J Immunol* (2022) 208(4):793–8. doi: 10.4049/jimmunol.2100652

29. Szefel J, Ślebioda T, Walczak J, Kruszewski WJ, Szajewski M, Ciesielski M, et al. The effect of l-arginine supplementation and surgical trauma on the frequency of myeloid-derived suppressor cells and T lymphocytes in tumour and blood of colorectal cancer patients. *Adv Med Sci* (2022) 67(1):66–78. doi: 10.1016/j.advms.2021.12.005

30. Hajaj E, Sciacovelli M, Frezza C, Erez A. The context-specific roles of urea cycle enzymes in tumorigenesis. *Mol Cell* (2021) 81(18):3749–59. doi: 10.1016/j.molcel.2021.08.005

31. Yao S, Nguyen TV, Rolfe A, Agrawal AA, Ke J, Peng S, et al. Small molecule inhibition of CPS1 activity through an allosteric pocket. *Cell Chem Biol* (2020) 27 (3):259–68.e5. doi: 10.1016/j.chembiol.2020.01.009

32. Spinelli JB, Yoon H, Ringel AE, Jeanfavre S, Clish CB, Haigis MC. Metabolic recycling of ammonia via glutamate dehydrogenase supports breast cancer biomass. *Science.* (2017) 358(6365):941–6. doi: 10.1126/science.aam9305

33. Lercher A, Bhattacharya A, Popa AM, Caldera M, Schlapansky MF, Baazim H, et al. Type I interferon signaling disrupts the hepatic urea cycle and alters systemic metabolism to suppress T cell function. *Immunity.* (2019) 51(6):1074–87.e9. doi: 10.1016/j.immuni.2019.10.014

34. Cruzat V, Macedo Rogero M, Noel Keane K, Curi R, Newsholme P. Glutamine: metabolism and immune function, supplementation and clinical translation. *Nutrients.* (2018) 10(11):1564. doi: 10.3390/nu10111564

35. Hakvoort TB, He Y, Kulik W, Vermeulen JL, Duijst S, Ruijter JM, et al. Pivotal role of glutamine synthetase in ammonia detoxification. *Hepatology.* (2017) 65(1):281–93. doi: 10.1002/hep.28852

36. Scalise M, Pochini L, Galluccio M, Console L, Indiveri C. Glutamine transport and mitochondrial metabolism in cancer cell growth. *Front Oncol* (2017) 7:306. doi: 10.3389/fonc.2017.00306

37. Sinclair LV, Rolf J, Emslie E, Shi YB, Taylor PM, Cantrell DA. Control of amino-acid transport by antigen receptors coordinates the metabolic reprogramming essential for T cell differentiation. *Nat Immunol* (2013) 14(5):500–8. doi: 10.1038/ni.2556

38. Yang WH, Qiu Y, Stamatatos O, Janowitz T, Lukey MJ. Enhancing the efficacy of glutamine metabolism inhibitors in cancer therapy. *Trends Cancer.* (2021) 7(8):790–804. doi: 10.1016/j.trecan.2021.04.003

39. Son J, Lyssiotis CA, Ying H, Wang X, Hua S, Ligorio M, et al. Glutamine supports pancreatic cancer growth through a KRAS-regulated metabolic pathway. *Nature.* (2013) 496(7443):101–5. doi: 10.1038/nature12040

40. Mukha A, Kahya U, Linge A, Chen O, Löck S, Lukiyanchuk V, et al. GLS-driven glutamine catabolism contributes to prostate cancer radiosensitivity by regulating the redox state, stemness and ATG5-mediated autophagy. *Theranostics.* (2021) 11 (16):7844–68. doi: 10.7150/thno.58655

41. Gross MI, Demo SD, Dennison JB, Chen L, Chernov-Rogan T, Goyal B, et al. Antitumor activity of the glutaminase inhibitor CB-839 in triple-negative breast cancer. *Mol Cancer Ther* (2014) 13(4):890–901. doi: 10.1158/1535-7163.MCT-13-0870

42. Jin H, Wang S, Zaal EA, Wang C, Wu H, Bosma A, et al. A powerful drug combination strategy targeting glutamine addiction for the treatment of human liver cancer. *Elife* (2020) 9:e56749. doi: 10.7554/eLife.56749

43. Hassanein M, Hoeksema MD, Shiota M, Qian J, Harris BK, Chen H, et al. SLC1A5 mediates glutamine transport required for lung cancer cell growth and survival. *Clin Cancer Res* (2013) 19(3):560–70. doi: 10.1158/1078-0432.CCR-12-2334

44. Nagarajan A, Malvi P, Wajapeyee N. Oncogene-directed alterations in cancer cell metabolism. *Trends Cancer.* (2016) 2(7):365–77. doi: 10.1016/j.trecan.2016.06.002

45. Wang Y, Bai C, Ruan Y, Liu M, Chu Q, Qiu L, et al. Coordinative metabolism of glutamine carbon and nitrogen in proliferating cancer cells under hypoxia. *Nat Commun* (2019) 10(1):201. doi: 10.1038/s41467-018-08033-9

46. Oh MH, Sun IH, Zhao L, Leone RD, Sun IM, Xu W, et al. Targeting glutamine metabolism enhances tumor-specific immunity by modulating suppressive myeloid cells. *J Clin Invest.* (2020) 130(7):3865–84. doi: 10.1172/JCI131859

47. Nabe S, Yamada T, Suzuki J, Toriyama K, Yasuoka T, Kuwahara M, et al. Reinforce the antitumor activity of CD8(+) T cells via glutamine restriction. *Cancer Sci* (2018) 109(12):3737–50. doi: 10.1111/cas.13827

48. Leone RD, Zhao L, Englert JM, Sun IM, Oh MH, Sun IH, et al. Glutamine blockade induces divergent metabolic programs to overcome tumor immune evasion. *Science.* (2019) 366(6468):1013–21. doi: 10.1126/science.aav2588

49. Johnson MO, Wolf MM, Madden MZ, Andrejeva G, Sugiura A, Contreras DC, et al. Distinct regulation of Th17 and Th1 cell differentiation by glutaminase-dependent metabolism. *Cell.* (2018) 175(7):1780–95.e19. doi: 10.1016/j.cell.2018.10.001

50. Presnell SR, Spear HK, Durham J, Riddle T, Applegate A, Lutz CT. Differential fuel requirements of human NK cells and human CD8 T cells: glutamine regulates glucose uptake in strongly activated CD8 T cells. *Immunohorizons.* (2020) 4(5):231–44. doi: 10.4049/immunohorizons.2000020

51. Best SA, Gubser PM, Sethumadhavan S, Kersbergen A, Negrón Abril YL, Goldford J, et al. Glutaminase inhibition impairs CD8 T cell activation in STK11-/Lkb1-deficient lung cancer. *Cell Metab* (2022) 34(6):874–87.e6. doi: 10.1016/j.cmet.2022.04.003

52. Fu Q, Xu L, Wang Y, Jiang Q, Liu Z, Zhang J, et al. Tumor-associated macrophage-derived interleukin-23 interlinks kidney cancer glutamine addiction with immune evasion. *Eur Urol.* (2019) 75(5):752–63. doi: 10.1016/j.eururo.2018.09.030

53. Blair MC, Neinast MD, Arany Z. Whole-body metabolic fate of branched-chain amino acids. *Biochem J* (2021) 478(4):765–76. doi: 10.1042/BCJ20200686

54. Cuomo P, Capparelli R, Iannelli A, Iannelli D. Role of branched-chain amino acid metabolism in type 2 diabetes, obesity, cardiovascular disease and non-alcoholic fatty liver disease. *Int J Mol Sci* (2022) 23(8):4325. doi: 10.3390/ijms23084325

55. Holeček M. Branched-chain amino acid supplementation in treatment of liver cirrhosis: updated views on how to attenuate their harmful effects on cataplerosis and ammonia formation. *Nutrition.* (2017) 41:80–5. doi: 10.1016/j.nut.2017.04.003

56. Yudkoff M. Interactions in the metabolism of glutamate and the branched-chain amino acids and ketoacids in the CNS. *Neurochem Res* (2017) 42(1):10–8. doi: 10.1007/s11064-016-2057-z

57. Siddik MAB, Shin AC. Recent progress on branched-chain amino acids in obesity, diabetes, and beyond. *Endocrinol Metab* (2019) 34(3):234–46. doi: 10.3803/EnM.2019.34.3.234

58. Wang W, Zou W. Amino acids and their transporters in T cell immunity and cancer therapy. *Mol Cell* (2020) 80(3):384–95. doi: 10.1016/j.molcel.2020.09.006

59. Yoneshiro T, Wang Q, Tajima K, Matsushita M, Maki H, Igarashi K, et al. BCAA catabolism in brown fat controls energy homeostasis through SLC25A44. *Nature.* (2019) 572(7771):614–9. doi: 10.1038/s41586-019-1503-x

60. Neinast M, Murashige D, Arany Z. Branched chain amino acids. *Annu Rev Physiol* (2019) 81:139–64. doi: 10.1146/annurev-physiol-020518-114455

61. Mayers JR, Wu C, Clish CB, Kraft P, Torrence ME, Fiske BP, et al. Elevation of circulating branched-chain amino acids is an early event in human pancreatic adenocarcinoma development. *Nat Med* (2014) 20(10):1193–8. doi: 10.1038/nm.3686

62. Lee K, Blanton C. The effect of branched-chain amino acid supplementation on cancer treatment. *Nutr Health* (2023), 2601060231153428. doi: 10.1177/02601060231153428

63. Chi R, Yao C, Chen S, Liu Y, He Y, Zhang J, et al. Elevated BCAA suppresses the development and metastasis of breast cancer. *Front Oncol* (2022) 12:887257. doi: 10.3389/fonc.2022.887257

64. Ananieva EA, Bostic JN, Torres AA, Glanz HR, McNitt SM, Brenner MK, et al. Mice deficient in the mitochondrial branched-chain aminotransferase (BCATm) respond with delayed tumour growth to a challenge with EL-4 lymphoma. *Br J Cancer.* (2018) 119(8):1009–17. doi: 10.1038/s41416-018-0283-7

65. Budhathoki S, Iwasaki M, Yamaji T, Yamamoto H, Kato Y, Tsugane S. Association of plasma concentrations of branched-chain amino acids with risk of colorectal adenoma in a large Japanese population. *Ann Oncol* (2017) 28(4):818–23. doi: 10.1093/annonc/mdw680

66. Li JT, Li KY, Su Y, Shen Y, Lei MZ, Zhang F, et al. Diet high in branched-chain amino acid promotes PDAC development by USP1-mediated BCAT2 stabilization. *Natl Sci Rev* (2022) 9(5):nwab212. doi: 10.1093/nsr/nwab212

67. Ikeda K, Kinoshita M, Kayama H, Nagamori S, Kongpracha P, Umemoto E, et al. Slc3a2 mediates branched-chain amino-Acid-Dependent maintenance of regulatory T cells. *Cell Rep* (2017) 21(7):1824–38. doi: 10.1016/j.celrep.2017.10.082

68. Ananieva EA, Patel CH, Drake CH, Powell JD, Hutson SM. Cytosolic branched chain aminotransferase (BCATc) regulates mTORC1 signaling and glycolytic metabolism in CD4+ T cells. *J Biol Chem* (2014) 289(27):18793–804. doi: 10.1074/jbc.M114.554113

69. Papathanassiu AE, Ko JH, Imprialou M, Bagnati M, Srivastava PK, Vu HA, et al. BCAT1 controls metabolic reprogramming in activated human macrophages and is associated with inflammatory diseases. *Nat Commun* (2017) 8:16040. doi: 10.1038/ncomms16040

70. Ko J-H, Olona A, Papathanassiu AE, Buang N, Park K-S, Costa ASH, et al. BCAT1 affects mitochondrial metabolism independently of leucine transamination in activated human macrophages. *J Cell Sci* (2020) 133(22). doi: 10.1242/jcs.247957

71. Bader JE, Voss K, Rathmell JC. Targeting metabolism to improve the tumor microenvironment for cancer immunotherapy. *Mol Cell* (2020) 78(6):1019–33. doi: 10.1016/j.molcel.2020.05.034

72. Vettore L, Westbrook RL, Tennant DA. New aspects of amino acid metabolism in cancer. *Br J Cancer.* (2020) 122(2):150–6. doi: 10.1038/s41416-019-0620-5

73. Ren W, Liu G, Yin J, Tan B, Wu G, Bazer FW, et al. Amino-acid transporters in T-cell activation and differentiation. *Cell Death Dis* (2017) 8(3):e2655. doi: 10.1111/jpi.12394

74. Lopes C, Pereira C, Medeiros R. ASCT2 and LAT1 contribution to the hallmarks of cancer: from a molecular perspective to clinical translation. *Cancers (Basel).* (2021) 13(2):203. doi: 10.3390/cancers13020203

75. Nachef M, Ali AK, Almutairi SM, Lee SH. Targeting SLC1A5 and SLC3A2/SLC7A5 as a potential strategy to strengthen anti-tumor immunity in the tumor microenvironment. *Front Immunol* (2021) 12:624324. doi: 10.3389/fimmu.2021.624324

76. Häfliger P, Charles RP. The l-type amino acid transporter LAT1-an emerging target in cancer. *Int J Mol Sci* (2019) 20(10):2428. doi: 10.3390/ijms20102428

77. You S, Zhu X, Yang Y, Du X, Song K, Zheng Q, et al. SLC7A1 overexpression is involved in energy metabolism reprogramming to induce tumor progression in epithelial ovarian cancer and is associated with immune-infiltrating cells. *J Oncol* (2022) 2022:5864826. doi: 10.1155/2022/5864826

78. Bröer A, Gauthier-Coles G, Rahimi F, van Geldermalsen M, Dorsch D, Wegener A, et al. Ablation of the ASCT2 (SLC1A5) gene encoding a neutral amino acid transporter reveals transporter plasticity and redundancy in cancer cells. *J Biol Chem* (2019) 294(11):4012–26. doi: 10.1074/jbc.RA118.006378

79. Kurozumi S, Kaira K, Matsumoto H, Kurosumi M, Yokobori T, Kanai Y, et al. Association of l-type amino acid transporter 1 (LAT1) with the immune system and prognosis in invasive breast cancer. *Sci Rep* (2022) 12(1):2742. doi: 10.1038/s41598-022-06615-8

80. Shimizu A, Kaira K, Kato M, Yasuda M, Takahashi A, Tominaga H, et al. Prognostic significance of l-type amino acid transporter 1 (LAT1) expression in cutaneous melanoma. *Melanoma Res* (2015) 25(5):399–405. doi: 10.1097/CMR.0000000000000181

81. Cibrian D, Castillo-González R, Fernández-Gallego N, de la Fuente H, Jorge I, Saiz ML, et al. Targeting l-type amino acid transporter 1 in innate and adaptive T cells efficiently controls skin inflammation. *J Allergy Clin Immunol* (2020) 145(1):199–214.e11. doi: 10.1016/j.jaci.2019.09.025

82. Yang L, Venneti S, Nagrath D. Glutaminolysis: a hallmark of cancer metabolism. *Annu Rev BioMed Eng.* (2017) 19:163–94. doi: 10.1146/annurev-bioeng-071516-044546

83. Lian J, Liang Y, Zhang H, Lan M, Ye Z, Lin B, et al. The role of polyamine metabolism in remodeling immune responses and blocking therapy within the tumor immune microenvironment. *Front Immunol* (2022) 13:912279. doi: 10.3389/fimmu.2022.912279

84. Kuo MT, Chen HHW, Feun LG, Savaraj N. Targeting the proline-Glutamine-Asparagine-Arginine metabolic axis in amino acid starvation cancer therapy. *Pharmaceuticals* (2021) 14(1):72. doi: 10.3390/ph14010072

85. Kurmi K, Haigis MC. Nitrogen metabolism in cancer and immunity. *Trends Cell Biol* (2020) 30(5):408–24. doi: 10.1016/j.tcb.2020.02.005

86. Mayers JR, Torrence ME, Danai LV, Papagiannakopoulos T, Davidson SM, Bauer MR, et al. Tissue of origin dictates branched-chain amino acid metabolism in mutant kras-driven cancers. *Science.* (2016) 353(6304):1161–5. doi: 10.1126/science.aaf5171

87. Lowman XH, Hanse EA, Yang Y, Ishak Gabra MB, Tran TQ, Li H, et al. p53 promotes cancer cell adaptation to glutamine deprivation by upregulating Slc7a3 to increase arginine uptake. *Cell Rep* (2019) 26(11):3051–60.e4. doi: 10.1016/j.celrep.2019.02.037

88. Metzler B, Gfeller P, Guinet E. Restricting glutamine or glutamine-dependent purine and pyrimidine syntheses promotes human T cells with high FOXP3 expression and regulatory properties. *J Immunol* (2016) 196(9):3618–30. doi: 10.4049/jimmunol.1501756

89. Chen CL, Hsu SC, Ann DK, Yen Y, Kung HJ. Arginine signaling and cancer metabolism. *Cancers (Basel).* (2021) 13(14):3541. doi: 10.3390/cancers13143541

90. Kim J, Guan KL. mTOR as a central hub of nutrient signalling and cell growth. *Nat Cell Biol* (2019) 21(1):63–71. doi: 10.1038/s41556-018-0205-1

91. Waickman AT, Powell JD. mTOR, metabolism, and the regulation of T-cell differentiation and function. *Immunol Rev* (2012) 249(1):43–58. doi: 10.1111/j.1600-065X.2012.01152.x

92. Bodineau C, Tomé M, Murdoch PDS, Durán RV. Glutamine, MTOR and autophagy: a multiconnection relationship. *Autophagy.* (2022) 18(11):2749–50. doi: 10.1080/15548627.2022.2062875

93. Meng D, Yang Q, Wang H, Melick CH, Navlani R, Frank AR, et al. Glutamine and asparagine activate mTORC1 independently of rag GTPases. *J Biol Chem* (2020) 295(10):2890–9. doi: 10.1074/jbc.AC119.011578

94. Saxton RA, Knockenhauer KE, Wolfson RL, Chantranupong L, Pacold ME, Wang T, et al. Structural basis for leucine sensing by the Sestrin2-mTORC1 pathway. *Science.* (2016) 351(6268):53–8. doi: 10.1126/science.aad2087

95. Chen J, Ou Y, Luo R, Wang J, Wang D, Guan J, et al. SAR1B senses leucine levels to regulate mTORC1 signalling. *Nature.* (2021) 596(7871):281–4. doi: 10.1038/s41586-021-03768-w

96. Wyant GA, Abu-Remaileh M, Wolfson RL, Chen WW, Freinkman E, Danai LV, et al. mTORC1 activator SLC38A9 is required to efflux essential amino acids from lysosomes and use protein as a nutrient. *Cell.* (2017) 171(3):642–54.e12. doi: 10.1016/j.cell.2017.09.046

97. Lemberg KM, Vornov JJ, Rais R, Slusher BS. We're not "DON" yet: optimal dosing and prodrug delivery of 6-Diazo-5-oxo-L-norleucine. *Mol Cancer Ther* (2018) 17(9):1824–32. doi: 10.1158/1535-7163.MCT-17-1148

98. Edwards DN, Ngwa VM, Raybuck AL, Wang S, Hwang Y, Kim LC, et al. Selective glutamine metabolism inhibition in tumor cells improves antitumor T lymphocyte activity in triple-negative breast cancer. *J Clin Invest* (2021) 131(4):e140100. doi: 10.1172/JCI140100

99. Fultang L, Booth S, Yogev O, Martins da Costa B, Tubb V, Panetti S, et al. Metabolic engineering against the arginine microenvironment enhances CAR-T cell proliferation and therapeutic activity. *Blood.* (2020) 136(10):1155–60. doi: 10.1182/blood.2019004500

100. Zhang J, Wang S, Guo X, Lu Y, Liu X, Jiang M, et al. Arginine supplementation targeting tumor-killing immune cells reconstructs the tumor microenvironment and enhances the antitumor immune response. *ACS Nano.* (2022) 16(8):12964–78. doi: 10.1021/acsnano.2c05408

101. Lim JW, Son HY, Huh YM, Haam S. Cationic poly(amino acid) surface functionalized manganese nanoparticles for nitric oxide-based immunotherapy and magnetic resonance imaging. *J Mater Chem B* (2022) 10(28):5402–9. doi: 10.1039/D2TB00794K

10.3389/fonc.2023.1186539

Glossary

BCAA	Branched chain amino acids
TME	Tumor microenvironment
TILs	Tumor infiltrating lymphocytes
BCKA	Branched chain keto acid
ASS1	Arginosuccinate synthase 1
ASL	Arginosuccinate lyase
CAT	Cationic amino acid transporter
NO	Nitric oxide
mTOR	Mammalian target of rapamycin
Arg1	Arginase 1
Arg2	Arginase 2
NOS	Nitric oxide synthase
M-MDSCs	Mononuclear myeloid-derived suppressor cells
BMDCs	Bone marrow derived dendritic cells
PMN-MDSCs	Polymorphonuclear myeloid derived suppressor cells
GS	Glutamine synthase
GLS-1	Glutaminase-1
GLS-2	Glutaminase-2
ASCT2	Alanine/Serine/Cysteine transporter
SLC	Sodium dependent transporter
LAT1	L-type amino acid transporter 1
L-DON	6-diazo-5-oxo-L-norleucine
NK cells	Natural killer cells
TAMs	Tumor associated macrophages
Treg	Regulatory T cells
HIF1α	Hypoxia inducible factor 1 α
BCATc	Cytosolic branched chain aminotransferase
BCATm	Mitochondrial branched chain aminotransferase
BCKDC	Mitochondrial branched chain alpha-keto acid dehydrogenase complex
PDAC	Pancreatic ductal adenocarcinoma
ER	Estrogen receptor
PD-L1	Programed death receptor ligand-1
NSCLC	Non-small cell lung carcinoma
CAR-T	Chimeric antigen receptor T cells
ccRCC	Clear cell renal cell carcinoma

frontiers | Frontiers in Oncology

TYPE Original Research
PUBLISHED 28 June 2023
DOI 10.3389/fonc.2023.1173424

OPEN ACCESS

EDITED BY
Martin Böttcher,
Otto-von-Guericke University Magdeburg, Germany

REVIEWED BY
Benedikt Jacobs,
University Hospital Erlangen, Germany
Steve Symes,
University of Tennessee at Chattanooga, United States

*CORRESPONDENCE
Chongxu Han
Hanchongxu@126.com
Wei Sun
sunwei1018@sina.com

†These authors have contributed equally to this work

RECEIVED 24 February 2023
ACCEPTED 14 June 2023
PUBLISHED 28 June 2023

CITATION
Yi Y, Wang J, Liang C, Ren C, Lian X, Han C and Sun W (2023) LC–MS-based serum metabolomics analysis for the screening and monitoring of colorectal cancer. *Front. Oncol.* 13:1173424. doi: 10.3389/fonc.2023.1173424

LC–MS-based serum metabolomics analysis for the screening and monitoring of colorectal cancer

Yanan Yi[1†], Jianjian Wang[1†], Chengtong Liang[1], Chuanli Ren[1], Xu Lian[1], Chongxu Han[1*] and Wei Sun[2*]

[1]Department of Laboratory Medicine, Northern Jiangsu People's Hospital Affiliated to Yangzhou University, Yangzhou, Jiangsu, China, [2]Institute of Basic Medical Sciences, Chinese Academy of Medical Sciences, School of Basic Medicine, Peking Union Medical College, Beijing, China

Background: Colorectal Cancer (CRC) is a prevalent digestive system tumour with significant mortality and recurrence rates. Serum metabolomics, with its high sensitivity and high throughput, has shown potential as a tool to discover biomarkers for clinical screening and monitoring of the CRC patients.

Methods: Serum metabolites of 61 sex and age-matched healthy controls and 62 CRC patients (before and after surgical intervention) were analyzed using a ultra-performance liquid chromatography-high resolution mass spectrometer (UPLC-MS). Statistical methods and pathway enrichment analysis were used to identify potential biomarkers and altered metabolic pathways.

Results: Our analysis revealed a clear distinction in the serum metabolic profile between CRC patients and healthy controls (HCs). Pathway analysis indicated a significant association with arginine biosynthesis, pyrimidine metabolism, pantothenate, and CoA biosynthesis. Univariate and multivariate statistical analysis showed that 9 metabolites had significant diagnostic value for CRC, among them, Guanosine with Area Under the Curve (AUC) values of 0.951 for the training group and0.998 for the validation group. Furthermore, analysis of four specific metabolites (N-Phenylacetylasparticacid, Tyrosyl-Gamma-glutamate, Tyr-Ser and Sphingosine) in serum samples of CRC patients before and after surgery indicated a return to healthy levels after an intervention.

Conclusion: Our results suggest that serum metabolomics may be a valuable tool for the screening and monitoring of CRC patients.

KEYWORDS

colorectal cancer, serum metabolomics, liquid chromatography-mass spectrometer, biomarkers, screening, monitoring

Introduction

Colorectal cancer (CRC) is currently the third most prevalent malignant tumour and the second leading cause of cancer death worldwide (1).Early detection and treatment are critical in enhancing the 5-year survival rate. Currently, stage I and II patients have a cure rate of approximately 90% (2). Therefore, early screening for CRC is essential for improving patients' cure and survival rates. Carcinoembryonic antigen (CEA) and faecal occult blood tests are currently the main non-invasive early screening methods, but their clinical value is limited due to their low sensitivity and specificity (3). Endoscopy combined with pathological examination is the gold standard for diagnosing CRC, allowing for an initial evaluation of tumour shape, size, depth of invasion, and pathological classification. However, as an invasive and expensive procedure, it cannot be used for large-scale population screening. Thus, there is an urgent need to develop novel, accurate, and non-invasive techniques for detecting CRC.

Metabolomics is a rapidly developing field that studies the composition, distribution, and regulation of small molecular metabolites. By detecting the metabolic spectrum of biological fluids or tissues and monitoring the effects of different disturbance factors on the body's metabolic profile (4), it has become a powerful tool for identifying biomarkers for diseases, including cancer. In recent years, metabolomics has been widely applied to the biomarker discovery and pathway analysis of CRC. In 2012, by comparing the area under the receiver operating characteristic curve (AUROC) analysis of 11 amino acids, Leichtle AB et al. found that the model consisting of carcinoembryonic antigen, glycine, and tyrosine had better differentiation for CRC compared to carcinoembryonic antigen alone, with an AUROC of 0.878 (5). Nishiumietal. analyzed serum samples using gas-chromatography/mass-spectrometry (GC/MS) and generated a metabolite panel for CRC detection with an AUC of 0.91 (6). There is an increasing focus on exploring changes in CRC pathways. In 2021, Zhu et al. analyzed the tissue and serum metabonomic profiles of 48 CRC patients using non-targeted GC-MS and found that the most important pathways affecting CRC were phosphate inositol metabolism, primary bile acid biosynthesis, and linoleic acid metabolism pathway (7). Shen et al. applied LC-MS to perform tissue metabolomics for 10 paired CRC tissues and adjacent normal tissues and found alterations in levels of glutathione metabolism, fatty acid metabolism, and amino acid intermediates (8). These studies demonstrate the potential of metabolomics as a promising tool for improving CRC diagnosis and understanding the underlying disease mechanisms.

Metabolomics research of cancer typically relies on biological body fluid samples, withblood and urine being the primary fluids of interest. Blood samples offer a rich source of biological information, with changes in metabolite levels reflecting various pathological changes caused by cancer. Consequently, serum metabolomics has emerged as a promising approach for identifying CRC biomarkers (5, 6). Most studies have focused on identifying markers for the diagnosis of CRC comparing the metabolite profiles of cancer and healthy subjects,demonstrating the potential to distinguish between different stages of cancer based on differential serum metabolite profiles. However, few studies have examined changes in metabolite levels in postoperative patients. Thus, there is an urgent need for further metabolomics research on CRC to fill this gap in knowledge.

In this study, we conducted a non-targeted analysis of human serum using liquid chromatography-high resolution mass spectrometry (LC-HRMS) metabolomics. Specifically, we measured serum metabolites in both newly diagnosed CRC patients and healthy subjects and compared the differential metabolite levels in preoperative and postoperative CRC patients. The objective of this study was to identify potential biomarkers for CRC screening and monitoring and to make a meaningful contribution to clinical research in this area.

Materials and methods

Sample collection

All samples were collected from January to August in 2022, according to a standardized sample collection scheme. Specifically, 62 patients with CRC were diagnosed pathologically by the pathology department of Northern Jiangsu People's Hospital and were not subjected to surgery, chemotherapy, or radiotherapy. The admission criteria of CRC patients included (1): age between 30 and 89 years old (2). clear preoperative diagnosis with complete pathological examination and various examination data (3). absence of other metabolic or immune system diseases, such as diabetes, rheumatoid arthritis, etc. (4) normal laboratory tests including liver function, renal function, and blood routine (5). absence of primary tumours in other parts (6). no prior treatment or medication. Post-operative serum samples were collected one week after the operation.

All samples were collected using a serum collection tube with inert separation gel after an 8-hour overnight fast in the morning. After collection, serum samples were obtained by centrifugation at 3000rpm for 10 minutes and stored at -80 °C for subsequent analysis.

This study was approved by the Ethics Committee of Northern Jiangsu People's Hospital Affiliated with Yangzhou University (approval number: 2022ky134), and all subjects gave informed consent before participating in this study.

Sample pre-processing

50 µl serum was mixed with 150 µl acetonitrile and vortexed for 30 seconds, followed by centrifugation at 15,000 × g for 10 minutes. The supernatant was then dried in a vacuum and stored at -80 °C. Before analysis, the dry powder was resuspended in 100 µl 2% acetonitrile, vortexed till it was completely dissolved, and centrifuged at 15,000 × g for 10 minutes. Quality control (QC) samples were combined 5 µl serum samples prepared by mixing the 40 samples randomly from the healthy group, CRC group and the the post-operative group.

LC-MS/MS analysis

The samples were analysed by Waters ACQUITY H class LC system (Waters, USA) and LTQ Orbitrap Fusion Lumos mass spectrometer (Thermo Fisher, Scientific, MA, USA). The serum metabolites were separated by running a gradient at a flow rate of 0.5 ml/min for 8 minutes on a Waters Acquity UPLC HSS T3 column (100 mm × 3.0 mm, 1.8 µm). The mobile phase A was a 0.1% formic acid aqueous solution, and the mobile phase B was acetonitrile. The gradient elution procedure is as follows: 0-1.0 min, 2%B;1-3 min, 2%-55% B; 3-8min, 55%-100% B.The washing gradient procedure is as follows: 0-3.0 min, 100%B; 3.0-3.1 min, 100-2% B; 3.1-5.0 min, 2% B. The column temperature was set at 40°C, and the injection volume was 20 µl. The electrospray ion source (ESI source), the sheath gas was 40 arb, and the spray voltage was 3.20 kV (positive ion). The range of quality scanning was from 100 to 1000 m/z. The data acquisition mode was set to Full Scan + ddMS2. The goal of MS2 automatic gain control (AGC) was 5×10^5, and the maximum injection time (IT) was 100 ms. High energy collision dissociation (HCD) pyrolysis mode for dissociation has the best collision energy of 20, 35, and 60.

Data analysis

The original MS data were imported into Progenesis QI (Waters, USA) software for peak alignment, peak picking, and peak recognition. The annotation of metabolites was determined from the accurate mass composition, the isotope goodness-of-fit of the predicted molecular formula and the MS/MS fragments matching with the databases (HMDB, METLIN, and in-house standard libraries). The metabolite score was calculated using the sum of three similarity metrics including mass similarity, isotope similarity, and fragmentation score. The score was used to assess reliability of each metabolite. A CSV file containing sample information, retention time, peak area, score and other data sets was obtained. The CSV file was then imported into MetaboAnalyst5.0 (https://www.metaboanalyst.ca/) for data processing. For following statistical analysis the peak area in each sample were firstly performed normalization to the total compound. Then the missing variables were removed from more than 50% of the samples for further statistical analysis. Student's t-test was used to evaluate the significance between groups, and α value was set to 0.05. Principal component analysis (PCA) and orthogonal partial least square discriminant analysis (OPLS-DA) were performed using SIMCA14.1 (Umetrics, Sweden) software. The differential metabolites was defined as follows (1): P-value < 0.05 (2); fold change > 1.5 and < 0.67. We used the "pathway analysis" module in MetaboAnalyst 5.0 to analyse the differential metabolites and the "biomarker discovery" module for ROC analysis. In addition, we performed box chart analysis using the R software package (version 3.6.3) to show individual metabolite differences between different groups.

Results

Subjects

The methodology of this study is illustrated in (Figure 1). Our study enrolled a total of 123 subjects, including 61 healthy controls and 62 CRC patients diagnosed pathologically. The samples were randomly divided into a discovery group and a validation group in a 2:1 ratio, with age and sex-matched between the two groups. Differential metabolites were identified through the comparative analysis in 41 age-and sex-matched CRC patients and 41 healthy controls, using a selection criterion of p-value < 0.05 and fold change (FC) >1.5. The identified differential metabolites were subjected to functional

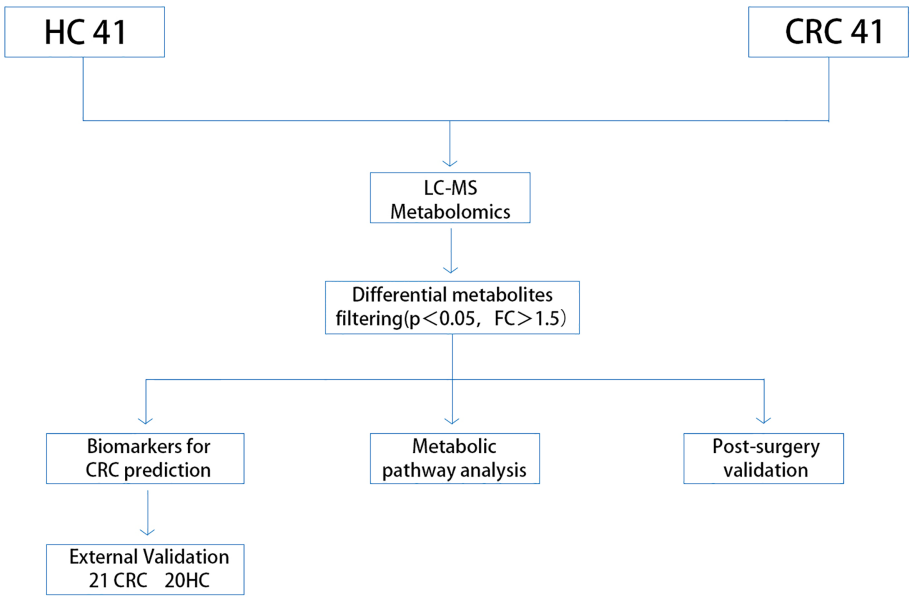

FIGURE 1
Study workflow. CRC, colorectal cancer; HC, healthy control.

annotation and pathway analysis. Moreover, potential biomarkers for CRC diagnosis were discovered through receiver operating characteristic curve (ROC) analysis, which was then validated using an independent set of 21 CRC and 20 healthy control samples. In addition, we collected serum samples from 62 patients one week after the operation and compared the changes in differential metabolites before and after the operation, aiming to identify biomarkers for monitoring prognosis.The details of all study participants are provided in Table 1 and Table S1.

Quality control

In this study, sample analysis was performed in random order. We evaluated the repeatability of the instrument analysis according to QC correlation. QC sample were randomly run during the sample analysis process. A total of 9 QC samples were injected. The Pearson correlation coefficient analysis was calculated between pairwise pairs of QC results (9). 'Wu Kong' platform (https://www.omicsolution.com/wkomics/main/) was used for relative Pearson correlation coefficient analysis of QC samples. The QC chart (Figure S1) revealed that the r values (correlation coefficient) were close to 1, indicating the good correlation between QC samples and the LC/MS system stability. This suggested that the observed differences between groups were primarily due to metabolic variations among the samples, rather than any other confounding factors. Moreover, a serum chromatogram of QC sample was provided in Figure S2.

Distinguishing CRC patients from healthy controls using serum metabolomics

In this study, we conducted unsupervised PCA analysis to identify potential biomarkers distinguishing between CRC patients and healthy controls (Figure S3A). We then used supervised pattern recognition with an OPLS-DA model, which showed better separation between the two groups (Figure 2A). To ensure the reliability and stability of the supervisory model, we performed 100 permutation tests (Figure S3B).

We selected 240 metabolic molecules with statistical differences based on criteria of P-value < 0.05, fold change > 1.5 and < 0.67 (Table S2). Of these, 145 metabolites were up-regulated and 95 were down-regulated in the CRC group (Figure 2B). Pathway analysis revealed significant disruptions in amino acid metabolism, energy metabolism, and nucleotide metabolism in colon cancer (Figure 2C, Table 2).We used ROC curve analysis to evaluate the predictive ability of potential biomarkers in distinguishing CRC from healthy controls (Table S3). Our results identified 9 metabolites with potential diagnostic value, all of which had AUC higher than 0.9 in the discovery group. In the validation group, the AUC values for these 9 differential metabolites were all above 0.8, indicating good diagnostic value (Table 3). Notably, three metabolites- Tyrosyl-Gamma-glutamate, Tyr Ser,and N-Phenylacetylaspartic acid-had AUC values of 0.945, 0.931and 0.916, respectively, in the discovery group (Figure 2D), and AUC values of 0.993, 0.981 and 0.986, respectively, in the validation group (Figure 2E). Furthermore, mass spectrum of the 9 metabolites were in Figure S4.

TABLE 1 Basic clinical information of samples.

	Discovery group		Validation group	
	CRC	HC	CRC	HC
Cases	41	41	21	20
Age	66.7 ± 11.0	67.7 ± 7.8	66.4 ± 10.5	61.8 ± 8.3
Sex(M/F)	27/14	27/14	13/9	15/5
Tumour site				
colon	32		14	
rectum	9		7	
AJCC				
I	6		4	
II	15		10	
III	17		7	
IV	3		0	
Lymphatic metastasis	20		7	
Distant metastasis	3		0	

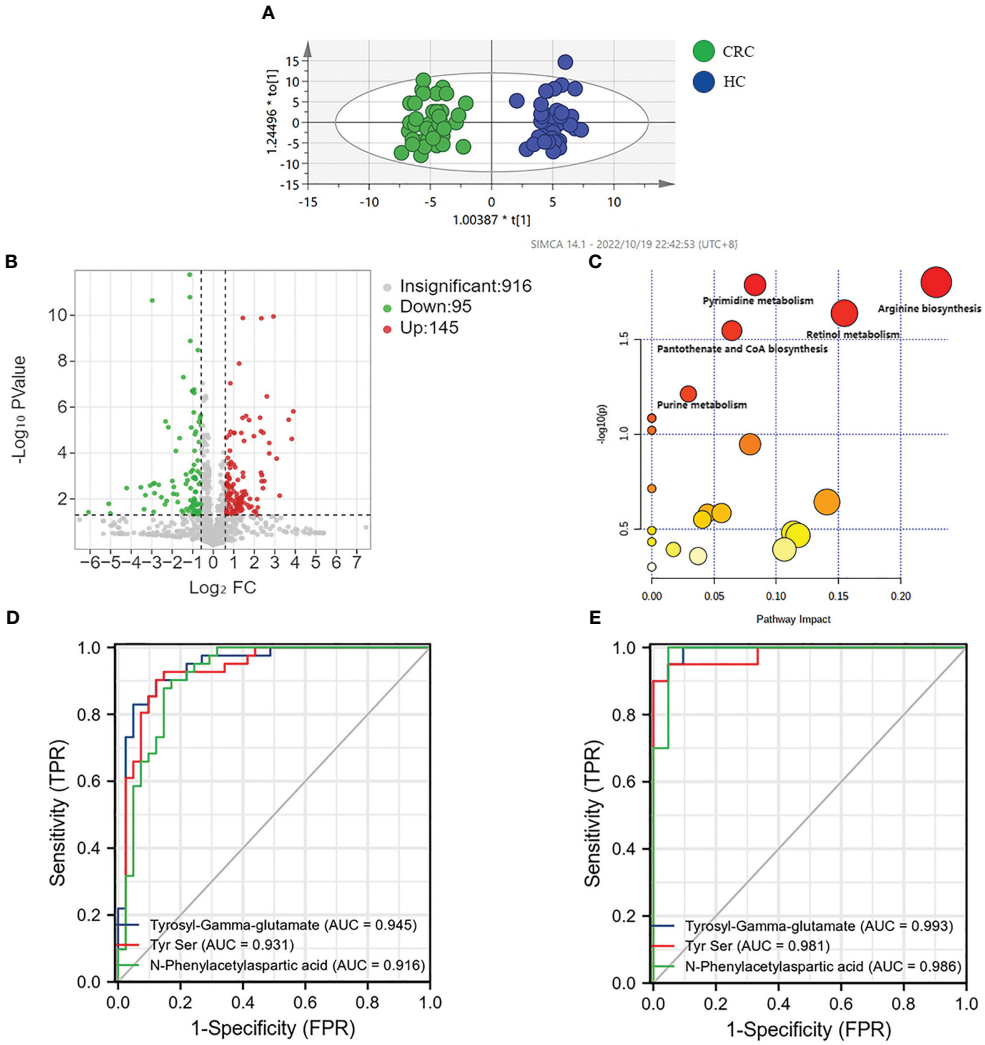

FIGURE 2
Analysis of metabolic profiling of CRC and HC. **(A)** Metabolic score plot of OPLS-DA. **(B)** Volcano analysis of the metabolites of CRC group and HC group in the discovery group. **(C)** Altered metabolic pathways in colorectal cancer. **(D)** AUC value of three metabolites in the discovery group. **(E)** AUC value of three metabolites in the validation group.

Discovery of metabolic markers for postoperative monitoring of CRC

In this study, postoperative specimens from CRC patients were analyzed to evaluate the association of the identified differential metabolites with tumour load. These metabolites may serve as potential biomarkers for monitoring CRC after surgery. Therefore, we collected serum samples about a week after the operation from 62 cases and examined the changing trend of the 9 metabolites identified earlier in preoperative and postoperative cases to evaluate the biological correlation between the potential biomarkers and CRC tumour load. We analyzed the mean intensity

TABLE 2 Pathway analysis results in the MetaboAnalyst 5.0.

Pathway name	Match status	p	FDR	Impact
Arginine biosynthesis	2/14	0.01579	0.59693	0.22843
Pyrimidine metabolism	3/39	0.016295	0.59693	0.08289
Retinol metabolism	2/17	0.022998	0.59693	0.15464
Pantothenate and CoA biosynthesis	2/19	0.028425	0.59693	0.06429
Purine metabolism	3/65	0.061347	0.98789	0.02939
D-Glutamine and D-glutamate metabolism	1/6	0.082324	0.98789	0

TABLE 3 Differential metabolites for colorectal cancer distinction in the discovery group and validation group.

Compounds	Discovery Group			Validation group		
	AUC	Sensitivity	Specificity	AUC	Sensitivity	Specificity
Guanosine	0.951	0.840	0.913	0.998	0.956	0.958
2-Hydroxyadenine	0.950	0.946	0.856	0.998	0.956	0.958
Tyrosyl-Gamma-glutamate	0.945	0.867	0.878	0.993	0.944	0.958
Tyr Ser	0.931	0.883	0.878	0.981	0.944	0.910
Lyciumoside VI	0.919	0.818	0.832	0.958	1	0.905
3-Hydroxypimelyl-CoA	0.919	0.797	0.889	0.882	0.750	0.952
N-Phenylacetylaspartic acid	0.916	0.892	0.821	0.986	1	0.952
Sphingosine	0.914	0.878	0.818	0.843	0.789	0.836
Val Arg	0.908	0.805	0.878	0.840	0.878	0.683

heatmap (Figure 3A) and serum levels of the 9 specific metabolites before and after the operation (Figure 3B, Figure S5, Table 4).

The intensity heatmap showed that seven metabolites were remarkably up-regulated in CRC and decreased after operation. These metabolites were related to amino acid metabolism and purine metabolism. Several studies have reported that the up-regulation of amino acids and purine metabolism was to promote the proliferation of cancer cells (10, 11). And the rest two down-regulated metabolites, 3-Hydroxypimelyl-CoA and Sphingosine, were involved in lipid metabolism. Lipid metabolism was associated with tumor progression and metastasis, which was to maintain high energy demand and division of cancer cells (12, 13). Moreover, previous research reported that the changes of lipidomic signatures could be served as promising potential biomarkers (12, 14).

The results showed significant differences in the levels of the 9 specific metabolites in preoperative and postoperative cases. Among these, 3-Hydroxypimelyl-CoA and Sphingosine were higher in healthy controls than in CRC, while Guanosine, 2-Hydroxyadenine, Tyrosyl-Gamma-glutamate, Tyrs Ser, Lyciumoside VI, N-Phenylacetylasparticacid, and Val Arg were higher in CRC. Four of the 9 specific metabolites, including N-Phenylacetylasparticacid, Tyrosyl-Gamma-glutamate,Tyr Ser and Sphingosine returned to normal levels, and there was no significant difference between post-operation and healthy controls (Figure 3B). These metabolites may be related to tumour load and can be used to monitor the treatment of CRC after surgery. These results further confirm the biological correlation of these metabolites in CRC and highlight their potential value for the screening and monitoringof CRC. The remaining five metabolites exhibited statistical differences between preoperative CRC samples and healthy controls and tended to return to normal levels after the operation. However, further validation may be required to confirm this (Figure S5).

Moreover, we explored whether these 9 metabolites were statistically significant in different genders, tumor locations, AJCC stage and TNM classification. There was no statistical significance among different groups (Table S4). Only Val Arg was statistically different ($P<0.05$) in the comparison of left and right-sided colorectal cancer. However, the specific mechanism is still unclear and needs to be further investigated.

Discussion

Serum metabolomics analysis using mass spectrometry offers high-throughput and high-sensitivity advantages for the screening of CRC. In this study, we comprehensively characterized the serum metabolomic profiles of healthy controls, preoperative CRC patients andpostoperative CRC patients. We identified 9specific differential metabolites that exhibit good discriminatory power for distinguishing CRC patients from healthy controls. Moreover, the 9 metabolites exhibited significant differences between preoperative and one-week post-operative samples, with four metabolites including N-Phenylacetylasparticacid, Tyrosyl-Gamma-glutamate, Tyr Ser and Sphingosine returning to normal levels and displaying no significant difference compared to healthy controls after surgery. Thus, these four metabolites may serve as potential biomarkers for monitoring CRC.

In this study, we observed changes in several metabolic pathways, including arginine biosynthesis, purine metabolism, and pantothenate and CoA biosynthesisin patients with CRC group. These metabolic changes are typical of tumour cells, which must adapt to the nutrition-deficient environment, and obtain the necessary nutrients to support their rapid proliferation and the establishment of a new biological microenvironment (10). Our findings indicated that Guanosine, an intermediate metabolite in the purine pathway and a common precursor of DNA, was significantly increased in the CRC group compared to the control group. This up-regulated metabolite change suggested that purine metabolism was upregulated in CRC. Consistent with our results, previous metabolomics analyses of CRC tissues have reported upregulation of urea cycle intermediates, purines, and most amino acids (15). Abnormal proliferation of cancer cells is one of

10.3389/fonc.2023.1173424

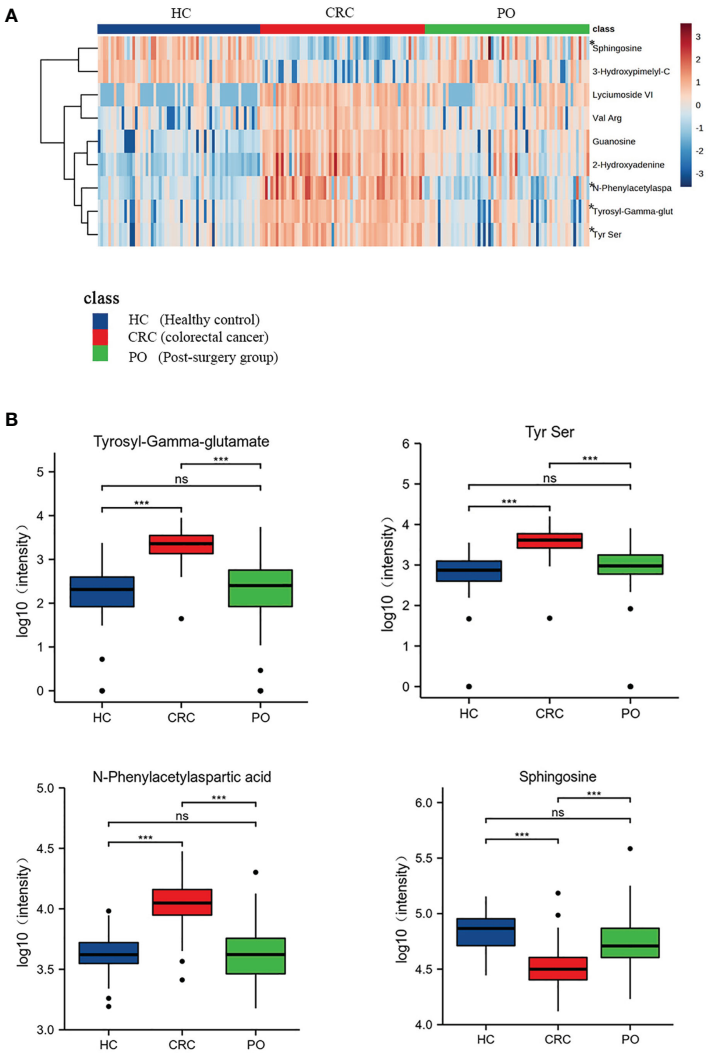

FIGURE 3
Heat map of 9 CRC-related differential metabolites in CRC,healthy control and post-surgery group. "*" marked the four metabolites which returned to normal levels **(A)**. The box plots of these 4 metabolites of healthy controls, CRC group and the post-surgery group **(B)**. "ns" p >0.05; "***"p < 0.001.

TABLE 4 The intensity changes of differential metabolites before and after operation.

Compounds	HC		CRC		PO	
	Mean	SD	Mean	SD	Mean	SD
Guanosine	557.31	763.49	8005.65	8798.36	2462.23	3680.06
2-Hydroxyadenine	923.64	602.04	5929.21	5268.45	2405.23	2514.34
Tyrosyl-Gamma-glutamate*	306.35	397.89	2589.12	1772.56	548.71	934.24
Tyr Ser*	945.63	809.55	4695.36	2886.14	1388.29	1526.21
Lyciumoside VI	1664.32	3882.26	29353.63	37950.91	6065.67	7345.01
3-Hydroxypimelyl-CoA	52332.62	35776.92	7681.90	8146.51	40996.07	44496.98
N-Phenylacetylaspartic acid*	4490.92	1612.21	12460.65	5980.75	4975.19	3143.40
Sphingosine*	72805.68	27915.05	36202.03	21451.68	67715.09	52913.39
Val Arg	1484.90	2532.48	6160.23	6194.21	2523.44	3256.98

CRC, colorectal cancer; HC, healthy control; PO, post-surgery group."*" refer to four metabolites which returned to normal levels.

the hallmarks of cancer, and purine is one of the basic nucleotides needed for cell proliferation, underscoring the close relationship between purine metabolism and cancer (11). Furthermore, increased purine levels are also considered an indicator of enhanced DNA synthesis (16). In 2017, Tian et al. examined the expression level of a rate-limiting enzyme gene in the purine synthesis pathway in different cancers and found that purine metabolism was significantly upregulated in colorectal adenocarcinoma, bladder cancer, breast cancer, and other cancers (17). The decrease in guanosine levels after surgery in our study further confirmed that solid tumour resection led to the cessation of abnormal cancer cell proliferation and that purine metabolism gradually returned to normal.

Amino acids are known to be essential for cell proliferation, and certain cancer cells rely on specific amino acids as their primary energy sources (18). Hirayama A et al. conducted a study comparing the metabolites of colon cancer and normal tissues and observed significantly higher levels of most amino acids and their primary derivatives in tumours compared to normal colon tissues (10). Arginine biosynthesis, a critical pathway upregulated in CRC compared with healthy controls, is of particular interest. Two intermediates involved in this pathway, L-citrulline and L-glutamine were found to exhibit contrasting changes in the CRC group. While L-citrulline decreased, L-glutamine increased in the CRC group. L-citrulline is mainly produced in the small intestine and converted to arginine through the actions of arginine succinate synthase (ASS) and arginine succinate lyase (ASL) (19). Glutamine, on the other hand, is the most abundant free amino acid in serum (20), and serves as an essential energy source for cancer cell proliferation (21). It also acts as a nitrogen donor, necessary for *de novo* synthesis of purines and pyrimidines, promoting nucleotide production during cancer cell proliferation (22). Within cells, glutamine is synthesized from glutamate and ammonia by glutamine synthetase (Glutamine synthetase, GS), which is highly expressed in hepatocellular carcinoma (HCC) and glioblastoma (23, 24). Extracellular glutamine can act as a signal transducer, activating transcriptional activator 3 (STAT3) to promote cancer cell proliferation (21). Arginine is one of the essential amino acids in the human body, and it plays a vital role in the ornithine cycle and promotes the formation of urea. The ammonia produced in the human body is converted into urea through the ornithine cycle and excreted through the urine. Arginine is the precursor of nitric oxide (NO) synthesis, and NO is an important signal molecule involved in immune and vascular tone regulation (25). Previous studies have shown that the potential link between arginine and colorectal cancer is the regulation of the immune system by arginine through nitric oxide (25, 26). Whereas low concentrations of NO amplify the Ras signal by inducing conformational changes of membrane-bound Ras protein to promote cancer cell proliferation (27). high concentrations of NO may lead to apoptosis, invasion, and metastasis (28). Catabolic disease states (such as sepsis, injury, and cancer) can lead to increased arginine utilization, resulting in increased arginine synthesis. Arginine is the precursor of proline, which is necessary for the synthesis of collagen. Moreover, it produces polyamines under the action of ornithine decarboxylase to promote the occurrence of CRC and cell proliferation (29, 30). As the arginine metabolic pathway is highly active in colorectal cancer, multiple molecules or enzymes involved in this pathway may be promising targets for targeted therapy for colorectal cancer (31). It has been found that tumour-infiltrating dendritic cells inhibit the proliferation and activation of CD8 cells through L-arginine metabolism (32). In addition, the expression of enzymes involved in arginine metabolism is increased in CRC tumour cells, and increasing research is focusing on potential ways to interfere with the regulatory mechanism of the L-arginine pathway by targeting transporters (10).

In this study, we also observed disruption of the pantothenate and CoA biosynthesis pathways in the CRC group. Currently, there are very few reports on the status of pantothenate and CoA biosynthesis pathways in cancer. Pantothenate, also known as vitamin B5, is one of the components of coenzyme A. Coenzyme A(CoA) plays a key role in energy and lipid synthesis (16). The increased concentration of coenzyme A in the body promotes the transition from glucose oxidation to fatty acid oxidation, thus stimulating gluconeogenesis (33). Recent studies have found that TC22 cells in CD8+-effector T cells highly express the pantothenate-CoA pathway, and CoA enhances the anti-tumour ability of TC22 by promoting oxidative phosphorylation (34, 35). These results suggest that the disruption of this pathway may be partly caused by the limited energy supply and deficiency of anti-tumour effector T cells in patients with CRC.

Tyrosyl-Gamma-glutamate is a dipeptide synthesized by tyrosine and γ-glutamate, and was significantly increased in the CRC group (AUC>0.9 in both the discovery group and validation group) and returned to normal levels after the operation. Therefore, it can have utility as a metabolic marker for detection and postoperative monitoring. When tyrosine is phosphorylated by tyrosine kinase, it regulates the signal transduction pathway and activates pyruvate dehydrogenase kinase 1 (PDHK1), which promotes solid tumour growth and Warburg metabolism (36, 37). Glutamine is deaminated to glutamic acid under the catalysis of glutaminase (GLS), which is then deaminated by glutamate dehydrogenase (GDH) to form α-ketoglutarate, which enters the TCA cycle and serves as a precursor for the synthesis of certain amino acids (38). In a previous study, analysis of levels of intracellular ROS in different cancers revealed a strong positive correlation between the estimated change in ROS levels in cancer and the change in levels of glutamate metabolism ($r = 0.655$, $P = 0.029$) (17). This may be related to the synthesis of glutathione by glutamate (39). Previous studies found that the increase of glutamate and glutathione levels is an important signal for oxidative stress, which may be due to the metabolism of rapidly proliferating CRC cells and glutathione metabolism is upregulated to combat the oxidative stress (8). Tyrosine and γ-glutamate, which are involved in dipeptide synthesis, are directly or indirectly implicated in colorectal tumours. The increased protein catabolism in CRC patients results in elevated levels of Tyrosyl-Gamma-glutamate in the serum. The observed decrease in the levels of Tyrosyl-Gamma-glutamate after the surgical removal of the tumour may be due to the decrease in energy metabolism and oxidative stress, which could result in a gradual shift toward normal levels of protein metabolism. However, currently, there is a lack of

literature on the regulation/transformation mechanism of dipeptides in colorectal tissues.

N-Phenylacetylaspartic acid belongs to a class of aspartic acidderivatives. Aspartic acid is produced by oxaloacetic acid, an intermediate product involved in the tricarboxylic acid cycle (TCA). TCA disorders are related to the occurrence and development of colon cancer (10, 16). Aspartic acid also reacts with citrulline to form arginine, which enters the urea cycle. In this study, we found that the level of serum N-Phenylacetylasparticacid in CRC patients was higher than that in healthy controls. This may be because aspartic acid is also utilized by cells for nucleotide biosynthesis, which is very important for cancer cell proliferation and is often up-regulated in tumors (40). Through comparing metabolite profiles at various stages of CRC, previous studies have found that serum aspartic acid and other amino acids peak significantly enhanced in patients with stage 3-4 CRC (6). Consistent with our findings,the level of N-Phenylacetylasparticacid decreases after the operation, which can be attributed to the decrease or absence of cancer cell proliferation, which would bring nucleotide metabolism back to normal. Therefore, N-Phenylacetylasparticacid may be an effective biomarker for monitoring patients' metabolism patterns before and after surgery.

Our results confirmed that Sphingosine reduced in the CRC group and returned to normal levels in the post-operative group. Sphingosine is the major component of sphingolipids, which belongs to cell membrane lipids. Phosphorylate Sphingosine forms the bioactive lipid sphingosine 1-phosphate (S1P), catalyzed by sphingosine kinase1 (Sphk1) (41). Several studies have revealed that the SIP/Sphk1 signaling plays oncogenic roles and it is overexpressed in colon cancer tissue which is correlated with poor survival (41–43). Therefore, decreased Sphingosine levels in CRC group may be due to increased utilization of lipids or enhanced SIP synthesis, which is needed for increased membrane synthesis or tumour development.

Conclusion

In conclusion, we performed LC-MS-based comparative metabolomics to evaluate the serum metabolite profiles of healthy controls and preoperative and postoperative CRC patients. 9 metabolites were identified as potential biomarkers of CRC. Of these, N-Phenylacetylasparticacid, Tyrosyl-Gamma-glutamate, Tyr-Ser and Sphingosine, showed similar levels in healthy controls and post-operative CRC patients, which indicates their potential value in screening and postoperative monitoring of CRC.

Nonetheless, further detailed studies are required to validate our findings. There are several ways in which this could be achieved. First, in this pilot study, we tentatively explored CRC-associated serum metabolite changes and potential biomarkers. We provided some clues for functional analysis and subsequent study. Due to the small sample size, our analysis is preliminary. In the future, larger sample cohorts from multicenter analyses should be analyzed and standards validation will be necessary. Second, a grouping study of inflammatory bowel disease should be included, which could reveal deeper mechanisms of CRC development. Third, patients with infections and metabolic diseases were not enrolled in this study, which may limit the application of our conclusions. We will include these patients in future analysis for a more comprehensive validation. Forth, in this study, we collected post-operative serum samples only once, one week after the operation. However, we did not subsequently perform a follow-up analysis on postoperative patient samples.Therefore, future studies could include an analysis of samples collected over longer periods after the surgery, which could be useful in dynamically monitoring the preoperative and postoperative metabolic changes. Additionally, among the 9 potential biomarkers, three did not have standard secondary mass spectra. Further studies will be done for the validation of the 3 metabolites.

Data availability statement

The datasets presented in this study can be found in online repositories. The names of the repository/repositories and accession number(s) can be found in the article/Supplementary Material.

Ethics statement

The studies involving human participants were reviewed and approved by Ethics Committee of Northern Jiangsu People's Hospital Affiliated with Yangzhou University (approval number: 2022ky134). The patients/participants provided their written informed consent to participate in this study. Written informed consent was obtained from the individual(s) for the publication of any potentially identifiable images or data included in this article.

Author contributions

YY and WS designed the study, performed data processing and statistical analysis. XL collected the serum samples. The article was written by YY. CL and CR contributed to the final version of the manuscript. CH and WS participated in generation of the manuscript and are the corresponding authors. All authors contributed to the article and approved the submitted version.

Funding

This work was supported by National Key Research and Developemnt Program of China (No. 2015CB755402), National Natural Science Foundation of China (82172345, 81573220), Natural Science Foundation of Jiangsu Province (BK20221281), Foundation of Yangzhou Science and Technology Planning (YZ2020076) and Northern Jiangsu People's Hospital (No. SBJC21017, SBJC220009).

Acknowledgments

We thank Bullet Edits Limited for the linguistic editing and proofreading of the manuscript. We also thank excellent colleagues from Northern Jiangsu People's Hospital for their help (Xuefen Zhao, Meichen Tang, Bingqian Liu, Lin Yuan, Pengfei Sun, et al).

Conflict of interest

The authors declare that the research was conducted in the absence of any commercial or financial relationships that could be construed as a potential conflict of interest.

Publisher's note

Supplementary material

The Supplementary Material for this article can be found online at: https://www.frontiersin.org/articles/10.3389/fonc.2023.1173424/full#supplementary-material

References

1. Sung H, Ferlay J, Siegel RL, Laversanne M, Soerjomataram I, Jemal A, et al. Global cancer statistics 2020: GLOBOCAN estimates of incidence and mortality worldwide for 36 cancers in 185 countries. *CA Cancer J Clin* (2021) 71(3):209–49. doi: 10.3322/caac.21660

2. Weitz J, Koch M, Debus J, Höhler T, Galle PR, Büchler MW. Colorectal cancer. *Lancet* (2005) 365(9454):153–65. doi: 10.1016/S0140-6736(05)17706-X

3. Chan EC, Koh PK, Mal M, Cheah PY, Eu KW, Backshall A, et al. Metabolic profiling of human colorectal cancer using high-resolution magic angle spinning nuclear magnetic resonance (HR-MAS NMR) spectroscopy and gas chromatography mass spectrometry (GC/MS). *J Proteome Res* (2009) 8(1):352–61. doi: 10.1021/pr8006232

4. Kikuchi K, Kakeya H. A bridge between chemistry and biology. *Nat Chem Biol* (2006) 2(8):392–4. doi: 10.1038/nchembio0806-392

5. Leichtle AB, Nuoffer JM, Ceglarek U, Kase J, Conrad T, Witzigmann H, et al. Serum amino acid profiles and their alterations in colorectal cancer. *Metabolomics* (2012) 8(4):643–53. doi: 10.1007/s11306-011-0357-5

6. Nishiumi S, Kobayashi T, Ikeda A, Yoshie T, Kibi M, Izumi Y, et al. A novel serum metabolomics-based diagnostic approach for colorectal cancer. *PloS One* (2012) 7(7):e40459. doi: 10.1371/journal.pone.0040459

7. Zhu G, Wang Y, Wang W, Shang F, Pei B, Zhao Y, et al. Untargeted GC-MS-Based metabolomics for early detection of colorectal cancer. *Front Oncol* (2021) 11:729512. doi: 10.3389/fonc.2021.729512

8. Shen Y, Sun M, Zhu J, Wei M, Li H, Zhao P, et al. Tissue metabolic profiling reveals major metabolic alteration in colorectal cancer. *Mol Omics.* (2021) 17(3):464–71. doi: 10.1039/D1MO00022E

9. Wang S, Zhu H, Zhou H, Cheng J, Yang H. MSpectraAI: a powerful platform for deciphering proteome profiling of multi-tumor mass spectrometry data by using deep neural networks. *BMC Bioinf* (2020) 21:439. doi: 10.1186/s12859-020-03783-0

10. Hirayama A, Kami K, Sugimoto M, Sugawara M, Toki N, Onozuka H, et al. Quantitative metabolome profiling of colon and stomach cancer microenvironment by capillary electrophoresis time-of-flight mass spectrometry. *Cancer Res* (2009) 69 (11):4918–25. doi: 10.1158/0008-5472.CAN-08-4806

11. Yin J, Ren W, Huang X, Deng J, Li T, Yin Y. Potential mechanisms connecting purine metabolism and cancer therapy. *Front Immunol* (2018) 9:1697. doi: 10.3389/fimmu.2018.01697

12. Mozolewska P, Duzowska K, Pakiet A, Mika A, ŚledziŃski T. Inhibitors of fatty acid synthesis and oxidation as potential anticancer agents in colorectal cancer treatment. *Anticancer Res* (2020) 40:4843–56. doi: 10.21873/anticanres.14487

13. Răchieriu C, Eniu DT, Moiş E, Graur F, Socaciu C, Socaciu MA, et al. Lipidomic signatures for colorectal cancer diagnosis and progression using UPLC-QTOF-ESI(+) MS. *Biomolecules* (2021) 11(3):417. doi: 10.3390/biom11030417

14. Coleman O, Ecker M, Haller D. Dysregulated lipid metabolism in colorectal cancer. *Curr Opin Gastroenterol* (2022) 38:162–7. doi: 10.1097/MOG.0000000000000811

15. Denkert C, Budczies J, Weichert W, Wohlgemuth G, Scholz M, Kind T, et al. Metabolite profiling of human colon carcinoma–deregulation of TCA cycle and amino acid turnover. *Mol Cancer.* (2008) 7:72. doi: 10.1186/1476-4598-7-72

16. Naquet P, Kerr EW, Vickers SD, Leonardi R. Regulation of coenzyme a levels by degradation: the 'Ins and outs'. *Prog Lipid Res* (2020) 78:101028. doi: 10.1016/j.plipres.2020.101028

17. Tian Y, Du W, Cao S, Wu Y, Dong N, Wang Y, et al. Systematic analyses of glutamine and glutamate metabolisms across different cancer types. *Chin J Cancer.* (2017) 36(1):88. doi: 10.1186/s40880-017-0255-y

18. Argilés JM, Azcón-Bieto J. The metabolic environment of cancer. *Mol Cell Biochem* (1988) 81(1):3–17. doi: 10.1007/BF00225648

19. Morris SMJr. Arginine metabolism revisited. *J Nutr* (2016) 146(12):2579S–86S. doi: 10.3945/jn.115.226621

20. Brosnan JT. Interorgan amino acid transport and its regulation. *J Nutr* (2003) 133(6 Suppl 1):2068S–72S. doi: 10.1093/jn/133.6.2068S

21. Cacace A, Sboarina M, Vazeille T, Sonveaux P. Glutamine activates STAT3 to control cancer cell proliferation independently of glutamine metabolism. *Oncogene* (2017) 36(15):2074–84. doi: 10.1038/onc.2016.364

22. DeBerardinis RJ, Cheng T. Q's next: the diverse functions of glutamine in metabolism, cell biology and cancer. *Oncogene* (2010) 29(3):313–24. doi: 10.1038/onc.2009.358

23. Long J, Lang ZW, Wang HG, Wang TL, Wang BE, Liu SQ. Glutamine synthetase as an early marker for hepatocellular carcinoma based on proteomic analysis of resected small hepatocellular carcinomas. *Hepatobiliary Pancreat Dis Int* (2010) 9 (3):296–305.

24. Rosati A, Poliani PL, Todeschini A, Cominelli M, Medicina D, Cenzato M, et al. Glutamine synthetase expression as a valuable marker of epilepsy and longer survival in newly diagnosed glioblastoma multiforme. *Neuro Oncol* (2013) 15(5):618–25. doi: 10.1093/neuonc/nos338

25. Tong BC, Barbul A. Cellular and physiological effects of arginine. *Mini Rev Med Chem* (2004) 4(8):823–32. doi: 10.2174/1389557043403305

26. Ma Q, Wang Y, Gao X, Ma Z, Song Z. L-arginine reduces cell proliferation and ornithine decarboxylase activity in patients with colorectal adenoma and adenocarcinoma. *Clin Cancer Res* (2007) 13(24):7407–12. doi: 10.1158/1078-0432.CCR-07-0751

27. Pervin S, Singh R, Hernandez E, Wu G, Chaudhuri G. Nitric oxide in physiologic concentrations targets the translational machinery to increase the proliferation of human breast cancer cells: involvement of mammalian target of rapamycin/eIF4E pathway. *Cancer Res* (2007) 67(1):289–99. doi: 10.1158/0008-5472.CAN-05-4623

28. Choudhari SK, Chaudhary M, Bagde S, Gadbail AR, Joshi V. Nitric oxide and cancer: a review. *World J Surg Oncol* (2013) 11:118. doi: 10.1186/1477-7819-11-118

29. Witte MB, Barbul A. Arginine physiology and its implication for wound healing. *Wound Repair Regen.* (2003) 11(6):419–23. doi: 10.1046/j.1524-475X.2003.11605.x

30. Gerner EW, Meyskens FLJr. Combination chemoprevention for colon cancer targeting polyamine synthesis and inflammation. *Clin Cancer Res* (2009) 15(3):758–61. doi: 10.1158/1078-0432.CCR-08-2235

31. Uchiyama K, Yagi N, Mizushima K, Higashimura Y, Hirai Y, Okayama T, et al. Serum metabolomics analysis for early detection of colorectal cancer. *J Gastroenterol* (2017) 52(6):677–94. doi: 10.1007/s00535-016-1261-6

32. Norian LA, Rodriguez PC, O'Mara LA, Zabaleta J, Ochoa AC, Cella M, et al. Tumor-infiltrating regulatory dendritic cells inhibit CD8+ T cell function *via* l-arginine metabolism. *Cancer Res* (2009) 69(7):3086–94. doi: 10.1158/0008-5472.CAN-08-2826

33. Leonardi R, Rehg JE, Rock CO, Jackowski S. Pantothenate kinase 1 is required to support the metabolic transition from the fed to the fasted state. *PloS One* (2010) 5(6): e11107. doi: 10.1371/journal.pone.0011107

34. St Paul M, Saibil SD, Han S, Israni-Winger K, Lien SC, Laister RC, et al. Coenzyme a fuels T cell anti-tumor immunity. *Cell Metab* (2021) 33(12):2415–2427.e6. doi: 10.1016/j.cmet.2021.11.010

35. Tabata R, Chi S, Yuda J, Minami Y. Emerging immunotherapy for acute myeloid leukemia. *Int J Mol Sci* (2021) 22(4):1944. doi: 10.3390/ijms22041944

36. Hitosugi T, Fan J, Chung TW, Lythgoe K, Wang X, Xie J, et al. Tyrosine phosphorylation of mitochondrial pyruvate dehydrogenase kinase 1 is important for cancer metabolism. *Mol Cell* (2011) 44(6):864–77. doi: 10.1016/j.molcel.2011.10.015

37. Taddei ML, Pardella E, Pranzini E, Raugei G, Paoli P. Role of tyrosine phosphorylation in modulating cancer cell metabolism. *Biochim Biophys Acta Rev Cancer*. (2020) 1874(2):188442. doi: 10.1016/j.bbcan.2020.188442

38. Lu W, Pelicano H, Huang P. Cancer metabolism: is glutamine sweeter than glucose. *Cancer Cell* (2010) 18(3):199–200. doi: 10.1016/j.ccr.2010.08.017

39. Traverso N, Ricciarelli R, Nitti M, Marengo B, Furfaro AL, Pronzato MA, et al. Role of glutathione in cancer progression and chemoresistance. *Oxid Med Cell Longev* (2013) 2013:972913. doi: 10.1155/2013/972913

40. Shuvalov O, Petukhov A, Daks A, Fedorova O, Vasileva E, Barlev NA. One-carbon metabolism and nucleotide biosynthesis as attractive targets for anticancer therapy. *Oncotarget* (2017) 8(14):23955–77. doi: 10.18632/oncotarget.15053

41. Bao Y, Guo Y, Zhang C, Fan F, Yang W. Sphingosine kinase 1 and sphingosine-1-Phosphate signaling in colorectal cancer. *Int J Mol Sci* (2017) 18(10):2109. doi: 10.3390/ijms18102109

42. Olivera A, Kohama T, Edsall L, Nava V, Cuvillier O, Poulton S, et al. Sphingosine kinase expression increases intracellular sphingosine-1-phosphate and promotes cell growth and survival. *J Cell Biol* (1999) 147:545–58. doi: 10.1083/jcb.147.3.545

43. Liu SQ, Su YJ, Qin MB, Mao YB, Huang JA, Tang GD. Sphingosine kinase 1 promotes tumor progression and confers malignancy phenotypes of colon cancer by regulating the focal adhesion kinase pathway and adhesion molecules. *Int J Oncol* (2013) 42:617–26. doi: 10.3892/ijo.2012.1733

frontiers | Frontiers in Oncology

TYPE Review
PUBLISHED 14 November 2023
DOI 10.3389/fonc.2023.1259034

OPEN ACCESS

EDITED BY
Sascha Kahlfuss,
Universitätsklinikum Magdeburg, Germany

REVIEWED BY
Carla Guenther,
Osaka University, Japan
Caroline Perner,
Universitätsmedizin Greifswald, Germany

*CORRESPONDENCE
Natalia Baran
nbaran@mdanderson.org

RECEIVED 15 July 2023
ACCEPTED 17 October 2023
PUBLISHED 14 November 2023

CITATION
Aizaz M, Khan A, Khan F, Khan M, Musad Saleh EA, Nisar M and Baran N (2023) The cross-talk between macrophages and tumor cells as a target for cancer treatment.
Front. Oncol. 13:1259034.
doi: 10.3389/fonc.2023.1259034

The cross-talk between macrophages and tumor cells as a target for cancer treatment

Muhammad Aizaz[1], Aakif Khan[2], Faisal Khan[2], Maria Khan[3], Ebraheem Abdu Musad Saleh[4], Maryum Nisar[5] and Natalia Baran[6]*

[1]Shandong Provincial Key Laboratory of Animal Resistance Biology, College of Life Sciences, Shandong Normal University, Jinan, China, [2]Centre of Excellence in Molecular Biology, University of the Punjab, Lahore, Pakistan, [3]Center of Biotechnology and Microbiology, University of Peshawar, Peshawar, Pakistan, [4]Department of Chemistry, College of Arts & Science, Prince Sattam Bin Abdulaziz University, Alkharj, Saudi Arabia, [5]School of Interdisciplinary Engineering & Sciences, National University of Sciences and Technology, Islamabad, Pakistan, [6]Department of Leukemia, The University of Texas MD Anderson Cancer Center, Houston, TX, United States

Macrophages represent an important component of the innate immune system. Under physiological conditions, macrophages, which are essential phagocytes, maintain a proinflammatory response and repair damaged tissue. However, these processes are often impaired upon tumorigenesis, in which tumor-associated macrophages (TAMs) protect and support the growth, proliferation, and invasion of tumor cells and promote suppression of antitumor immunity. TAM abundance is closely associated with poor outcome of cancer, with impediment of chemotherapy effectiveness and ultimately a dismal therapy response and inferior overall survival. Thus, cross-talk between cancer cells and TAMs is an important target for immune checkpoint therapies and metabolic interventions, spurring interest in it as a therapeutic vulnerability for both hematological cancers and solid tumors. Furthermore, targeting of this cross-talk has emerged as a promising strategy for cancer treatment with the antibody against CD47 protein, a critical macrophage checkpoint recognized as the "don't eat me" signal, as well as other metabolism-focused strategies. Therapies targeting CD47 constitute an important milestone in the advancement of anticancer research and have had promising effects on not only phagocytosis activation but also innate and adaptive immune system activation, effectively counteracting tumor cells' evasion of therapy as shown in the context of myeloid cancers. Targeting of CD47 signaling is only one of several possibilities to reverse the immunosuppressive and tumor-protective tumor environment with the aim of enhancing the antitumor response. Several preclinical studies identified signaling pathways that regulate the recruitment, polarization, or metabolism of TAMs. In this review, we summarize the current understanding of the role of macrophages in cancer progression and the mechanisms by which they communicate with tumor cells. Additionally, we dissect various therapeutic strategies developed to target macrophage–tumor cell cross-talk, including modulation of macrophage polarization, blockade of signaling pathways, and

disruption of physical interactions between leukemia cells and macrophages. Finally, we highlight the challenges associated with tumor hypoxia and acidosis as barriers to effective cancer therapy and discuss opportunities for future research in this field.

KEYWORDS

macrophages, TAMs, tumor cells, cross-talk, hematological malignancies, cancer progression

1 Introduction

The tumor microenvironment (TME), the environment surrounding cancer cells, is crucial to cancer development, providing a stage for several hallmarks of cancer like tumor growth, uncontrolled tumor cell proliferation, evasion of growth suppression, immune system evasion, angiogenesis, tumor migration and invasion, tumor progression, metastasis, or emergence of treatment resistance to occur (1, 2). The TME consists of diverse cellular and extracellular components (3, 4). The cellular compartment of the TME consists of stromal cells, including cancer-associated fibroblasts (CAFs), endothelial cells (ECs), pericytes, and mesenchymal stem cells, as well as diverse immune cells, which typically include tumor-infiltrating lymphocytes, microglia, macrophages, and dendritic cells (DCs) (5, 6). This compartment of the TME can be divided further into two functional subcategories of cells: immune-stimulating cells, which facilitate the anticancer immune response, and immunosuppressive cells, which inhibit the anticancer immune response to promote tumor progression (7). The ongoing interaction between these elements and tumor cells creates a dynamic network that promotes tumorigenesis (5). These interactions among different cell types occur within a unique environment for each cancer type and cancer stage noncellular component of the TME. The non-cellular TME consists of the extracellular matrix (ECM), mainly including structural proteins (e.g., collagen, elastin, and tenascin), glycosaminoglycans (e.g., hyaluronic acid), proteoglycans (e.g., chondroitin sulfate, dermatan sulfate, heparin sulfate, heparan sulfate, and keratan sulfate), matricellular proteins (e.g., osteonectin, osteopontin, and thrombospondin), adhesion proteins (e.g., fibronectin and laminin), and a variety of signaling chemicals (e.g., cytokines, chemokines, and growth factors) (5, 6, 8).

TME composition, both cellular and extracellular, may change depending on the stage of tumor progression and undergoes continuous reorganization via several intrinsic and extrinsic processes (9, 10). The key intrinsic factors influencing the risk of tumor development and progression are genetic alterations, whereas extrinsic contributors to TME remodeling are hypoxia, acidosis, and inflammation, which impact the final composition of both the cellular construction of TME and the extracellular TME matrix (5).

Although the specific composition of a TME may depend on the tissue origin of the tumor, independent of cancer type, increased infiltration of tumor-associated macrophages (TAMs), monocytes, and DCs is common to protumorigenic TMEs (11). Also, protumorigenic TMEs are frequently accompanied by T helper 2 (Th2) cells, myeloid-derived suppressor cells (MDSCs), neutrophils (particularly of type N2), tolerogenic DCs (with immunosuppressive properties, priming the immune system into a tolerogenic state against various antigens, causing clonal T-cell deletion and anergy, suppressing memory and effector T-cell responses, and producing and activating regulatory T cells [Tregs]), and other Tregs (5, 12) as shown in Table 1. In comparison, antitumorigenic TMEs are often enriched in $CD8^+$ cytotoxic T lymphocytes, Th1 cells, classically activated M1 macrophages, neutrophils, and natural killer (NK) cells.

These differences in cellular tumor composition, particularly in the nature, density, immune functional orientation, and distribution of immune cells within a tumor, became a further basis for identifying immune tumor profiles associated with distinct responses to treatment with immune checkpoint inhibitors and therefore distinct survival and patient outcomes (3, 4, 9, 10). This stratification of patients with solid tumors according to

TABLE 1 The components of antitumorigenic and protumorigenic TMEs [adapted from Hourani et al. (6)].

	TME	
Component	Antitumorigenic	Protumorigenic
Macrophages	M1 (CD86, TLR4)	M2 (CD163, CD206)
Th cells	Th1 cells	Th2 cells
DCs	Mature DCs	Tolerogenic DCs ($CD80^{low}$, $CD86^{low}$)
T cells	Cytotoxic $CD8^+$ T cells	Tregs
Other cells	NK cells	MDSCs
Cytokines	IL-2, IL-12, IFN-γ	IL-4, IL-6, IL-10, TGF-β, IFN-γ
Growth/angiogenic factors	GM-CSF	GM-CSF, EGF, HGF, FGF, VEGF
Chemokines	CXCL9, CXCL10	CCL2

Tolerogenic DCs consist of a heterogeneous pool of DCs with immunosuppressive properties that prime the immune system into a tolerogenic state in response to various antigens. GM-CSF, granulocyte-macrophage colony-stimulating factor; HGF, hepatocyte growth factor.

composition of immune environment demonstrated the central role of the immune system in guiding therapeutic decisions and enables one to distinguish four types of tumors: hot, cold, altered-excluded, and altered-immunosuppressed tumors (9, 10, 13, 14).

Hot tumors are attributed to infiltration of TMEs mostly by T cells (15–17). They intensify the immune response, engaging it to recognize and attack tumor cells and produce a good response to immunotherapy, including that with immune checkpoint inhibitors (17). Cold tumors, on the other hand, are characterized by deficient immune cell infiltration in the TME, resulting in evasion of immune detection and responses to immune effector cells via several mechanisms, such as immunosuppressive growth factors and cytokines produced by tumor cells. A hot TME is generally seen as more favorable than cold TME in the context of cancer treatment because it suggests that the immune system is aggressively combating the tumor (15). Furthermore, an altered-excluded tumor is characterized by TME infiltration of $CD8^{+}$T cells located at the edge of the invasive margin of the tumor dominated by an abnormal vasculature (and consequent hypoxia) and a dense stroma, while altered-immunosuppressed tumors are characterized by the presence of a low degree of immune infiltration and an immunosuppressive, often hypoxic TME that limits further recruitment of immune cells and promotes an expansion of tumor (9, 10, 13–17).

Besides differences in the cellular composition of TME, distinctions in cytokines and secreted growth factors can also be found in TME, which help in the identification and characterization (8, 16–19). Most common in the latter milieu are growth factors associated with inflammation, such as granulocyte-macrophage colony-stimulating factor, epidermal growth factor (EGF), hepatocyte growth factor, and fibroblast growth factor (FGF) which are accompanied by vascular endothelial growth factor (VEGF) and stimulate angiogenesis (3, 5, 7, 8, 12, 20, 21). A protumorigenic TME is saturated with several supporting tumor growth cytokines like interleukin (IL)-4, IL-6, and IL-10 as well as transforming growth factor (TGF)-β, interferon (IFN)-γ, and chemokines such as chemokine (C-C motif) ligand 2 (CCL2) (3, 5, 7, 8, 12, 20, 21). Conversely, an antitumorigenic TME is frequently enriched in IL-2 and IL-12 along with IFN-γ, granulocyte macrophage-stimulating factor, and chemokines like C-X-C motif chemokine ligand 9 (CXCL9) and CXCL10 (22). However, the role of specific cell populations and signaling molecules in TME depends on many other factors, such as the presence of programmed death-ligand 1 (PD-L1) receptors that are often upregulated in tumor tissue and, through cooperation with IFN-γ, can induce tumor growth-promoting properties (23–26). Like IFN-γ, granulocyte macrophage-stimulating factor is known to effectively elicit anticancer immune responses, but it can also trigger tumor development and metastasis, demonstrating its context-dependent mechanism of action (27, 28).

Remodeling of the ECM and lymphatic and blood vessels caused by autocrine and paracrine signaling between the TME and cancer cells may control invasion of the cells (29). CAFs and TAMs are the two crucial cell populations impacting and modulating the maturation and modulation of the TME, remodeling of the ECM, and modulation of metabolism and angiogenesis as well as cross-talk between tumor cells and tumor-infiltrating immune cells via the production of growth factors, cytokines, and chemokines (30). Upon interaction with tumor cells, CAFs secrete or shed diverse proteins such as collagens, glycoproteins, and proteoglycans. They can also transmit autocrine and paracrine signals, including cytokines/chemokines, growth factors, mRNAs, microRNAs, and other proteins like enzymes. Through secretion of these signals, CAFs can establish the physical barrier surrounding cancer cells and thus directly supporting cancer progression via immune cell polarization, leading to a protumoral, immunosuppressive status (21, 31–33). Depending on the stage of tumor progression, CAFs contribute to the characteristics of the TME including the ECM through direct humoral interaction with TAMs (34). They remodel the ECM via qualitative and quantitative changes in the production of collagen, laminins, or fibronectins or tenascins through reorganization of protein synthesis and structure (12, 21). CAFs and cancer cells cooperate with each other through secretion of proteolytic enzymes such as matrix metalloproteinases (MMPs) that destroy the ECM and control the modification and cross-talk linking of ECM proteins (e.g., lysyl oxidases), leading to increased stiffness of ECM and its altered composition (21, 30, 35–38). This induces desmoplasia and fibrosis, establishing a physical barrier between tumor cells and therapeutic drugs as well as immune cells and enabling cancer cells to invade and metastasize (39).

CAFs may increase monocyte recruitment through secretion of monocyte chemoattractant protein-1 and stromal cell-derived factor 1 (SDF-1) and differentiation into TAMs, particularly M2 cells (35, 38). CAFs can promote tumor development by maintaining monocyte chemotactic protein-1-mediated macrophage infiltration and chronic inflammation and have been associated with infiltration of $CD204^{+}$ TAMs (40, 41). CAFs and M2 macrophages were demonstrated to cooperate with each other during cancer progression, and they are able to alter each other's functions through constant cross-talk (37, 42–45).

Finally, the TME restricts the entry of any cytotoxic antitumor substance or antitumor immune cells to the tumor cells by establishing cellular and noncellular barriers around the malignant cells (29, 36). Together with the vascular network, the ECM, and necrotic tissues, CAFs may shield tumor cells from outside signaling, completing the TME framework. Table 1 lists different components of antitumorigenic and protumorigenic microenvironments. A remodeled TME with rewired macrophage function is considered one of the key mechanisms of resistance to chemotherapy and immune checkpoint inhibitors, which we characterize and discuss below.

2 Types of macrophages and their characteristics and impact on tumorigenesis

Macrophages and other myeloid cells constitute more than 50% of a tumor mass and are crucial to its development (31, 46). The significant infiltration of macrophages in tumor metastases has been recognized as an independent biomarker of poor prognosis (3,

11, 13, 14, 47–50). Although macrophages exhibit high heterogeneity, three main populations of macrophages can be distinguished: TAMs, tissue-resident macrophages, and MDSCs (51). Among these populations, TAMs are the most abundant infiltrating cells in the TME (52). Because of their extreme plasticity and ability to adapt to external stimuli, macrophages can differentiate into specific subpopulations in response to environmental changes, in a process known as polarization, and perform functions dictated by the environment (51–53).

The two main types of macrophages commonly recognized are M1, also referred to as classically activated macrophages, and M2, alternatively activated macrophages (53). Despite the considerable plasticity of macrophages and their capacity to differentiate through polarization, researchers have proposed using various markers to characterize and distinguish between M1 and M2 morphology (54, 55). The utilization of these markers has demonstrated that M1 macrophages are often characterized by the presence of CD68 and CD80 and exhibit high expression of the MHC-II complex (56), whereas M2 macrophages are characterized by high expression of CD23 [the low-affinity receptor for immunoglobulin (Ig)E], CD163 (hemoglobin scavenger receptor), CD204 (class A macrophage scavenger receptor, SR), or CD206 (mannose receptor, C type 1, MR); a low expression of the MHC-II complex; and expression of arginase 1 (21, 35, 36, 57).

In terms of their function, M1 macrophages are involved in immune defense against external pathogens and promoting antitumor immunity (2, 53). They exert their immunostimulatory and tumoricidal effects through the release of various chemicals and molecules, including lipopolysaccharides, IFN-γ, tumor necrosis factor (TNF)-α, IL-12, IL-18, reactive nitrogen and oxygen species, inducible nitric oxide synthase, CXCL9, CXCL10, and major histocompatibility complex (MHC)-II. Additionally, they participate in the process of antigen presentation (20, 58).

On the other hand, M2 macrophages, which naturally occur in normal physiological conditions, are involved in Th2-mediated immune response, particularly in humoral immunity, wound healing, and tissue remodeling (52). However, in the presence of tumor cells, alternatively activated M2 macrophages assume an immunosuppressive and tumor-promoting role (52). The characteristics of tumor-associated M2 macrophages are orchestrated by the action of IL-4, IL-10, IL-13, macrophage colony-stimulating factor 1 (CSF-1), CCL2, or VEGF-A (2, 22, 51, 53, 59) (Figure 1).

The specific polarization state of TAMs can be influenced by certain chemokines and other substances secreted by tumors. The expression pattern of surface markers in M2 macrophages is heavily influenced by the presence of IL-4, -10, and -13 or MMPs such as MMP-1, MMP-3, MMP-10, and MMP-14, which are secreted by the tumor. The levels of these factors can vary among organs and types of tumors (2, 51–53) (Figure 1). Further distinctions between M1 and M2 macrophages can be made based on the quality and quantity of secreted cytokines and chemokines. Upon exposure to

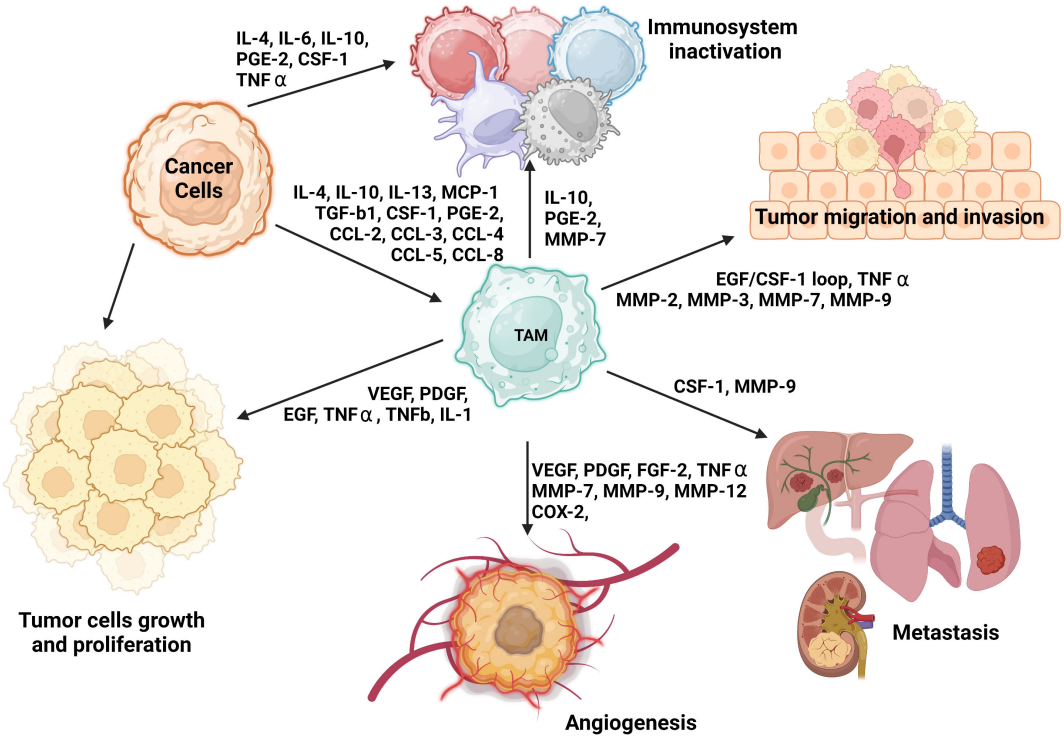

FIGURE 1
The role of M2 TAMs and their impact on tumorigenesis and immune system evasion. TAMs engage in several phases of tumorigenesis by secreting growth factors, chemokines, cytokines, and TGF-β (51, 60–63). These cells can foster a susceptible to modulation microenvironment by polarizing $CD25^+$ T cells to Th2 and Treg phenotypes. They can also restrict the antitumor ability of NK cells and cytotoxic T cells ($CD8^+$ T cells) by generating TGF-β (64). Additionally, TAMs may promote the invasion of cancer cells by producing EGF and CCL2 in the TME (65).

inflammatory signals, M1 macrophages secrete IL-1β, IL-6, IL-12, IL-23, CXCL9, CXCL10, TNF-α, nitric oxide, and reactive oxygen species (52, 53, 55). In contrast, in response to secretion of cytokines by tumor cells, M2 macrophages may release hepatocyte growth factor, TGF-β, VEGF-A, FGF-2, platelet-derived growth factors, placental growth factor, insulin-like growth factor-1, IL-1, IL-10, IL-8, CCL17, CCL22, SDF-1 (CXCL12), PD-L1, PD-L2, arginase, and prostaglandin E2 (22, 48, 59, 66–68). Additionally, M2 macrophages can synthesize and release MMP-2, MMP-7, MMP-9, MMP-13, cathepsin B and S, and serine proteolytic enzymes that break down the ECM as well as secrete growth factors necessary for EC proliferation and microvessel development (48), as shown in Figure 1.

Notably, researchers have shown M1 and M2 macrophages to have distinct angiogenic potential *in vitro*, with the M2 phenotype expressing more proangiogenic cytokines and other growth factors than does the M1 phenotype, which is discussed below in detail (48). Furthermore, M1 and M2 macrophages can be distinguished by their metabolic state. M2 macrophages mainly have a preponderance of glycolysis, fatty acid synthesis, and the pentose phosphate pathway, whereas M2 macrophages largely depend on oxidative phosphorylation (OXPHOS) for their biosynthetic and bioenergetic needs (69). TAMs are closely involved in angiogenesis, suppression of the immune system, impairment of the other immune cells' function, and support of tumor-cell metastasis. TAMs consist mostly of M2 macrophages and are thus thought to resemble M2 macrophages with their wide array of secreted cytokines, chemokines, and enzymes, and Th2 immune response (22, 70); therefore for the purpose of simplicity, we will further refer to TAMs or tumor-associated M2 macrophages equally. Figure 1 provides an overview of the various roles of M2 TAMs in tumorigenesis, including an immune system inactivation, which is discussed in detail in the next section.

3 The role of TAMs in suppression of immune responses

Immune surveillance against cancer involves immune cells such as $CD4^+$ Th cells, $CD8^+$ cytotoxic T cells, NK cells, and DCs (Figure 2). TAMs disrupt the function of these cells via secretion of specific cytokines. TGF-β is one of the key regulators of immunosuppression that may prevent the production of cytotoxicity-promoting receptors like natural cytotoxicity triggering receptor 3 (also known as NKp30) and NK group 2 member D protein upon binding of its receptors on the surface of NK cells (71). TGF-β may also affect T cells by impairing their ability to express lysing genes like granzyme A and B together with IFN-γ and FAS ligand, thus inhibiting their cytotoxic function. TGF-β also may induce expression of FOXP3 in $CD4^+CD25^+$ T cells, contributing to recruitment and an increase in the pool of Tregs in the TME (72), which can weaken the immune functions of

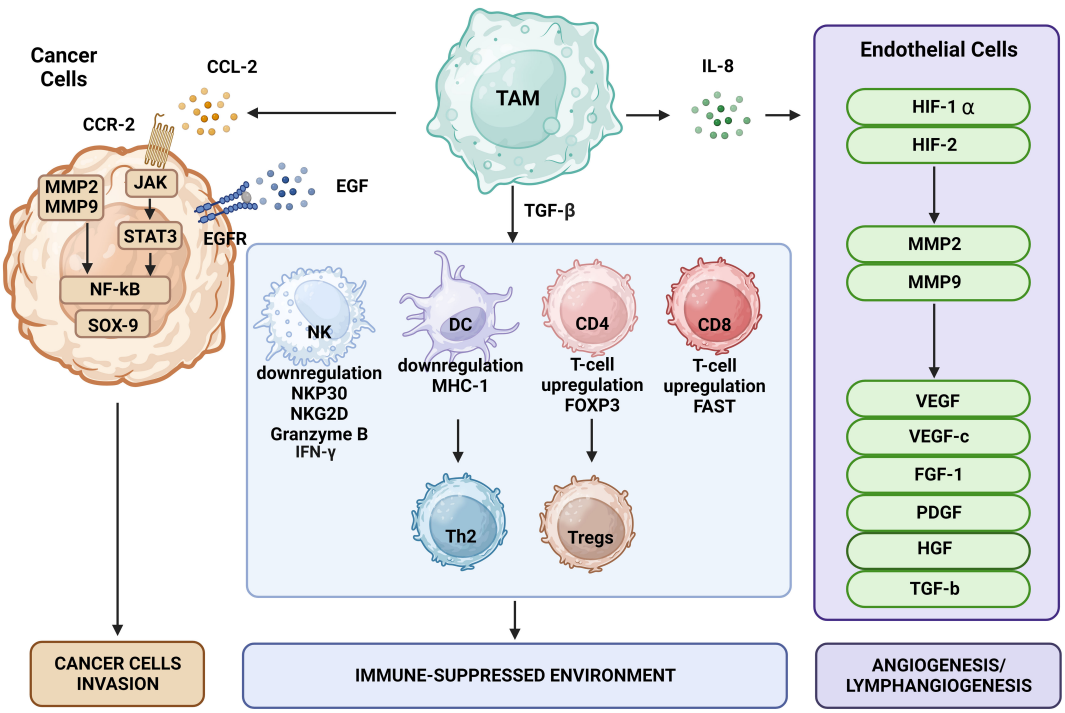

FIGURE 2
The effects of TAMs on tumor cells include promotion of tumor growth, angiogenesis, induction of tumor infiltration and immune suppression by Tregs, metabolic deprivation of T cells, inactivation of T cells, induction of growth and proliferation of cancer stem cells, EMT, invasion, migration, and metastasis. TAMs encourage the growth of tumors by secreting certain substances and expressing specific proteins. MMPs, CSF-1, and EGF produced by TAMs promote tumor invasion and migration. Moreover, TAMs release VEGF and platelet-derived growth factor, which encourage angiogenesis and tumor growth.

$CD4^+$ and $CD8^+$ T cells (73). Thymus-derived $CD4^+CD25^+FOXP3^+$ Tregs may increase the pool of $CD206^+CD163^+$ macrophages that differentiate from monocytes and upregulate CCL18 and IL-1Ra produced by macrophages (74).

By triggering $CD4^+$ T cells to differentiate into the Th2 phenotype, TGF-β and its receptor in DCs decrease adaptive immune responses through apoptosis induction and reduction of antigen-presentation ability. Thus, TGF-β changes the balance between Th1 and Th2 cells in favor of Th2 cells and enhances the immunosuppressive structure of the TME (63, 75, 76). In addition to interacting with local immune cells in an inflammatory TME, secreted TGF-β may stimulate tumor cells and MDSCs to release IL-10. The latter could be further enhanced by synergistic interaction of IL-10 with TGF-β and prostaglandin E2 via EP2 and EP4 receptors, which direct TAMs to further sustain the secretion of IL-10 (77). This cascade continues to transform naïve T cells into Tregs and inhibit the antitumor immunity maintained by NK cells (78).

IL-10 may decrease the production of proinflammatory cytokines such as IL-6, TNF-α, and IFN-γ and thus promote polarization of macrophages toward the protumorigenic M2 phenotype and thus ultimately enable tumor cells to evade immune surveillance (79). IL-10 may also inhibit or downregulate macrophage IL-2 production and thus induce macrophage polarization into the M2 phenotype (79). Furthermore, secreted IL-10 may induce release of PD-L1 and cytotoxic T-lymphocyte-associated antigen-4 as well as expression and activation of the corresponding receptors to further reduce the antitumor activity of T cells. The binding of PD-L1, followed by its activation of programmed cell death protein 1 (PD-1; CD279), or receptors B7-1 (CD80), and B7-2 (CD86) on the surface of TAMs, DCs, and B cells, triggers inhibitory signals, leading to a state of immunological tolerance and negative regulation of T-cell immune response, including apoptosis, anergy, and exhaustion (80–82). PD-L1's activation of CD80/CD86 and CD28 receptors also causes decreased proliferation, cytokine production, and T-cell anergy (80–82). Thus, to reactivate the immune response and enhance antitumor results of anti-PD1 therapy, blocking or reversing these interactions among T cells and macrophages is crucial. This immunosuppression mechanism plays a crucial role in tumor immune evasion.

TAMs also subvert immune surveillance by expressing cell surface proteins or releasing other soluble factors such as arginase 1, indoleamine 2,3-dioxygnease, and inducible nitric oxide synthase, which are oxygen and nitrogen radicals that harbor immunosuppressive functions and inhibit proliferation of NK and T cells (83, 84). TAMs restrained T-cell-specific response and crippled $CD8^+$ T-cell proliferation and killing activity via the release of extracellular vesicles (EVs), which led to tumor immune evasion (85, 86). Investigators showed that T-cell exhaustion was induced by leukemia-cell-derived EVs transporting the microRNA miR-21-5p. EVs harboring miR-21-5p also enhanced $CD8^+$ T-cell exhaustion in mice with primary hepatocellular carcinoma by targeting of YOD1 and activating the YAP/β-catenin signaling pathway (87).

To induce macrophage polarization toward the M2 phenotype, renal cell carcinoma (RCC)-derived EVs containing *lncARSR* delivered to macrophages acted as competing endogenous RNA for the microRNAs *miR-34*/*miR-449*, thus increasing signal transducer and activator of transcription 3 (STAT3) expression as the primary type of signaling of macrophage polarization (88). In addition, glioblastoma-derived EVs reprogram M1 macrophages to become TAMs and enhance protumor functions of the M2 macrophages (89). Similarly, M2-polarized TAM-derived EVs showed an activity to influence proliferation, migration, invasion, and tumorigenesis of meningioma tumors through activation of TGF-β signaling, and with delivery of *oncomiR-21* and *AKT*, *STAT3*, *MTOR*, and *ACTB* mRNA expression showed to support progression, migration, tumor sphere generation, and cisplatin resistance of bladder cancer (52, 90). Furthermore, TAM-derived exosomes promote the migration, growth, and proliferation of glioblastoma cells (50). Finally, EC-derived EVs in the TME were shown to recruit macrophages to tumors, resulting in transferring microRNAs via EVs to M2-like macrophages and causing an immunomodulatory phenotype that permits tumor growth (91).

In summary, TAMs govern immunosuppression by inducing phenotypic changes in other immune cells, recruitment and migration of myeloid DCs, stimulation of immunosuppressive cells, and production of chemokines and cytokines that regulate both the function of immunosuppressive cells and promotion of tumor-cell growth, thus impairing the effectiveness of chemotherapy and contributing to chemotherapy and immunotherapy resistance. Hence, targeting TAMs may enhance chemotherapy and immune therapy responses of tumor cells by boosting the immune system.

4 The roles of TAMs in tumor cell initiation, growth, and progression

Tumorigenesis is strongly associated with inflammation. In the process of establishing an inflammatory environment, TAMs play an essential role (53, 73) by producing mediators that remodel the TME or directly support tumor cell proliferation, protect tumor cells from apoptosis, and modulate tissue composition to favor cell migration, invasion, and metastasis. Investigators demonstrated these functions of TAMs in solid tumors such as colon and gastric cancer (73, 92, 93), in which underlying chronic inflammation or activation of specific oncogenes may cause activation and expression of proinflammatory transcription factors. The most examined transcription factors associated with inflammation include nuclear factor (NF)-κB, STAT3, hypoxia-inducible factor (HIF)-1α, and HIF-2 (73). Activation of these signaling pathways in cancer cells leads to a cascade of events with the release of cytokines and chemokines such as TNF-α and IL-6, which authors reported led to the recruitment, migration, and polarization of MDSCs and monocytes; differentiation of monocytes to macrophages; and ultimately the polarization of macrophages toward the M2 phenotype (56, 73, 79).

Macrophages might initially produce several proinflammatory mediators (IL-6, TNF-α, and IFN-γ), growth factors (EGF and Wnt), enzymes like proteases, and free radicals. This cocktail of substances, chemokines, and growth factors boosts the creation of a mutagenic microenvironment that favors and facilitates cancer

initiation, and in consequence macrophage polarization toward M2 phenotype (81, 94). TAMs may also release other ILs such as IL-6, IL-17, and IL-23 that can support tumor growth and progression as shown in models of colon cancer and hepatocellular carcinoma, in which tumor progression was associated with activation of the STAT3 signaling pathway (95, 96). In summary, as depicted in Figures 1, 2, the impact of TAMs on the initiation of tumorigenesis involves secretion of diverse factors and chemokines that lead to an accelerated tumor expansion and spread, which is discussed in the next section.

5 The role of TAMs in angiogenesis and lymphangiogenesis

In addition to tumor initiation and growth-supporting activities, TAMs can promote neovascularization to maintain the supply of nutrients and growth factors necessary for increasing the energy and biosynthesis demands of tumor cells required for expansion, invasion, and metastasis. In this context, angiogenesis and lymphangiogenesis are often discussed in association with factors like hypoxia, acidosis, and hyperosmotic pressure that, together with angiogenic factors such as VEGF-A (97–100), TGF-β (63), cyclooxygenase-2, placental growth factor, FGF-2 (62), EGF, platelet-derived growth factor, insulin-like growth factor-1, angiotensin-1, and chemokines like SDF-1, stimulate these processes (Figure 1) (48, 66, 68, 92, 101–104). The precise mechanism underlying cell-to-cell contacts between ECs and macrophage subsets as well as that underlying macrophage-stimulated angiogenesis has yet to be fully determined. However, TAMs may contribute to these processes by controlling responses to inflammatory stimuli through the release of angiogenesis- and lymphangiogenesis-stimulating factors such as VEGF-C and VEGF-D (62, 105–108). VEGF-C-mediated lymphangiogenesis may also result from a process associated with overexpression of MMP-2, MMP-3, and MMP-9 or MMP-13 that degrades the ECM and thereby indirectly facilitates angiogenic invasion, linking neovascularization with TME and matrix remodeling (48, 62, 68, 104, 109, 110). Production of proangiogenic factors such as VEGF and FGF-2 is commonly increased in hypoxic areas and has been linked to elevated expression of HIF-1α, a transcription factor that plays a central role in regulating the activation of genes in response to decreased/low oxygen levels in cells (91, 111, 112). Under elevated hypoxic conditions, due to the uncontrolled cell growth and tumor expansion especially in the middle of the tumor mass, HIF-1α was shown to interact with the transcriptional co-factor p300/CBP, activating a wide range of genes, upregulating expression of the SLC2A1/GLUT1 receptor, and increasing glycolytic activity (46, 111–114). This in consequence leads to increasing distance between blood vessels and individual cells within the tumor mass, reducing an intratumoral oxygen level, and thus deepening further the level of hypoxia within the tumor due to limitations in oxygen diffusion and oxygen availability for selected cells (115). Increased hypoxia together with elevated glycolytic activity as shown for most of solid tumors, increased the production and secretion of VEGFs, thereby promoting neovascularization and finally increasing the release of TGF-α/β to induce angiogenesis and impediment of immune cells' tumor growth–inhibitory properties (59, 116) as shown in Figures 1, 3 (92, 119, 120).

Researchers also demonstrated upregulated expression of VEGF-A in tyrosine kinase with immunoglobulin and EGF homology domain 2 (Tie2)-positive macrophages. VEGF-A secreted by Tie-2-expressing macrophages (TEMs) induced proliferation of ECs, which led to tumor angiogenesis (121). Furthermore, Tie2 on TEMs binds to angiopoietins 1–4, which initiates vascular development or neoangiogenesis (122, 123) and is a homing mechanism for ECs and vessel development (122, 123). Of note, Tie2 is frequently co-expressed with CXCR4, a chemokine receptor for SDF-1 linked to cell migration (124, 125). SDF-1 is a membrane-bound or released chemoattractant cytokine that promotes inflammation, thereby primarily attracting leukocytes, hematopoietic stem cells from adult bone marrow, and macrophages (126). SDF-1 is predominantly expressed by ECs (127), and its expression and secretion results in consistent recruitment of $CD11b^{+}$ monocytes/macrophages and retention of these cells in the tumor environment (128). Besides the presence of Tie2 (109), CXCR4 or CD11b (CD18/MAC-1) TAMs express and secrete angiogenic cytokines like MMP-9 and MMP-13 (50) stimulating further the process of neovascularization (129). Of note, during brain vascularization, yolk-sac-derived macrophages expressing Tie2 make up most of tissue macrophages and work with the endothelial tip cells to enhance vascular anastomosis following VEGF-mediated tip-cell proliferation and sprout formation (50). Also, EGF secretion by TAMs may activate EGFR on tumor cells, further upregulate VEGF/VEGFR signaling, and thus increase cancer cell proliferation and invasion (130). TAMs may also promote angiogenesis by increasing the secretion of TGF-β and IL-10, resulting in the proliferation of vessel ECs (131). Stimulation of ECs by Wnt family ligand 7B (WNT7B) aberrantly expressed in TAMs, which regulates the Wnt/β-catenin signaling pathway and VEGF production, and thereby triggers angiogenesis, tumor progression, growth, tumor cell invasion, and metastasis, was demonstrated in models of luminal breast cancer (73, 132, 133). Furthermore, myeloid Wnt7b caused an overexpression of VEGF-A in ECs, leading to angiogenic switching and tumor neovascularization (132).

In summary, the contribution of TAMs to tumor neovascularization provides solid evidence that TAM targeting may diminish or reduce tumor progression and metastasis directly by reducing TAM abundance and indirectly by impairing the release of angiogenesis-stimulating factors. Combinatorial approaches to targeting tumor cells such as classical chemotherapy together with strategies aimed at targeting TAMs and neoangiogenesis may be superior to chemotherapy or immunotherapy alone. Alternatively, approaches targeting TAMs combined with immunotherapy targeting EGFR or VEGFR and/or HIF-1/2 may warrant preclinical and clinical testing and inhibit tumor expansion.

6 The role of TAMs in tumor metastasis and invasion

The migration of tumor cells to ectopic sites requires both angiogenesis and lymphangiogenesis (134, 135). In line with TAMs'

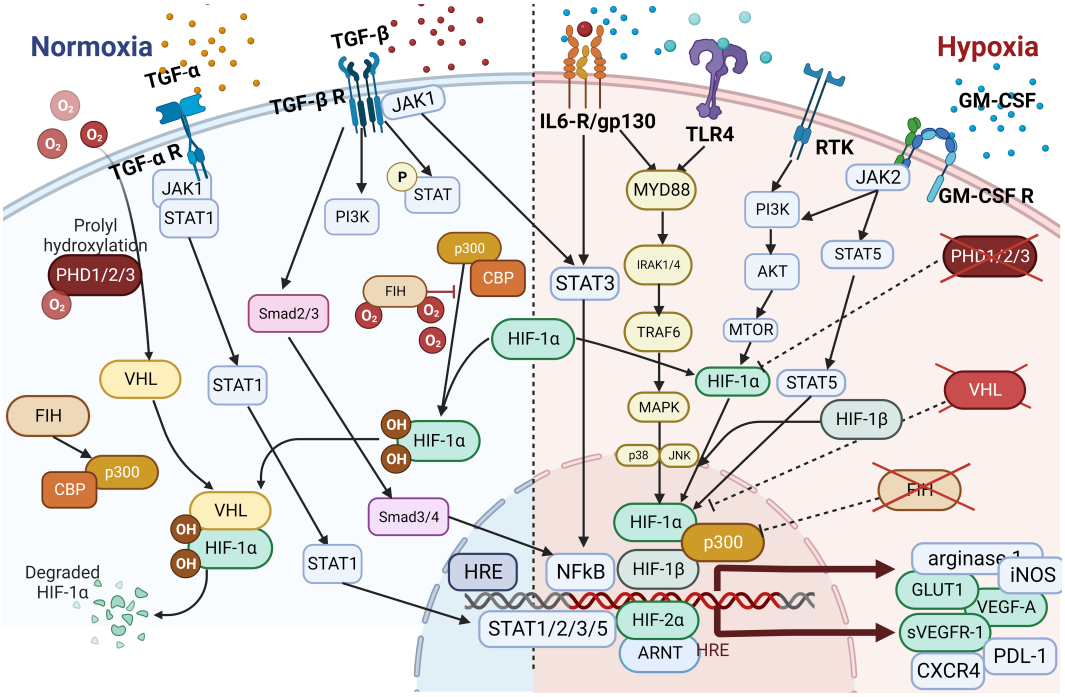

FIGURE 3
Effects of hypoxia and acidosis on TAMs. The TME is influenced by hypoxia and acidosis, which significantly impact TAMs. Hypoxia induces an M2-like phenotype, supporting tumor growth, whereas acidosis shifts TAMs toward immunosuppression and reduces proinflammatory cytokine output. These factors contribute to tissue remodeling, ECM disintegration, and angiogenesis (92, 117–119). Together, hypoxia and acidosis shape TAM activities, promoting tumor growth, blood vessel formation, and immune system evasion (119).

involvement in angiogenesis, a plethora of evidence has emphasized the importance of TAMs to tumor invasion and metastasis (136). For example, neovascularization is essential for metastasis, enabling cancer cells to spread from the primary tumor to distant sites. It enables cancer cells to enter blood or lymphatic vessels, allowing them to adhere to vessel's walls, penetrate barriers, and establish secondary tumors. The tumor vasculature's permeability and angiogenesis create a supportive microenvironment for cancer cell survival and growth. Given that metastasis is the main cause of death in cancer patients, targeting tumors at this stage is an urgent need. A common feature of cancer cells is their ability to move and release digestive enzymes that enable escape from the primary tumor and to break into the vascular and lymphoid systems to further colonize distant sites (85, 93, 133, 137).

Invasion and metastasis can also be conferred via initiation of epithelial-to-mesenchymal transition (EMT), a process enabling epithelial cells to acquire mesenchymal features (138). EMT is a crucial biological process in cancer development in which epithelial cells become more motile and invasive mesenchymal-like cells. This process facilitates invasion, metastasis, and therapeutic resistance of cancer cells. Cancer cells thus lose adhesion, become more motile, and resist apoptosis. EMT also aids in angiogenesis and immune evasion, making tumors more resistant to various treatments. EMT is linked to resistance to various treatments, including chemotherapies and targeted therapies. Understanding and targeting EMT in cancer research may lead to potential techniques for reducing metastasis, increasing therapy responses, and improving outcomes. Recent studies demonstrated that EMT is regulated by TAMs, further facilitating metastasis (132, 139).

TAMs interact with cancer cells, promoting EMT-related genetic alterations and facilitating cell migration and invasion. They also contribute to ECM remodeling and promote an immunosuppressive milieu, supporting EMT indirectly by suppressing immune responses. This interaction creates an EMT-friendly microenvironment, enabling cancer cells to penetrate tissues, enter the circulation, and metastasize to other organs. EGF production by tumor-infiltrating M2 TAMs within the TME can stimulate the NF-κB, STAT3, EGFR, and extracellular signal-regulated kinase signaling axes in tumor cells, promoting their invasive traits (140, 141). For instance, TAMs increase cancer cell invasion and capability for metastasis through induction of EMT by interfering with JAK2/STAT3/miR-506-3p/FoxQ1 regulation of colorectal cancer development (139). Additionally, EGF may prevent expression of the long noncoding RNA LIMIT, increasing the capacity for cancer cells to move (142).

The expression of EGF by TAMs may be adversely affected by CSF-1 synthesized by tumor cells, which may enhance the metastatic potential of tumor cells (143). EGF secreted by TAMs activates the EGFR/extracellular signal-regulated kinase 1/2 signal pathway in some types of cancer cells, which results in the promotion of EMT (144). Additionally, authors suggested that TGF-β generated by these TAMs in lung cancers boosts the expression of SOX9 and triggers EMT, thereby causing tumor cell migration (145). TAMs also support tumor metastasis through increased expression and release of MMPs such as MMP-2 and MMP-9 (143). MMPs together with VEGF-C, activates the CCL2/CCR2 signaling pathway and attracts circulating monocytes into the

TME, thereby promoting tumor growth, expansion, and metastasis (132, 137, 146). These infiltrating monocytes may facilitate tumor growth, expansion, and metastasis by releasing tumor-promoting factors. For example, monocytes can secrete growth factors such as VEGF-C, which induce angiogenesis and lymphangiogenesis, resulting in the creation of new blood vessels that deliver oxygen and nutrients to tumors. These cells can also produce cytokines and chemokines, which attract additional immune cells to the TME, where they dampen the immune response and promote tumor growth. Furthermore, monocytes can develop into TAMs, which are already demonstrated to enhance tumor progression by releasing a variety of substances that encourage tumor cell proliferation, invasion, and metastasis (147).

Activation of the JAK2/STAT3/miR-506-3p/FoxQ1 axis may also result in the generation of CCL2 and thereby facilitate the recruitment of macrophages (139). Furthermore, increased CCL2 expression in the TME is accompanied by increased CCR2 expression on TAMs and by the polarization of macrophages toward the M2 phenotype, whereas CCL2 overexpression and high TCF4 expression correlate with cancer metastasis to lymph nodes and have been linked to poor prognosis because the TCF4/CCL2/CCR2 regulation axis regulated TAM polarization (146). Of note, preclinical studies demonstrated M2 macrophages' potent induction of an invasive phenotype in previously healthy epithelial cells through the release of CCL2 and upregulation of endoplasmic reticulum oxidoreductase 1α as well as MMP-9, leading to acquisition of an invasive EMT phenotype (101, 148–151). TAMs may also release CCL5, which, through activation of the β-catenin/STAT3 signaling pathway, significantly promoted invasion, metastasis, and EMT in studies using prostate cancer cells (24, 86, 146, 150–152). Of note, CCL5, which is released by malignant phyllodes tumors, can trigger recruitment and repolarization of TAMs through activation of the CCR5 receptor and the AKT signaling pathway.

Furthermore, TAM-secreted CCL18 can bind to the membrane-associated phosphatidylinositol transfer protein 3 receptor, which further facilitates differentiation and invasion of myofibroblasts (83). Infiltration of TAMs and invasion and metastasis of colorectal cancer cells were promoted by the phosphatase of regenerating liver-3 (PRL3)-stimulated upregulation of cytokine CCL26 and activation of CCR3 receptor (85). Whereas EMT and metastasis induction in a model of non-small cell lung cancer (NSCLC) were facilitated by upregulation of αβ-crystallin upon co-culture of TAMs with cancer cells (153), phosphorylated STAT3 with upregulation of cyclooxygenase-2 and MMP-9 led to EMT induction, invasion, and metastasis in animal models of osteosarcoma (154).

Taken together, these findings demonstrate that TAMs can express and release a variety of factors to induce EMT. Therefore, targeting TAMs, even in advanced stages of cancer development, may have life-extending benefits for patients.

7 The role of TAMs in chemoresistance

Depending on the tumor type, most cancer treatments consist of a combination of chemotherapy, immune therapy, hormonal therapy, immune checkpoint blockade (ICB), and/or radiotherapy. Acquired resistance to treatment is the most common reason for treatment failure, and researchers have extensively investigated the contribution of TMEs including TAMs to treatment resistance. Macrophages can be prompted by their environment to adopt multiple phenotypes, and most TAMs are commonly polarized toward a cancer-promoting phenotype, which confers treatment resistance (102, 152). Treatment resistance may either reduce or completely impair the effectiveness of therapy. Investigators have identified several mechanisms of resistance conferred by TAMs. Changes in the profiles of secreted cytokines, expression of different receptors, activation of transcription factors and signaling pathways mostly associated with inflammation or hypoxia, changes in polarization of TAMs, rewiring of metabolism, and initiation of dynamic changes in the microvasculature are only some of the resistance mechanisms (Figure 4). Overall, TAMs limit the effectiveness of cancer therapies, triggering detrimental reactive responses to tumor-induced tissue damage cues and rapidly reprogramming the TME toward a proremodeling state (53, 56, 120, 158). For instance, in prostate cancer models, secretion of CCL5, activation of STAT3, and upregulation of the transcription factor Nanog resulted in chemotherapeutic drug resistance, whereas secretion of CXCL12 and activation of CXCR4 by TAMs occurred following combined docetaxel/androgen deprivation therapy in cases of castration-resistant prostate cancer tumors with poor response (84, 103, 159).

Researchers found markedly greater TAM abundance in patients with NSCLC who experienced progressive disease upon treatment with an EGFR tyrosine kinase inhibitor (137) than in those with nonprogressive disease. Moreover, as described previously, high TAM counts were significantly associated with poor progression-free and overall survival, suggesting that TAMs are related to reduced treatment responsiveness after administration of not only EGFR tyrosine kinase inhibitors but also several commonly used treatment combinations (159) and mediate resistance to antiangiogenic therapies via compensatory pathways such as cathepsin B and angiopoietin-2. Also, TAMs are key players in the antitumor activity of selected monoclonal antibodies (mAbs) such as rituximab (anti-CD20), trastuzumab (anti-HER2), cetuximab (anti-EGFR), and daratumumab (anti-CD38), as they express FcγR to perform tumor-cell killing and phagocytosis (127, 160). However, functional polymorphisms in human FcγRIIIA that affect the killing ability of macrophages correlate with low rates of response to treatment with mAbs in patients with lymphoma, breast cancer, or myeloma (127, 160).

In addition, the effects of hormonal therapy on disease progression and survival are impacted by inflammatory pathways orchestrated by macrophages. Inflammatory cytokines such as IL-1 and IL-6 can activate estrogen or androgen receptor signaling on tumor cells, linking inflammation to tumor growth and endocrine resistance (159). A new level of therapeutic intervention was introduced with the development of ICB. However, shortly after its introduction into the therapeutic armament, authors reported new resistance mechanisms mainly driven by macrophages. For instance, as key cell types participating in tumor-extrinsic pathways of primary and adaptive resistance, macrophages express several

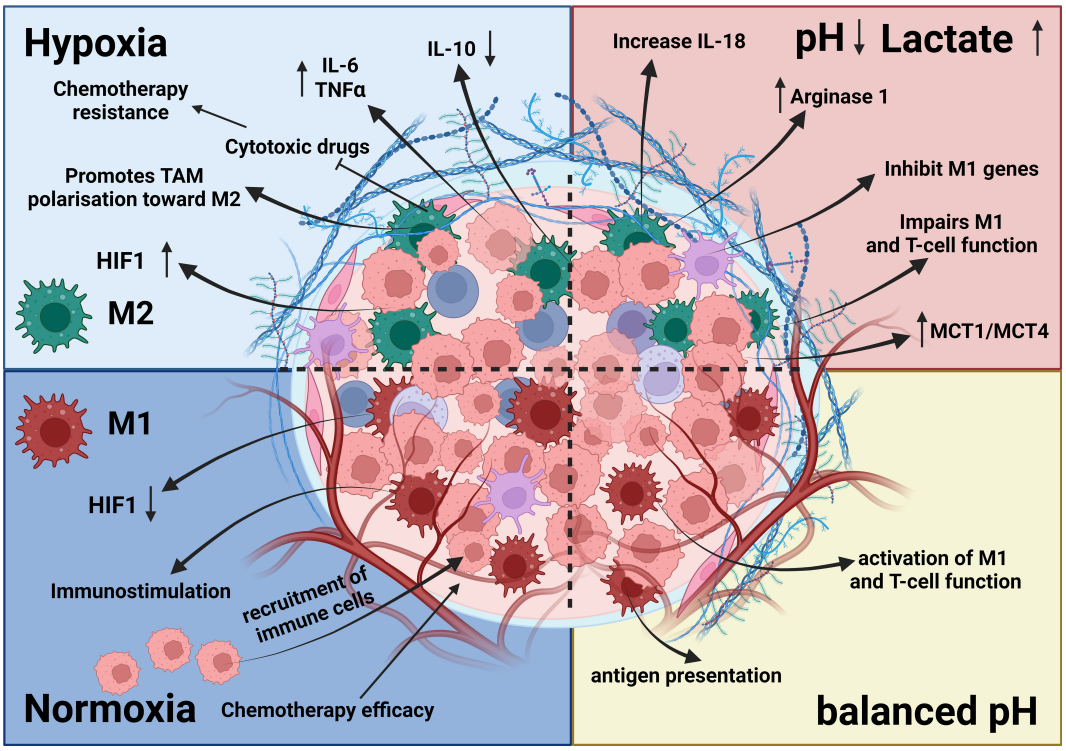

FIGURE 4
The Hypoxia pathway. Overactivated STAT3 and NF-κB activate the transcription of HIF-1α, which has resulted in the overexpression of HIF-1α (116). In combination with HIF-1β, HIF-1α triggers the transcription of TGF-α and TGF-β. Moreover, HIF-1α indirectly activates VEGF, leading to angiogenesis via overactivation of TGF-α. HIF is a transcription factor that plays a central role in regulating the activation of genes in response to low oxygen levels in cells. HIF-dependent mechanisms influence gene expression by affecting epigenetic factors such as DNA methylation and histone acetylation (155). HIF binds to DNA and associates with distinct nuclear co-factors under low-oxygen conditions. Oxygen depletion causes HIF-α to interact with the transcriptional co-factor p300/CBP. This association activates a wide range of genes, initiating diverse adaptive processes such as glycolysis (SLC2A1/GULT1), angiogenesis (VEGF-A), and angiogenesis and loss of growth-inhibitory effects (TGFα/β) (156, 157).

immunosuppressive molecules, including checkpoint ligands such as PD-L1, PD-L2, poliovirus receptor (CD155), and TIGIT ligands. Researchers showed these and other molecules to be overexpressed and to impede the efficacy of ICB for NSCLC and other types of cancer (83, 84, 151). Also, whereas PD-L1 expression in tumor-infiltrating immune cells but not macrophages correlated with positive response to anti-PD-L1/2 therapy, expression of PD-1 in macrophages was negatively correlated with their ability to phagocytose tumor cells (58, 81, 161, 162). Another inhibitory receptor found on macrophages is VISTA, which cooperates with negative regulators of T and NK cells such as P-selectin glycoprotein ligand 1 and acts as a T-cell checkpoint-inhibitory ligand. Thus, targeting VISTA with mAbs led to transcriptional and functional changes that produced increased antigen presentation, activation, and migration (22, 163). Another aspect of resistance to ICB is the cellular composition of tumors. The presence of tumor-infiltrating neutrophils together with tumor-infiltrating macrophages accompanied by T-cell elimination/depletion has contributed to the lack of response of liver cancer cells to ICB (164). For instance, abundant M2 macrophages in renal cell cancer were associated with resistance to ICB. In particular, the presence of a macrophage subpopulation expressing TIM4 suppressed $CD8^+$ T-cell responses, impairing the efficacy of ICB. However, ICB efficacy may be restored by targeting $TIM4^+$ macrophages via anti-TIM4 antibody-mediated blockade (165).

Additionally, a new dimension of complexity in the effectiveness of and resistance to immunotherapies was revealed by studies of the microbiome, suggesting that the specific composition of the microbiome shapes the components of the TEM and thus enhances or impairs therapy response. The composition of the microbiota and the cellular composition of the TEM may result from complex cross-talk and exchange of cytokines and oncometabolites among the microbiota, tumor cells, and cellular immune environment. For instance, abundant and diverse gut bacteria enriched for Bacteroides species, shaped tumor myeloid infiltration, and thus increased the effectiveness of anti-cytotoxic T-lymphocyte-associated antigen and anti-PD-1 therapy for melanoma (166). Taken together, these findings suggest that macrophages, particularly TAMs, have an important influence on the activity of chemotherapy, radiotherapy, antiangiogenic agents, hormonal therapy, and ICB. Their role is complex, as they frequently serve as inhibitors of antineoplastic activity. Despite progress in dissecting the role of macrophages in conventional antineoplastic treatment modalities, the actual translation of these findings into more effective cancer treatments remains challenging. Depletion of macrophages can potentiate various chemotherapeutic

and immunotherapeutic strategies. Several preclinical and clinical trials combining different therapeutic strategies, such as immune checkpoint inhibitors and anti-CSF-1R antibodies or other TAM-centered therapeutic strategies in combination with chemotherapy, are currently under way and are discussed below.

8 TAM-targeted therapies

Macrophages, the most prevalent immune cells within the TME, have a dual function in immunomodulation (19, 51). As discussed above, macrophages in cancer patients are an incredibly diverse mixture ranging from tumor suppressors (M1 phenotype) to tumor protectors (M2 phenotype) (19). Via sequestration of the release of proinflammatory cytokines and display of more than immunostimulatory markers, classically activated macrophages (M1 phenotype) support anticancer immunity (6, 19, 51). In contrast, M2 macrophages, which constitute most of TAMs, have a low antigen-presenting capacity and strong immunosuppressive features and produce higher numbers of proangiogenic cytokines than M1 macrophages (103, 167). Thus, limiting the number of TAMs or switching TAMs within the TME to the M1 phenotype is essential for cancer therapy because TAMs' overall activity promotes tumor development and metastasis (19, 51). Figure 5 summarizes selected therapeutic strategies targeting TAMs.

8.1 Blockade of TAMs migration/depletion of TAMs from the TME

8.1.1 The CCL2/CCR2 axis

Blocking the CCL2 or CCR2 signaling pathway, an axis that draws circulating monocytes into the TME and induces their differentiation into macrophages, is one way to eliminate TAMs from the TME (101, 148–151). CCL2 blockade can stop tumor spread, angiogenesis, and growth, and researchers have demonstrated CCL2 restriction in animal studies to increase the antitumor effects of cytotoxic T lymphocytes and decrease the number of TAMs in the TME (168). Additionally, a CCR2 antagonist has exhibited tumor-burden-reducing efficacy in animal models of adenoid cystic carcinoma of the salivary glands by reducing the number of infiltrated TAMs (168). Studies demonstrated that targeting the CCL2/CCR2 axis with the antibody carlumab (CNTO 888) as well as with a specific inhibitor of the CCR2 receptor (PF-04136309) specifically blocks the CCL2-mediated activation and migration of macrophages into tumors and tumor's infiltration by macrophages in patients with diverse types of cancers (149).

8.1.2 CSF-1 and CSF-1R

Another valuable target for the removal of TAMs from the TME is CSF-1R. CSF-1 is a cytokine that is essential for the survival, proliferation, and differentiation of mononuclear phagocytes (84,

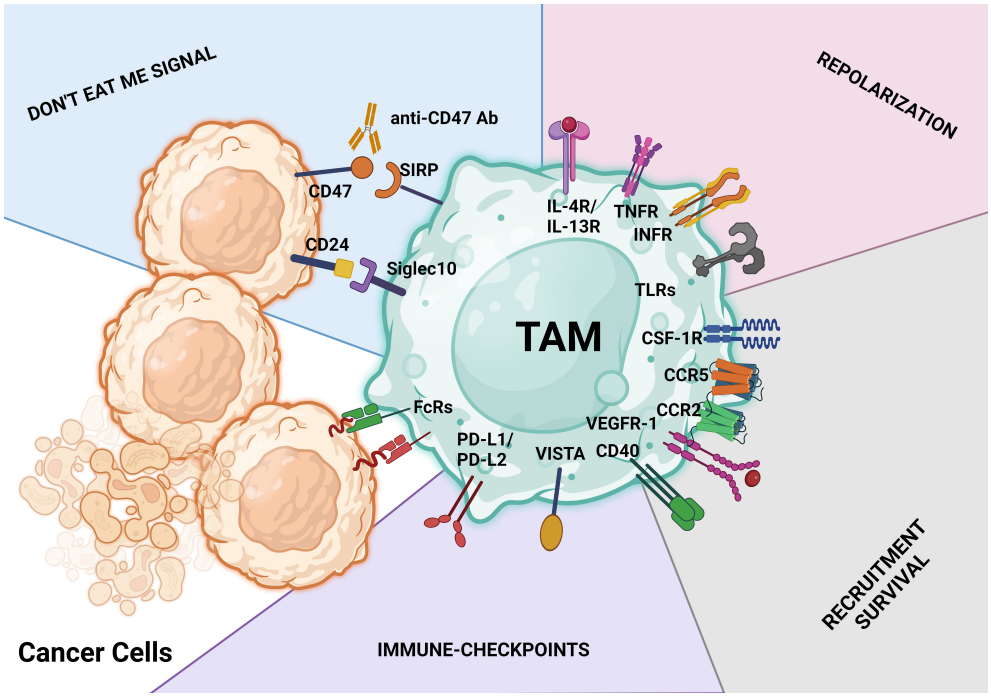

FIGURE 5
TAM-targeting strategies. These treatment approaches aim to either activate the antitumor behavior of TAMs or limit macrophage infiltration, survival, and protumoral actions. Identification of therapeutic antibodies using Fc receptors (FcRs) on TAMs is a key step in the macrophage-mediated antibody-dependent cellular cytotoxicity process. The CD47/SIRPα axis and CD24/SIGLEC10 pathway are both parts of the don't eat me signal for tumor cells. Activating macrophage-mediated antibody-dependent cellular cytotoxicity phagocytosis is possible with antibodies against the CD47/SIRPα and CD24/SIGLEC10 pathways (antibody-dependent cellular phagocytosis). Don't eat me signal pathways, repolarization, limiting and reducing the infiltration and survival of tumor cells, and ICB with antibodies are just a few of the major therapeutic approaches used to target TAMs.

159, 169). CSF-1R is a tyrosine kinase transmembrane receptor that belongs to the CSF-1/platelet-derived growth factor receptor family of protein tyrosine kinases. It has an important role in the formation and maintenance of microglia in the brain (84, 159, 169, 170). CSF-1R promotes myeloid cell survival when activated by two ligands, CSF-1 and IL-34. Inhibiting CSF-1/CSF-1R prevented murine M2 macrophages from differentiating, proliferating, and surviving in one study (169). In addition, blockade of the CSF-1/CSF-1R axis with the specific CSF-1R inhibitors PLX3397, BLZ945, and GW2580 directly impacted macrophage viability and differentiation, improving their function as well as antigen presentation ability. Furthermore, CSF-1R inhibitors induced repolarization of macrophages toward the M1 phenotype and thereby boosted the antitumor T-cell response (84, 171). In an animal model of glioblastoma, CSF-1R blockade demonstrated significant potential to reduce tumor growth, suggesting that CSF-1R inhibitors can block TAM-mediated immunosuppression and make tumor cells more susceptible to chemotherapeutics (120). For instance, treatment with PLX3397 prevented the differentiation of myeloid monocytes into TAMs and improved the response of glioblastoma to ionizing radiotherapy, which delayed the recurrence of glioblastoma (152, 172). Authors reported that the number of TAMs and polymorphonuclear MDSCs in the TME were successfully reduced by the co-targeting of CSF-1R and CXCR2 inhibitors. Importantly, in diverse animal models of cancer, this drug combination reduced tumor burdens and inhibited tumor growth (54, 168, 173).

Also, antibodies against CSF-1 and CSF-1R are used to target macrophages by inhibiting their recruitment and depleting and re-educating them. Given promising results in preclinical data, investigators are further evaluating this combinatorial approach in the setting of breast cancer and other solid tumors in ongoing clinical studies (172). Even though CSF-1R inhibition enhances TAMs' ability to present antigens in animal models of aggressive pancreatic ductal adenocarcinoma, it may cause exhausted phenotypes of cytotoxic T cells, highlighting the importance of combining immune checkpoint inhibitors and CSF-1R inhibitors in treating these tumors (172).

8.2 Polarization of M2 TAMs into tumor-suppressive macrophages

Given the fact that protumor macrophages (M2 phenotype) create an immune-resistant TME whereas antitumor macrophages (M1 phenotype) stop or slow down cancer growth and metastasis, potential strategies for cancer therapy include switching M2 macrophages to the M1 phenotype (120, 162, 173, 174). This change in phenotype may be helpful for cancer treatment because M1 macrophages create an immune-vulnerable microenvironment for cancer cells. Additionally, changing the phenotype of M2 macrophages may stop cancer cells from growing and forming metastases (173, 175). Various substances and modalities to change the state of TAMs within the TEM were investigated including T-cell immunoglobulin and mucin domain 3 and 4 blockade and treatment with macrophage receptor with collagenous structure (MARCO) or Toll-like receptor (TLR) agonists (145, 176–178). TIMs are phosphatidylserine receptors mainly expressed on antigen −presenting cells that are involved in the recognition and efferocytosis of apoptotic cells. They are expressed in immune cells such as NK, T, B, and mast cells and participate in multiple aspects of immune regulation but are also abnormally expressed in cancer cells, contributing to immunosuppression (64, 179, 180). Studies demonstrated that blockade of TIMs improved the anticancer effectiveness of T-cell responses in cancer patients and enhanced the immune cells' stimulatory properties (64, 180). Investigators achieved similar effects by targeting the scavenger receptor MARCO, which reversed the immunosuppressive effects of TAMs and reduced tumor progression in several murine models of solid tumors (181–183).

Also, use of phosphoinositide 3-kinase γ (PI3Kγ) inhibitors such as IPI-549, mammalian target of rapamycin inhibitors, CD40 agonists, TLR agonists, and class IIa histone deacetylase (HDAC) inhibitors helps repolarize TAMs toward the proinflammatory M1 state (171). Specifically, HDAC inhibitors improved the effectiveness of both chemotherapeutic drugs and immune checkpoint inhibitors in breast cancer treatment by inducing M1 polarization of TAMs (81, 184). The phenotype switch toward M1 was also achieved through PI3Kγ suppression in pancreatic ductal adenocarcinoma, a tactic used to modify the TAM phenotype in solid tumors like melanoma, pancreatic cancer, and lung cancer. They also observed that blocking the PI3Kγ/Akt signaling pathway could decrease the recruitment of integrin α4-dependent MDSCs, increase the recruitment of mature DCs, impede macrophage polarization toward the M2 phenotype, and strengthen T-cell anticancer defenses (185). BKM120 and IPI-549 are two highly effective PI3K inhibitors with direct modifying effects on macrophages and anticancer effectiveness alone or in combination with immune checkpoint inhibitors (83, 90).

Use of TLR agonists has also produced positive results in reversing TAM polarization toward the M1 phenotype. For instance, TLR3 stimulation enhanced the production of MHC-II and other co-stimulatory elements on macrophages by activating the IFN-α/β signaling pathway, exhibited M2/M1 polarization-changing properties, and switched M2 macrophages to the M1 phenotype (186). Also, TLR4 and IFN-γ receptors on macrophages are commonly involved in M1 activation. The major signals associated with M1 macrophage polarization are STAT1 and NF-κB. Immunomodulatory compounds such as Lachnum polysaccharide and glycocalyx-mimicking nanoparticles can interact with TLRs, influencing TAMs to release IL-12, exhibit the M1 phenotype, or reverse the M2 phenotype (158, 187). Of note, glycocalyx-mimicking nanoparticles are internalized by TAMs via lectin receptors, stimulating production of IL-12 and inhibiting production of IL-10, arginase 1, and CCL22 to activate macrophages' antitumor responses (187, 188). This macrophage phenotype reversion was further controlled by suppressing STAT6 and activating NF-κB phosphorylation (187). Furthermore, glycocalyx effectively reduced tumor burdens in *in vivo* studies and had positive synergistic effects when combined with anti-PD-L1 therapy (145, 187).

Additional targeted nanocarriers have demonstrated efficacy by conveying mRNA-encoding transcription factors responsible for M1

polarization to the M2 phenotype (189, 190). In addition, nanoparticle injections prepared with mRNAs expressing IFN-regulatory factor 5 along with IKKβ switched M2 subsets to antitumor M1 macrophages in animal studies of ovarian cancer, melanoma, and glioblastoma (142). Lately, targeted delivery of chlorogenic acid (CHA) encapsulated in mannosylated liposomes can reduce the immune-suppressive effects of the TME on glioblastoma cells by causing TAMs with the M2 phenotype to adopt an M1 state (191). Remodeling of the TAM phenotype was also caused by infusion of IL-12 in hepatocellular carcinoma models. IL-12 injection lowered the expression of STAT3 and c-Myc, which led to induction of the M1 phenotype in macrophages (192). In another study of hepatocellular carcinoma, IL-37 converted M2 TAMs into M1 cells by inhibiting the IL-6/STAT3 signaling pathway (163). Also, studies using ureido tetrahydrocarbazole derivatives confirmed the potent transformation of M2 macrophages to the M1 phenotype to instill antitumor activity both *in vitro* and *in vivo*. According to Pei et al. (193), the ureido tetrahydrocarbazole derivatives were effective at slowing the growth of tumors in tumor-bearing mouse models and had effective results when combined with anti-PD-1 antibodies. Considering all of these data, altering the phenotype of TAMs to become M1 cells appears to be an effective tactic for increasing the sensitivity of tumor cells to both chemotherapeutic drugs and immunotherapies.

8.3 Checkpoints for macrophage-induced phagocytosis

Investigators have identified several tumor-phagocytosis-related checkpoints, including the CD47/signal regulatory protein α (SIRPα) axis, the PD-1/PD-L1 axis, the MHC-I/leukocyte immunoglobulin-like receptor subfamily B (LILRB1) axis, and the CD24/SIGLEC10 axis. This was followed by the development of several mAbs or protein fusions directed against these checkpoints, with some of them exhibiting promising effectiveness in ongoing clinical trials.

8.3.1 CD47/SIRPα checkpoint

The first checkpoint to be connected to tumor phagocytosis was CD47/SIRP cross-talk, commonly referred to as the don't eat me signal (123). CD47 was first described as a membrane protein in healthy red blood cells (123). Previous studies revealed that senescent red blood cells with reduced CD47 expression are swiftly removed by the macrophages residing in the splenic red pulp, liver tissue, or bone marrow erythroblastic island (6, 72, 194–196). However, in normal erythroid cells, CD47 expression prevents clearance by attaching to the macrophage inhibitory receptor SIRPα (128, 176, 197–199). Recent reports pointed to SIRPα as a membrane protein belonging to the immunoglobulin superfamily that is primarily expressed by myeloid cells like macrophages and other DCs (54). The mechanism behind inhibition of phagocytosis by macrophages was further dissected with the discovery that macrophages and SIRPα interact with CD47 expressed on nearby cells, causing the SIRPα cytoplasmic immunoreceptor to phosphorylate its tyrosine-based inhibitory motif. Src homology 1 and 2 phosphatases are subsequently recruited because of this mechanism (200).

Inhibition of phagocytosis results from the downstream signaling cascade's prevention of myosin-IIA aggregation at the phagocytic synapse (200). As a result, the CD47/SIRPα axis is mainly thought of as a don't eat me signal that enables CD47-expressing cells to avoid being phagocytosed by macrophages (200). In contrast, cells lacking CD47 are quickly destroyed by wild-type macrophages (201). Thus, most cell types, including erythroblasts, platelets, and hematopoietic stem cells, express CD47 on their surfaces to avoid being phagocytosed by macrophages (200). However, a similar mechanism of elevating the expression of CD47, and thereby inhibiting macrophage phagocytosis, was found in numerous hematological and solid tumors (129, 198, 202–206). These findings demonstrate that CD47/SIRPα cross-talk acts as a protective immunological checkpoint associated with phagocytosis. Furthermore, authors documented a substantial positive connection between high CD47 expression and poor prognosis for cancer (125, 203, 207–209), leading to several approaches aimed at blockade of this signaling axis. CD47-targeting approaches include the anti-CD47 antibodies Hu5F9-G4 (NCT02216409), SRF231 (NCT035123), and IBI188 (NCT03763149) and the anti-SIRPα antibody BI-765063 (NCT03990233). The anti-CD47 mAb Magrolimab is reported to be the first therapeutic drug to target macrophages (54). These findings demonstrate that suppression of CD47/SIRP cross-talk may indeed improve antitumor activity of macrophages and that using this approach in combination with other therapies may further improve results of immunotherapy (127, 128). Furthermore, clinical studies demonstrated the significance of blocking the CD47/SIRP interaction in animals bearing xenograft models with a variety of hematological cancers, such as acute myeloid leukemia, myelodysplastic syndrome, and refractory non-Hodgkin lymphoma (47, 97, 124, 177, 200, 210).

The results of the studies described above demonstrated that anti-CD47 antibodies facilitate tumor-cell detection and phagocytosis by macrophages (211). Furthermore, macrophage removal reversed tumor development following CD47 blockage, demonstrating that macrophages are essential for suppressing the proliferation of cancer cells after CD47 dampening. Targeting cancer cells with CD47 blockage is carried out using four major strategies (54, 126, 127, 208). (1) Direct killing of cancerous cells. Anti-CD47 mAbs cause tumor cells to die via a process unrelated to caspases (212). (2) Macrophage-regulated antibody-dependent cellular phagocytosis. The use of anti-CD47 mAbs reduces CD47/SIRPα cross-talk, thereby causing macrophages to phagocytose tumor cells (213). Furthermore, inhibiting CD47/SIRPα cross-talk causes tumor cells to be phagocytosed by all macrophage populations, particularly M1 and M2c macrophages (214–216). That study also demonstrated that preventing CD47/SIRPα cross-talk causes a variety of polarized macrophages to engulf tumor cells and that this action is necessary for producing FcγRs (217). This suggests that inhibiting CD47 efficiently causes the diverse macrophage population seen in *in vivo* studies to start destroying tumor cells. Enhancement of antigen presentation ability and $CD8^+$ T-cell proliferation *in vitro* are primarily caused by increased cancer cell phagocytosis brought on by the interruption of CD47/SIRPα cross-talk. (3) T-cell-induced immunological responses and DC-mediated antigen presentation. Studies demonstrated that anti-CD47 mAbs stimulate DCs to phagocytose tumor cells, which is followed by antigen presentation to $CD8^+$ T cells to trigger an anticancer adaptive immune response

(217). (4) NK-cell-modulated antibody-dependent cellular cytotoxicity and complement-dependent cytotoxicity. SIRPα is a notable suppressor of NK-cell-modulated cytotoxicity, whereas anti-CD47 mAbs kill cancerous cells via the antibody-dependent cellular cytotoxicity and complement-dependent cytotoxicity pathways (197). Consequently, preventing CD47/SIRPα cross-talk stimulates the innate and adaptive immune responses, resulting in tumor-cell apoptosis.

Table 2 includes a list of potential targets and the phases of clinical trials of cancer treatments using these targets performed thus far. Also, in several preclinical studies, researchers have investigated potential therapeutic approaches combining anti-CD47 strategies with anti-CD20 strategies for lymphoma, anti-HER2 strategies for breast cancer, and anti-EGFR strategies for colorectal cancer. The results of these studies indicated that the mechanisms of action of these tumor-opsonizing mAbs can be greatly potentiated by anti-CD47 strategies (240–245). Concerns related to CD47 expression in healthy platelets and red blood cells led to the development of antibodies with weaker anti-CD47 properties and selective SIRPα inhibitors. Several anti-CD47 agents, such as TTI-621 (NCT03530683), TTI-622 (NCT02890368), and ALX148 (NCT04675333), have undergone clinical trial evaluation. In addition to the use of immunomodulatory agents, targeting immune checkpoint pathways could constitute an additional approach. A series of bispecific antibodies combining anti-CD47 specificity with anti-PD-L1, -EGFR, -CD19, or -CD20 activity may preserve tumor-specific phagocytosis-stimulating activities while sparing the host cells that do not express the tumor antigen, thus limiting toxicity. As discussed above, M2 TAMs may possess only low capacity for phagocytosis or the ability to present antigens to cytotoxic T lymphocytes, and thus showing impaired immunological activity. Treatment with antibodies targeting CD47 may be a tactic to help TAMs regain their immunological characteristics. By blocking the connection between CD47 and SIRPα, anti-CD47 antibodies may improve macrophages' ability to fight tumors (246, 247). Blocking the CD47/SIRPα pathway had promising results in treatment of several solid tumors and hematological cancers such as glioblastoma, lymphoma, and breast cancer and may compel TAMs to phagocytose tumor cells (246, 248–255). Other strategies for harnessing or restoring antitumor properties of macrophages are discussed below.

8.3.2 Other checkpoint signaling pathways

Additional don't eat me signals have been identified, such as SIGLEC1 (CD169), the PD-1/PD-L1 axis (161), LILRB, and targeting scavenger antigens. SIGLEC1 (sialoadhesin/CD169) is a membrane protein that binds to sialic acid and mediates cell–cell interactions. CD169 is expressed by a fraction of macrophages that undergo M2 polarization and is upregulated in human cancer cells. As observed with CD47, expression of CD169 correlates with a dismal prognosis in cancer patients (126, 256). Depletion of $CD169^+$ TAMs was effective in reducing tumor burdens and metastasis in mouse models of breast cancer, whereas targeting of SIGLEC7 and SIGLEC9 led to a significant reduction in tumor burdens in transgenic mice expressing the human transgenes for SIGLEC7 and SIGLEC9 but lacking expression of the murine homolog Siglec-E that were transplanted with murine B16 and B16-FUT3 lung cancer cells (257). SIGLEC proteins contain immunoreceptor tyrosine-based inhibitory motifs in the cytoplasmic tail, which, through their inhibitory and suppressive activation signals, regulate the functions of several immune cells (51). Another molecule that is frequently overexpressed by diverse tumor types is CD24. Binding of CD24 to SIGLEC10, which is overexpressed by TAMs, leads to phagocytosis inhibition (256). Experimental targeting of SIGLEC10 with mAb against SIGLEC10 restored the phagocytosis properties of macrophages in preclinical models of ovarian cancer (51).

Another approach to stimulating macrophages to regain their antitumor activity may be inhibition of LILRB, a receptor that engages with MHC-I protein (256). Suppression of MHC-I molecules is one of the best-known mechanisms cancer cells use to circumvent recognition by T cells (51, 258). The expression of MHC-I protein by tumor cells was shown to correlate with the level of tumor resistance to anti-CD47 therapy. Of note, like SIGLECs and CD24, LILRB was shown to contain an immunoreceptor tyrosine-based inhibitory motif that exerts an inhibitory activity on immune cells and to be widely expressed by immune cells and enriched in TAMs. Anti-CD47 therapy resistance of tumor cells may be restored by treatment with an LILRB1-blocking antibody. Furthermore, LILRB antagonists such as MK-4830 (NCT03564691), a human mAb directed against LILRB2, in conjunction with IL-4 or macrophage colony-stimulating factor, may alter the ECM composition, limit the recruitment of Tregs to the TME, inhibit the function of MDSCs, and enhance proinflammatory activation and phagocytic activity of macrophages (30, 256, 258, 259). In phase 1 dose-escalation studies in patients with advanced solid tumors, treatment with MK-4830 alone or in combination with anti-PD-1 therapy produced durable responses that correlated with enhanced cytotoxic T-lymphocyte-mediated antitumor immune response. Therapeutic approaches are also targeting LILRB4, and blockade of it had potent activity in reshaping tumor-infiltrating T cells and reversing the M2-suppressive phenotype of TAMs (258).

Other molecules abundantly expressed in TAMs include several types of scavenging receptors. These receptors not only identify specific types of TAMs but also are apparent therapeutic targets with the aim of potentiation of a proinflammatory switch toward the M1 phenotype. Specifically, researchers observed significant correlation between expression of CD163 and progression of several types of solid tumors (139, 167, 260). CD163 enables macrophages to remove erythrocyte debris by binding to haptoglobin. Of note, depletion of $CD163^+$ TAMs resulted in tumor regression in a mouse model of anti-PD-1-resistant melanoma (261–264). Furthermore, depletion of $CD163^+$ TAMs led to restoration of cytotoxic T-cell and inflammatory monocyte activity, leading to resensitization of tumor cells to anti-PD-1 therapy (265).

Other receptors highly expressed on TAMs, related to the M2 phenotype, are mannose receptor 1 (CD206) and MARCO (181–183). CD206 is a macrophage scavenger receptor that binds to several endogenous ligands in addition to pathogen moieties such as tumor mucins (186, 213). CD206 engages on macrophages maintaining the endocytosis and phagocytosis, and thus immune homeostasis by scavenging unwanted mannoglycoproteins; however, through their interactions with tumor mucins or upon an agonist anti-mannose receptor mAbs, they induced an

TABLE 2 Clinical trials of macrophage-targeting therapies for cancer.

Target	Treatment	Phase	Cancer Type	Trial Status	Reference
CSF-1R	Emactuzumab	2	Breast cancer	Closed	(18, 172)
	JNJ-40346527	3	Tenosynovial solid tumors	Closed	(18, 218, 219)
	Cabiralizumab	1	Pancreatic cancer	Open	(18)
	Cabiralizumab + APX005 + nivolumab	1	Melanoma, non-small cell lung cancer, renal cell carcinoma	Active	(18)
	Cabiralizumab (FPA008) + nivolumab (Opdivo)	1/2	Advanced solid tumors	Closed	(18)
	Cabiralizumab (FPA008) + nivolumab (Opdivo)	2	Head and neck tumors	Active	(18)
	Cabiralizumab (FPA008) + nivolumab (Opdivo)	2	Lymphoma	Active	(18)
	Emactuzumab + PD-L1 inhibitor (atezolizumab)	1/2	Advanced solid tumors	Open	(18)
CD47/ SIRPα	Hu5F9-G4	1	Solid tumors	Closed	(220)
	Magrolimab	1/2	Acute myeloid leukemia	Closed	(88)
CD40/ CD40L	APX005M	1/2	Pancreatic cancer	Closed	(221, 222)
	Selicrelumab	1/2	Melanoma, pancreatic cancer	Open	(49, 223, 224)
CD68	ADG116	1/2	Solid tumors, melanoma, head and neck cancer	Closed	(57, 225–228)
CCR2	PF-04136309	1	Pancreatic cancer	Closed	(57, 98, 146, 149–151)
	CCX872	1/2	Solid tumors	Closed	(57, 98, 146, 149–151)
TLR7/8/9	GSK2831781	1	Solid tumors	Closed	(57, 98, 146, 149–151)
	IMO-2125	1/2	Melanoma, head and neck cancer	Closed	(57, 98, 146, 149–151)
CD206	ANG4043	1	Solid tumors	Closed	(229)
ATM/TTK	AZD1390	1/2	Solid tumors	Closed	(230, 231)
	CFI-402257	1/2	Advanced solid tumors	Closed	(232–234)
CD47	TTI-621	1/2	Solid tumors and hematological cancers	Open	(198)
	AO-176	1	Solid tumors	Closed	(235)
	CC-90002 + nivolumab (Opdivo)	1b/2	Advanced solid tumors	Open	(236)
	Hu5F9-G4 + rituximab	1	Non-Hodgkin lymphoma	Open	(237, 238) (220)
CD115/ CSF1R	LY3022855	1	Solid tumors	Closed	(18, 84, 159, 169)
PD-1/PD-L1	Lenvatinib and pembrolizumab	1	Solid tumors	Closed	(239)

immunosuppressive phenotype with increased production of cytokines such IL-10 by TAMs (74, 94). Treatment with RP-182 peptide, which binds to CD206/mannose receptor 1 and induces a conformational switch of the receptor, partially depletes $CD206^+$ macrophages and reprograms the remaining TAMs into antitumor M1-like effectors with increased inflammatory cytokine production and the ability to phagocytose cancer cells (6, 266). In murine cancer models, RP-182 suppressed tumor growth, extended survival, and synergized with combined immunotherapy (266). Of note, targeting MARCO with mAbs induced mainly an antitumor immune response through reprogramming of TAMs (267).

Immunosuppressive M2-like macrophages also express the receptor Clever-1 (stabilin-1), an adhesion and scavenger receptor. Clever-1 binds to several ligands, primarily lipoproteins and carbohydrates, mediating endocytosis of scavenged material and its delivery to the endosomal compartment, ultimately resulting in suppression of macrophages and impaired activation of Th1 lymphocytes (268, 269). Antibody blockade of Clever-1 with FP-1305

caused a phenotypic switch in TAMs from immunosuppressive to proinflammatory and activation of T-cell responses and delayed tumor growth in preclinical studies (269–272). These preclinical results led to a phase 1 trial to determine the safety and preliminary effectiveness of FP-1305, a humanized anti-Clever-1 antibody administered to heavily pretreated patients with metastatic solid tumors (269). Encouraging results of this trial indicated a proinflammatory switch of monocytes, enhanced capability of macrophages to cross-present scavenged antigens, and activation of T cells (270). TAMs also express PD-1, which inhibits phagocytosis and tumor immunity, impairing the PD-1/PD-L1 axis in macrophages. Of note, PD-L1 expression in cancer cells may concomitantly enable evasion from not only T-cell cytotoxicity but also macrophage-mediated phagocytosis (273–275). Therefore, blockade of the PD-1/PD-L1 axis may enhance an antitumor immunity of both adaptive and innate mechanisms.

Of note, the receptors PD-1, LILRB1, and SIRPα all contain an immunoreceptor tyrosine-based inhibitory motif domain, which may be instrumental for downstream signals that inhibit phagocytosis (258, 259, 274, 276, 277). Based on this, in studies aimed at monitoring response in patients with cancer undergoing treatment with immune checkpoint inhibitors, researchers should consider the myeloid compartment as a potential target and predictive biomarker (104, 160). TAMs were also shown to upregulate triggering receptor expressed on myeloid cells 2 (104, 237, 274, 278). This protein scavenges large molecules like lipoproteins and phospholipids as well as cell debris. Targeting of triggering receptor expressed on myeloid cells^{+} TAMs led to restricted tumor growth and resensitization to anti-PD-1 therapy. Investigators recently evaluated PY414, a humanized mAb targeting triggering receptor expressed on myeloid cells 2^{+} macrophages, in a phase 1 clinical trial in patients with advanced solid tumors (NCT04691375) (237, 278). Finally, another ligand strongly upregulated in M2 macrophages and expressed in TAMs is P-selectin glycoprotein ligand-1 (279). This protein has high affinity for VISTA (B7-H5 and PD-1H) and selectins, and upon activation, it contributes to T-cell dysfunction in cancer patients (280). Targeting of P-selectin glycoprotein ligand-1 should be a subject of further investigation.

8.4 Targeting epigenetic and metabolic changes in TAMs

Therapy resistance may be a consequence of metabolic rewiring in both tumor cells and cellular immune compartment of TME. Downstream metabolic rewiring of macrophage function following polarization changes involves complex changes in amino acid, lipid, and iron metabolism (19, 69, 134, 196, 281, 282). This complex series of events provides potential targets to rewire macrophage function at the metabolic level. One of the promising approaches to harnessing the antitumor potential of macrophages is epigenetic regulation by class IIa HDACs. TMP195, a selective class IIa HDAC inhibitor, exhibited the ability to effectively modify the transcription profile of macrophages, resulting in macrophage-mediated reduction of tumor growth in a breast cancer model (81, 184). Another HDAC inhibitor, tefinostat (CHR-2845), is cleaved to an active acid form CHR-2847 via nonspecific esterase liver carboxylesterase 1, an enzyme selectively present only in monocytoid-lineage cells and some hepatocytes. Because of this feature, tefinostat has been successfully tested in a phase 1 clinical trial in patients with advanced hematological cancers such as myelodysplastic syndrome and chronic myeloid leukemia (NCT00820508). Also, carboxylesterase 1 may be used as an elegant tool for developing drugs with macrophage-selective targeting features.

Also, hypoxia and acidosis (Figures 3, 4) play a crucial role in the TME and can modulate the function of TAMs. For instance, the oxygen demand of initially fast-proliferating tumor cells may enhance the hypoxic gradient across tumor tissue, forcing both tumor cells and immune cells to adapt to new conditions. Metabolic wiring may therefore promote nonoxidative pathways of energy generation, which leads to increased tumor acidification. Hypoxia can trigger the expression of genes like TNF-α, IL-18, and H1F-1 in TAMs, which may cause inflammation, angiogenesis, and tumor growth. Both hypoxia and acidification were shown to promote polarization of macrophages toward the M2 phenotype and therefore may consolidate the protumorigenic milieu. Therapeutic interventions impeding hypoxia or hypoxia-inducible changes such as blockade of HIF-2 with belzutifan in renal cell cancer cells and use of hypoxia-activated prodrugs may constitute an important backbone of macrophage-targeted therapies (111, 116, 283).

Another opportunity for targeting TAMs and antitumor therapy may be blockade of other metabolic pathways, such as OXPHOS. Given the fact that M2 macrophages and some subsets of hematological cancers and stem cell populations in solid tumors rely more on OXPHOS than other metabolic pathways for biosynthetic and bioenergetic demands, selective blockade of OXPHOS (281, 284) may be synergistic together with anti-CD47 therapy, in both achieving direct eradication of OXPHOS-dependent tumor cells and reshaping the TME through elimination of protumorigenic, OXPHOS-dependent M2 macrophages. Along this line, treatment with the respiratory complex I inhibitor metformin, an antidiabetic agent, reduced the density of TAMs, remodulated their function in the TME, and increased their phagocytic function, and its antitumor efficacy has been tested in several clinical trials for the treatment of diverse types of cancer (260).

M2 TAMs are often characterized by increased consumption of glutamine, which is essential for biosynthetic processes and redox balance. Thus, combined small-molecule inhibitors such as CB-839 and DON downstream from glutamine receptors may be therapeutic options for modulation of myelosuppressive cells (285). Another amino acid of great interest in macrophage targeting is tryptophan. Increased consumption of tryptophan by TAMs owing to elevated expression of the enzyme indoleamine 2,3-dioxygenase 1 results in reduced tryptophan access for T cells and accumulation of kynurenine, leading to severe impairment of cytotoxic T-cell function, and inhibits T lymphocytes division and favors T-cell differentiation toward Treg generation (286). Whereas some results of ongoing clinical trials testing indoleamine 2,3-dioxygenase 1 inhibitors alone or combined with other agents such as pembrolizumab have been negative, results for other

combinations using anti-PD-1 agents are pending (190, 239, 287–292).

Another metabolic vulnerability of TAMs is lipid metabolism. Researchers showed that TAMs possess a defective mechanism of lipid utilization that is most likely linked to activation of immunosuppressive pathways and mediated by the oxysterol receptor and transcription factor LXR (293). Strategies targeting LXR such as exposure to LXR agonists have induced anti-inflammatory actions and reduced the pool of macrophages in affected lesions. Another group of lipid derivatives, prostaglandins, particularly tumor-derived prostaglandin E2, blocked early activation of NK cells and inflammatory activation of myeloid cells, consolidating the immune-suppressive phenotypes of the TME (77). Furthermore, altered prostaglandin pathways have negatively impacted the effectiveness of ICB, which could be reversed and enhanced by use of prostaglandin G/H synthase 2 (cyclooxygenase-2) inhibitors or antagonists of the prostaglandin E2 receptors EP1 and EP2 (51, 77).

Another metabolic factor facilitating cancer therapy resistance is acidosis, particularly lactic acidosis. Lactic acid produced by tumor cells as a by-product of glycolysis can lead to upregulation of the CD206 and CD163 genes in TAMs, which is linked to M2 polarization and immunosuppression. Lactate functionally polarizes macrophages toward an M2-like phenotype and leads to elevated expression of arginase 1 (294) (Figure 4), suggesting that targeting glycolysis in general or lactate flux inhibition in particular positively influences TAM polarization and activity. Other synergistic effects of metabolic interventions that may impair acidosis-driven TAM polarization toward the M2 phenotype or reuse of lactate in solid tumors can be achieved via selective blockade of lactate transporters such as monocarboxylate transporters 1–4 (MCT1–4) (295) or inhibition of glycolysis pathways, for which novel MCT receptor family inhibitors warrant further investigation on their efficacy to inhibit lactate release into TME. Recently, authors discussed the role of metabolic reprogramming in the context of ICB failure. Therefore, combined metabolic and immune interventions may be novel, promising solutions for counteracting the ICB resistance (282).

Moreover, hypoxia and acidosis can negatively impact the secretion of cytokines such as IL-10 by TAMs, which can hinder the immune response and promote tumor survival. Overall, the effects of hypoxia and acidosis on TAMs are multifaceted and rely on specific genes and cytokines. Comprehending these effects can provide valuable insight into the mechanisms of tumor immune evasion and may open doors for developing innovative immunotherapeutic strategies for cancer as summarized in Figures 3–5.

8.5 Chimeric antigen receptor macrophages

As described above, TAMs can make up almost half of the cellular mass of a tumor (31, 46). However, the TAM pool undergoes continuous restructuring through the recruitment of new circulating monocytes (35, 74, 82). Compared with hematological cancers, which are effectively targeted in many cases by chimeric antigen receptor (CAR) T cells, treatment of solid tumors with CAR-T therapy owing to vascular remodeling, hypoxia, and acidosis is often less effective (7, 57, 80, 120, 129, 177). Given the constant trafficking of monocytes into tumors, macrophage-based cell therapies may constitute a feasible alternative to overcome obstacles to treat solid tumors, associated with the use of CAR T cells (15, 57, 80, 120, 129, 177). Thus, engineering macrophages to deliver cytokines or nanoparticles to the TME or equipping them with specific receptors may be a promising therapeutic approach. Researchers have looked at using monocytes replenished with drug-loaded nanoparticles or capable of delivering IFN-α to a tumor site and consequently activating an immune response in preclinical studies. They subjected hematopoietic progenitors under the Tie2 promoter to IFNA1 gene transduction. Tie2-expressing monocytes, which have a high level of tumor-homing ability, successfully migrated to tumors and delivered IFN-α to the TME, triggering the activation of immune cells and inhibiting tumor growth and angiogenesis (108, 145, 177).

Furthermore, studies using soft particles as “backpacks” containing cytokines demonstrated that backpacks were stuck on macrophage surfaces, causing acquisition of the M1 phenotype regardless of the presence of an immunosuppressive TME and leading to significant reduction of tumor growth and metastatic burdens (296). Another approach to modify macrophages was genetic engineering of myeloid cells to express IL-12. This approach elicited a type 1 immune response and reduced metastasis and primary tumor growth (51, 297).

Although transducing human macrophages remains a challenge in developing mononuclear-phagocyte-based cellular therapies for cancer, investigators recently developed several innovative therapies to overcome this obstacle. New-generation CAR macrophages armed with receptors recognizing carcinoembryonic antigen-related cell adhesion molecule 5, CD19, CD22, HER2, and CD5 to improve macrophage’s detection and clearance in patients with hematological malignancies and solid tumors are undergoing preclinical and clinical evaluation (80, 105–108, 145, 177). Despite first promising results, there is still an unmet need to enhance CAR-macrophage-mediated phagocytosis of tumor cells and to provide a solution on maintaining the M1 shape and functions in a stable way regardless of tumor environment together with improving the trafficking of CAR-M into primary and metastatic tumors that should be further investigated.

9 Future recommendations and conclusions

The cross-talk between macrophages and tumor cells plays a critical role in cancer progression and represents a promising target for cancer treatment. However, further research is needed to understand the molecular mechanisms underlying this complex cell–cell communication. Modulation of macrophage polarization, blockade of signaling pathways, and disruption of physical interactions among macrophages and tumor cells are strategies developed to target this cross-talk. The preclinical and clinical evidence supporting the effectiveness of these strategies is promising. To provide better, more targeted, safe, effective cell-

specific therapeutic strategies, more research is warranted to fully understand the molecular mechanisms of these processes. In fact, combinatorial therapies that target multiple aspects of the macrophage–tumor cell cross-talk may be more effective than single-agent therapies, such as modulation of macrophage polarization, blockade of signaling pathways, and disruption of physical interactions. In addition, development of imaging techniques together with *in vitro* and *in vivo* studies of potential biomarkers to monitor the presence, activation state, and function of macrophages in tumors will aid in selecting patients who could benefit from macrophage-targeted therapies. Preclinical and clinical studies of TAMs in cancer should focus on the specific roles of macrophages in different types of tumors to identify the most promising tumor-type-specific targets for therapy. Development of *in vitro* and *in vivo* models that accurately recapitulate the complex interactions between macrophages and tumor cells will be essential to further our understanding of this cross-talk and test new therapeutic strategies. Finally, further study is needed to understand the potential side effects and toxicity of macrophage-targeted therapy, mainly when combined with other cancer treatments. Careful monitoring of potential side and toxic effects therefore is essential when developing macrophage-targeted therapies, particularly in combination with other cancer treatments.

Author contributions

MA: Visualization, Writing – original draft, Writing – review & editing. AK: Visualization, Writing – original draft, Writing – review & editing. FK: Visualization, Writing – original draft, Writing – review & editing. MK: Visualization, Writing – original draft, Writing – review & editing. EM: Visualization, Writing – original draft, Writing – review & editing. MN: Visualization, Writing – original draft, Writing – review & editing. NB: Visualization, Writing – original draft, Writing – review & editing, Funding acquisition, Supervision.

Funding

The author(s) declare that no financial support was received for the research, authorship, and/or publication of this article.

Acknowledgments

All figures were created using BioRender software. The authors thank Don Norwood, Scientific Editor, Research Medical Library, MD Anderson Cancer Center, for editing the manuscript.

Conflict of interest

The authors declare that the research was conducted in the absence of any commercial or financial relationships that could be construed as a potential conflict of interest.

Publisher's note

References

1. Alhudaithi SS, Almuqbil RM, Zhang H, Bielski ER, Du W, Sunbul FS, et al. Local targeting of lung-tumor-associated macrophages with pulmonary delivery of a CSF-1R inhibitor for the treatment of breast cancer lung metastases. *Mol Pharm* (2020) 17:4691–703. doi: 10.1021/acs.molpharmaceut.0c00983

2. Cavalleri T, Greco L, Rubbino F, Hamada T, Quaranta M, Grizzi F, et al. Tumor-associated macrophages and risk of recurrence in stage III colorectal cancer. *J Pathol Clin Res* (2022) 8:307–12. doi: 10.1002/cjp2.267

3. Baghban R, Roshangar L, Jahanban-Esfahlan R, Seidi K, Ebrahimi-Kalan A, Jaymand M, et al. Tumor microenvironment complexity and therapeutic implications at a glance. *Cell Commun Signal* (2020) 18:59. doi: 10.1186/s12964-020-0530-4

4. Prasad S, Saha P, Chatterjee B, Chaudhary AA, Lall R, Srivastava AK. Complexity of tumor microenvironment: therapeutic role of curcumin and its metabolites. *Nutr Cancer* (2023) 75:1–13. doi: 10.1080/01635581.2022.2096909

5. Giraldo NA, Sanchez-Salas R, Peske JD, Vano Y, Becht E, Petitprez F, et al. The clinical role of the TME in solid cancer. *Br J Cancer* (2019) 120:45–53. doi: 10.1038/s41416-018-0327-z

6. Hourani T, Holden JA, Li W, Lenzo JC, Hadjigol S, O'Brien-Simpson NM. Tumor associated macrophages: origin, recruitment, phenotypic diversity, and targeting. *Front Oncol* (2021) 11:788365. doi: 10.3389/fonc.2021.788365

7. Salemme V, Centonze G, Cavallo F, Defilippi P, Conti L. The crosstalk between tumor cells and the immune microenvironment in breast cancer: implications for immunotherapy. *Front Oncol* (2021) 11:610303. doi: 10.3389/fonc.2021.610303

8. Yuan Z, Li Y, Zhang S, Wang X, Dou H, Yu X, et al. Extracellular matrix remodeling in tumor progression and immune escape: from mechanisms to treatments. *Mol Cancer* (2023) 22:48. doi: 10.1186/s12943-023-01744-8

9. Galon J, Bruni D. Approaches to treat immune hot, altered and cold tumours with combination immunotherapies. *Nat Rev Drug Discovery* (2019) 18:197–218. doi: 10.1038/s41573-018-0007-y

10. Petrovic M, Porcello A, Tankov S, Majchrzak O, Kiening M, Laingoniaina AC, et al. Synthesis, formulation and characterization of immunotherapeutic glycosylated dendrimer/cGAMP complexes for CD206 targeted delivery to M2 macrophages in cold tumors. *Pharmaceutics* (2022) 14. doi: 10.3390/pharmaceutics14091883

11. Cassetta L, Fragkogianni S, Sims AH, Swierczak A, Forrester LM, Zhang H, et al. Human tumor-associated macrophage and monocyte transcriptional landscapes reveal cancer-specific reprogramming, biomarkers, and therapeutic targets. *Cancer Cell* (2019) 35:588–602.e10. doi: 10.1016/j.ccell.2019.02.009

12. Nagarsheth N, Wicha MS, Zou W. Chemokines in the cancer microenvironment and their relevance in cancer immunotherapy. *Nat Rev Immunol* (2017) 17:559–72. doi: 10.1038/nri.2017.49

13. Bruni D, Angell HK, Galon J. The immune contexture and Immunoscore in cancer prognosis and therapeutic efficacy. *Nat Rev Cancer* (2020) 20:662–80. doi: 10.1038/s41568-020-0285-7

14. Camus M, Tosolini M, Mlecnik B, Pages F, Kirilovsky A, Berger A, et al. Coordination of intratumoral immune reaction and human colorectal cancer recurrence. *Cancer Res* (2009) 69:2685–93. doi: 10.1158/0008-5472.CAN-08-2654

15. Hao C, Li R, Lu Z, He K, Shen J, Wang T, et al. Predicting prognosis, immunotherapy and distinguishing cold and hot tumors in clear cell renal cell carcinoma based on anoikis-related lncRNAs. *Front Immunol* (2023) 14:1145450. doi: 10.3389/fimmu.2023.1145450

16. Ullman NA, Burchard PR, Dunne RF, Linehan DC. Immunologic strategies in pancreatic cancer: making cold tumors hot. *J Clin Oncol* (2022) 40:2789–805. doi: 10.1200/JCO.21.02616

17. Zhang J, Huang D, Saw PE, Song E. Turning cold tumors hot: from molecular mechanisms to clinical applications. *Trends Immunol* (2022) 43:523–45. doi: 10.1016/j.it.2022.04.010

18. Wang S, Yang Y, Ma P, Huang H, Tang Q, Miao H, et al. Landscape and perspectives of macrophage -targeted cancer therapy in clinical trials. *Mol Ther Oncolytics* (2022) 24:799–813. doi: 10.1016/j.omto.2022.02.019

19. Zhang X, Li S, Malik I, Do MH, Ji L, Chou C, et al. Reprogramming tumour-associated macrophages to outcompete cancer cells. *Nature* (2023) 619:616–23. doi: 10.1038/s41586-023-06256-5

20. Kaymak I, Williams KS, Cantor JR, Jones RG. Immunometabolic interplay in the tumor microenvironment. *Cancer Cell* (2021) 39:28–37. doi: 10.1016/j.ccell.2020.09.004

21. Komohara Y, Takeya M. CAFs and TAMs: maestros of the tumour microenvironment. *J Pathol* (2017) 241:313–5. doi: 10.1002/path.4824

22. Pathria P, Louis TL, Varner JA. Targeting tumor-associated macrophages in cancer. *Trends Immunol* (2019) 40:310–27. doi: 10.1016/j.it.2019.02.003

23. Chaganty BKR, Qiu S, Gest A, Lu Y, Ivan C, Calin GA, et al. Trastuzumab upregulates PD-L1 as a potential mechanism of trastuzumab resistance through engagement of immune effector cells and stimulation of IFNgamma secretion. *Cancer Lett* (2018) 430:47–56. doi: 10.1016/j.canlet.2018.05.009

24. Dan H, Liu S, Liu J, Liu D, Yin F, Wei Z, et al. RACK1 promotes cancer progression by increasing the M2/M1 macrophage ratio *via* the NF-kappaB pathway in oral squamous cell carcinoma. *Mol Oncol* (2020) 14:795–807. doi: 10.1002/1878-0261.12644

25. Korbecki J, Grochans S, Gutowska I, Barczak K, Baranowska-Bosiacka I. CC chemokines in a tumor: A review of pro-cancer and anti-cancer properties of receptors CCR5, CCR6, CCR7, CCR8, CCR9, and CCR10 ligands. *Int J Mol Sci* (2020) 21. doi: 10.3390/ijms21207619

26. Mimura K, Teh JL, Okayama H, Shiraishi K, Kua LF, Koh V, et al. PD-L1 expression is mainly regulated by interferon gamma associated with JAK-STAT pathway in gastric cancer. *Cancer Sci* (2018) 109:43–53. doi: 10.1111/cas.13424

27. Hong IS. Stimulatory versus suppressive effects of GM-CSF on tumor progression in multiple cancer types. *Exp Mol Med* (2016) 48:e242. doi: 10.1038/emm.2016.64

28. Yonemitsu K, Pan C, Fujiwara Y, Miyasato Y, Shiota T, Yano H, et al. GM-CSF derived from the inflammatory microenvironment potentially enhanced PD-L1 expression on tumor-associated macrophages in human breast cancer. *Sci Rep* (2022) 12:12007. doi: 10.1038/s41598-022-16080-y

29. Hanahan D, Coussens LM. Accessories to the crime: functions of cells recruited to the tumor microenvironment. *Cancer Cell* (2012) 21:309–22. doi: 10.1016/j.ccr.2012.02.022

30. Chen Y, McAndrews KM, Kalluri R. Clinical and therapeutic relevance of cancer-associated fibroblasts. *Nat Rev Clin Oncol* (2021) 18:792–804. doi: 10.1038/s41571-021-00546-5

31. Boesch M, Onder L, Cheng HW, Novkovic M, Morbe U, Sopper S, et al. Interleukin 7-expressing fibroblasts promote breast cancer growth through sustenance of tumor cell stemness. *Oncoimmunology* (2018) 7:e1414129. doi: 10.1080/2162402X.2017.1414129

32. Kikuchi K, McNamara KM, Miki Y, Moon JY, Choi MH, Omata F, et al. Effects of cytokines derived from cancer-associated fibroblasts on androgen synthetic enzymes in estrogen receptor-negative breast carcinoma. *Breast Cancer Res Treat* (2017) 166:709–23. doi: 10.1007/s10549-017-4464-5

33. Liubomirski Y, Lerrer S, Meshel T, Rubinstein-Achiasaf L, Morein D, Wiemann S, et al. Tumor-stroma-inflammation networks promote pro-metastatic chemokines and aggressiveness characteristics in triple-negative breast cancer. *Front Immunol* (2019) 10:757. doi: 10.3389/fimmu.2019.00757

34. Comito G, Giannoni E, Segura CP, Barcellos-de-Souza P, Raspollini MR, Baroni G, et al. Cancer-associated fibroblasts and M2-polarized macrophages synergize during prostate carcinoma progression. *Oncogene* (2014) 33:2423–31. doi: 10.1038/onc.2013.191

35. Gok Yavuz B, Gunaydin G, Gedik ME, Kosemehmetoglu K, Karakoc D, Ozgur F, et al. Cancer associated fibroblasts sculpt tumour microenvironment by recruiting monocytes and inducing immunosuppressive PD-1(+) TAMs. *Sci Rep* (2019) 9:3172. doi: 10.1038/s41598-019-39553-z

36. Tajaldini M, Saeedi M, Amiriani T, Amiriani AH, Sedighi S, Mohammad Zadeh F, et al. Cancer-associated fibroblasts (CAFs) and tumor-associated macrophages (TAMs); where do they stand in tumorigenesis and how they can change the face of cancer therapy? *Eur J Pharmacol* (2022) 928:175087. doi: 10.1016/j.ejphar.2022.175087

37. Timperi E, Gueguen P, Molgora M, Magagna I, Kieffer Y, Lopez-Lastra S, et al. Lipid-associated macrophages are induced by cancer-associated fibroblasts and mediate immune suppression in breast cancer. *Cancer Res* (2022) 82:3291–306. doi: 10.1158/0008-5472.CAN-22-1427

38. Ziani L, Chouaib S, Thiery J. Alteration of the antitumor immune response by cancer-associated fibroblasts. *Front Immunol* (2018) 9:414. doi: 10.3389/fimmu.2018.00414

39. Feng B, Wu J, Shen B, Jiang F, Feng J. Cancer-associated fibroblasts and resistance to anticancer therapies: status, mechanisms, and countermeasures. *Cancer Cell Int* (2022) 22:166. doi: 10.1186/s12935-022-02599-7

40. Sakai T, Aokage K, Neri S, Nakamura H, Nomura S, Tane K, et al. Link between tumor-promoting fibrous microenvironment and an immunosuppressive microenvironment in stage I lung adenocarcinoma. *Lung Cancer* (2018) 126:64–71. doi: 10.1016/j.lungcan.2018.10.021

41. Zhang J, Chen L, Xiao M, Wang C, Qin Z. FSP1+ fibroblasts promote skin carcinogenesis by maintaining MCP-1-mediated macrophage infiltration and chronic inflammation. *Am J Pathol* (2011) 178:382–90. doi: 10.1016/j.ajpath.2010.11.017

42. Pich-Bavastro C, Yerly L, Di Domizio J, Tissot-Renaud S, Gilliet M, Kuonen F. Activin A-mediated polarization of cancer-associated fibroblasts and macrophages confers resistance to checkpoint immunotherapy in skin cancer. *Clin Cancer Res* (2023) 29(17):3498–513. doi: 10.1158/1078-0432.c.6731683

43. Qi J, Sun H, Zhang Y, Wang Z, Xun Z, Li Z, et al. Single-cell and spatial analysis reveal interaction of FAP(+) fibroblasts and SPP1(+) macrophages in colorectal cancer. *Nat Commun* (2022) 13:1742. doi: 10.1038/s41467-022-29366-6

44. Sathe A, Mason K, Grimes SM, Zhou Z, Lau BT, Bai X, et al. Colorectal cancer metastases in the liver establish immunosuppressive spatial networking between tumor-associated SPP1+ Macrophages and fibroblasts. *Clin Cancer Res* (2023) 29:244–60. doi: 10.1158/1078-0432.CCR-22-2041

45. Zhang R, Qi F, Zhao F, Li G, Shao S, Zhang X, et al. Cancer-associated fibroblasts enhance tumor-associated macrophages enrichment and suppress NK cells function in colorectal cancer. *Cell Death Dis* (2019) 10:273. doi: 10.1038/s41419-019-1435-2

46. Bronikowska I, Swietochowska E, Morawski R, Sowa P, Czecior E. Concentration of hypoxia-inducible factor-1, glucose transporter 1 and vascular endothelial growth factor in tissue samples and serum in patients with primary laryngeal carcinoma. *Acta Otolaryngol* (2022) 142:532–6. doi: 10.1080/00016489.2022.2085885

47. Advani R, Flinn I, Popplewell L, Forero A, Bartlett NL, Ghosh N, et al. CD47 blockade by Hu5F9-G4 and rituximab in non-Hodgkin's lymphoma. *N Engl J Med* (2018) 379:1711–21. doi: 10.1056/NEJMoa1807315

48. Butler JM, Kobayashi H, Rafii S. Instructive role of the vascular niche in promoting tumour growth and tissue repair by angiocrine factors. *Nat Rev Cancer* (2010) 10:138–46. doi: 10.1038/nrc2791

49. Byrne KT, Betts CB, Mick R, Sivagnanam S, Bajor DL, Laheru DA, et al. Neoadjuvant selicrelumab, an agonist CD40 antibody, induces changes in the tumor microenvironment in patients with resectable pancreatic cancer. *Clin Cancer Res* (2021) 27:4574–86. doi: 10.1158/1078-0432.CCR-21-1047

50. Cao X, Wang Y, Zhang W, Zhong X, Gunes EG, Dang J, et al. Targeting macrophages for enhancing CD47 blockade-elicited lymphoma clearance and overcoming tumor-induced immunosuppression. *Blood* (2022) 139:3290–302. doi: 10.1182/blood.2021013901

51. Mantovani A, Allavena P, Marchesi F, Garlanda C. Macrophages as tools and targets in cancer therapy. *Nat Rev Drug Discovery* (2022) 21:799–820. doi: 10.1038/s41573-022-00520-5

52. Dehne N, Mora J, Namgaladze D, Weigert A, Brune B. Cancer cell and macrophage cross-talk in the tumor microenvironment. *Curr Opin Pharmacol* (2017) 35:12–9. doi: 10.1016/j.coph.2017.04.007

53. Sica A, Mantovani A. Macrophage plasticity and polarization: in *vivo* veritas. *J Clin Invest* (2012) 122:787–95. doi: 10.1172/JCI59643

54. Jiang Z, Sun H, Yu J, Tian W, Song Y. Targeting CD47 for cancer immunotherapy. *J Hematol Oncol* (2021) 14:180. doi: 10.1186/s13045-021-01197-w

55. Xue J, Schmidt SV, Sander J, Draffehn A, Krebs W, Quester I, et al. Transcriptome-based network analysis reveals a spectrum model of human macrophage activation. *Immunity* (2014) 40:274–88. doi: 10.1016/j.immuni.2014.01.006

56. Biswas SK, Allavena P, Mantovani A. Tumor-associated macrophages: functional diversity, clinical significance, and open questions. *Semin Immunopathol* (2013) 35:585–600. doi: 10.1007/s00281-013-0367-7

57. Duan Z, Luo Y. Targeting macrophages in cancer immunotherapy. *Signal Transduct Target Ther* (2021) 6:127. doi: 10.1038/s41392-021-00506-6

58. Elomaa H, Ahtiainen M, Vayrynen SA, Ogino S, Nowak JA, Lau MC, et al. Spatially resolved multimarker evaluation of CD274 (PD-L1)/PDCD1 (PD-1) immune checkpoint expression and macrophage polarisation in colorectal cancer. *Br J Cancer* (2023) 128:2104–15. doi: 10.1038/s41416-023-02238-6

59. Al-Matary YS, Botezatu L, Opalka B, Hones JM, Lams RF, Thivakaran A, et al. Acute myeloid leukemia cells polarize macrophages towards a leukemia supporting state in a Growth factor independence 1 dependent manner. *Haematologica* (2016) 101:1216–27. doi: 10.3324/haematol.2016.143180

60. Baradaran A, Asadzadeh Z, Hemmat N, Baghbanzadeh A, Shadbad MA, Khosravi N, et al. The cross-talk between tumor-associated macrophages and tumor endothelium: Recent advances in macrophage-based cancer immunotherapy. *BioMed Pharmacother* (2022) 146:112588. doi: 10.1016/j.biopha.2021.112588

61. Di Somma S, Napolitano F, Portella G, Malfitano AM. Cross talk of macrophages with tumor microenvironment cells and modulation of macrophages in cancer by Virotherapy. *Biomedicines* (2021) 9. doi: 10.3390/biomedicines9101309

62. Riabov V, Gudima A, Wang N, Mickley A, Orekhov A, Kzhyshkowska J. Role of tumor associated macrophages in tumor angiogenesis and lymphangiogenesis. *Front Physiol* (2014) 5:75. doi: 10.3389/fphys.2014.00075

63. Sanjabi S, Oh SA, Li MO. Regulation of the immune response by TGF-beta: from conception to autoimmunity and infection. *Cold Spring Harb Perspect Biol* (2017) 9. doi: 10.1101/cshperspect.a022236

64. Chen H, Zha J, Tang R, Chen G. T-cell immunoglobulin and mucin-domain containing-3 (TIM-3): Solving a key puzzle in autoimmune diseases. *Int Immunopharmacol* (2023) 121:110418. doi: 10.1016/j.intimp.2023.110418

65. Nasrollahzadeh E, Razi S, Keshavarz-Fathi M, Mazzone M, Rezaei N. Pro-tumorigenic functions of macrophages at the primary, invasive and metastatic tumor site. *Cancer Immunol Immunother* (2020) 69:1673–97. doi: 10.1007/s00262-020-02616-6

66. Forder A, Hsing CY, Trejo Vazquez J, Garnis C. Emerging role of extracellular vesicles and cellular communication in metastasis. *Cells* (2021) 10. doi: 10.3390/cells10123429

67. Knapinska AM, Fields GB. The expanding role of MT1-MMP in cancer progression. *Pharm (Basel)* (2019) 12. doi: 10.3390/ph12020077

68. Quintero-Fabian S, Arreola R, Becerril-Villanueva E, Torres-Romero JC, Arana-Argaez V, Lara-Riegos J, et al. Role of matrix metalloproteinases in angiogenesis and cancer. *Front Oncol* (2019) 9:1370. doi: 10.3389/fonc.2019.01370

69. Koo SJ, Garg NJ. Metabolic programming of macrophage functions and pathogens control. *Redox Biol* (2019) 24:101198. doi: 10.1016/j.redox.2019.101198

70. Marchesi F, Cirillo M, Bianchi A, Gately M, Olimpieri OM, Cerchiara E, et al. High density of CD68+/CD163+ tumour-associated macrophages (M2-TAM) at diagnosis is significantly correlated to unfavorable prognostic factors and to poor clinical outcomes in patients with diffuse large B-cell lymphoma. *Hematol Oncol* (2015) 33:110–2. doi: 10.1002/hon.2142

71. Siemaszko J, Marzec-Przyszlak A, Bogunia-Kubik K. NKG2D natural killer cell receptor-A short description and potential clinical applications. *Cells* (2021) 10. doi: 10.3390/cells10061420

72. Li W, Wang Y, Zhao H, Zhang H, Xu Y, Wang S, et al. Identification and transcriptome analysis of erythroblastic island macrophages. *Blood* (2019) 134:480–91. doi: 10.1182/blood.2019000430

73. Szebeni GJ, Vizler C, Kitajka K, Puskas LG. Inflammation and cancer: extra- and intracellular determinants of tumor-associated macrophages as tumor promoters. *Mediators Inflammation* (2017) 2017:9294018. doi: 10.1155/2017/9294018

74. Tiemessen MM, Jagger AL, Evans HG, van Herwijnen MJ, John S, Taams LS. CD4+CD25+Foxp3+ regulatory T cells induce alternative activation of human monocytes/macrophages. *Proc Natl Acad Sci U.S.A.* (2007) 104:19446–51. doi: 10.1073/pnas.0706832104

75. Li S, Mirlekar B, Johnson BM, Brickey WJ, Wrobel JA, Yang N, et al. STING-induced regulatory B cells compromise NK function in cancer immunity. *Nature* (2022) 610:373–80. doi: 10.1038/s41586-022-05254-3

76. Mirlekar B, Wang Y, Li S, Zhou M, Entwistle S, De Buysscher T, et al. Balance between immunoregulatory B cells and plasma cells drives pancreatic tumor immunity. *Cell Rep Med* (2022) 3:100744. doi: 10.1016/j.xcrm.2022.100744

77. Finetti F, Travelli C, Ercoli J, Colombo G, Buoso E, Trabalzini L. Prostaglandin E2 and cancer: insight into tumor progression and immunity. *Biol (Basel)* (2020) 9. doi: 10.3390/biology9120434

78. Zou W, Restifo NP. T(H)17 cells in tumour immunity and immunotherapy. *Nat Rev Immunol* (2010) 10:248–56. doi: 10.1038/nri2742

79. Dutta P, Bishayi B. IL-10 in combination with IL-12 and TNF-alpha attenuates CXCL8/CXCR1 axis in peritoneal macrophages of mice infected with Staphylococcus aureus through the TNFR1-IL-1R-NF-kappaB pathway. *Int Immunopharmacol* (2023) 120:110297. doi: 10.1016/j.intimp.2023.110297

80. Anderson NR, Minutolo NG, Gill S, Klichinsky M. Macrophage-based approaches for cancer immunotherapy. *Cancer Res* (2021) 81:1201–8. doi: 10.1158/0008-5472.CAN-20-2990

81. Kim YD, Park SM, Ha HC, Lee AR, Won H, Cha H, et al. HDAC inhibitor, CG-745, enhances the anti-cancer effect of anti-PD-1 immune checkpoint inhibitor by modulation of the immune microenvironment. *J Cancer* (2020) 11:4059–72. doi: 10.7150/jca.44622

82. Kuang DM, Peng C, Zhao Q, Wu Y, Chen MS, Zheng L. Activated monocytes in peritumoral stroma of hepatocellular carcinoma promote expansion of memory T helper 17 cells. *Hepatology* (2010) 51:154–64. doi: 10.1002/hep.23291

83. Sai J, Owens P, Novitskiy SV, Hawkins OE, Vilgelm AE, Yang J, et al. PI3K inhibition reduces mammary tumor growth and facilitates antitumor immunity and anti-PD1 responses. *Clin Cancer Res* (2017) 23:3371–84. doi: 10.1158/1078-0432.CCR-16-2142

84. Zhu Y, Knolhoff BL, Meyer MA, Nywening TM, West BL, Luo J, et al. CSF1/CSF1R blockade reprograms tumor-infiltrating macrophages and improves response to T-cell checkpoint immunotherapy in pancreatic cancer models. *Cancer Res* (2014) 74:5057–69. doi: 10.1158/0008-5472.CAN-13-3723

85. Lan J, Sun L, Xu F, Liu L, Hu F, Song D, et al. M2 macrophage-derived exosomes promote cell migration and invasion in colon cancer. *Cancer Res* (2019) 79:146–58. doi: 10.1158/0008-5472.CAN-18-0014

86. Pu J, Xu Z, Nian J, Fang Q, Yang M, Huang Y, et al. M2 macrophage-derived extracellular vesicles facilitate CD8+T cell exhaustion in hepatocellular carcinoma *via* the miR-21-5p/YOD1/YAP/beta-catenin pathway. *Cell Death Discovery* (2021) 7:182. doi: 10.1038/s41420-021-00556-3

87. Cui J, Li Q, Luo M, Zhong Z, Zhou S, Jiang L, et al. Leukemia cell-derived microvesicles induce T cell exhaustion *via* miRNA delivery. *Oncoimmunology* (2018) 7: e1448330. doi: 10.1080/2162402X.2018.1448330

88. Daver N, Jonas BA, Medeiros BC, Patil U, Yan M. Phase 1b, open-label study evaluating the safety and pharmacokinetics of atezolizumab (anti-PD-L1 antibody) administered in combination with Hu5F9-G4 to patients with relapsed and/or refractory acute myeloid leukemia. *Leuk Lymphoma* (2022) 63:2711–4. doi: 10.1080/10428194.2022.2092853

89. Azambuja JH, Ludwig N, Yerneni SS, Braganhol E, Whiteside TL. Arginase-1+ Exosomes from reprogrammed macrophages promote glioblastoma progression. *Int J Mol Sci* (2020) 21. doi: 10.3390/ijms21113990

90. De Henau O, Rausch M, Winkler D, Campesato LF, Liu C, Cymerman DH, et al. Overcoming resistance to checkpoint blockade therapy by targeting PI3Kgamma in myeloid cells. *Nature* (2016) 539:443–7. doi: 10.1038/nature20554

91. Dekker Y, Le Devedec SE, Danen EHJ, Liu Q. Crosstalk between hypoxia and extracellular matrix in the tumor microenvironment in breast cancer. *Genes (Basel)* (2022) 13. doi: 10.3390/genes13091585

92. Jiang J, Wang GZ, Wang Y, Huang HZ, Li WT, Qu XD. Hypoxia-induced HMGB1 expression of HCC promotes tumor invasiveness and metastasis *via* regulating macrophage-derived IL-6. *Exp Cell Res* (2018) 367:81–8. doi: 10.1016/j.yexcr.2018.03.025

93. Xiao P, Long X, Zhang L, Ye Y, Guo J, Liu P, et al. Neurotensin/IL-8 pathway orchestrates local inflammatory response and tumor invasion by inducing M2 polarization of Tumor-Associated macrophages and epithelial-mesenchymal transition of hepatocellular carcinoma cells. *Oncoimmunology* (2018) 7:e1440166. doi: 10.1080/2162402X.2018.1440166

94. Ghosh S, Mukherjee S, Choudhury S, Gupta P, Adhikary A, Baral R, et al. Reactive oxygen species in the tumor niche triggers altered activation of macrophages and immunosuppression: Role of fluoxetine. *Cell Signal* (2015) 27:1398–412. doi: 10.1016/j.cellsig.2015.03.013

95. Grivennikov SI, Wang K, Mucida D, Stewart CA, Schnabl B, Jauch D, et al. Adenoma-linked barrier defects and microbial products drive IL-23/IL-17-mediated tumour growth. *Nature* (2012) 491:254–8. doi: 10.1038/nature11465

96. Kong L, Zhou Y, Bu H, Lv T, Shi Y, Yang J. Deletion of interleukin-6 in monocytes/macrophages suppresses the initiation of hepatocellular carcinoma in mice. *J Exp Clin Cancer Res* (2016) 35:131. doi: 10.1186/s13046-016-0412-1

97. Liu X, Guo A, Tu Y, Li W, Li L, Liu W, et al. Fruquintinib inhibits VEGF/VEGFR2 axis of choroidal endothelial cells and M1-type macrophages to protect against mouse laser-induced choroidal neovascularization. *Cell Death Dis* (2020) 11:1016. doi: 10.1038/s41419-020-03222-1

98. Wu Y, Jennings NB, Sun Y, Dasari SK, Bayraktar E, Corvigno S, et al. Targeting CCR2(+) macrophages with BET inhibitor overcomes adaptive resistance to anti-VEGF therapy in ovarian cancer. *J Cancer Res Clin Oncol* (2022) 148:803–21. doi: 10.1007/s00432-021-03885-z

99. Yu Y, Dai K, Gao Z, Tang W, Shen T, Yuan Y, et al. Sulfated polysaccharide directs therapeutic angiogenesis via endogenous VEGF secretion of macrophages. *Sci Adv* (2021) 7. doi: 10.1126/sciadv.abd8217

100. Zhang Y, Zhang C, Li L, Liang X, Cheng P, Li Q, et al. Lymphangiogenesis in renal fibrosis arises from macrophages *via* VEGF-C/VEGFR3-dependent autophagy and polarization. *Cell Death Dis* (2021) 12:109. doi: 10.1038/s41419-020-03385-x

101. Kitamura T, Qian BZ, Soong D, Cassetta L, Noy R, Sugano G, et al. CCL2-induced chemokine cascade promotes breast cancer metastasis by enhancing retention of metastasis-associated macrophages. *J Exp Med* (2015) 212:1043–59. doi: 10.1084/jem.20141836

102. Pollard JW. Tumour-educated macrophages promote tumour progression and metastasis. *Nat Rev Cancer* (2004) 4:71–8. doi: 10.1038/nrc1256

103. Wu N, Wang Y, Wang K, Zhong B, Liao Y, Liang J, et al. Cathepsin K regulates the tumor growth and metastasis by IL-17/CTSK/EMT axis and mediates M2 macrophage polarization in castration-resistant prostate cancer. *Cell Death Dis* (2022) 13:813. doi: 10.1038/s41419-022-05215-8

104. Yan S, Wan G. Tumor-associated macrophages in immunotherapy. *FEBS J* (2021) 288:6174–86. doi: 10.1111/febs.15726

105. Li S, Song L, Zhang Y, Zhan Z, Yang Y, Yu L, et al. Optimizing the method for differentiation of macrophages from human induced pluripotent stem cells. *Stem Cells Int* (2022) 2022:6593403. doi: 10.1155/2022/6593403

106. Takata K, Kozaki T, Lee CZW, Thion MS, Otsuka M, Lim S, et al. Induced-pluripotent-stem-cell-derived primitive macrophages provide a platform for modeling tissue-resident macrophage differentiation and function. *Immunity* (2020) 52:417–8. doi: 10.1016/j.immuni.2020.01.004

107. Xue D, Lu S, Zhang H, Zhang L, Dai Z, Kaufman DS, et al. Induced pluripotent stem cell-derived engineered T cells, natural killer cells, macrophages, and dendritic cells in immunotherapy. *Trends Biotechnol* (2023) 41:907–22. doi: 10.1016/j.tibtech.2023.02.003

108. Zhang J, Webster S, Duffin B, Bernstein MN, Steill J, Swanson S, et al. Generation of anti-GD2 CAR macrophages from human pluripotent stem cells for cancer immunotherapies. *Stem Cell Rep* (2023) 18:585–96. doi: 10.1016/j.stemcr.2022.12.012

109. Du S, Qian J, Tan S, Li W, Liu P, Zhao J, et al. Tumor cell-derived exosomes deliver TIE2 protein to macrophages to promote angiogenesis in cervical cancer. *Cancer Lett* (2022) 529:168–79. doi: 10.1016/j.canlet.2022.01.005

110. Moradi-Gharibvand N, Hashemibeni B. The effect of stem cells and vascular endothelial growth factor on cancer angiogenesis. *Adv BioMed Res* (2023) 12:124. doi: 10.4103/abr.abr_378_21

111. Baran N, Konopleva M. Molecular pathways: hypoxia-activated prodrugs in cancer therapy. *Clin Cancer Res* (2017) 23:2382–90. doi: 10.1158/1078-0432.CCR-16-0895

112. Chen G, Wu K, Li H, Xia D, He T. Role of hypoxia in the tumor microenvironment and targeted therapy. *Front Oncol* (2022) 12:961637. doi: 10.3389/fonc.2022.961637

113. Midha AD, Zhou Y, Queliconi BB, Barrios AM, Haribowo AG, Chew BTL, et al. Organ-specific fuel rewiring in acute and chronic hypoxia redistributes glucose and fatty acid metabolism. *Cell Metab* (2023) 35:504–16.e5. doi: 10.1016/j.cmet.2023.02.007

114. Zhou J, Lin Y, Kang X, Liu Z, Zou J, Xu F. Hypoxia-mediated promotion of glucose metabolism in non-small cell lung cancer correlates with activation of the EZH2/FBXL7/PFKFB4 axis. *Cell Death Dis* (2023) 14:326. doi: 10.1038/s41419-023-05795-z

115. Roodink I, van der Laak J, Kusters B, Wesseling P, Verrijp K, de Waal R, et al. Development of the tumor vascular bed in response to hypoxia-induced VEGF-A differs from that in tumors with constitutive VEGF-A expression. *Int J Cancer* (2006) 119:2054–62. doi: 10.1002/ijc.22072

116. Choueiri TK, McDermott DF, Merchan J, Bauer TM, Figlin R, Heath EI, et al. Belzutifan plus cabozantinib for patients with advanced clear cell renal cell carcinoma previously treated with immunotherapy: an open-label, single-arm, phase 2 study. *The Lancet Oncol* (2023) 24(5):553–62. doi: 10.1016/S1470-2045(23)00097-9

117. Bai R, Li Y, Jian L, Yang Y, Zhao L, Wei M. The hypoxia-driven crosstalk between tumor and tumor-associated macrophages: mechanisms and clinical treatment strategies. *Mol Cancer* (2022) 21:177. doi: 10.1186/s12943-022-01645-2

118. Cui Z, Ruan Z, Li M, Ren R, Ma Y, Zeng J, et al. Intermittent hypoxia inhibits anti-tumor immune response *via* regulating PD-L1 expression in lung cancer cells and tumor-associated macrophages. *Int Immunopharmacol* (2023) 122:110652. doi: 10.1016/j.intimp.2023.110652

119. Henze AT, Mazzone M. The impact of hypoxia on tumor-associated macrophages. *J Clin Invest* (2016) 126:3672–9. doi: 10.1172/JCI84427

120. DeNardo DG, Ruffell B. Macrophages as regulators of tumour immunity and immunotherapy. *Nat Rev Immunol* (2019) 19:369–82. doi: 10.1038/s41577-019-0127-6

121. Harney AS, Arwert EN, Entenberg D, Wang Y, Guo P, Qian BZ, et al. Real-time imaging reveals local, transient vascular permeability, and tumor cell intravasation stimulated by TIE2hi macrophage-derived VEGFA. *Cancer Discovery* (2015) 5:932–43. doi: 10.1158/2159-8290.CD-15-0012

122. Blazar BR, Lindberg FP, Ingulli E, Panoskaltsis-Mortari A, Oldenborg PA, Iizuka K, et al. CD47 (integrin-associated protein) engagement of dendritic cell and macrophage counterreceptors is required to prevent the clearance of donor lymphohematopoietic cells. *J Exp Med* (2001) 194:541–9. doi: 10.1084/jem.194.4.541

123. Oldenborg PA, Gresham HD, Lindberg FP. CD47-signal regulatory protein alpha (SIRPalpha) regulates Fcgamma and complement receptor-mediated phagocytosis. *J Exp Med* (2001) 193:855–62. doi: 10.1084/jem.193.7.855

124. Eladl E, Tremblay-LeMay R, Rastgoo N, Musani R, Chen W, Liu A, et al. Role of CD47 in hematological Malignancies. *J Hematol Oncol* (2020) 13:96. doi: 10.1186/s13045-020-00930-1

125. Uger R, Johnson L. Blockade of the CD47-SIRPalpha axis: a promising approach for cancer immunotherapy. *Expert Opin Biol Ther* (2020) 20:5–8. doi: 10.1080/14712598.2020.1685976

126. Theruvath J, Menard M, Smith BAH, Linde MH, Coles GL, Dalton GN, et al. Anti-GD2 synergizes with CD47 blockade to mediate tumor eradication. *Nat Med* (2022) 28:333–44. doi: 10.1038/s41591-021-01625-x

127. Upton R, Banuelos A, Feng D, Biswas T, Kao K, McKenna K, et al. Combining CD47 blockade with trastuzumab eliminates HER2-positive breast cancer cells and overcomes trastuzumab tolerance. *Proc Natl Acad Sci U S A* (2021) 118. doi: 10.1073/pnas.2026849118

128. Behrens LM, van den Berg TK, van Egmond M. Targeting the CD47-SIRPalpha innate immune checkpoint to potentiate antibody therapy in cancer by neutrophils. *Cancers (Basel)* (2022) 14. doi: 10.3390/cancers14143366

129. Lee P, Yim R, Yung Y, Chu HT, Yip PK, Gill H. Molecular targeted therapy and immunotherapy for myelodysplastic syndrome. *Int J Mol Sci* (2021) 22. doi: 10.3390/ijms221910232

130. Yin M, Li X, Tan S, Zhou HJ, Ji W, Bellone S, et al. Tumor-associated macrophages drive spheroid formation during early transcoelomic metastasis of ovarian cancer. *J Clin Invest* (2016) 126:4157–73. doi: 10.1172/JCI87252

131. Cui X, Morales RT, Qian W, Wang H, Gagner JP, Dolgalev I, et al. Hacking macrophage-associated immunosuppression for regulating glioblastoma angiogenesis. *Biomaterials* (2018) 161:164–78. doi: 10.1016/j.biomaterials.2018.01.053

132. Chen Y, Wen H, Zhou C, Su Q, Lin Y, Xie Y, et al. TNF-alpha derived from M2 tumor-associated macrophages promotes epithelial-mesenchymal transition and cancer stemness through the Wnt/beta-catenin pathway in SMMC-7721 hepatocellular carcinoma cells. *Exp Cell Res* (2019) 378:41–50. doi: 10.1016/j.yexcr.2019.03.005

133. Yeo EJ, Cassetta L, Qian BZ, Lewkowich I, Li JF, Stefater ,JA 3rd, et al. Myeloid WNT7b mediates the angiogenic switch and metastasis in breast cancer. *Cancer Res* (2014) 74:2962–73. doi: 10.1158/0008-5472.CAN-13-2421

134. Jiang M, Cui H, Liu Z, Zhou X, Zhang L, Cao L, et al. The role of amino acid metabolism of tumor associated macrophages in the development of colorectal cancer. *Cells* (2022) 11. doi: 10.3390/cells11244106

135. Tan Y, Zhao L, Yang YG, Liu W. The role of osteopontin in tumor progression through tumor-associated macrophages. *Front Oncol* (2022) 12:953283. doi: 10.3389/fonc.2022.953283

136. Chen QY, Chen YX, Han QY, Zhang JG, Zhou WJ, Zhang X, et al. Prognostic significance of immune checkpoints HLA-G/ILT-2/4 and PD-L1 in colorectal cancer. *Front Immunol* (2021) 12:679090. doi: 10.3389/fimmu.2021.679090

137. Chen Y, Song Y, Du W, Gong L, Chang H, Zou Z. Tumor-associated macrophages: an accomplice in solid tumor progression. *J BioMed Sci* (2019) 26:78. doi: 10.1186/s12929-019-0568-z

138. Yang C, Dou R, Wei C, Liu K, Shi D, Zhang C, et al. Tumor-derived exosomal microRNA-106b-5p activates EMT-cancer cell and M2-subtype TAM interaction to facilitate CRC metastasis. *Mol Ther* (2021) 29:2088–107. doi: 10.1016/j.ymthe.2021.02.006

139. Wei C, Yang C, Wang S, Shi D, Zhang C, Lin X, et al. Crosstalk between cancer cells and tumor associated macrophages is required for mesenchymal circulating tumor cell-mediated colorectal cancer metastasis. *Mol Cancer* (2019) 18:64. doi: 10.1186/s12943-019-0976-4

140. Zhu S, Luo Z, Li X, Han X, Shi S, Zhang T. Tumor-associated macrophages: role in tumorigenesis and immunotherapy implications. *J Cancer* (2021) 12:54–64. doi: 10.7150/jca.49692

141. Zhu S, Yi M, Wu Y, Dong B, Wu K. Roles of tumor-associated macrophages in tumor progression: implications on therapeutic strategies. *Exp Hematol Oncol* (2021) 10:60. doi: 10.1186/s40164-021-00252-z

142. Zhang T, Hu H, Yan G, Wu T, Liu S, Chen W, et al. Long Non-Coding RNA and Breast Cancer. *Technol Cancer Res Treat* (2019) 18:1533033819843889. doi: 10.1177/1533033819843889

143. Guo XY, Zhang JY, Shi XZ, Wang Q, Shen WL, Zhu WW, et al. Upregulation of CSF-1 is correlated with elevated TAM infiltration and poor prognosis in oral squamous cell carcinoma. *Am J Transl Res* (2020) 12:6235–49.

144. Gao L, Zhang W, Zhong WQ, Liu ZJ, Li HM, Yu ZL, et al. Tumor associated macrophages induce epithelial to mesenchymal transition *via* the EGFR/ERK1/2 pathway in head and neck squamous cell carcinoma. *Oncol Rep* (2018) 40:2558–72. doi: 10.3892/or.2018.6657

145. Zhang L, Tian L, Dai X, Yu H, Wang J, Lei A, et al. Pluripotent stem cell-derived CAR-macrophage cells with antigen-dependent anti-cancer cell functions. *J Hematol Oncol* (2020) 13:153. doi: 10.1186/s13045-020-00983-2

146. Tu W, Gong J, Zhou Z, Tian D, Wang Z. TCF4 enhances hepatic metastasis of colorectal cancer by regulating tumor-associated macrophage *via* CCL2/CCR2 signaling. *Cell Death Dis* (2021) 12:882. doi: 10.1038/s41419-021-04166-w

147. Karlen SJ, Miller EB, Wang X, Levine ES, Zawadzki RJ, Burns ME. Monocyte infiltration rather than microglia proliferation dominates the early immune response to rapid photoreceptor degeneration. *J Neuroinflamm* (2018) 15:344. doi: 10.1186/s12974-018-1365-4

148. Fang WB, Yao M, Brummer G, Acevedo D, Alhakamy N, Berkland C, et al. Targeted gene silencing of CCL2 inhibits triple negative breast cancer progression by blocking cancer stem cell renewal and M2 macrophage recruitment. *Oncotarget* (2016) 7:49349–67. doi: 10.18632/oncotarget.9885

149. Fei L, Ren X, Yu H, Zhan Y. Targeting the CCL2/CCR2 axis in cancer immunotherapy: one stone, three birds? *Front Immunol* (2021) 12:771210. doi: 10.3389/fimmu.2021.771210

150. Hajal C, Shin Y, Li L, Serrano JC, Jacks T, Kamm RD. The CCL2-CCR2 astrocyte-cancer cell axis in tumor extravasation at the brain. *Sci Adv* (2021) 7. doi: 10.1126/sciadv.abg8139

151. Miyamoto T, Murakami R, Hamanishi J, Tanigaki K, Hosoe Y, Mise N, et al. B7-H3 suppresses antitumor immunity *via* the CCL2-CCR2-M2 macrophage axis and contributes to ovarian cancer progression. *Cancer Immunol Res* (2022) 10:56–69. doi: 10.1158/2326-6066.CIR-21-0407

152. Anagnostakis F, Piperi C. Targeting options of tumor-associated macrophages (TAM) activity in gliomas. *Curr Neuropharmacol* (2023) 21:457–70. doi: 10.2174/1570159X20666220120120203

153. Guo Z, Song J, Hao J, Zhao H, Du X, Li E, et al. M2 macrophages promote NSCLC metastasis by upregulating CRYAB. *Cell Death Dis* (2019) 10:377. doi: 10.1038/s41419-019-1618-x

154. Han Y, Guo W, Ren T, Huang Y, Wang S, Liu K, et al. Tumor-associated macrophages promote lung metastasis and induce epithelial-mesenchymal transition in osteosarcoma by activating the COX-2/STAT3 axis. *Cancer Lett* (2019) 440-441:116–25. doi: 10.1016/j.canlet.2018.10.011

155. Choudhry H, Harris AL. Advances in hypoxia-inducible factor biology. *Cell Metab* (2018) 27:281–98. doi: 10.1016/j.cmet.2017.10.005

156. Greer SN, Metcalf JL, Wang Y, Ohh M. The updated biology of hypoxia-inducible factor. *EMBO J* (2012) 31:2448–60. doi: 10.1038/emboj.2012.125

157. Zhao L, Ma R, Zhang L, Yuan X, Wu J, He L, et al. Inhibition of HIF-1a-mediated TLR4 activation decreases apoptosis and promotes angiogenesis of placental microvascular endothelial cells during severe pre-eclampsia pathogenesis. *Placenta* (2019) 83:8–16. doi: 10.1016/j.placenta.2019.06.375

158. Nguyen KG, Vrabel MR, Mantooth SM, Hopkins JJ, Wagner ES, Gabaldon TA, et al. Localized interleukin-12 for cancer immunotherapy. *Front Immunol* (2020) 11:575597. doi: 10.3389/fimmu.2020.575597

159. Guan W, Li F, Zhao Z, Zhang Z, Hu J, Zhang Y. Tumor-Associated Macrophage Promotes the Survival of Cancer Cells upon Docetaxel Chemotherapy via the CSF1/CSF1R-CXCL12/CXCR4 Axis in Castration-Resistant Prostate Cancer. *Genes (Basel)* (2021) 12. doi: 10.3390/genes12050773

160. Yan Z, Li L, Fu D, Wu W, Qiao N, Huang Y, et al. Immunosuppressive tumor microenvironment contributes to tumor progression in diffuse large B-cell lymphoma upon anti-CD19 chimeric antigen receptor T therapy. *Front Med* (2023) 17. doi: 10.1007/s11684-022-0972-8

161. Gordon SR, Maute RL, Dulken BW, Hutter G, George BM, McCracken MN, et al. PD-1 expression by tumour-associated macrophages inhibits phagocytosis and tumour immunity. *Nature* (2017) 545:495–9. doi: 10.1038/nature22396

162. Rosenzweig N, Dvir-Szternfeld R, Tsitsou-Kampeli A, Keren-Shaul H, Ben-Yehuda H, Weill-Raynal P, et al. PD-1/PD-L1 checkpoint blockade harnesses monocyte-derived macrophages to combat cognitive impairment in a tauopathy mouse model. *Nat Commun* (2019) 10:465. doi: 10.1038/s41467-019-08352-5

163. Pan Y, Yu Y, Wang X, Zhang T. Tumor-associated macrophages in tumor immunity. *Front Immunol* (2020) 11:583084. doi: 10.3389/fimmu.2020.583084

164. Yu J, Green MD, Li S, Sun Y, Journey SN, Choi JE, et al. Liver metastasis restrains immunotherapy efficacy *via* macrophage-mediated T cell elimination. *Nat Med* (2021) 27:152–64. doi: 10.1038/s41591-020-1131-x

165. Chow A, SChad S, Green MD, Hellmann MD, Allaj V, Ceglia N, et al. Tim-4(+) cavity-resident macrophages impair anti-tumor CD8(+) T cell immunity. *Cancer Cell* (2021) 39:973–88.e9. doi: 10.1016/j.ccell.2021.05.006

166. Vetizou M, Pitt JM, Daillere R, Lepage P, Waldschmitt N, Flament C, et al. Anticancer immunotherapy by CTLA-4 blockade relies on the gut microbiota. *Science* (2015) 350:1079–84. doi: 10.1126/science.aad1329

167. Wu MF, Lin CA, Yuan TH, Yeh HY, Su SF, Guo CL, et al. The M1/M2 spectrum and plasticity of Malignant pleural effusion-macrophage in advanced lung cancer. *Cancer Immunol Immunother* (2021) 70:1435–50. doi: 10.1007/s00262-020-02781-8

168. Ge Z, Ding S. The crosstalk between tumor-associated macrophages (TAMs) and tumor cells and the corresponding targeted therapy. *Front Oncol* (2020) 10:590941. doi: 10.3389/fonc.2020.590941

169. Rojo R, Raper A, Ozdemir DD, Lefevre L, Grabert K, Wollscheid-Lengeling E, et al. Deletion of a Csf1r enhancer selectively impacts CSF1R expression and development of tissue macrophage populations. *Nat Commun* (2019) 10:3215. doi: 10.1038/s41467-019-11053-8

170. Yeung J, Yaghoobi V, Miyagishima D, Vesely MD, Zhang T, Badri T, et al. Targeting the CSF1/CSF1R axis is a potential treatment strategy for Malignant meningiomas. *Neuro Oncol* (2021) 23:1922–35. doi: 10.1093/neuonc/noab075

171. Han J, Chitu V, Stanley ER, Wszolek ZK, Karrenbauer VD, Harris RA. Inhibition of colony stimulating factor-1 receptor (CSF-1R) as a potential therapeutic strategy for neurodegenerative diseases: opportunities and challenges. *Cell Mol Life Sci* (2022) 79:219. doi: 10.1007/s00018-022-04225-1

172. Gomez-Roca C, Cassier P, Zamarin D, Machiels JP, Perez Gracia JL, Stephen Hodi F, et al. Anti-CSF-1R emactuzumab in combination with anti-PD-L1 atezolizumab in advanced solid tumor patients naive or experienced for immune checkpoint blockade. *J Immunother Cancer* (2022) 10. doi: 10.1136/jitc-2021-004076

173. Li M, He L, Zhu J, Zhang P, Liang S. Targeting tumor-associated macrophages for cancer treatment. *Cell Biosci* (2022) 12:85. doi: 10.1186/s13578-022-00823-5

174. Li X, Liu R, Su X, Pan Y, Han X, Shao C, et al. Harnessing tumor-associated macrophages as aids for cancer immunotherapy. *Mol Cancer* (2019) 18:177. doi: 10.1186/s12943-019-1102-3

175. Li M, Yu H, Qi F, Ye Y, Hu D, Cao J, et al. Anti-CD47 immunotherapy in combination with BCL-2 inhibitor to enhance anti-tumor activity in B-cell lymphoma. *Hematol Oncol* (2022) 40:596–608. doi: 10.1002/hon.3009

176. Chang R, Chu X, Zhang J, Fu R, Feng C, Jia D, et al. Liposome-based co-immunotherapy with TLR agonist and CD47-SIRPalpha checkpoint blockade for efficient treatment of colon cancer. *Molecules* (2023) 28. doi: 10.3390/molecules28073147

177. Klichinsky M, Ruella M, Shestova O, Lu XM, Best A, Zeeman M, et al. Human chimeric antigen receptor macrophages for cancer immunotherapy. *Nat Biotechnol* (2020) 38:947–53. doi: 10.1038/s41587-020-0462-y

178. Liu H, Pan C, Song W, Liu D, Li Z, Zheng L. Novel strategies for immuno-oncology breakthroughs with cell therapy. *biomark Res* (2021) 9:62. doi: 10.1186/s40364-021-00316-6

179. Li P, Li X, Wu W, Hou M, Yin G, Wang Z, et al. Tim-3 protects against cisplatin nephrotoxicity by inhibiting NF-kappaB-mediated inflammation. *Cell Death Discovery* (2023) 9:218. doi: 10.1038/s41420-023-01519-6

180. Sauer N, Janicka N, Szlasa W, Skinderowicz B, Kolodzinska K, Dwernicka W, et al. TIM-3 as a promising target for cancer immunotherapy in a wide range of tumors. *Cancer Immunol Immunother* (2023) 72:3405–25. doi: 10.1007/s00262-023-03516-1

181. Gu C, Wiest M, Zhang W, Halder K, Zurawski S, Zurawski G, et al. Cancer cells promote immune regulatory function of macrophages by upregulating scavenger receptor MARCO expression. *J Immunol* (2023) 211:57–70. doi: 10.4049/jimmunol.2300029

182. Jeremiasen M, Borg D, Hedner C, Svensson M, Nodin B, Leandersson K, et al. Tumor-associated CD68(+), CD163(+), and MARCO(+) macrophages as prognostic biomarkers in patients with treatment-naive gastroesophageal adenocarcinoma. *Front Oncol* (2020) 10:534761. doi: 10.3389/fonc.2020.534761

183. La Fleur L, Botling J, He F, Pelicano C, Zhou C, He C, et al. and IL37R on immunosuppressive macrophages in lung cancer blocks regulatory T cells and supports cytotoxic lymphocyte function. *Cancer Res* (2021) 81:956–67. doi: 10.1158/0008-5472.CAN-20-1885

184. Guerriero JL, Sotayo A, Ponichtera HE, Castrillon JA, Pourzia AL, SChad S, et al. Class IIa HDAC inhibition reduces breast tumours and metastases through anti-tumour macrophages. *Nature* (2017) 543:428–32. doi: 10.1038/nature21409

185. Foubert P, Kaneda MM, Varner JA. PI3Kgamma Activates Integrin alpha(4) and Promotes Immune Suppressive Myeloid Cell Polarization during Tumor Progression. *Cancer Immunol Res* (2017) 5:957–68. doi: 10.1158/2326-6066.CIR-17-0143

186. Vidyarthi A, Khan N, Agnihotri T, Negi S, Das DK, Aqdas M, et al. TLR-3 stimulation skews M2 macrophages to M1 through IFN-alphabeta signaling and restricts tumor progression. *Front Immunol* (2018) 9:1650. doi: 10.3389/fimmu.2018.01650

187. Zhang Y, Wu L, Li Z, Zhang W, Luo F, Chu Y, et al. Glycocalyx-mimicking nanoparticles improve anti-PD-L1 cancer immunotherapy through reversion of tumor-associated macrophages. *Biomacromolecules* (2018) 19:2098–108. doi: 10.1021/acs.biomac.8b00305

188. Su L, Zhang W, Wu X, Zhang Y, Chen X, Liu G, et al. Glycocalyx-mimicking nanoparticles for stimulation and polarization of macrophages *via* specific interactions. *Small* (2015) 11:4191–200. doi: 10.1002/smll.201403838

189. Li X, Guo X, Ling J, Tang Z, Huang G, He L, et al. Nanomedicine-based cancer immunotherapies developed by reprogramming tumor-associated macrophages. *Nanoscale* (2021) 13:4705–27. doi: 10.1039/D0NR08050K

190. Mathur R, Chauhan RP, Singh G, Singh S, Varshney R, Kaul A, et al. Tryptophan conjugated magnetic nanoparticles for targeting tumors overexpressing indoleamine 2,3 dioxygenase (IDO) and L-type amino acid transporter. *J Mater Sci Mater Med* (2020) 31:87. doi: 10.1007/s10856-020-06438-x

191. Ye J, Yang Y, Jin J, Ji M, Gao Y, Feng Y, et al. Targeted delivery of chlorogenic acid by mannosylated liposomes to effectively promote the polarization of TAMs for the treatment of glioblastoma. *Bioact Mater* (2020) 5:694–708. doi: 10.1016/j.bioactmat.2020.05.001

192. Zhou ZF, Peng F, Li JY, Ye YB. Intratumoral IL-12 gene therapy inhibits tumor growth in A HCC-Hu-PBL-NOD/SCID murine model. *Onco Targets Ther* (2019) 12:7773–84. doi: 10.2147/OTT.S222097

193. Pei H, Qin J, Wang F, Tan B, Zhao Z, Peng Y, et al. Discovery of potent ureido tetrahydrocarbazole derivatives for cancer treatments through targeting tumor-associated macrophages. *Eur J Med Chem* (2019) 183:111741. doi: 10.1016/j.ejmech.2019.111741

194. Li W, Wang X, Li C, Chen T, Yang Q. Exosomal non-coding RNAs: Emerging roles in bilateral communication between cancer cells and macrophages. *Mol Ther* (2022) 30:1036–53. doi: 10.1016/j.ymthe.2021.12.002

195. Li W, Xin X, Li X, Geng J, Sun Y. Exosomes secreted by M2 macrophages promote cancer stemness of hepatocellular carcinoma *via* the miR-27a-3p/TXNIP pathways. *Int Immunopharmacol* (2021) 101:107585. doi: 10.1016/j.intimp.2021.107585

196. Li W, Zeng H, Xu M, Huang C, Tao L, Li J, et al. Oleanolic acid improves obesity-related inflammation and insulin resistance by regulating macrophages activation. *Front Pharmacol* (2021) 12:697483. doi: 10.3389/fphar.2021.697483

197. Deuse T, Hu X, Agbor-Enoh S, Jang MK, Alawi M, Saygi C, et al. The SIRPalpha-CD47 immune checkpoint in NK cells. *J Exp Med* (2021) 218. doi: 10.1084/jem.20200839

198. Petrova PS, Viller NN, Wong M, Pang X, Lin GH, Dodge K, et al. TTI-621 (SIRPalphaFc): A CD47-blocking innate immune checkpoint inhibitor with broad antitumor activity and minimal erythrocyte binding. *Clin Cancer Res* (2017) 23:1068–79. doi: 10.1158/1078-0432.CCR-16-1700

199. Yang H, Shao R, Huang H, Wang X, Rong Z, Lin Y. Engineering macrophages to phagocytose cancer cells by blocking the CD47/SIRPa axis. *Cancer Med* (2019) 8:4245–53. doi: 10.1002/cam4.2332

200. Logtenberg MEW, Scheeren FA, Schumacher TN. The CD47-SIRPalpha immune checkpoint. *Immunity* (2020) 52:742–52. doi: 10.1016/j.immuni.2020.04.011

201. Morrissey MA, Kern N, Vale RD. CD47 ligation repositions the inhibitory receptor SIRPA to suppress integrin activation and phagocytosis. *Immunity* (2020) 53:290–302.e6. doi: 10.1016/j.immuni.2020.07.008

202. Hassan EM, Zou S. Novel nanocarriers for silencing anti-phagocytosis CD47 marker in acute myeloid leukemia cells. *Colloids Surf B Biointerfaces* (2022) 217:112609. doi: 10.1016/j.colsurfb.2022.112609

203. Majeti R, Chao MP, Alizadeh AA, Pang WW, Jaiswal S, Gibbs KD Jr., et al. CD47 is an adverse prognostic factor and therapeutic antibody target on human acute myeloid leukemia stem cells. *Cell* (2009) 138:286–99. doi: 10.1016/j.cell.2009.05.045

204. Pena-Martinez P, Ramakrishnan R, Hogberg C, Jansson C, Nord DG, Jaras M. Interleukin 4 promotes phagocytosis of murine leukemia cells counteracted by CD47 upregulation. *Haematologica* (2022) 107:816–24. doi: 10.3324/haematol.2020.270421

205. Simonis A, Russkamp NF, Mueller J, Wilk CM, Wildschut MHE, Myburgh R, et al. Disruption of CSF-1R signaling inhibits growth of AML with inv(16). *Blood Adv* (2021) 5:1273–7. doi: 10.1182/bloodadvances.2020003125

206. Willingham SB, Volkmer JP, Gentles AJ, Sahoo D, Dalerba P, Mitra SS, et al. The CD47-signal regulatory protein alpha (SIRPa) interaction is a therapeutic target for human solid tumors. *Proc Natl Acad Sci U S A* (2012) 109:6662–7. doi: 10.1073/pnas.1121623109

207. Chao MP, Alizadeh AA, Tang C, Myklebust JH, Varghese B, Gill S, et al. Anti-CD47 antibody synergizes with rituximab to promote phagocytosis and eradicate non-Hodgkin lymphoma. *Cell* (2010) 142:699–713. doi: 10.1016/j.cell.2010.07.044

208. Chao MP, Tang C, Pachynski RK, Chin R, Majeti R, Weissman IL. Extranodal dissemination of non-Hodgkin lymphoma requires CD47 and is inhibited by anti-CD47 antibody therapy. *Blood* (2011) 118:4890–901. doi: 10.1182/blood-2011-02-338020

209. Chao MP, Weissman IL, Majeti R. The CD47-SIRPalpha pathway in cancer immune evasion and potential therapeutic implications. *Curr Opin Immunol* (2012) 24:225–32. doi: 10.1016/j.coi.2012.01.010

210. Haddad F, Daver N. Targeting CD47/SIRPalpha in acute myeloid leukemia and myelodysplastic syndrome: preclinical and clinical developments of magrolimab. *J Immunother Precis Oncol* (2021) 4:67–71. doi: 10.36401/JIPO-21-X2

211. Tseng D, Volkmer JP, Willingham SB, Contreras-Trujillo H, Fathman JW, Fernhoff NB, et al. Anti-CD47 antibody-mediated phagocytosis of cancer by macrophages primes an effective antitumor T-cell response. *Proc Natl Acad Sci U S A* (2013) 110:11103–8. doi: 10.1073/pnas.1305569110

212. Treffers LW, Ten Broeke T, Rosner T, Jansen JHM, van Houdt M, Kahle S, et al. IgA-mediated killing of tumor cells by neutrophils is enhanced by CD47-SIRPalpha checkpoint inhibition. *Cancer Immunol Res* (2020) 8:120–30. doi: 10.1158/2326-6066.CIR-19-0144

213. Zhang Y, Sime W, Juhas M, Sjolander A. Crosstalk between colon cancer cells and macrophages *via* inflammatory mediators and CD47 promotes tumour cell migration. *Eur J Cancer* (2013) 49:3320–34. doi: 10.1016/j.ejca.2013.06.005

214. Suter EC, Schmid EM, Harris AR, Voets E, Francica B, Fletcher DA. Antibody: CD47 ratio regulates macrophage phagocytosis through competitive receptor phosphorylation. *Cell Rep* (2021) 36:109587. doi: 10.1016/j.celrep.2021.109587

215. Wang C, Sun C, Li M, Xia B, Wang Y, Zhang L, et al. Novel fully human anti-CD47 antibodies stimulate phagocytosis and promote elimination of AML cells. *J Cell Physiol* (2021) 236:4470–81. doi: 10.1002/jcp.30163

216. Zhang H, Wang C, Fan J, Zhu Q, Feng Y, Pan J, et al. CD47 promotes the proliferation and migration of adamantinomatous craniopharyngioma cells by activating the MAPK/ERK pathway, and CD47 blockade facilitates microglia-mediated phagocytosis. *Neuropathol Appl Neurobiol* (2022) 48:e12795. doi: 10.1111/nan.12795

217. Liu X, Pu Y, Cron K, Deng L, Kline J, Frazier WA, et al. CD47 blockade triggers T cell-mediated destruction of immunogenic tumors. *Nat Med* (2015) 21:1209–15. doi: 10.1038/nm.3931

218. Genovese MC, Hsia E, Belkowski SM, Chien C, Masterson T, Thurmond RL, et al. Results from a phase IIA parallel group study of JNJ-40346527, an oral CSF-1R inhibitor, in patients with active rheumatoid arthritis despite disease-modifying antirheumatic drug therapy. *J Rheumatol* (2015) 42:1752–60. doi: 10.3899/jrheum.141580

219. von Tresckow B, Morschhauser F, Ribrag V, Topp MS, Chien C, Seetharam S, et al. Multicenter, phase I/II study of JNJ-40346527, a CSF-1R inhibitor, in patients with relapsed or refractory hodgkin lymphoma. *Clin Cancer Res* (2015) 21:1843–50. doi: 10.1158/1078-0432.CCR-14-1845

220. Sikic BI, Lakhani N, Patnaik A, Shah SA, Chandana SR, Rasco D, et al. First-in-human, first-in-class phase I trial of the anti-CD47 antibody Hu5F9-G4 in patients with advanced cancers. *J Clin Oncol* (2019) 37:946–53. doi: 10.1200/JCO.18.02018

221. O'Hara MH, O'Reilly EM, Varadhachary G, Wolff RA, Wainberg ZA, Ko AH, et al. CD40 agonistic monoclonal antibody APX005M (sotigalimab) and chemotherapy, with or without nivolumab, for the treatment of metastatic pancreatic adenocarcinoma: an open-label, multicentre, phase 1b study. *Lancet Oncol* (2021) 22:118–31. doi: 10.1016/S1470-2045(20)30532-5

222. Reni M. APX005M, a CD40 monoclonal antibody, for patients with pancreatic adenocarcinoma. *Lancet Oncol* (2021) 22:10–1. doi: 10.1016/S1470-2045(20)30724-5

223. Machiels JP, Gomez-Roca C, Michot JM, Zamarin D, Mitchell T, Catala G, et al. Phase Ib study of anti-CSF-1R antibody emactuzumab in combination with CD40 agonist selicrelumab in advanced solid tumor patients. *J Immunother Cancer* (2020) 8. doi: 10.1136/jitc-2020-001153

224. Mukhtar M, Ali H, Ahmed N, Munir R, Talib S, Khan AS, et al. Drug delivery to macrophages: a review of nano-therapeutics targeted approach for inflammatory disorders and cancer. *Expert Opin Drug Delivery* (2020) 17:1239–57. doi: 10.1080/17425247.2020.1783237

225. Iglesias M, Brennan DC, Larsen CP, Raimondi G. Targeting inflammation and immune activation to improve CTLA4-Ig-based modulation of transplant rejection. *Front Immunol* (2022) 13:926648. doi: 10.3389/fimmu.2022.926648

226. Ma Y, Xue J, Zhao Y, Zhang Y, Huang Y, Yang Y, et al. Phase I trial of KN046, a novel bispecific antibody targeting PD-L1 and CTLA-4 in patients with advanced solid tumors. *J Immunother Cancer* (2023) 11. doi: 10.1136/jitc-2022-006654

227. Zhang A, Ren Z, Tseng KF, Liu X, Li H, Lu C, et al. Dual targeting of CTLA-4 and CD47 on T(reg) cells promotes immunity against solid tumors. *Sci Transl Med* (2021) 13. doi: 10.1126/scitranslmed.abg8693

228. Zhou Y, Song S, Yuan B, Wu Y, Gao Y, Wan G, et al. A Novel CTLA-4 affinity peptide for cancer immunotherapy by increasing the integrin alphavbeta3 targeting. *Discovery Oncol* (2022) 13:99. doi: 10.1007/s12672-022-00562-6

229. Regina A, Demeule M, Tripathy S, Lord-Dufour S, Currie JC, Iddir M, et al. ANG4043, a novel brain-penetrant peptide-mAb conjugate, is efficacious against HER2-positive intracranial tumors in mice. *Mol Cancer Ther* (2015) 14:129–40. doi: 10.1158/1535-7163.MCT-14-0399

230. Tew BY, Kalfa AJ, Yang Z, Hurth KM, Simon T, Abnoosian E, et al. ATM-inhibitor AZD1390 is a radiosensitizer for breast cancer CNS metastasis. *Clin Cancer Res* (2023) 16:CCR-23-0290. doi: 10.1158/1078-0432.CCR-23-0290

231. Yang S, Song D, Wang Z, Su Y, Chen J, Xian Y, et al. AKT/GSK3beta/NFATc1 and ROS signal axes are involved in AZD1390-mediated inhibitory effects on osteoclast and OVX-induced osteoporosis. *Int Immunopharmacol* (2022) 113:109370. doi: 10.1016/j.intimp.2022.109370

232. Chan CY, Chiu DK, Yuen VW, Law CT, Wong BP, Thu KL, et al. CFI-402257, a TTK inhibitor, effectively suppresses hepatocellular carcinoma. *Proc Natl Acad Sci U S A* (2022) 119:e2119514119. doi: 10.1073/pnas.2119514119

233. Liu Y, Laufer R, Patel NK, Ng G, Sampson PB, Li SW, et al. Discovery of pyrazolo [1,5-a]pyrimidine TTK inhibitors: CFI-402257 is a potent, selective, bioavailable anticancer agent. *ACS Med Chem Lett* (2016) 7:671–5. doi: 10.1021/acsmedchemlett.5b00485

234. Mason JM, Wei X, Fletcher GC, Kiarash R, Brokx R, Hodgson R, et al. Functional characterization of CFI-402257, a potent and selective Mps1/TTK kinase inhibitor, for the treatment of cancer. *Proc Natl Acad Sci U S A* (2017) 114:3127–32. doi: 10.1073/pnas.1700234114

235. Puro RJ, Bouchlaka MN, Hiebsch RR, Capoccia BJ, Donio MJ, Manning PT, et al. Development of AO-176, a next-generation humanized anti-CD47 antibody with novel anticancer properties and negligible red blood cell binding. *Mol Cancer Ther* (2020) 19:835–46. doi: 10.1158/1535-7163.MCT-19-1079

236. Zeidan AM, DeAngelo DJ, Palmer J, Seet CS, Tallman MS, Wei X, et al. Phase 1 study of anti-CD47 monoclonal antibody CC-90002 in patients with relapsed/refractory acute myeloid leukemia and high-risk myelodysplastic syndromes. *Ann Hematol* (2022) 101:557–69. doi: 10.1007/s00277-021-04734-2

237. Binnewies M, Pollack JL, Rudolph J, Dash S, Abushawish M, Lee T, et al. Targeting TREM2 on tumor-associated macrophages enhances immunotherapy. *Cell Rep* (2021) 37:109844. doi: 10.1016/j.celrep.2021.109844

238. Xiang X, Wang J, Lu D, Xu X. Targeting tumor-associated macrophages to synergize tumor immunotherapy. *Signal Transduct Target Ther* (2021) 6:75. doi: 10.1038/s41392-021-00484-9

239. Toulmonde M, Penel N, Adam J, Chevreau C, Blay JY, Le Cesne A, et al. Use of PD-1 targeting, macrophage infiltration, and IDO pathway activation in sarcomas: A phase 2 clinical trial. *JAMA Oncol* (2018) 4:93–7. doi: 10.1001/jamaoncol.2017.1617

240. Hu Z, Li W, Chen S, Chen D, Xu R, Zheng D, et al. Design of a novel chimeric peptide *via* dual blockade of CD47/SIRPalpha and PD-1/PD-L1 for cancer immunotherapy. *Sci China Life Sci* (2023) 66(10):2310–28. doi: 10.1007/s11427-022-2285-6

241. Liu Y, Xue R, Duan X, Shang X, Wang M, Wang F, et al. PARP inhibition synergizes with CD47 blockade to promote phagocytosis by tumor-associated macrophages in homologous recombination-proficient tumors. *Life Sci* (2023) 326:121790. doi: 10.1016/j.lfs.2023.121790

242. Lu J, Li J, Lin Z, Li H, Lou L, Ding W, et al. Reprogramming of TAMs *via* the STAT3/CD47-SIRPalpha axis promotes acquired resistance to EGFR-TKIs in lung cancer. *Cancer Lett* (2023) 564:216205. doi: 10.1016/j.canlet.2023.216205

243. Ribeiro ML, Profitos-Peleja N, Santos JC, Blecua P, Reyes-Garau D, Armengol M, et al. G protein-coupled receptor 183 mediates the sensitization of Burkitt lymphoma tumors to CD47 immune checkpoint blockade by anti-CD20/PI3Kdeltai dual therapy. *Front Immunol* (2023) 14:1130052. doi: 10.3389/fimmu.2023.1130052

244. Su Z, Dong S, Chen Y, Huang T, Qin B, Yang Q, et al. Microfluidics-enabled nanovesicle delivers CD47/PD-L1 antibodies to enhance antitumor immunity and reduce immunotoxicity in lung adenocarcinoma. *Adv Sci (Weinh)* (2023) 10:e2206213. doi: 10.1002/advs.202206213

245. Ye L, Lv W, He W, Li S, Min Z, Gong L, et al. Reduced Malignant glioblastoma recurrence post-resection through the anti-CD47 antibody and Temozolomide co-embedded in-situ hydrogel system. *J Control Release* (2023) 359:224–33. doi: 10.1016/j.jconrel.2023.05.046

246. Hutter G, Theruvath J, Graef CM, Zhang M, Schoen MK, Manz EM, et al. Microglia are effector cells of CD47-SIRPalpha antiphagocytic axis disruption against glioblastoma. *Proc Natl Acad Sci U S A* (2019) 116:997–1006. doi: 10.1073/pnas.1721434116

247. Yu J, Li S, Chen D, Liu D, Guo H, Yang C, et al. SIRPalpha-Fc fusion protein IMM01 exhibits dual anti-tumor activities by targeting CD47/SIRPalpha signal pathway *via* blocking the "don't eat me" signal and activating the "eat me" signal. *J Hematol Oncol* (2022) 15:167. doi: 10.1186/s13045-022-01385-2

248. Hendriks M, Britsch I, Ke X, van Wijngarden AP, Samplonius DF, Ploeg EM, et al. Cancer cells under immune attack acquire CD47-mediated adaptive immune resistance independent of the myeloid CD47-SIRPalpha axis. *Oncoimmunology* (2021) 10:2005344. doi: 10.1080/2162402X.2021.2005344

249. Jia X, Yan B, Tian X, Liu Q, Jin J, Shi J, et al. CD47/SIRPalpha pathway mediates cancer immune escape and immunotherapy. *Int J Biol Sci* (2021) 17:3281–7. doi: 10.7150/ijbs.60782

250. Li Y, Zhou H, Liu P, Lv D, Shi Y, Tang B, et al. SHP2 deneddylation mediates tumor immunosuppression in colon cancer via the CD47/SIRPalpha axis. *J Clin Invest* (2023) 133. doi: 10.1172/JCI162870

251. Logtenberg MEW, Jansen JHM, Raaben M, Toebes M, Franke K, Brandsma AM, et al. Glutaminyl cyclase is an enzymatic modifier of the CD47- SIRPalpha axis and a target for cancer immunotherapy. *Nat Med* (2019) 25:612–9. doi: 10.1038/s41591-019-0356-z

252. Luo X, Shen Y, Huang W, Bao Y, Mo J, Yao L, et al. Blocking CD47-SIRPalpha signal axis as promising immunotherapy in ovarian cancer. *Cancer Control* (2023) 30:10732748231159706. doi: 10.1177/10732748231159706

253. Wang H, Sun Y, Zhou X, Chen C, Jiao L, Li W, et al. CD47/SIRPalpha blocking peptide identification and synergistic effect with irradiation for cancer immunotherapy. *J Immunother Cancer* (2020) 8. doi: 10.1136/jitc-2020-000905

254. Yu J, Li S, Chen D, Liu D, Guo H, Yang C, et al. IMM0306, a fusion protein of CD20 mAb with the CD47 binding domain of SIRPalpha, exerts excellent cancer killing efficacy by activating both macrophages and NK cells *via* blockade of CD47-SIRPalpha interaction and Fc?R engagement by simultaneously binding to CD47 and CD20 of B cells. *Leukemia* (2022) 37(3):695–8. doi: 10.1038/s41375-022-01805-9

255. Zhou X, Jiao L, Qian Y, Dong Q, Sun Y, Zheng WV, et al. Repositioning azelnidipine as a dual inhibitor targeting CD47/SIRPalpha and TIGIT/PVR pathways for cancer immuno-therapy. *Biomolecules* (2021) 11. doi: 10.3390/biom11050706

256. Barkal AA, Brewer RE, Markovic M, Kowarsky M, Barkal SA, Zaro BW, et al. CD24 signalling through macrophage Siglec-10 is a target for cancer immunotherapy. *Nature* (2019) 572:392–6. doi: 10.1038/s41586-019-1456-0

257. Ibarlucea-Benitez I, Weitzenfeld P, Smith P, Ravetch JV. Siglecs-7/9 function as inhibitory immune checkpoints in vivo and can be targeted to enhance therapeutic antitumor immunity. *Proc Natl Acad Sci U S A* (2021) 118. doi: 10.1073/pnas.2107424118

258. Zhao J, Zhong S, Niu X, Jiang J, Zhang R, Li Q. The MHC class I-LILRB1 signalling axis as a promising target in cancer therapy. *Scand J Immunol* (2019) 90: e12804. doi: 10.1111/sji.12804

259. Zeller T, Lutz S, Munnich IA, Windisch R, Hilger P, Herold T, et al. Dual checkpoint blockade of CD47 and LILRB1 enhances CD20 antibody-dependent phagocytosis of lymphoma cells by macrophages. *Front Immunol* (2022) 13:929339. doi: 10.3389/fimmu.2022.929339

260. Wang S, Lin Y, Xiong X, Wang L, Guo Y, Chen Y, et al. Low-dose metformin reprograms the tumor immune microenvironment in human esophageal cancer: results of a phase II clinical trial. *Clin Cancer Res* (2020) 26:4921–32. doi: 10.1158/1078-0432.CCR-20-0113

261. Blanc F, Bertho N, Piton G, Leplat JJ, Egidy G, Bourneuf E, et al. Deciphering the immune reaction leading to spontaneous melanoma regression: initial role of MHCII(+) CD163(-) macrophages. *Cancer Immunol Immunother* (2023) 72(11):3507–21. doi: 10.1007/s00262-023-03503-6

262. Lee WJ, Lee MH, Kim HT, Won CH, Lee MW, Choi JH, et al. Prognostic significance of CD163 expression and its correlation with cyclooxygenase-2 and vascular endothelial growth factor expression in cutaneous melanoma. *Melanoma Res* (2019) 29:501–9. doi: 10.1097/CMR.0000000000000549

263. Najem H, Marisetty A, Horbinski C, Long J, Huse JT, Glitza Oliva IC, et al. CD11c+CD163+ Cells and signal transducer and activator of transcription 3 (STAT3) expression are common in melanoma leptomeningeal disease. *Front Immunol* (2021) 12:745893. doi: 10.3389/fimmu.2021.745893

264. Tremble LF, McCabe M, Walker SP, McCarthy S, Tynan RF, Beecher S, et al. Differential association of CD68(+) and CD163(+) macrophages with macrophage enzymes, whole tumour gene expression and overall survival in advanced melanoma. *Br J Cancer* (2020) 123:1553–61. doi: 10.1038/s41416-020-01037-7

265. Shinohara H, Kobayashi M, Hayashi K, Nogawa D, Asakawa A, Ohata Y, et al. Spatial and quantitative analysis of tumor-associated macrophages: intratumoral CD163-/PD-L1+ TAMs as a marker of favorable clinical outcomes in triple-negative breast cancer. *Int J Mol Sci* (2022) 23. doi: 10.3390/ijms232113235

266. Jaynes JM, Sable R, Ronzetti M, Bautista W, Knotts Z, Abisoye-Ogunniyan A, et al. Mannose receptor (CD206) activation in tumor-associated macrophages enhances adaptive and innate antitumor immune responses. *Sci Transl Med* (2020) 12. doi: 10.1126/scitranslmed.aax6337

267. Eisinger S, Sarhan D, Boura VF, Ibarlucea-Benitez I, Tyystjarvi S, Oliynyk G, et al. Targeting a scavenger receptor on tumor-associated macrophages activates tumor cell killing by natural killer cells. *Proc Natl Acad Sci U S A* (2020) 117:32005–16. doi: 10.1073/pnas.2015343117

268. Dunkel J, Viitala M, Karikoski M, Rantakari P, Virtakoivu R, Elima K, et al. Enhanced antibody production in clever-1/stabilin-1-deficient mice. *Front Immunol* (2018) 9:2257. doi: 10.3389/fimmu.2018.02257

269. Hollmen M, Maksimow M, Rannikko JH, Karvonen MK, Vainio M, Jalkanen S, et al. Nonclinical characterization of bexmarilimab, a clever-1-targeting antibody for supporting immune defense against cancers. *Mol Cancer Ther* (2022) 21:1207–18. doi: 10.1158/1535-7163.MCT-21-0840

270. Mutka M, Virtakoivu R, Joensuu K, Hollmen M, Heikkila P. Clever-1 positive macrophages in breast cancer. *Breast Cancer Res Treat* (2022) 195:237–48. doi: 10.1007/s10549-022-06683-4

271. Viitala M, Virtakoivu R, Tadayon S, Rannikko J, Jalkanen S, Hollmen M. Immunotherapeutic blockade of macrophage clever-1 reactivates the CD8(+) T-cell response against immunosuppressive tumors. *Clin Cancer Res* (2019) 25:3289–303. doi: 10.1158/1078-0432.CCR-18-3016

272. Virtakoivu R, Rannikko JH, Viitala M, Vaura F, Takeda A, Lonnberg T, et al. Systemic blockade of clever-1 elicits lymphocyte activation alongside checkpoint molecule downregulation in patients with solid tumors: results from a phase I/II clinical trial. *Clin Cancer Res* (2021) 27:4205–20. doi: 10.1158/1078-0432.CCR-20-4862

273. Tichet M, Wullschleger S, Chryplewicz A, Fournier N, Marcone R, Kauzlaric A, et al. Bispecific PD1-IL2v and anti-PD-L1 break tumor immunity resistance by enhancing stem-like tumor-reactive CD8(+) T cells and reprogramming macrophages. *Immunity* (2023) 56:162–79.e6. doi: 10.1016/j.immuni.2022.12.006

274. Xia Q, Jia J, Hu C, Lu J, Li J, Xu H, et al. Tumor-associated macrophages promote PD-L1 expression in tumor cells by regulating PKM2 nuclear translocation in pancreatic ductal adenocarcinoma. *Oncogene* (2022) 41:865–77. doi: 10.1038/s41388-021-02133-5

275. Zhang J, Fu J, Zhang G. Assessing expression of PD-L1 in tumor-associated macrophages. *JAMA Oncol* (2020) 6:1634. doi: 10.1001/jamaoncol.2020.2698

276. Cho J, Kim E, Yoon SE, Kim SJ, Kim WS. TET2 and LILRB1 mutations are frequent in Epstein-Barr virus-positive diffuse large B-cell lymphoma especially in elderly patients. *Cancer* (2023) 129:1502–12. doi: 10.1002/cncr.34698

277. Zou R, Zhong X, Liang K, Zhi C, Chen D, Xu Z, et al. Elevated LILRB1 expression predicts poor prognosis and is associated with tumor immune infiltration in patients with glioma. *BMC Cancer* (2023) 23:403. doi: 10.1186/s12885-023-10906-2

278. Molgora M, Liu YA, Colonna M, Cella M. TREM2: A new player in the tumor microenvironment. *Semin Immunol* (2023) 67:101739. doi: 10.1016/j.smim.2023.101739

279. Fox R, Nhan TQ, Law GL, Morris DR, Liles WC, Schwartz SM. PSGL-1 and mTOR regulate translation of ROCK-1 and physiological functions of macrophages. *EMBO J* (2007) 26:505–15. doi: 10.1038/sj.emboj.7601522

280. Vivian Ma YH, Sparkes A, Saha S, Gariepy J. VISTA as a ligand downregulates LPS-mediated inflammation in macrophages and neutrophils. *Cell Immunol* (2022) 379:104581. doi: 10.1016/j.cellimm.2022.104581

281. Baran N, Lodi A, Dhungana Y, Herbrich S, Collins M, Sweeney S, et al. Inhibition of mitochondrial complex I reverses NOTCH1-driven metabolic reprogramming in T-cell acute lymphoblastic leukemia. *Nat Commun* (2022) 13:2801. doi: 10.1038/s41467-022-30396-3

282. Dora D, Ligeti B, Kovacs T, Revisnyei P, Galffy G, Dulka E, et al. Non-small cell lung cancer patients treated with Anti-PD1 immunotherapy show distinct microbial signatures and metabolic pathways according to progression-free survival and PD-L1 status. *Oncoimmunology* (2023) 12:2204746. doi: 10.1080/2162402X.2023.2204746

283. Choueiri TK, McDermott DF, Merchan J, Bauer TM, Figlin R, Heath EI, et al. Belzutifan plus cabozantinib for patients with advanced clear cell renal cell carcinoma previously treated with immunotherapy: an open-label, single-arm, phase 2 study. *Lancet Oncol* (2023) 24:553–62. doi: 10.1016/S1470-2045(23)00097-9

284. Yap TA, Daver N, Mahendra M, Zhang J, Kamiya-Matsuoka C, Meric-Bernstam F, et al. Complex I inhibitor of oxidative phosphorylation in advanced solid tumors and acute myeloid leukemia: phase I trials. *Nat Med* (2023) 29:115–26. doi: 10.1038/s41591-022-02103-8

285. Oh MH, Sun IH, Zhao L, Leone RD, Sun IM, Xu W, et al. Targeting glutamine metabolism enhances tumor-specific immunity by modulating suppressive myeloid cells. *J Clin Invest* (2020) 130:3865–84. doi: 10.1172/JCI131859

286. Stone TW, Williams RO. Modulation of T cells by tryptophan metabolites in the kynurenine pathway. *Trends Pharmacol Sci* (2023) 44:442–56. doi: 10.1016/j.tips.2023.04.006

287. Hu C, Song Y, Zhang Y, He S, Liu X, Yang X, et al. Sequential delivery of PD-1/PD-L1 blockade peptide and IDO inhibitor for immunosuppressive microenvironment remodeling *via* an MMP-2 responsive dual-targeting liposome. *Acta Pharm Sin B* (2023) 13:2176–87. doi: 10.1016/j.apsb.2023.02.009

288. Kapron B, Czarnomysy R, Radomska D, Bielawski K, Plech T. Thiosemicarbazide derivatives targeting human topoIIalpha and IDO-1 as small-molecule drug candidates for breast cancer treatment. *Int J Mol Sci* (2023) 24. doi: 10.3390/ijms24065812

289. Li Q, Liu J, Fan H, Shi L, Deng Y, Zhao L, et al. IDO-inhibitor potentiated immunogenic chemotherapy abolishes primary tumor growth and eradicates metastatic lesions by targeting distinct compartments within tumor microenvironment. *Biomaterials* (2021) 269:120388. doi: 10.1016/j.biomaterials.2020.120388

290. Lorentzen CL, Kjeldsen JW, Ehrnrooth E, Andersen MH, Marie Svane I. Long-term follow-up of anti-PD-1 naive patients with metastatic melanoma treated with IDO/PD-L1 targeting peptide vaccine and nivolumab. *J Immunother Cancer* (2023) 11. doi: 10.1136/jitc-2023-006755

291. Zhai L, Bell A, Ladomersky E, Lauing KL, Bollu L, Sosman JA, et al. Immunosuppressive IDO in cancer: mechanisms of action, animal models, and targeting strategies. *Front Immunol* (2020) 11:1185. doi: 10.3389/fimmu.2020.01185

292. Zheng Q, Gan G, Gao X, Luo Q, Chen F. Targeting the IDO-BCL2A1-cytochrome c pathway promotes apoptosis in oral squamous cell carcinoma. *Onco Targets Ther* (2021) 14:1673–87. doi: 10.2147/OTT.S288692

293. Qiao X, Hu Z, Xiong F, Yang Y, Peng C, Wang D, et al. Lipid metabolism reprogramming in tumor-associated macrophages and implications for therapy. *Lipids Health Dis* (2023) 22:45. doi: 10.1186/s12944-023-01807-1

294. Colegio OR, Chu NQ, Szabo AL, Chu T, Rhebergen AM, Jairam V, et al. Functional polarization of tumour-associated macrophages by tumour-derived lactic acid. *Nature* (2014) 513:559–63. doi: 10.1038/nature13490

295. Goldberg FW, Kettle JG, Lamont GM, Buttar D, Ting AKT, McGuire TM, et al. Discovery of clinical candidate AZD0095, a selective inhibitor of monocarboxylate transporter 4 (MCT4) for oncology. *J Med Chem* (2023) 66:384–97. doi: 10.1021/acs.jmedchem.2c01342

296. Shields CW, Evans MA, Wang LL, Baugh N, Iyer S, Wu D, et al. Cellular backpacks for macrophage immunotherapy. *Sci Adv* (2020) 6:eaaz6579. doi: 10.1126/sciadv.aaz6579

297. Kaczanowska S, Beury DW, Gopalan V, Tycko AK, Qin H, Clements ME, et al. Genetically engineered myeloid cells rebalance the core immune suppression program in metastasis. *Cell* (2021) 184:2033–52.e21. doi: 10.1016/j.cell.2021.02.048

frontiers | Frontiers in Oncology

TYPE Review
PUBLISHED 14 March 2024
DOI 10.3389/fonc.2024.1287010

OPEN ACCESS

EDITED BY
Martin Böttcher,
Otto-von-Guericke University
Magdeburg, Germany

REVIEWED BY
Musaddiq Javvad Awan,
Medical College of Wisconsin, United States
Chad Brenner,
University of Michigan, United States

*CORRESPONDENCE
Stephen Y. Lai
sylai@mdanderson.org
Vlad C. Sandulache
Vlad.Sandulache@bcm.edu

RECEIVED 01 September 2023
ACCEPTED 20 February 2024
PUBLISHED 14 March 2024

CITATION
Sandulache VC, Kirby RP and Lai SY (2024) Moving from conventional to adaptive risk stratification for oropharyngeal cancer. *Front. Oncol.* 14:1287010. doi: 10.3389/fonc.2024.1287010

Moving from conventional to adaptive risk stratification for oropharyngeal cancer

Vlad C. Sandulache[1,2,3]*, R. Parker Kirby[1] and Stephen Y. Lai[4,5,6]*

[1]Bobby R. Alford Department of Otolaryngology- Head and Neck Surgery, Baylor College of Medicine, Houston, TX, United States, [2]Ear Nose and Throat Section (ENT), Operative Care Line, Michael E. DeBakey Veterans Affairs Medical Center, Houston, TX, United States, [3]Center for Translational Research on Inflammatory Diseases, Michael E. DeBakey Veterans Affairs Medical Center, Houston, TX, United States, [4]Department of Head and Neck Surgery, Division of Surgery, University of Texas MD Anderson Cancer Center, Houston, TX, United States, [5]Department of Molecular and Cellular Oncology, Division of Surgery, University of Texas MD Anderson Cancer Center, Houston, TX, United States, [6]Department of Radiation Oncology, Division of Surgery, University of Texas MD Anderson Cancer Center, Houston, TX, United States

Oropharyngeal cancer (OPC) poses a complex therapeutic dilemma for patients and oncologists alike, made worse by the epidemic increase in new cases associated with the oncogenic human papillomavirus (HPV). In a counterintuitive manner, the very thing which gives patients hope, the high response rate of HPV-associated OPC to conventional chemo-radiation strategies, has become one of the biggest challenges for the field as a whole. It has now become clear that for ~30-40% of patients, treatment intensity could be reduced without losing therapeutic efficacy, yet substantially diminishing the acute and lifelong morbidity resulting from conventional chemotherapy and radiation. At the same time, conventional approaches to de-escalation at a population (selected or unselected) level are hampered by a simple fact: we lack patient-specific information from individual tumors that can predict responsiveness. This results in a problematic tradeoff between the deleterious impact of de-escalation on patients with aggressive, treatment-refractory disease and the beneficial reduction in treatment-related morbidity for patients with treatment-responsive disease. True precision oncology approaches require a constant, iterative interrogation of solid tumors prior to and especially during cancer treatment in order to tailor treatment intensity to tumor biology. Whereas this approach can be deployed in hematologic diseases with some success, our ability to extend it to solid cancers with regional metastasis has been extremely limited in the curative intent setting. New developments in metabolic imaging and quantitative interrogation of circulating DNA, tumor exosomes and whole circulating tumor cells, however, provide renewed opportunities to adapt and individualize even conventional chemo-radiation strategies to diseases with highly variable biology such as OPC. In this review, we discuss opportunities to deploy developing technologies in the context of institutional and cooperative group clinical trials over the coming decade.

KEYWORDS

oropharynx, hyperpolarized MRI, circulating tumor cells, cell free DNA, smoking, radiation

Introduction

OPC incidence is increasing

With more than 63,000 cases annually in the US, head and neck cancer (HNC) represents a significant health burden (1). The epidemic increase in human papillomavirus (HPV)-associated HNC will dramatically increase this burden over the coming decades. Given the epidemiologic shift toward HPV-mediated diseases and lagging vaccination rates, the rise in HNC incidence is projected to not *begin* to abate until the 2050s. The US healthcare system will need to accommodate medical conditions related to HNC and HNC treatment for well over 4 million patients projected to be diagnosed between 2000 and 2060 (2). Previously a relatively rare entity, HNC was primarily attributable to tobacco and alcohol exposure and was predominantly a disease of elderly male patients (3, 4). The rise in HPV-associated HNC (3, 5) affects most age groups and crosses gender and racial/ethnic barriers (6). Long known to be a cause of cervical, penile, and anal cancer (7–9), HPV has been shown to be the primary driver of the increase in HNC diagnoses particularly for the oropharynx site (OPC). Preclinical and clinical studies have now conclusively linked HPV to OPC tumorigenesis in a majority of new diagnoses in the United States, with an increasing incidence across much of the world (10–19).

Survival is highly variable

The shift toward HPV-associated disease was accompanied by the first significant improvements in HNC treatment response and survival in the last 50 years of clinical research and medicine. First brought to light by the landmark retrospective analysis of RTOG 0129 by Ang et al. (10), HPV-associated OPC demonstrates a drastically improved survival compared to its HPV-independent counterpart. At a population level, younger OPC patients, without a history of tobacco exposure and early T-stage tumors were shown to have a significantly improved survival in the early 2000s compared to the previous half century (3). Despite these promising shifts in survival, the same analysis showed that a subset of OPC patients continues to demonstrate poor disease free and overall survival, consistent with historical data, despite application of new therapeutic strategies (3, 10).

Following a decade of clinical trial and retrospective data analysis, the AJCC Staging Manual received a significant update in its 8th Edition, with a dichotomization of OPC into HPV-associated and HPV-independent disease, and a concomitant reduction in stage in the context of HPV-associated OPC meant to more accurately reflect the improved survival of patients with what in the past would have been considered Stage II-III and even Stage IV disease (20). The newest large scale clinical trials conducted in OPC, including RTOG1016 and De-ESCALaTE confirmed that the survival parameters for HPV-associated OPC had indeed shifted critically compared to historical data (21, 22).

This improvement in survival, predicated on an excellent response to conventional radiation and chemotherapy strategies in a large subset of HPV-associated OPC has given hope to patients and clinicians alike, given the prevailing failures to improve HNC survival over previous decades. Yet at the same time, the same improvement in survival has drastically complicated the clinical management of the disease, at a time when its increasing incidence is exacerbating potential errors in an exponential fashion. Although as a group, HPV-associated OPC patients do well compared to their HPV-independent OPC counterparts, this effect is not uniform. There remains considerable heterogeneity in HPV-associated OPC response to treatment. Among Veterans with high rates of heavy tobacco exposure, survival for HPV-associated OPC remains lower compared to non-smokers by approximately 20% (4, 23) in line with the Ang et al. intermediate-risk rates (4, 24). These characteristics are conserved in both white and black patients, resulting in similar disease behavior and oncologic outcomes (25). Re-analyzed data from RTOG 0129 and RTOG 0522 demonstrated that the overall (OS) and progression free survival (PFS) rates for low-, intermediate- and high-risk OPC patients persisted with a difference in PFS between low- and intermediate- risk groups of over 15% (26). Our recent analysis of over 600 OPC patients treated in the modern era showed that heavy tobacco exposure reduced survival by the same amount as a shift in disease stage of 1 (e.g., stage I migrated to stage II) (27), in line with data published earlier by Vawda et al. (28).

Whereas some risk factors (e.g., tobacco) portend inferior survival in a subset of HPV-associated OPC patients, there is increasing evidence that a subset of HPV-associated OPC patients demonstrates excellent response to chemo-radiation. A recent analysis of over 1000 HPV-associated OPC patients showed that low levels of multinucleation identified on analysis of pre-treatment biopsy specimens were associated with dramatic improvements in overall, disease free and distant metastasis free survival, with hazard ratios ranging from 1.78 to 1.94 (29). In parallel, even when the analysis is restricted by stage, as was done by our collaborative group in a cohort of 439 stage I patients, infiltrative lymphocyte levels can drive further stratification of survival with hazard ratios >2.0 (30).

Together these data indicate that new HPV-associated OPC patients cannot be expected to demonstrate uniform response to chemo-radiation and thus equivalent survival. Furthermore, there is no evidence that this divergent survival is likely to change over the coming decades due to significant shifts in treatment paradigms. Surgery has not replaced radiation for most patients and there is no evidence that post-treatment function will be better with surgery (31–33). Targeted agents are inferior to conventional chemotherapy and no less toxic (21, 22). Immunotherapy has not yet demonstrated utility in the definitive, frontline setting for HNC and thus will be unlikely to replace conventional chemotherapy as a radiosensitizer in the near future (34). The only viable option to achieve a precision oncology approach that appropriately balances treatment effectiveness and toxicity is to maximize separation of patients into high-risk and low-risk groups.

Limitations to conventional risk stratification

Although largely self-evident, it remains important to understand why it is critical that we accurately risk-stratify OPC patients. Standard NCCN guidelines for OPC treatment include definitive external beam radiation (EBRT) regimens (66-70Gy) or surgical resection followed by adjuvant EBRT with a slight reduction in dose based on pathologic features of the disease and conventional chemotherapy with cisplatin being the current standard of care (21, 22). As indicated above, these conventional approaches are extremely effective in a majority of HPV-associated OPC patients but they carry significant acute toxicity and the potential for life-long debilitating morbidity (e.g., chronic renal insufficiency, peripheral neurotoxicity, chronic aspiration, lower cranial nerve neuropathies) (35–43). There is currently no definitive evidence that we can safely shift away from current NCCN guidelines for HPV-associated OPC disease as a whole. Omission of cisplatin has not been shown to be safe at a population level prospectively (HN002) (44) and direct replacement of cisplatin with cetuximab has failed in 2 prospective clinical trials (21, 22). Replacement of cisplatin with immune checkpoint inhibitors does not appear to be on the horizon for at least another decade based on the most recent negative clinical trial data (34). Altered fractionation regimens designed to reduce EBRT toxicity have been investigated for over 3 decades without a significant impact, although IMRT has indeed greatly reduced toxicity over previous EBRT delivery approaches (35). Dose de-escalation appears promising in very select patients, but has not yet been shown to be safe across the broader HPV-associated OPC population in large randomized clinical trials. Incorporation of surgery into treatment paradigms for OPC has shown promise as it relates to risk stratification and tailoring adjuvant treatment to disease burden. In EA3311, investigators were able to show that patients deemed intermediate-risk based on surgical pathologic parameters could receive a reduced dose of adjuvant radiation of 50Gy without a clear decrease in treatment efficacy as measured using progression free survival (PFS) (45).

Recurrence from HPV-associated OPC is deadly; no less so compared to that from HPV-independent disease. Salvage with surgery, re-irradiation or systemic treatment fails in >60% of recurrent disease patients (46–49). Taken together, the severe toxicity from current treatment regimens and the nearly uniform fatality of recurrent disease create a Hobson's choice for patients and a difficult balancing act for oncologists. Reducing treatment intensity at a population level will undoubtedly result in more recurrences yet failure to reduce treatment intensity will result in overtreatment and unnecessary toxicity in a large fraction of the OPC population. Importantly, some of this toxicity will translate into treatment related mortality (e.g., aspiration), making the need for accurate risk-stratification of OPC patients critical.

Conventional risk stratification has been standard for HNC ever since the first introduction of TNM classification and has continued throughout the 8 editions of the AJCC Staging Manual. That conventional risk stratification is clinically useful is evidenced by the significant divergence of survival by disease stage across tens of thousands of treated patients; that incorporation of HPV status into OPC staging has been impactful is similarly made plain by both prospective and retrospective datasets (10, 11, 21, 27, 46, 50). Yet at the same time, conventional risk stratification has had a modest impact on our ability to develop treatment regimens better tailored to disease biology. Whereas positive margins and extra-nodal extension (ENE) were shown to be useful in assigning patients to treatment escalation with the addition of conventional chemotherapy in the adjuvant setting, their utility in the setting of HPV-associated disease may be more limited (47). For aggressive, advanced-stage disease, attempted escalation with induction chemotherapy failed to improve survival in the PARADIGM and DECIDE trials (51, 52), and in a recent in-depth retrospective analysis appeared to be associated with reduced survival in OPC patients (53). As mentioned above, changing from cisplatin to cetuximab, a drug assumed to be more tolerable and thus better suited for the lower risk HPV-associated OPC population failed to maintain adequate survival in both RTOG1016 (which included intermediate-risk OPC) and De-ESCALaTE (which included exclusively low-risk OPC) trials (21). HN002 concluded that although a modest reduction in EBRT dose was safe, the omission of cisplatin could not be deemed safe even in non-smokers with HPV-associated OPC (low-risk OPC) (44).

One limitation of conventional risk stratification is that it requires very large signals (difference in survival), very large cohorts or both. An excellent example of this is the initial Ang et al. study in which HPV-associated OPC demonstrated ~75% survival at 2 years compared to HPV-independent OPC patients which demonstrated ~30% survival at 2 years, with HPV-associated smokers essentially in the middle (10). These very large differences have persisted in retrospective analysis across multiple cohorts and are reproduced in the aggregate when data from RTOG1016 and De-ESCALaTE are analyzed head to head. Despite decades of investigation, no other biological variable in HNC has demonstrated such dramatic stratifying effects (e.g., *TP53*) across multiple prospective and retrospective cohorts and thus, no other biological variables are included in the AJCC staging or considered in NCCN guidelines for HNC treatment generally. Effect sizes from shifts in treatment are similarly small. When averaged over tens of thousands of patients, the effect size for adding conventional chemotherapy to radiation in the definitive setting results in merely a 7-8% improvement in survival in the latest MACH-NC analysis, yet its elimination in the setting of low risk disease has not been shown to be safe (54). For decades, nodal metastasis was considered one of the most compelling predictors of survival in HNC, and indeed for HPV-independent disease it remains so as was recently show in oral cavity disease (47). In contrast, HPV-associated OPC demonstrates excellent survival even when nodal metastasis is present, which resulted in the substantial down-staging of tumors with significant nodal disease in the 8th edition of the AJCC Staging Manual (20).

A second limitation of conventional risk stratification is a fundamental lack of knowledge - we simply don't know what we don't know. Decades were required to properly observe the presence of, measure the impact for, and develop risk stratification based on, HPV status alone in OPC. More recent

work from us and others has now identified other potential stratifiers for treatment response and survival, including multinucleation, infiltration of tumors by cytotoxic immunocytes, the presence of complex immune frameworks in a subset of OPC tumors and differential tumor mutational burden (30, 46, 55, 56). Yet none of these potential risk-stratification markers are fully proven, and it is unlikely that they would be incorporated into staging and used for treatment de-intensification without extensive prospective testing.

One critical limitation to incorporating biologically specific biomarkers into risk stratification algorithms stems from the potential for false negative findings. Many individual genomic events (e.g., *TP53* mutation, *KEAP1* mutation) can be quite rare depending on the subtype of OPC and thus most retrospective and prospective institutional datasets and even cooperative group trial cohorts will be underpowered to truly examine their risk stratification potential. The need to develop large cohorts, with comprehensive clinical data and appropriate matching tissue has now been recognized by investigators and funding agencies alike (e.g., National Institute of Dental and Craniofacial Research).

Risk-stratification and therapeutic response drivers

Many aspects of tumor biology can confer "risk" as manifested by reduced survival. However, only those biological events which drive treatment response can really inform our ability to modulate existing therapeutic strategies in a meaningful way to reduce toxicity or improve overall response. In breast cancer and prostate cancer, hormonal receptor status is utilized to characterize the disease because it fundamentally influences response to hormonal blockade (57, 58). In melanoma and to a lesser degree in thyroid carcinoma, *BRAF* mutational status is a critical biomarker because it predicts response to a specific treatment, namely BRAF +/- MEK inhibition. Unlike in these diseases, and multiple other examples in adjacent solid tumors (e.g., lung cancer) (59, 60), HNC broadly and OPC in particular manifests few, if any, examples of biologically consistent drivers of response to chemotherapy and radiation which can be used to *mechanistically inform modulation of therapy, especially de-escalation strategies*.

Even within the context of HPV-driven disease, the superior response of disease to conventional chemotherapy and radiation remains unclear. Some speculate that maintenance of a wild-type *TP53* status allows for activation of the tumor suppressor under oxidative stress conditions (e.g., during treatment) and may explain the improved response rate (61). Others, including us, believe that an improved tumor immune micro-environment (i.e., enriched for functional immunocytes) may somehow result in an improved response, although this is somewhat mechanistically unclear since HPV-associated tumors do not demonstrate a substantially better response to immune checkpoint inhibitors compared to their HPV-independent counterparts (46, 62, 63). Another subset of investigators suggest that higher levels of oncogene-driven replication stress in HPV-associated tumors allows them to more easily activate programmed cell death pathways (61) or that non-canonical p16 signaling may be key to enhanced radiation response in this disease subset (64). The fact that we cannot consistently explain WHY HPV-associated OPC responds better to radiation (with or without chemotherapy) provides a clear impediment to a logical escalation or de-escalation strategy for this patient population. Whereas HPV oncogenic infections and their downstream impact on intra-cellular tumor suppressors and signaling cascades have been studied for years, some of the more recent pathomic and radiomic features correlated with improved survival in HPV-associated disease have never been mechanistically explored and thus are highly unlikely to really impact treatment intensity decisions for the near future without extensive preclinical and clinical investigation.

This limitation also applies to what many consider the treatment of the future, namely immunotherapy in the form of immune checkpoint inhibitors (ICIs). Starting with CheckMate141 and followed by Keynote048, ICIs have now demonstrated meaningful activity in HNC broadly and OPC specifically in the recurrent metastatic disease setting (63, 65). However, their use has encountered some of the same difficulties experienced when trying to improve upon the radiation vs surgery +/- conventional chemotherapy approach with targeted agents (e.g., cetuximab) or conventional induction chemotherapy in previous decades: treatment optimization. Combinatorial therapy studies have failed in the definitive upfront setting to date (e.g., JAVELIN Head and Neck 100) (34). In part, this is likely driven by the same limitation we face with conventional treatment. We have no predictive biomarker of ICI response in HNC or OPC specifically. PDL1 status although utilized, is far from being informative enough to further optimize utilization beyond the dichotomous chemotherapy versus no chemotherapy decision point. More sophisticated transcriptomic approaches published in recent years (e.g., TGEP) or our pathomic approaches (MuNI, OP-TIL) remain far from being prospectively validated and even with validation they remain poorly linked mechanistically to ICI effects (29, 30, 66, 67). It is also important to note, that immunotherapy in the form of existing ICIs, is not quite as benign as was initially hoped. Significant levels of immunotherapy-related adverse events (irAEs) have been reported in non-small cell lung cancer (NSCLC) (68, 69), melanoma (70) and HNSCC (71) especially when multiple ICIs are combined. Particularly problematic is the consistent observation that ICI toxicity and effectiveness are extremely correlated suggesting a substantial hurdle to ICI deployment for HNSCC particularly when combined with other toxic regimens/treatments.

Adaptive risk stratification

In the second half of the last century, John Boyd introduced the OODA (observe, orient, decide, act) loop concept, first in the context of military conflict and then more generally in the context of human behavior and interaction. Conventional risk stratification for cancers has optimized the utilization of the OODA concept, even more so with the revolution in genomic, transcriptomic and

proteomic characterization of tumors. However, a key component of Boyd's approach to action was the loop itself, the iterative and ever informative nature of a repetitive cycle. Modern risk stratification runs the loop once; after the decision to act is made, no further information is easily available to the oncologist until the complete course of chemo-radiation runs its course. This approach violates basic principles of biology, which is adaptive in the setting of exogenous stress (particularly in highly flexible cancer cells) in addition to reducing the proven benefits of the loop. Oncologists are not to blame for this failure. The failure stems from the difficulties of obtaining new information from solid tumors that are meaningful, actionable, and timely. Yet new techniques are being increasingly deployed which may make this a reality in the not-too-distant future.

In addition to the difficulties associated with conventional risk stratification outlined above, conventional risk-stratification suffers from a fatal flaw. It is static; it ignores the effect of the treatment itself which can manifest in many ways. Radiation can impact ICI response through local destruction of immunocytes. Chemotherapy can impact ICI effectiveness through systemic myelosuppression. Both can generate significant shifts in tumor biology which may be anti-immunogenic (72). Conversely, these interactions can occur in a positive feedback loop through damage-associated molecular patterns (DAMPs) or generation of mutational or more commonly expression-based neoantigens (73, 74). Unlike other solid cancers, truly ingrained events such as *BRAF*, *ALK* and *EGFR* mutations simply do not exist in OPC or even HNC with sufficient frequency to drive treatment selection on the basis of predicted response. As a result, all biological shifts during treatment, small and subtle as they may be, can greatly impact the effectiveness of the chosen treatment and affect the predictive potential of any risk stratification schema (Figure 1). This limitation applies to ICIs as well which still lack a robustly informative biomarker of response in OPC and to some degree in many other solid tumors.

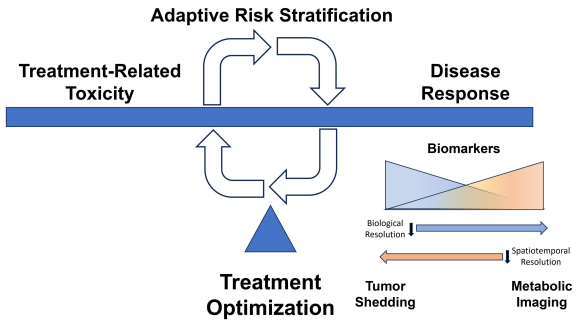

FIGURE 1
Dynamic Adaptive Risk Stratification. Treatment decisions for our patients balance maximizing disease response and minimizing treatment-related toxicity. There is currently a scarcity of clear biologically consistent drivers of response to therapy which can be used to mechanistically inform modulation of therapy, especially de-escalation strategies. Dynamic assessment of treatment response may allow therapeutic modification to balance disease control with toxicity. Tumor shedding creates a multitude of circulating biomarkers (e.g., viral DNA, tumor exosomes, viable circulating tumor cells) that provide high biological resolution regarding response to therapy, while imaging-based parameters may afford high spatiotemporal resolution reflective of tumor heterogeneity in response to treatment.

Leveraging tumor shedding for adaptive risk stratification

While hematopoietic malignancies have an intrinsic circulating component, solid tumors are highly anatomically restricted and defined (even in the metastatic setting). However, the presence of solid tumors can be detected at a systemic level through a multitude of circulating markers, including viral DNA (for oncogenic viruses such as EBV and HPV), tumor exosomes, cell free DNA (cfDNA), and even fully viable circulating tumor cells. These markers provide a compelling avenue to indirectly interrogate events in solid tumors to inform treatment selection and make clinical decisions in an iterative fashion for an individual patient.

Plasma EBV DNA levels have been capable of detecting a prior infection and associated malignancies for over 2 decades (75, 76). Nearly 80% of patients with active nasopharyngeal cancer mediated by EBV shed detectable EBV DNA prior to treatment and EBV remains systemically detectable in the post-treatment setting when patients presented with initially higher stage disease (77). In contrast to serology, circulating DNA levels can be at least partially correlated to relative tumor burden generating a more useful biomarker of relative tumor burden in the post treatment setting (78). Recent studies have extended this approach to the HPV counterpart of EBV leveraging the fact that both are oncogenic viruses with a direct link to the biological genesis of the underlying disease. Oncogenic HPV infection can be detected at a single-cell level in basal keratinocytes suggestive of potential for a mechanistic biomarker with a high sensitivity albeit likely a low specificity for development of cancer in the short term (79). HPV viral loads have been correlated with survival in patients with OPC (80) in both retrospective and prospective series. The ability to detect measurable changes in circulating tumor tissue modified viral DNA (TTMV) during treatment holds some potential to inform de-escalation strategies for patients with HPV-associated OPC. Although the accuracy of such a biomarker would need to be extremely high, a more proximate application of this approach is as early biomarker of recurrence. TTMV has been utilized in large series (81) of patients (>1000) to track recurrence post-treatment with an overall positive predictive value for recurrent disease of 95% and a point-in-time negative predictive value is 95% (with the caveat that some patients with a one-time negative test did go on to develop recurrence). Detection of EBV and HPV can thus be useful but is not currently actionable as it does not reflect events downstream from the individual viral oncogenes and thus cannot inform how chemotherapy, radiation or ICIs might interact with an individual tumor's biological features.

Whereas viral DNA can be useful in the setting of virally mediated HNC, circulating tumor DNA (ctDNA) can be broadly utilized regardless of underlying tumor pathogenesis. We and others have previously deployed ctDNA to detect actionable oncogenic events in solid tumors including melanoma and anaplastic thyroid carcinoma such as the V600E BRAF mutation

(82). Other investigators (83) have used ctDNA and phylogenetic analysis to track the evolution of lung cancer and development of chemotherapy resistance. In contrast to HNC and NSCLC, in SCLC high rates of hematogenous spread are commonly encountered resulting in rapid and widespread distant metastasis. In this setting ctDNA is thought to be particularly informative and representative of the intrinsic tumor biology (84) as was shown via paired analysis of primary tumors and ctDNA of variant allele frequency of clonal mutations. Simply put, shifts in ctDNA during and post-treatment can reflect, albeit with caveats, similar shifts within the primary and metastatic tumor sites which may be indicative of cure or recurrence as a function of clonal expansion and/extinction. Recent work by Cao et al. highlighted the utility of a combined ctDNA/imaging-based approach to early detection of treatment response in AJCC (8^{th} edition) stage III OPC patients and demonstrate significant correlation with freedom from disease progression (85). Similarly, Chera et al. showed that rapid clearance of HPV ctDNA (defined as a favorable clearance profile) achieved cure with conventional chemo-radiation in contrast to patients with an unfavorable clearance profile (86).

A broader biological approach is to assess exosomes (87), sub-micrometer tumor cell vesicles, which can be stable in body fluids and contain not just DNA, but also RNA, tumor proteins, lipids, and metabolites. In some cases, proteins can be particularly informative as in the case of PDL1 (88) which has been correlated to HNC disease progression as compared to non-exosomal plasma PDL1 levels. Exosomes and their counterpart microvesicles (89) can be used in a largely agnostic fashion to characterize data from both tumor and viral DNA as well as associated proteins and metabolites, forming a biologically rich dataset and providing increased stability for macromolecules in inhospitable fluid environments such as saliva which can be of critical importance to HNC. At the extreme end of the spectrum, the entire biological landscape of a subset of tumor clones can be captured in the form of whole, viable circulating tumor cells (CTCs) (90). In HNC, a pooled survival analysis of 22 studies eligible for systematic review found that presence of CTCs was associated with shorter disease-free survival (DFS, HR 4.62, 95% CI 2.51-8.52) with a very high overall specificity but low sensitivity. An important limitation to circulating biomarkers is that their actionability remains in question at this time in the context of OPSCC. All existing systemic treatments inclusive of ICIs incur significant toxicity for limited survival benefit and almost none for lasting cure. As such, treatment in the recurrent/metastatic setting is reserved for either imaging identifiable lesions (e.g. radiation based treatment of oligometastasis, surgical resection of isolated regional recurrence) or for symptomatic disease (e.g. palliative intent chemotherapy and/or chemo-ICIs). Since there is limited evidence that earlier initiation of treatment is either feasible, in the setting of imaging invisible disease, or beneficial, in the setting of disseminated disease, the utility of early detection of recurrence/metastasis for this particular disease site remains unclear, particularly since it often precedes conventionally detectable disease by only several weeks to months. As such, utility may be initially limited to early detection of response to primary treatment that could assist escalation/de-escalation decision making.

Leveraging metabolic imaging for adaptive risk stratification

Whereas ctDNA, CTCs and exosomes can provide high biologic resolution and identify a multitude of genomic, transcriptomic, and proteomic events related to tumorigenesis and evolution prior to and during treatment delivery, spatial resolution is absent. Although a signal may be detected, we have no idea where that signal is coming from (i.e., primary tumor, regional or distant metastases, etc). In contrast, imaging can provide outstanding spatial resolution, but significantly lower biological resolution. It is not the goal of this review to summarize the massive literature on the subject of biologic imaging of solid tumors, but rather to highlight some recent advances in imaging which may be applicable to dynamic or adaptive risk stratification strategies for OPC.

Starting with extensive work using F-labeled fluoromisonidazole (F-FMISO) (91), pre-treatment measurements of tumor hypoxia have long been utilized to ascertain potential radio-sensitivity/radio-resistance of whole tumors or individual tumor voxels given the known correlation between tumor hypoxia and radiation responsiveness. The counterpart of hypoxia, namely vascularity can be ascertained with fairly high sensitivity and specificity using dynamic contrast-enhanced MRI (DCE-MRI). DCE-MRI can be deployed in translationally relevant settings particularly when utilizing anti-angiogenic agents where imaging parameters may be altered prior to clinical effect (92). By capturing vascular parameters throughout the entire treatment field (tumor and adjacent normal tissue) DCE-MRI has the additional potential to be a real-time biomarker of normal tissue toxicity driven by shifts in vascularity. One such application pioneered by our group is the use of DCE-MRI for early detection of subclinical osteoradionecrosis (ORN) and identification of patients at high risk for severe ORN (93–95).

Extension of this work using multi-parametric (MRI) (96) has been used to predict complete response (CR) in patients with OPC prior to treatment completion in a manner suitable for potential treatment de-escalation in responders. Although additional work will be required to optimize multi-parametric and even DCE-MRI to fully capture biological data from the primary tumor and associated cervical lymphadenopathy common to OPC, preliminary findings are promising (97). This is particularly true since the approach appears to be scalable across institutions as shown in a comprehensive analysis (98) of the accuracy of diffusion-weighted imaging (DWI) for predicting locoregional failure of chemo-radiation in HNC across 9 studies and 421 patients, with a sensitivity of 82%, specificity of 70% and an area under the sROC curve of 84%.

While tumor vascularity, cellularity and hypoxia are transient on a slow scale (days-weeks), tumor metabolism is a continuously changing biological variable that has extremely high temporal

resolution (minutes-hours), and when interrogated via metabolic imaging can be analyzed with an equally high spatial resolution. Over the last 2 decades, both FDG-PET and hyperpolarized magnetic resonance imaging (HP-MRI) techniques have been used to assess the aggressiveness of solid tumors including HNC and have been explored as tools to predict treatment response in preclinical models and patients (99–109). Although FDG-PET is available in clinical settings, prospective clinical trial data suggest that measurement of mid-therapy glucose uptake does not allow for adaptive reduction in tumor volumes (110–115). Furthermore, glucose uptake does not correlate with radiation response and provides no information on intracellular metabolic fluxes (116–118). In contrast HP-MRI of labeled pyruvate and lactate provides a unique opportunity to obtain real-time metabolic information from within solid tumors. Its ability to detect differential metabolic activity in tumor tissue has been established (99, 109). Substantial work from other groups has advanced the development of HP-MRI into a clinically viable tool for characterization of intrinsic tumor aggressiveness (prostate) and towards deployment of HP-MRI as a tool to measure treatment response (e.g., breast cancer) (101, 103, 119–121). HNC sensitivity to genotoxic agents is a function of multiple discrete biological events, such as activation of pathways associated with the human papillomavirus (HPV) or mutation of tumor suppressors such as *TP53*. Unfortunately, we and others have shown that individual patient responses are not completely uniform across patient groups (e.g., HPV-associated vs. HPV-independent, wildtype vs. mutant *TP53*), and this may be due in large part to the heterogenous activation of acquired resistance pathways once treatment starts (3, 4, 10, 122–127). Therefore, even if genomic biomarkers such as *TP53* and HPV start to be used in treatment-selection decisions at baseline, tailoring treatment intensity to *individual* patients in the face of acquired resistance potentially based upon changes in metabolic response will still be required for true precision oncology approaches and personalized cancer treatment.

In 2014, we were the first to show that k_{PL} measured with noninvasive HP [1- (13)C]-pyruvate MRI is decreased under conditions of depleted REDOX following genotoxic stress in animal models of HNC and other tumors (128). We have developed a multi-compartment model of intracellular k_{PL} which increases the fidelity of our measurements (129). In 2020, for the first time, we measured these metabolic changes in a patient during treatment. This first-in-human assessment of metabolic response to treatment serves as a critical proof-of-principle and demonstrates our technical capability to execute the proposed studies. On the basis of these robust preliminary data, we propose to test the potential of metabolic interrogation as a clinical tool that can (1) predict treatment response and (2) be used to develop treatment strategies tailored to individual tumor biology. Our innovative approach is supported by (1) studies that link reducing potential to genotoxic stress (127, 130–136); (2) clinical and preclinical data that link lactate to tumor progression and treatment response (137–139); and (3) studies that confirm the excellent spatiotemporal resolution of HP [1- (13)C]-pyruvate MRI (128, 140–143).

The biologically rich data from anatomic and metabolic studies can be enhanced by nearly an order of magnitude when combined with artificial intelligence (AI)/machine learning (ML) approaches. Utilization of machine learning approaches (144) can generate meaningful data even from relatively data poor CECT studies to identify radiomic features which when combined can distinguish invasive cancer from more benign solid tumors. This approach has also been deployed (145) to generate combined radiomic risk scores which can predict disease free and overall survival in the context of either conventional treatment or in the presence of immunomodulatory combinatorial strategies.

A path toward clinical translation

Conventional and adaptive risk stratification are not mutually exclusive. They represent 2 aspects of a combined approach designed to deliver maximal anti-tumor activity, using the most appropriate agents, at the lowest possible dose that will achieve a durable cure. In order to maximize the therapeutic index of both conventional and targeted strategies the most effective future algorithms will start with conventional risk stratification that combines biological data with clinical risk factors. Upon this baseline approach, treatment algorithms will then incorporate a complex adaptive risk stratification strategy that combines feasible aspects of biological interrogation using circulating and imaging tumor markers (Figure 1). Critically, this second layer of data will be truly personalized, specific not only to the individual tumor, but also to the interaction between the individual tumor and the chosen treatment regimen. Successful implementation of such an approach will require a rigorous process, outlined by Pepe et al. nearly 2 decades ago (146), whose key ingredients include carefully defining the target population (carefully selected based on clinically relevant criteria and relevant disease biology) and the expected outcome for each individual biomarker (e.g. impact on local recurrence vs distant metastasis rates), testing in populations large enough to reduce the number of false negative studies, and *a priori* definitions of expected effect size and clinical impact. For solid tumors, which present challenges to repetitive interrogation with high biological and spatial resolution (see above), an "n of 1" precision oncology algorithm is somewhat unlikely using existing approaches and technologies, however, careful integrated of layered biomarkers can provide a significant advantage over current clinical paradigms for OPC. For widespread clinical translation it is critical to identify circulating markers (high biological resolution) and imaging modalities (high temporal and spatial resolution) which can be rapidly deployed and relatively cost-effective. Finally, the entire platform and associated algorithms must be readily replicated across institutions and healthcare delivery systems. Our patients deserve no less.

Author contributions

SL: Conceptualization, Formal analysis, Funding acquisition, Project administration, Supervision, Writing – original draft, Writing – review & editing. VS: Conceptualization, Formal analysis, Funding acquisition, Project administration, Supervision,

Writing – original draft, Writing – review & editing. RK: Writing – original draft, Writing – review & editing.

Funding

The author(s) declare financial support was received for the research, authorship, and/or publication of this article. This work was supported by a Career Development Award to VS from the Veterans Administration Clinical Science Research and Development division (1IK2CX001953). VS is supported by an American Cancer Society Research Scholar Grant RSG-21-182-01-CDP. SL and VS receive research support from R01DE025248, R01CA280980, U01DE032168, and U54CA274321. SL has additional research funding from R01DE032521, R01DE028290, R21CA259839, and T32CA261856.

Conflict of interest

The authors declare that the research was conducted in the absence of any commercial or financial relationships that could be construed as a potential conflict of interest.

Publisher's note

References

1. Siegel RL, Miller KD, Fuchs HE, Jemal A. Cancer Statistics, 2021. *CA: A Cancer J Clin*. (2021) 71:7–33. doi: 10.3322/caac.21654

2. Zhang Y, Fakhry C, D'Souza G. Projected Association of Human Papillomavirus Vaccination With Oropharynx Cancer Incidence in the US, 2020-2045. *JAMA Oncol*. (2021) 7:e212907. doi: 10.1001/jamaoncol.2021.2907

3. Dahlstrom KR, Calzada G, Hanby JD, Garden AS, Glisson BS, Li G, et al. An evolution in demographics, treatment, and outcomes of oropharyngeal cancer at a major cancer center: a staging system in need of repair. *Cancer*. (2013) 119:81–9. doi: 10.1002/cncr.27727

4. Sandulache VC, Hamblin J, Lai S, Pezzi T, Skinner HD, Khan NA, et al. Oropharyngeal squamous cell carcinoma in the veteran population: Association with traditional carcinogen exposure and poor clinical outcomes. *Head Neck*. (2015) 37:1246–53. doi: 10.1002/hed.23740

5. Chaturvedi AK, Engels EA, Pfeiffer RM, Hernandez BY, Xiao W, Kim E, et al. Human Papillomavirus and Rising Oropharyngeal Cancer Incidence in the United States. *J Clin Oncol*. (2011) 29:4294–301. doi: 10.1200/jco.2011.36.4596

6. Lu DJ, Luu M, Mita A, Scher K, Shiao SL, Yoshida EP, et al. Human papillomavirus–associated oropharyngeal cancer among patients aged 70 and older: Dramatically increased prevalence and clinical implications. *Eur J Cancer*. (2018) 103:195–204. doi: 10.1016/j.ejca.2018.08.015

7. Gupta SM, Mania-Pramanik J. Molecular mechanisms in progression of HPV-associated cervical carcinogenesis. *J BioMed Sci*. (2019) 26:28. doi: 10.1186/s12929-019-0520-2

8. Castellsague X. Natural history and epidemiology of HPV infection and cervical cancer. *Gynecol Oncol*. (2008) 110:S4–7. doi: 10.1016/j.ygyno.2008.07.045

9. Shrestha AD, Neupane D, Vedsted P, Kallestrup P. cervical cancer prevalence, incidence and mortality in low and middle income countries: A systematic review. *Asian Pac J Cancer Prev*. (2018) 19:319–24. doi: 10.22034/APJCP.2018.19.2.319

10. Ang KK, Harris J, Wheeler R, Weber R, Rosenthal DI, Nguyen-Tan PF, et al. Human papillomavirus and survival of patients with oropharyngeal cancer. *N Engl J Med*. (2010) 363:24–35. doi: 10.1056/NEJMoa0912217

11. Gillison ML, D'Souza G, Westra W, Sugar E, Xiao W, Begum S, et al. Distinct risk factor profiles for human papillomavirus type 16-positive and human papillomavirus type 16-negative head and neck cancers. *J Natl Cancer Inst*. (2008) 100:407–20. doi: 10.1093/jnci/djn025

12. Gleber-Netto FO, Rao X, Guo T, Xi Y, Gao M, Shen L, et al. Variations in HPV function are associated with survival in squamous cell carcinoma. *JCI Insight*. (2019) 4 (1):e124762. doi: 10.1172/jci.insight.124762

13. Muller S, Khuri FR, Kono SA, Beitler JJ, Shin DM, Saba NF. HPV positive squamous cell carcinoma of the oropharynx. *Are we observing an unusual Pattern metastases? Head Neck Pathol*. (2012) 6:336–44. doi: 10.1007/s12105-012-0355-6

14. Shay SG, Chang E, Lewis MS, Wang MB. Characteristics of Human Papillomavirus- Associated Head and Neck Cancers in a Veteran Population. *JAMA Otolaryngol Head Neck Surg*. (2015) 141:790–6. doi: 10.1001/jamaoto.2015.1447

15. Garnaes E, Kiss K, Andersen L, Therkildsen MH, Franzmann MB, Filtenborg-Barnkob B, et al. A high and increasing HPV prevalence in tonsillar cancers in Eastern Denmark, 2000–2010: The largest registry-based study to date. *Int J Cancer*. (2015) 136:2196–203. doi: 10.1002/ijc.29254

16. Garnaes E, Kiss K, Andersen L, Therkildsen MH, Franzmann MB, Filtenborg-Barnkob B, et al. Increasing incidence of base of tongue cancers from 2000 to 2010 due to HPV: the largest demographic study of 210 Danish patients. *Br J Of Cancer*. (2015) 113:131. doi: 10.1038/bjc.2015.198. https://www.nature.com/articles/bjc2015198#supplementary-information.

17. Rietbergen MM, Leemans CR, Bloemena E, Heideman DAM, Braakhuis BJM, Hesselink AT, et al. Increasing prevalence rates of HPV attributable oropharyngeal squamous cell carcinomas in the Netherlands as assessed by a validated test algorithm. *Int J Cancer*. (2013) 132:1565–71. doi: 10.1002/ijc.27821

18. Shin A, Jung Y-S, Jung K-W, Kim K, Ryu J, Won Y-J. Trends of human papillomavirus-related head and neck cancers in Korea: National cancer registry data. *Laryngoscope*. (2013) 123:E30– E37. doi: 10.1002/lary.24243

19. Hwang T-Z, Hsiao J-R, Tsai C-R, Chang JS. Incidence trends of human papillomavirus-related head and neck cancer in Taiwan, 1995–2009. *Int J Cancer*. (2015) 137:395–408. doi: 10.1002/ijc.29330

20. O'Sullivan B, Huang SH, Su J, Garden AS, Sturgis EM, Dahlstrom K, et al. Development and validation of a staging system for HPV-related oropharyngeal cancer by the International Collaboration on Oropharyngeal cancer Network for Staging (ICON-S): a multicentre cohort study. *Lancet Oncol*. (2016) 17:440–51. doi: 10.1016/S1470-2045(15)00560-4

21. Gillison ML, Trotti AM, Harris J, Eisbruch A, Harari PM, Adelstein DJ, et al. Radiotherapy plus cetuximab or cisplatin in human papillomavirus-positive oropharyngeal cancer (NRG Oncology RTOG 1016): a randomised, multicentre, non-inferiority trial. *Lancet*. (2019) 393:40–50. doi: 10.1016/S0140-6736(18)32779-X

22. Mehanna H, Robinson M, Hartley A, Kong A, Foran B, Fulton-Lieuw T, et al. Radiotherapy plus cisplatin or cetuximab in low-risk human papillomavirus-positive oropharyngeal cancer (De- ESCALaTE HPV): an open-label randomised controlled phase 3 trial. *Lancet*. (2019) 393:51–60. doi: 10.1016/S0140-6736(18)32752-1

23. Park J, McPike V, Kambhampati S, Huang C, Fields-Meehan J, Verkruyse L, et al. Positivity Rates in Oropharyngeal and Nonoropharyngeal Head and Neck Cancer in the VA. *Fed Pract*. (2018) 35:S44– S47.

24. Feinstein AJ, Shay SG, Chang E, Lewis MS, Wang MB. Treatment outcomes in veterans with HPV-positive head and neck cancer. *Am J Otolaryngol*. (2017) 38:188–92. doi: 10.1016/j.amjoto.2017.01.005

25. Zevallos JP, Sandulache VC, Hamblin J, Skinner HD, Kramer J, Hartman CM, et al. Impact of race on oropharyngeal squamous cell carcinoma presentation and outcomes among veterans. *Head Neck*. (2016) 38:44–50. doi: 10.1002/hed.23836

26. Fakhry C, Zhang Q, Gillison ML, Nguyen-Tan PF, Rosenthal DI, Weber RS, et al. Validation of NRG oncology/RTOG-0129 risk groups for HPV-positive and HPV-negative oropharyngeal squamous cell cancer: Implications for risk-based therapeutic intensity trials. *Cancer*. (2019) 125:2027–38. doi: 10.1002/cncr.32025

27. Elhalawani H, Mohamed ASR, Elgohari B, Lin TA, Sikora AG, Lai SY, et al. Tobacco exposure as a major modifier of oncologic outcomes in human papillomavirus (HPV) associated oropharyngeal squamous cell carcinoma. *BMC Cancer*. (2020) 20:912. doi: 10.1186/s12885-020-07427-7

28. Vawda N, Banerjee RN, Debenham BJ. Impact of Smoking on Outcomes of HPV-related Oropharyngeal Cancer Treated with Primary Radiation or Surgery. *Int J Radiat Oncol Biol Phys*. (2019) 103:1125–31. doi: 10.1016/j.ijrobp.2018.11.046

29. Koyuncu CF, Lu C, Bera K, Zhang Z, Xu J, Andrea Toro Castano P, et al. Computerized tumor multinucleation index (MuNI) is prognostic in p16+ oropharyngeal carcinoma: A multi-site validation study. *J Clin Invest*. (2021) 131(8): e145488. doi: 10.1172/JCI145488

30. Corredor G, Toro P, Koyuncu C, Lu C, Buzzy C, Bera K, et al. An Imaging Biomarker of Tumor- Infiltrating Lymphocytes to Risk-Stratify Patients with HPV-Associated Oropharyngeal Cancer. *J Natl Cancer Inst*. (2021) 114(4):609–17. doi: 10.1093/jnci/djab215

31. Nichols AC, Theurer J, Prisman E, Read N, Berthelet E, Tran E, et al. Radiotherapy versus transoral robotic surgery and neck dissection for oropharyngeal squamous cell carcinoma (ORATOR): an open-label, phase 2, randomised trial. *Lancet Oncol*. (2019) 20:1349–59. doi: 10.1016/S1470-2045(19)30410-3

32. Nichols AC, Theurer J, Prisman E, Read N, Berthelet E, Tran E, et al. Randomized trial of radiotherapy versus transoral robotic surgery for oropharyngeal squamous cell carcinoma: long- term results of the ORATOR Trial. *J Clin Oncol*. (2022) 40:866–75. doi: 10.1200/JCO.21.01961

33. Nichols AC, Yoo J, Hammond JA, Fung K, Winquist E, Read N, et al. Early-stage squamous cell carcinoma of the oropharynx: radiotherapy vs. trans-oral robotic surgery (ORATOR)–study protocol for a randomized phase II trial. *BMC Cancer*. (2013) 13:133. doi: 10.1186/1471-2407-13-133

34. Lee NY, Ferris RL, Psyrri A, Haddad RI, Tahara M, Bourhis J, et al. Avelumab plus standard-of- care chemoradiotherapy versus chemoradiotherapy alone in patients with locally advanced squamous cell carcinoma of the head and neck: a randomised, double-blind, placebo-controlled, multicentre, phase 3 trial. *Lancet Oncol*. (2021) 22:450–62. doi: 10.1016/S1470-2045(20)30737-3

35. Beadle BM, Liao KP, Giordano SH, Garden AS, Hutcheson KA, Lai SY, et al. Reduced feeding tube duration with intensity-modulated radiation therapy for head and neck cancer: A Surveillance, Epidemiology, and End Results-Medicare Analysis. *Cancer*. (2017) 123:283–93. doi: 10.1002/cncr.30350

36. Bhayani MK, Hutcheson KA, Barringer DA, Lisec A, Alvarez CP, Roberts DB, et al. Gastrostomy tube placement in patients with oropharyngeal carcinoma treated with radiotherapy or chemoradiotherapy: factors affecting placement and dependence. *Head Neck*. (2013) 35:1634–40. doi: 10.1002/hed.23200

37. Goepfert RP, Lewin JS, Barrow MP, Fuller CD, Lai SY, Song J, et al. Predicting two-year longitudinal MD Anderson Dysphagia Inventory outcomes after intensity modulated radiotherapy for locoregionally advanced oropharyngeal carcinoma. *Laryngoscope*. (2017) 127:842–8. doi: 10.1002/lary.26153

38. Goepfert RP, Lewin JS, Barrow MP, Gunn GB, Fuller CD, Beadle BM, et al. Long-term, prospective performance of the md anderson dysphagia inventory in "Low-Intermediate Risk" oropharyngeal carcinoma after intensity modulated radiation therapy. *Int J Radiat Oncol Biol Phys*. (2017) 97:700–8. doi: 10.1016/j.ijrobp.2016.06.010

39. Hutcheson KA, Barrow MP, Lisec A, Barringer DA, Gries K, Lewin JS. What is a clinically relevant difference in MDADI scores between groups of head and neck cancer patients? *Laryngoscope*. (2016) 126:1108–13. doi: 10.1002/lary.25778

40. Hutcheson KA, Nurgalieva Z, Zhao H, Gunn GB, Giordano SH, Bhayani MK, et al. Two-year prevalence of dysphagia and related outcomes in head and neck cancer survivors: An updated SEER- Medicare analysis. *Head Neck*. (2019) 41:479–87. doi: 10.1002/hed.25412

41. Wong ATT, Lai SY, Gunn GB, Beadle BM, Fuller CD, Barrow MP, et al. Symptom burden and dysphagia associated with osteoradionecrosis in long-term oropharynx cancer survivors: A cohort analysis. *Oral Oncol*. (2017) 66:75–80. doi: 10.1016/j.oraloncology.2017.01.006

42. Chhabria K, Kansara S, Badr H, Stach C, Vernese M, Lerner A, et al. Gastrostomy utilization by oropharyngeal cancer patients is partially driven by swallowing function. *Laryngoscope*. (2019) 130(9):2153–9. doi: 10.1002/lary.28312

43. Harms A, Kansara S, Stach C, Richardson PA, Chen G, Lai S, et al. Swallowing function in survivors of oropharyngeal cancer is associated with advanced t classification. *Ann Otol Rhinol Laryngol*. (2019) 128:696–703. doi: 10.1177/0003489419839091

44. Yom SS, Torres-Saavedra P, Caudell JJ, Waldron JN, Gillison ML, Xia P, et al. Reduced-Dose Radiation Therapy for HPV-Associated Oropharyngeal Carcinoma (NRG Oncology HN002). *J Clin Oncol*. (2021) 39:956–65. doi: 10.1200/JCO.20.03128

45. Ferris RL, Flamand Y, Weinstein GS, Li S, Quon H, Mehra R, et al. Phase II randomized trial of transoral surgery and low-dose intensity modulated radiation therapy in resectable p16+ locally advanced oropharynx cancer: An ECOG-ACRIN cancer research group trial (E3311). *J Clin Oncol*. (2022) 40:138–49. doi: 10.1200/JCO.21.01752

46. Wilde DC, Castro PD, Bera K, Lai S, Madabhushi A, Corredor G, et al. Oropharyngeal cancer outcomes correlate with p16 status, multinucleation and immune infiltration. *Mod Pathol*. (2022) 35(8):1045–54. doi: 10.1038/s41379-022-01024-8

47. Sandulache VC, Michikawa C, Kataria P, Gleber-Netto FO, Bell D, Trivedi S, et al. High-risk TP53 mutations are associated with extranodal extension in oral cavity squamous cell carcinoma. *Clin Cancer Res*. (2018) 24:1727–33. doi: 10.1158/1078-0432.CCR-17-0721

48. Sandulache VC, Vandelaar LJ, Skinner HD, Cata J, Hutcheson K, Fuller CD, et al. Salvage total laryngectomy after external-beam radiotherapy: A 20-year experience. *Head Neck*. (2016) 38 Suppl 1:E1962–1968. doi: 10.1002/hed.24355

49. Sandulache VC, Kubik MW, Skinner HD, Malsky JA, Gelbard AH, Zevallos JP. Impact of race/ethnicity on laryngeal cancer in patients treated at a Veterans Affairs Medical Center. *Laryngoscope*. (2013) 123:2170–5. doi: 10.1002/lary.24058

50. Gillison ML, Chaturvedi AK, Anderson WF, Fakhry C. Epidemiology of Human Papillomavirus- Positive Head and Neck Squamous Cell Carcinoma. *J Clin Oncol*. (2015) 33:3235–42. doi: 10.1200/JCO.2015.61.6995

51. Haddad R, O'Neill A, Rabinowits G, Tishler R, Khuri F, Adkins D, et al. Induction chemotherapy followed by concurrent chemoradiotherapy (sequential chemoradiotherapy) versus concurrent chemoradiotherapy alone in locally advanced head and neck cancer (PARADIGM): a randomised phase 3 trial. *Lancet Oncol*. (2013) 14:257–64. doi: 10.1016/S1470-2045(13)70011-1

52. Cohen EE, Karrison TG, Kocherginsky M, Mueller J, Egan R, Huang CH, et al. Phase III randomized trial of induction chemotherapy in patients with N2 or N3 locally advanced head and neck cancer. *J Clin Oncol*. (2014) 32:2735–43. doi: 10.1200/JCO.2013.54.6309

53. Guo TW, Saiyed F, Yao C, Kiong KL, Martinez J, Sacks R, et al. Outcomes of patients with oropharyngeal squamous cell carcinoma treated with induction chemotherapy followed by concurrent chemoradiation compared with those treated with concurrent chemoradiation. *Cancer*. (2021) 127:2916–25. doi: 10.1002/cncr.33491

54. Lacas B, Carmel A, Landais C, Wong SJ, Licitra L, Tobias JS, et al. Meta-analysis of chemotherapy in head and neck cancer (MACH-NC): An update on 107 randomized trials and 19,805 patients, on behalf of MACH-NC Group. *Radiother Oncol*. (2021) 156:281–93. doi: 10.1016/j.radonc.2021.01.013

55. Koyuncu CF, Nag R, Lu C, Corredor G, Viswanathan VS, Sandulache VC, et al. Image analysis reveals differences in tumor multinucleations in Black and White patients with human papillomavirus-associated oropharyngeal squamous cell carcinoma. *Cancer*. (2022) 128:3831–42. doi: 10.1002/cncr.34446

56. Wahle BM, Zolkind P, Ramirez RJ, Skidmore ZL, Anderson SR, Mazul A, et al. Integrative genomic analysis reveals low T-cell infiltration as the primary feature of tobacco use in HPV-positive oropharyngeal cancer. *iScience*. (2022) 25:104216. doi: 10.1016/j.isci.2022.104216

57. Falato C, Schettini F, Pascual T, Braso-Maristany F, Prat A. Clinical implications of the intrinsic molecular subtypes in hormone receptor-positive and HER2-negative metastatic breast cancer. *Cancer Treat Rev*. (2022) 112:102496. doi: 10.1016/j.ctrv.2022.102496

58. Pagliuca M, Donato M, D'Amato AL, Rosanova M, Russo AOM, Scafetta R, et al. New steps on an old path: Novel estrogen receptor inhibitors in breast cancer. *Crit Rev Oncol Hematol*. (2022) 180:103861. doi: 10.1016/j.critrevonc.2022.103861

59. Giugliano F, Crimini E, Tarantino P, Zagami P, Uliano J, Corti C, et al. First line treatment of BRAF mutated advanced melanoma: Does one size fit all? *Cancer Treat Rev*. (2021) 99:102253. doi: 10.1016/j.ctrv.2021.102253

60. Bonomi PD, Gandara D, Hirsch FR, Kerr KM, Obasaju C, Paz-Ares L, et al. Predictive biomarkers for response to EGFR-directed monoclonal antibodies for advanced squamous cell lung cancer. *Ann Oncol*. (2018) 29:1701–9. doi: 10.1093/annonc/mdy196

61. Spiotto MT, Taniguchi CM, Klopp AH, Colbert LE, Lin SH, Wang L, et al. Biology of the Radio- and Chemo-Responsiveness in HPV Malignancies. *Semin Radiat Oncol*. (2021) 31:274–85. doi: 10.1016/j.semradonc.2021.02.009

62. Kemnade JO, Elhalawani H, Castro P, Yu J, Lai S, Ittmann M, et al. CD8 infiltration is associated with disease control and tobacco exposure in intermediate-risk oropharyngeal cancer. *Sci Rep*. (2020) 10:243. doi: 10.1038/s41598-019-57111-5

63. Ferris RL, Blumenschein G Jr., Fayette J, Guigay J, Colevas AD, Licitra L, et al. Nivolumab for Recurrent Squamous-Cell Carcinoma of the Head and Neck. *N Engl J Med*. (2016) 375:1856–67. doi: 10.1056/NEJMoa1602252

64. Molkentine DP, Molkentine JM, Bridges KA, Valdecanas DR, Dhawan A, Bahri R, et al. p16 Represses DNA Damage Repair *via* a Novel Ubiquitin-Dependent Signaling Cascade. *Cancer Res*. (2022) 82:916–28. doi: 10.1158/0008-5472.CAN-21-2101

65. Ferris RL, Blumenschein G Jr., Fayette J, Guigay J, Colevas AD, Licitra L, et al. Nivolumab vs investigator's choice in recurrent or metastatic squamous cell carcinoma of the head and neck: 2- year long-term survival update of CheckMate 141 with analyses by tumor PD-L1 expression. *Oral Oncol*. (2018) 81:45–51. doi: 10.1016/j.oraloncology.2018.04.008

66. Damotte D, Warren S, Arrondeau J, Boudou-Rouquette P, Mansuet-Lupo A, Biton J, et al. The tumor inflammation signature (TIS) is associated with anti-PD-1 treatment benefit in the CERTIM pan- cancer cohort. *J Transl Med*. (2019) 17:357. doi: 10.1186/s12967-019-2100-3

67. Danaher P, Warren S, Lu R, Samayoa J, Sullivan A, Pekker I, et al. Pan-cancer adaptive immune resistance as defined by the Tumor Inflammation Signature (TIS): results from The Cancer Genome Atlas (TCGA). *J Immunother Cancer*. (2018) 6:63. doi: 10.1186/s40425-018-0367-1

68. Cook S, Samuel V, Meyers DE, Stukalin I, Litt I, Sangha R, et al. Immune-Related Adverse Events and Survival Among Patients With Metastatic NSCLC Treated With Immune Checkpoint Inhibitors. *JAMA Netw Open*. (2024) 7:e2352302. doi: 10.1001/jamanetworkopen.2023.52302

69. Ghanbar MI, Suresh K. Pulmonary toxicity of immune checkpoint immunotherapy. *J Clin Invest*. (2024) 134(2):e170503. doi: 10.1172/JCI170503

70. Benhima N, Belbaraka R, Fontsa ML. Single agent vs combination immunotherapy in advanced melanoma: a review of the evidence. *Curr Opin Oncol*. (2024). doi: 10.1097/CCO.0000000000001014

71. Reyes-Gibby CC, Qdaisat A, Ferrarotto R, Fadol A, Bischof JJ, Coyne CJ, et al. Cardiovascular events after cancer immunotherapy as oncologic emergencies: Analyses of 610 head and neck cancer patients treated with immune checkpoint inhibitors. *Head Neck*. (2023) 46(3):627–35. doi: 10.1002/hed.27604

72. Kazi MA, Veeramachaneni R, Deng D, Putluri N, Cardinas M, Sikora A, et al. Glutathione peroxidase 2 is a metabolic driver of the tumor immune microenvironment and immune checkpoint inhibitor response. *J ImmunoTherapy Cancer*. (2022) 10(8):e004752.

73. Chen WY, Chen YL, Lin HW, Chang CF, Huang BS, Sun WZ, et al. Stereotactic body radiation combined with oncolytic vaccinia virus induces potent anti-tumor effect by triggering tumor cell necroptosis and DAMPs. *Cancer Lett*. (2021) 523:149–61. doi: 10.1016/j.canlet.2021.09.040

74. Zhu M, Yang M, Zhang J, Yin Y, Fan X, Zhang Y, et al. Immunogenic Cell Death Induction by Ionizing Radiation. *Front Immunol*. (2021) 12:705361. doi: 10.3389/fimmu.2021.705361

75. Niesters HG, van Esser J, Fries E, Wolthers KC, Cornelissen J, Osterhaus AD. Development of a real-time quantitative assay for detection of Epstein-Barr virus. *J Clin Microbiol*. (2000) 38:712–5. doi: 10.1128/JCM.38.2.712-715.2000

76. Bortolin MT, Pratesi C, Dolcetti R, Bidoli E, Vaccher E, Zanussi S, et al. Clinical value of Epstein- Barr virus DNA levels in peripheral blood samples of Italian patients with undifferentiated carcinoma of nasopharyngeal type. *Cancer Lett*. (2006) 233:247–54. doi: 10.1016/j.canlet.2005.03.015

77. Pow EH, Law MY, Tsang PC, Perera RA, Kwong DL. Salivary Epstein-Barr virus DNA level in patients with nasopharyngeal carcinoma following radiotherapy. *Oral Oncol*. (2011) 47:879–82. doi: 10.1016/j.oraloncology.2011.06.507

78. Fan H, Nicholls J, Chua D, Chan KH, Sham J, Lee S, et al. Laboratory markers of tumor burden in nasopharyngeal carcinoma: a comparison of viral load and serologic tests for Epstein-Barr virus. *Int J Cancer*. (2004) 112:1036–41. doi: 10.1002/ijc.20520

79. Lukowski SW, Tuong ZK, Noske K, Senabouth A, Nguyen QH, Andersen SB, et al. Detection of HPV E7 Transcription at Single-Cell Resolution in Epidermis. *J Invest Dermatol*. (2018) 138:2558–67. doi: 10.1016/j.jid.2018.06.169

80. Cohen EEW, Soulieres D, Le Tourneau C, Dinis J, Licitra L, Ahn MJ, et al. Pembrolizumab versus methotrexate, docetaxel, or cetuximab for recurrent or metastatic head-and-neck squamous cell carcinoma (KEYNOTE-040): a randomised, open-label, phase 3 study. *Lancet*. (2019) 393:156–67. doi: 10.1016/S0140-6736(18)31999-8

81. Berger BM, Hanna GJ, Posner MR, Genden EM, Lautersztain J, Naber SP, et al. Detection of Occult Recurrence Using Circulating Tumor Tissue Modified Viral HPV DNA among Patients Treated for HPV-Driven Oropharyngeal Carcinoma. *Clin Cancer Res*. (2022) 28:4292–301. doi: 10.1158/1078- 0432.CCR-22-0562

82. Sandulache VC, Williams MD, Lai SY, Lu C, William WN, Busaidy NL, et al. Real-Time Genomic Characterization Utilizing Circulating Cell-Free DNA in Patients with Anaplastic Thyroid Carcinoma. *Thyroid*. (2017) 27:81–7. doi: 10.1089/thy.2016.0076

83. Abbosh C, Birkbak NJ, Wilson GA, Jamal-Hanjani M, Constantin T, Salari R, et al. Phylogenetic ctDNA analysis depicts early-stage lung cancer evolution. *Nature*. (2017) 545:446–51. doi: 10.1038/nature22364

84. Nong J, Gong Y, Guan Y, Yi X, Yi Y, Chang L, et al. Circulating tumor DNA analysis depicts subclonal architecture and genomic evolution of small cell lung cancer. *Nat Commun*. (2018) 9:3114. doi: 10.1038/s41467-018-05327-w

85. Cao Y, Haring CT, Brummel C, Bhambhani C, Aryal M, Lee C, et al. Early HPV ctDNA kinetics and imaging biomarkers predict therapeutic response in p16+ oropharyngeal squamous cell carcinoma. *Clin Cancer Res*. (2022) 28:350–9. doi: 10.1158/1078-0432.CCR-21-2338

86. Chera BS, Kumar S, Beaty BT, Marron D, Jefferys S, Green R, et al. Rapid clearance profile of plasma circulating tumor HPV Type 16 DNA during chemoradiotherapy correlates with disease control in HPV-associated oropharyngeal cancer. *Clin Cancer Res*. (2019) 25:4682–90. doi: 10.1158/1078-0432.CCR-19-0211

87. Cao J, Zhang M, Xie F, Lou J, Zhou X, Zhang L, et al. Exosomes in head and neck cancer: Roles, mechanisms and applications. *Cancer Lett*. (2020) 494:7–16. doi: 10.1016/j.canlet.2020.07.005

88. Theodoraki MN, Yerneni SS, Hoffmann TK, Gooding WE, Whiteside TL. Clinical significance of PD-L1(+) exosomes in plasma of head and neck cancer patients. *Clin Cancer Res*. (2018) 24:896– 905. doi: 10.1158/1078-0432.CCR-17-2664

89. Principe S, Hui AB, Bruce J, Sinha A, Liu FF, Kislinger T. Tumor-derived exosomes and microvesicles in head and neck cancer: implications for tumor biology and biomarker discovery. *Proteomics*. (2013) 13:1608–23. doi: 10.1002/pmic.201200533

90. Wu XL, Tu Q, Faure G, Gallet P, Kohler C, Bittencourt Mde C. Diagnostic and prognostic value of circulating tumor cells in head and neck squamous cell carcinoma: a systematic review and meta-analysis. *Sci Rep*. (2016) 6:20210. doi: 10.1038/srep20210

91. Halmos GB, Bruine de Bruin L, Langendijk JA, van der Laan BF, Pruim J, Steenbakkers RJ. Head and neck tumor hypoxia imaging by 18F-fluoroazomycin-arabinoside (18F-FAZA)-PET: a review. *Clin Nucl Med*. (2014) 39:44–8. doi: 10.1097/RLU.0000000000000286

92. Gule MK, Chen Y, Sano D, Frederick MJ, Zhou G, Zhao M, et al. Targeted therapy of VEGFR2 and EGFR significantly inhibits growth of anaplastic thyroid cancer in an orthotopic murine model. *Clin Cancer Res*. (2011) 17:2281–91. doi: 10.1158/1078-0432.CCR-10-2762

93. Joint H, Neck Radiation Therapy MRIDC, Mohamed ASR, He R, Ding Y, Wang J, et al. Quantitative dynamic contrast-enhanced mri identifies radiation-induced vascular damage in patients with advanced osteoradionecrosis: Results of a prospective study. *Int J Radiat Oncol Biol Phys*. (2020) 108:1319–28. doi: 10.1016/j.ijrobp.2020.07.029

94. Joint H, Neck Radiotherapy MRIDC. Dynamic contrast-enhanced MRI detects acute radiotherapy-induced alterations in mandibular microvasculature: prospective assessment of imaging biomarkers of normal tissue injury. *Sci Rep*. (2016) 6:29864. doi: 10.1038/srep29864

95. Head MDANeck Cancer Symptom Working G. Dose-volume correlates of mandibular osteoradionecrosis in Oropharynx cancer patients receiving intensity-modulated radiotherapy: Results from a case-matched comparison. *Radiother Oncol*. (2017) 124:232–9. doi: 10.1016/j.radonc.2017.06.026

96. Ding Y, Hazle JD, Mohamed AS, Frank SJ, Hobbs BP, Colen RR, et al. Intravoxel incoherent motion imaging kinetics during chemoradiotherapy for human papillomavirus-associated squamous cell carcinoma of the oropharynx: preliminary results from a prospective pilot study. *NMR BioMed*. (2015) 28:1645–54. doi: 10.1002/nbm.3412

97. Ng SP, Cardenas CE, Bahig H, Elgohari B, Wang J, Johnson JM, et al. Changes in apparent diffusion coefficient (ADC) in serial weekly mri during radiotherapy in patients with head and neck cancer: results from the PREDICT-HN study. *Curr Oncol*. (2022) 29:6303–13. doi: 10.3390/curroncol29090495

98. Zhou Q, Zeng F, Ding Y, Fuller CD, Wang J. Meta-analysis of diffusion-weighted imaging for predicting locoregional failure of chemoradiotherapy in patients with head and neck squamous cell carcinoma. *Mol Clin Oncol*. (2018) 8:197–203. doi: 10.3892/mco.2017.1504

99. Aggarwal R, Vigneron DB, Kurhanewicz J. Hyperpolarized 1-[13C]-Pyruvate Magnetic Resonance Imaging Detects an Early Metabolic Response to Androgen Ablation Therapy in Prostate Cancer. *Eur Urol*. (2017) 72:1028–9. doi: 10.1016/j.eururo.2017.07.022

100. Autry AW, Park I, Kline C, Chen HY, Gordon JW, Raber S, et al. Pilot study of hyperpolarized (13)C metabolic imaging in pediatric patients with diffuse intrinsic pontine glioma and other cns cancers. *AJNR Am J Neuroradiol*. (2020) 42(1):178–84. doi: 10.3174/ajnr.A6937

101. Chen HY, Aggarwal R, Bok RA, Ohliger MA, Zhu Z, Lee P, et al. Hyperpolarized (13)C-pyruvate MRI detects real-time metabolic flux in prostate cancer metastases to bone and liver: a clinical feasibility study. *Prostate Cancer Prostatic Dis*. (2020) 23:269–76. doi: 10.1038/s41391-019-0180-z

102. Cunningham CH, Lau JY, Chen AP, Geraghty BJ, Perks WJ, Roifman I, et al. Hyperpolarized 13C Metabolic MRI of the Human Heart: Initial Experience. *Circ Res*. (2016) 119:1177–82. doi: 10.1161/CIRCRESAHA.116.309769

103. Gallagher FA, Woitek R, McLean MA, Gill AB, Manzano Garcia R, Provenzano E, et al. Imaging breast cancer using hyperpolarized carbon-13 MRI. *Proc Natl Acad Sci United States America*. (2020) 117:2092–8. doi: 10.1073/pnas.1913841117

104. Grist JT, McLean MA, Riemer F, Schulte RF, Deen SS, Zaccagna F, et al. Quantifying normal human brain metabolism using hyperpolarized [1-(13)C]pyruvate and magnetic resonance imaging. *Neuroimage*. (2019) 189:171–9. doi: 10.1016/j.neuroimage.2019.01.027

105. Miloushev VZ, Granlund KL, Boltyanskiy R, Lyashchenko SK, DeAngelis LM, Mellinghoff IK, et al. Metabolic imaging of the human brain with hyperpolarized (13)C pyruvate demonstrates (13)c lactate production in brain tumor patients. *Cancer Res*. (2018) 78:3755–60. doi: 10.1158/0008- 5472.CAN-18-0221

106. Park I, Larson PEZ, Gordon JW, Carvajal L, Chen HY, Bok R, et al. Development of methods and feasibility of using hyperpolarized carbon-13 imaging data for evaluating brain metabolism in patient studies. *Magn Reson Med*. (2018) 80:864–73. doi: 10.1002/mrm.27077

107. Stodkilde-Jorgensen H, Laustsen C, Hansen ESS, Schulte R, Ardenkjaer-Larsen JH, Comment A, et al. Pilot study experiences with hyperpolarized [1-(13) C]pyruvate mri in pancreatic cancer patients. *J Magn Reson Imaging*. (2020) 51:961–3. doi: 10.1002/jmri.26888

108. Tran M, Latifoltojar A, Neves JB, Papoutsaki MV, Gong F, Comment A, et al. First-in-human *in vivo* non-invasive assessment of intra-tumoral metabolic heterogeneity in renal cell carcinoma. *BJR Case Rep*. (2019) 5(3):20190003. doi: 10.1259/bjrcr.20190003

109. Woitek R, McLean MA, Gill AB, Grist JT, Provenzano E, Patterson AJ, et al. Hyperpolarized (13)C mri of tumor metabolism demonstrates early metabolic response to neoadjuvant chemotherapy in breast cancer. *Radiol Imaging Cancer*. (2020) 2:e200017. doi: 10.1148/rycan.2020200017

110. Moses WW. Fundamental Limits of Spatial Resolution in PET. *Nucl Instrum Methods Phys Res A 2011;*. (648) Supplement1:S236–40. doi: 10.1016/j.nima.2010.11.092

111. Levin CS, Hoffman EJ. Calculation of positron range and its effect on the fundamental limit of positron emission tomography system spatial resolution. *Phys Med Biol*. (1999) 44:781–99.

112. Fogarty GB, Peters LJ, Stewart J, Scott C, Rischin D, Hicks RJ. The usefulness of fluorine 18- labelled deoxyglucose positron emission tomography in the investigation of patients with cervical lymphadenopathy from an unknown primary tumor. *Head Neck*. (2003) 25:138–45. doi: 10.1002/hed.10191

113. Hentschel M, Appold S, Schreiber A, Abramyuk A, Abolmaali N, Kotzerke J, et al. Serial FDG- PET on patients with head and neck cancer: implications for radiation therapy. *Int J Radiat Biol*. (2009) 85:796–804. doi: 10.1080/09553000903039180

114. Porceddu SV, Pryor DI, Burmeister E, Burmeister BH, Poulsen MG, Foote MC, et al. Results of a prospective study of positron emission tomography-directed management of residual nodal abnormalities in node-positive head and neck cancer after definitive radiotherapy with or without systemic therapy. *Head Neck*. (2011) 33:1675–82. doi: 10.1002/hed.21655

115. Yao M, Graham MM, Smith RB, Dornfeld KJ, Skwarchuk M, Hoffman HT, et al. Value of FDG PET in assessment of treatment response and surveillance in head-and-neck cancer patients after intensity modulated radiation treatment: a preliminary report. *Int J Radiat Oncol Biol Phys*. (2004) 60:1410–8. doi: 10.1016/j.ijrobp.2004.05.058

116. Lin MY, Wu M, Brennan S, Campeau MP, Binns DS, Macmanus M, et al. Absence of a Relationship between Tumor 18F-fluorodeoxyglucose Standardized Uptake Value and Survival in Patients Treated with Definitive Radiotherapy for Non-Small-Cell Lung Cancer. *J Thorac Oncol*. (2014) 9:377–82. doi: 10.1097/JTO.0000000000000096

117. Schinagl DA, Span PN, Oyen WJ, Kaanders JH. Can FDG PET predict radiation treatment outcome in head and neck cancer? Results of a prospective study. *Eur J Nucl Med Mol Imaging*. (2011) 38:1449–58. doi: 10.1007/s00259-011-1789-x

118. Jacobson O, Chen X. Interrogating tumor metabolism and tumor microenvironments using molecular positron emission tomography imaging. *Theranostic approaches to improve Ther Pharmacol Rev*. (2013) 65:1214–56. doi: 10.1124/pr.113.007625

119. Albers MJ, Bok R, Chen AP, Cunningham CH, Zierhut ML, Zhang VY, et al. Hyperpolarized 13C lactate, pyruvate, and alanine: noninvasive biomarkers for prostate cancer detection and grading. *Cancer Res*. (2008) 68:8607–15. doi: 10.1158/0008-5472.CAN-08-0749

120. Chen AP, Chu W, Gu YP, Cunnhingham CH. Probing Early Tumor Response to Radiation Therapy Using Hyperpolarized [1-(13)C]pyruvate in MDA-MB-231 Xenografts. *PloS One*. (2013) 8:e56551. doi: 10.1371/journal.pone.0056551PONE-D-12-14990

121. Granlund KL, Tee SS, Vargas HA, Lyashchenko SK, Reznik E, Fine S, et al. Hyperpolarized MRI of human prostate cancer reveals increased lactate with tumor grade driven by monocarboxylate transporter 1. *Cell Metab*. (2020) 31:105–114 e103. doi: 10.1016/j.cmet.2019.08.024

122. Garden AS, Kies MS, Morrison WH, Weber RS, Frank SJ, Glisson BS, et al. Outcomes and patterns of care of patients with locally advanced oropharyngeal carcinoma treated in the early 21st century. *Radiat Oncol*. (2013) 8:21. doi: 10.1186/1748-717X-8-21

123. Lai S, Wenaas AE, Sandulache VC, Hartman C, Chiao E, Kramer J, et al. Prognostic Significance of p16 Cellular Localization in Oropharyngeal Squamous Cell Carcinoma. *Ann Clin Lab Sci*. (2016) 46:132–9.

124. Poeta ML, Manola J, Goldwasser MA, Forastiere A, Benoit N, Califano JA, et al. TP53 mutations and survival in squamous-cell carcinoma of the head and neck. *N Engl J Med*. (2007) 357:2552–61. doi: 10.1056/NEJMoa073770

125. Neskey DM, Osman AA, Ow TJ, Katsonis P, McDonald T, Hicks SC, et al. Evolutionary action score of TP53 identifies high-risk mutations associated with decreased survival and increased distant metastases in head and neck cancer. *Cancer Res*. (2015) 75:1527–36. doi: 10.1158/0008- 5472.CAN-14-2735

126. Osman AA, Neskey DM, Katsonis P, Patel AA, Ward AM, Hsu TK, et al. Evolutionary action score of TP53 coding variants is predictive of platinum response in head and neck cancer patients. *Cancer Res*. (2015) 75:1205–15. doi: 10.1158/0008-5472.CAN-14-2729

127. Skinner HD, Sandulache VC, Ow TJ, Meyn RE, Yordy JS, Beadle BM, et al. TP53 disruptive mutations lead to head and neck cancer treatment failure through inhibition of radiation-induced senescence. *Clin Cancer Res*. (2012) 18:290–300. doi: 10.1158/1078-0432.CCR-11-2260

128. Sandulache VC, Skinner HD, Wang Y, Chen Y, Dodge CT, Ow TJ, et al. Glycolytic inhibition alters anaplastic thyroid carcinoma tumor metabolism and improves response to conventional chemotherapy and radiation. *Mol Cancer Ther*. (2012) 11:1373–80. doi: 10.1158/1535-7163.MCT-12- 0041

129. Bankson JA, Walker CM, Ramirez MS, Stefan W, Fuentes D, Merritt ME, et al. Kinetic modeling and constrained reconstruction of hyperpolarized [1-13C]-pyruvate offers improved metabolic imaging of tumors. *Cancer Res*. (2015) 75:4708–17. doi: 10.1158/0008-5472.CAN-15-0171

130. Rosi A, Grande S, Luciani AM, Palma A, Giovannini C, Guidoni L, et al. Role of glutathione in apoptosis induced by radiation as determined by 1H MR spectra of cultured tumor cells. *Radiat Res*. (2007) 167:268–82. doi: 10.1667/RR0578.1

131. Sandulache VC, Ow TJ, Pickering CR, Frederick MJ, Zhou G, Fokt I, et al. Glucose, not glutamine, is the dominant energy source required for proliferation and survival of head and neck squamous carcinoma cells. *Cancer*. (2011) 117:2926–38. doi: 10.1002/cncr.25868

132. Sandulache VC, Skinner HD, Ow TJ, Zhang A, Xia X, Luchak JM, et al. Individualizing antimetabolic treatment strategies for head and neck squamous cell carcinoma based on TP53 mutational status. *Cancer*. (2012) 118:711–21. doi: 10.1002/cncr.26321

133. Sharma PK, Dwarakanath BS, Varshney R. Radiosensitization by 2-deoxy-D-glucose and 6- aminonicotinamide involves activation of redox sensitive ASK1-JNK/p38MAPK signaling in head and neck cancer cells. *Free Radic Biol Med*. (2012) 53:1500–13. doi: 10.1016/j.freeradbiomed.2012.07.001S0891-5849(12)00387-5

134. Simons AL, Ahmad IM, Mattson DM, Dornfeld KJ, Spitz DR. 2-Deoxy-D-glucose combined with cisplatin enhances cytotoxicity *via* metabolic oxidative stress in human head and neck cancer cells. *Cancer Res*. (2007) 67:3364–70. doi: 10.1158/0008-5472.CAN-06-3717

135. Simons AL, Fath MA, Mattson DM, Smith BJ, Walsh SA, Graham MM, et al. Enhanced response of human head and neck cancer xenograft tumors to cisplatin combined with 2-deoxy-D-glucose correlates with increased 18F-FDG uptake as determined by PET imaging. *Int J Radiat Oncol Biol Phys*. (2007) 69:1222–30. doi: 10.1016/j.ijrobp.2007.07.2343

136. Simons AL, Parsons AD, Foster KA, Orcutt KP, Fath MA, Spitz DR. Inhibition of glutathione and thioredoxin metabolism enhances sensitivity to perifosine in head and neck cancer cells. *J Oncol*. (2009) 2009:519563. doi: 10.1155/2009/519563

137. Brizel DM, Schroeder T, Scher RL, Walenta S, Clough RW, Dewhirst MW, et al. Elevated tumor lactate concentrations predict for an increased risk of metastases in head-and-neck cancer. *Int J Radiat Oncol Biol Phys*. (2001) 51:349–53.

138. Quennet V, Yaromina A, Zips D, Rosner A, Walenta S, Baumann M, et al. Tumor lactate content predicts for response to fractionated irradiation of human squamous cell carcinomas in nude mice. *Radiother Oncol*. (2006) 81:130–5. doi: 10.1016/j.radonc.2006.08.012

139. Sandulache VC, Chen Y, Lee J, Rubinstein A, Ramirez MS, Skinner HD, et al. Evaluation of hyperpolarized [1-(1)(3)C]-pyruvate by magnetic resonance to detect ionizing radiation effects in real time. *PloS One*. (2014) 9:e87031. doi: 10.1371/journal.pone.0087031

140. Ramirez MS, Lee J, Walker CM, Chen Y, Kingsley CV, de la Cerda J, et al. Feasibility of multianimal hyperpolarized (13) C MRS. *Magn Reson Med*. (2015) 73:1726–32. doi: 10.1002/mrm.25307

141. Ramirez MS, Lee J, Walker CM, Sandulache VC, Hennel F, Lai SY, et al. Radial spectroscopic MRI of hyperpolarized [1- C] pyruvate at 7 tesla. *Magn Reson Med*. (2014) 72(4):986–95. doi: 10.1002/mrm.25004

142. Ramirez MS, Lee J, Sandulache VC, Walker CM, Chen Y, Lai SY, et al. Salt Lake City, UT (2013).

143. Michel KA, Ragavan M, Walker CM, Merritt ME, Lai SY, Bankson JA. Comparison of Selective Excitation and Multi-Echo Chemical Shift Encoding for Imaging of Hyperpolarized [1-13C]Pyruvate. *J Magn Reson*. (2021) 325:106927.1016/j.jmr.2021.106927

144. Vaidya P, Bera K, Linden PA, Gupta A, Rajiah PS, Jones DR, et al. Combined Radiomic and Visual Assessment for Improved Detection of Lung Adenocarcinoma Invasiveness on Computed Tomography Scans: A Multi-Institutional Study. *Front Oncol*. (2022) 12:902056. doi: 10.3389/fonc.2022.902056

145. Jazieh K, Khorrami M, Saad A, Gad M, Gupta A, Patil P, et al. Novel imaging biomarkers predict outcomes in stage III unresectable non-small cell lung cancer treated with chemoradiation and durvalumab. *J Immunother Cancer*. (2022) 10(3):e003778. doi: 10.1136/jitc-2021-003778

146. Pepe MS, Feng Z, Janes H, Bossuyt PM, Potter JD. Pivotal evaluation of the accuracy of a biomarker used for classification or prediction: standards for study design. *J Natl Cancer Inst*. (2008) 100:1432–8. doi: 10.1093/jnci/djn326

Frontiers in Oncology

Advances knowledge of carcinogenesis and tumor progression for better treatment and management

The third most-cited oncology journal, which highlights research in carcinogenesis and tumor progression, bridging the gap between basic research and applications to imrpove diagnosis, therapeutics and management strategies.

Discover the latest Research Topics

See more →

Frontiers

Avenue du Tribunal-Fédéral 34
1005 Lausanne, Switzerland
frontiersin.org

Contact us

+41 (0)21 510 17 00
frontiersin.org/about/contact